

OPTIMIZATION OF LARGE-SCALE SUSTAINABLE RENEWABLE ENERGY SUPPLY  
CHAINS IN A STOCHASTIC ENVIRONMENT

A Dissertation  
Submitted to the Graduate Faculty  
of the  
North Dakota State University  
of Agriculture and Applied Science

By

Atif Osmani

In Partial Fulfillment  
for the Degree of  
DOCTOR OF PHILOSOPHY

Major Department:  
Industrial and Manufacturing Engineering

December 2013

Fargo, North Dakota

North Dakota State University  
Graduate School

---

**Title**

Optimization of large-scale sustainable renewable energy supply chains in a stochastic environment

---

**By**

Atif Osmani

---

The Supervisory Committee certifies that this *disquisition* complies with North Dakota State University's regulations and meets the accepted standards for the degree of

**DOCTOR OF PHILOSOPHY**

SUPERVISORY COMMITTEE:

Dr. Jun Zhang

---

Chair

Dr. Kambiz Farahmand

---

Dr. Jing Shi

---

Dr. Joseph Szmerekovsky

---

Approved:

12/8/2013

---

Date

Dr. Canan Bilen-Green

---

Department Chair

## ABSTRACT

Due to the increasing demand of energy and environmental concern of fossil fuels, it is becoming increasingly important to find alternative renewable energy sources. Biofuels produced from lignocellulosic biomass feedstock's show enormous potential as a renewable resource. Electricity generated from the combustion of biomass is also one important type of bioenergy. Renewable resources like wind also show great potential as a resource for electricity generation. In order to deliver competitive renewable energy products to the end-market, robust renewable energy supply chains (RESCs) are essential. Research is needed in two distinct types of RESCs, namely: 1) lignocellulosic biomass-to-biofuel supply chain (LBSC); and 2) wind and biomass to electricity supply chain (WBBRESC).

LBSC is a complex system which consists of multiple uncertainties, such as: 1) purchase price and availability of biomass feedstock; 2) sale price and demand of biofuels. To ensure LBSC sustainability, key logistics/supply chain decisions need to be optimized, such as: a) allocation of land for biomass cultivation; b) biorefinery sites selection; c) choice of biomass-to-biofuel conversion technology; and d) production capacity of biorefineries.

The major uncertainty in a WBBRESC concerns wind speeds which impact the power output of wind farms. To ensure WBBRESC sustainability, the following decisions need to be optimized: a) site selection for installation of wind farms, biomass power plants (BMPPs), and grid stations; b) generation capacity of wind farms and BMPPs; and c) transmission capacity of power lines.

The multiple uncertainties in RESCs if not jointly considered in the decision making process result in non-optimal (or even infeasible) solutions which might generate lower profits, increased environmental pollution, and reduced social benefits. This research proposes a number

of comprehensive mathematical models for the stochastic optimization of RESCs. The proposed large-scale stochastic mixed integer linear programming (SMILP) models are solved to optimality by using suitable decomposition methods (e.g. Bender's) and appropriate metaheuristic algorithms (e.g. Sample Average Approximation).

Overall, the research outcomes will help to design robust RESCs focused towards sustainability in order to optimally utilize the renewable resources in the near future. The findings can be used by renewable energy policy decision makers and investors to sustainably operate in an efficient (and cost effective) manner, boost the regional economy, and protect the environment.

## ACKNOWLEDGEMENT

By the grace of God almighty I have completed my dissertation. I would like to acknowledge the industrial engineering faculty and colleagues who have assisted me during the course of my research. Without their contributions, this dissertation would not have been possible. I gratefully acknowledge the advice of Dr. Om Yadav and Dr. Canan Bilen-Green. I thank Dawn Allmaras for her help and guidance. I specially appreciate Iddrisu Awudu, Vinay Gonela and Shah Limon for working with me, motivating me and helping me with all my research.

I also express my sincere and deepest gratitude to my advisor Dr. Jun Zhang without whom I would not have come so far in my research. I thank her for consistently motivating me, being patient with me and challenging me to go beyond my comfort zone to explore new ideas. Once I leave NDSU I will very much miss our weekly meetings.

A special thanks to the members of my advisory committee; Dr. Kambiz Farahmand, Dr. Jing Shi, and Dr. Joseph Szmerekovsky. I am most grateful for the opportunity, time and guidance. I state my gratitude for Dr. Farahmand and Dr. Shi for providing me with the opportunity to enroll in the IME PhD program at NDSU. I am truly indebted to you. I would also like to thank Dr. Szmerekovsky for being in my committee and giving me great insights during my research.

Finally, I would like to thank my family. I express my sincere obeisance to my mother, Iffat (*Ammi*), for her deep love for me. The pain taken by her to see me achieve my educational goals is immeasurable. "I thank her for all her sacrifices." I thank my late father, Ahsan (*Abbu*), whose love of knowledge and pride in me has always made me grow stronger and determined to succeed. I would also like to thank my elder sister, Saira (*Apa*), my younger sister Sumaira

(*Summo*), and my baby brother Fahad (*Faddu*), for their consistent help and motivation. I would like to remember my beautiful nieces Sarah (*Booboo*), Natasha (*Nanoo*), and Samar (*Timmy*) who have always made me happy and are my life and joy. As a student returning to graduate school after a gap of 15 years I would like to acknowledge the advice of my 10 year old niece Samar “... *he would not need to go back to school if only he had studied harder as a little boy*”.

Last but not least, to my wife and the love of my life, Samina. You have always been very patient with me. You are all I have. You are a kind hearted, loving and selfless person.

## DEDICATION

This work is dedicated to my grandmother (*Amma*) and grandfather (*Abba*). With your blessings, all things are possible.

## TABLE OF CONTENTS

ABSTRACT .....	iii
ACKNOWLEDGEMENT .....	v
DEDICATION .....	vii
LIST OF TABLES .....	xvi
LIST OF FIGURES .....	xvii
LIST OF APPENDIX TABLES .....	xx
CHAPTER 1. INTRODUCTION .....	1
1.1. Background .....	1
1.1.1. Biofuels .....	1
1.1.2. Renewable electricity .....	4
1.2. Research motivation .....	5
1.3. Research contribution and structure .....	7
CHAPTER 2. AN INTEGRATED OPTIMIZATION MODEL FOR SWITCHGRASS-BASED BIOETHANOL SUPPLY CHAIN .....	11
2.1. Abstract .....	11
2.2. Introduction and literature review .....	11
2.3. Problem statement .....	15
2.4. Assumptions .....	17
2.5. Model formulation .....	18
2.5.1. Objective function .....	18



2.5.2. Capacity constraints .....	22
2.5.3. Material flow constraints .....	24
2.6. Case study .....	26
2.6.1. Input parameters .....	26
2.7. Results and sensitivity analysis .....	27
2.7.1. Impact of different level of bioethanol demand on the SBSC decisions .....	29
2.7.2. Effect of different harvest methods on the total SBSC cost .....	30
2.7.3. Impact of biorefinery locations on the transportation and total SBSC costs .....	31
2.7.4. Impact of different levels of switchgrass yield on the SBSC decision variables .....	32
2.8. Conclusions .....	33
2.9. Nomenclature .....	34
2.9.1. Indices .....	34
2.9.2. Binary decision variables .....	35
2.9.3. Continuous decision variables .....	35
2.9.4. Parameters .....	35
2.10. References .....	37
<b>CHAPTER 3. OPTIMIZATION OF A MULTI FEEDSTOCK LIGNOCELLULOSIC-BASED BIOETHANOL SUPPLY CHAIN UNDER MULTIPLE UNCERTAINTIES .....</b>	<b>41</b>
3.1. Abstract .....	41
3.2. Introduction and literature review .....	41
3.3. Problem statement .....	45
3.3.1. Stochastic nature of the LBSC .....	47

3.4. Model formulation.....	48
3.4.1. Objective function of the LBSC .....	49
3.4.2. Capacity constraints.....	51
3.4.3. Material flow constraints .....	51
3.5. Case study setup .....	52
3.5.1. Model assumptions .....	53
3.6. Modeling the uncertainties in the LBSC .....	55
3.6.1. Modeling switchgrass yield.....	55
3.6.2. Modeling the purchase price for crop residues .....	56
3.6.3. Modeling the demand for bioethanol.....	57
3.6.4. Modeling the sale price for bioethanol .....	57
3.7. Solution procedure for the proposed stochastic MILP model .....	57
3.8. Comparison of the deterministic model vs. proposed stochastic model .....	58
3.8.1. For the base-case .....	59
3.8.2. Under different levels of variability .....	62
3.8.3. For different levels of recourse parameters.....	64
3.9. Sensitivity analysis .....	65
3.9.1. Impact of mean value of ethanol sale price on the LBSC logistic decisions .....	65
3.9.2. Impact of mean value of in-state ethanol demand on the LBSC logistic variables.....	67
3.9.3. Impact of mean value of rainfall (and crop residue price) on LBSC logistic variables .....	69
3.9.4. Impact of penalty cost of unmet bioethanol demand on the LBSC logistic variables.....	71

3.10. Conclusion .....	73
3.11. Nomenclature .....	75
3.11.1. Indices .....	75
3.11.2. First stage continuous decision variables.....	75
3.11.3. First stage binary decision variables .....	76
3.11.4. Second stage decision variables .....	76
3.11.5. Deterministic parameters .....	77
3.11.6. Stochastic parameters.....	78
3.12. References.....	78

<b>CHAPTER 4. ECONOMIC AND ENVIRONMENTAL OPTIMIZATION OF A LARGE SCALE SUSTAINABLE DUAL FEEDSTOCK LIGNOCELLULOSIC-BASED BIOETHANOL SUPPLY CHAIN IN A STOCHASTIC ENVIRONMENT.....</b>	<b>83</b>
4.1. Abstract.....	83
4.2. Introduction and literature review .....	84
4.3. Problem statement .....	88
4.4. Stochastic nature of the LBSC .....	91
4.4.1. Uncertainty in supply of biomass feedstock .....	91
4.4.2. Uncertainty in the demand for bioethanol.....	92
4.4.3. Uncertainty in the purchase prices for biomass feedstocks .....	92
4.4.4. Uncertainty in the sale prices for bioenergy products .....	92
4.5. Model formulation.....	93
4.5.1. Objective function of the LBSC .....	93

4.5.2. Capacity constraints.....	94
4.5.3. Material balance constraints.....	95
4.6. Solution procedure for the proposed stochastic MILP model .....	96
4.6.1. SAA algorithm .....	96
4.7. Case study set-up.....	99
4.7.1. Model assumptions .....	99
4.7.2. Modeling the uncertainties in a LBSC.....	101
4.7.3. Discretization of continuous stochastic parameters.....	101
4.8. Case study results .....	102
4.8.1. Comparison of outcomes in stand-alone vs. co-operation mode under uncertainties .....	102
4.8.2. Under co-operation mode.....	105
4.9. Sensitivity analysis .....	112
4.9.1. Impact of carbon price .....	113
4.9.2. Impact of bioethanol tax credit.....	114
4.10. Conclusion .....	115
4.11. Nomenclature .....	117
4.11.1. Indices .....	117
4.11.2. First stage decision variables.....	117
4.11.3. Second stage decision variables .....	118
4.11.4. Deterministic parameters .....	118
4.11.5. Stochastic parameters.....	120

4.12. References.....	120
<b>CHAPTER 5. MULTI-PERIOD STOCHASTIC OPTIMIZATION OF A SUSTAINABLE MULTI FEEDSTOCK SECOND GENERATION BIOETHANOL SUPPLY CHAIN.....</b>	<b>126</b>
5.1. Abstract.....	126
5.2. Introduction.....	126
5.3. Literature review and research significance .....	130
5.4. Problem statement .....	132
5.4.1. Modeling the stochastic nature of the LBSC .....	135
5.5. Model formulation.....	136
5.5.1. Objective functions of the LBSC .....	136
5.5.2. Environmental performance constraint.....	138
5.5.3. Capacity constraints .....	138
5.5.4. Material balance constraints.....	139
5.5.5. Link constraints .....	140
5.6. Two-step solution methodology for the proposed stochastic multi-period MILP model .....	141
5.6.1. Modified SAA method.....	142
5.6.2. Benders decomposition.....	143
5.6.3. Trade-off among different performance criteria .....	144
5.7. Case study set-up.....	145
5.7.1. Model assumptions .....	145
5.7.2. Modeling the uncertainties in a LBSC.....	146
5.7.3. Discretization of continuous stochastic parameters.....	146

5.7.4. Sequential application of modified SAA method and benders decomposition.....	148
5.8. Case study results .....	149
5.8.1. First-stage decisions during each planning period .....	149
5.8.2. Trade-off among economic, environmental and social performance criteria .....	155
5.8.3. Fixed vs. variable bioethanol production tax credit .....	159
5.9. Conclusions.....	161
5.10. Nomenclature .....	163
5.10.1. Indices .....	163
5.10.2. First stage decision variables.....	163
5.10.3. Second stage decision variables .....	163
5.10.4. Deterministic parameters .....	164
5.10.5. Stochastic parameters.....	165
5.11. References.....	166

**CHAPTER 6. OPTIMAL GRID DESIGN AND LOGISTIC PLANNING FOR BIOMASS AND WIND BASED RENEWABLE ELECTRICITY SUPPLY CHAINS UNDER UNCERTAINTIES ...170**

6.1. Abstract.....	170
6.2. Introduction.....	170
6.3. Problem statement .....	175
6.3.1. Logistics and supply chain decisions.....	176
6.3.2. Stochastic nature of the WBBRESC.....	178
6.4. Model formulation.....	180
6.4.1. Objective function of the WBBRESC .....	180

6.4.2 Constraints.....	181
6.5. Case study set-up and results .....	183
6.5.1. Model assumptions .....	183
6.5.2. Modeling the uncertainties in a WBBRESC .....	186
6.5.3. Comparison of the deterministic model vs. proposed stochastic model.....	187
6.5.4. Evaluating the decisions of the stochastic model.....	190
6.5.5. Sensitivity analysis .....	192
6.6. Conclusions.....	196
6.7. Nomenclature .....	198
6.7.1. Indices .....	198
6.7.2. First stage binary decision variables .....	198
6.7.3. First stage continuous decision variables.....	199
6.7.4. Second stage decision variables .....	199
6.7.4. Deterministic parameters .....	200
6.7.5. Stochastic parameters .....	201
6.8. References.....	201
APPENDIX A. INPUT PARAMETERS .....	207
APPENDIX B. CONVERSION FACTORS FROM METRIC (SI) UNITS TO U.S. UNITS .....	213
APPENDIX C. CONVERSION FACTORS FROM U.S. UNITS TO METRIC (SI) UNITS .....	214

## LIST OF TABLES

<u>Table</u>	<u>Page</u>
1. Optimal assignment of bioethanol demand zones to individual biorefineries.....	28
2. Percentage of gasoline demand met from cellulosic bioethanol (scenario planning).....	29
3. Discretized levels of independent random variables (IRVs).....	58
4. Comparison of deterministic model vs. proposed stochastic model for the base-case.....	60
5. Different levels of variability.....	62
6. VSS at different levels of crop residue price ( $\varepsilon$ ) and penalty for unmet demand ( $\varphi$ ).....	65
7. Indices used in the case study.....	99
8. Inter-state exchange of biomass and bioethanol under co-operation mode.....	105
9. Comparison of stochastic vs. deterministic model in co-op mode under uncertainty.....	106
10. Indices used in the case study.....	146
11. Discretized levels of independent random variables (IRVs).....	147
12. Modified SAA method vs. 2-step approach.....	149
13. LBSC performances under different optimization objectives.....	154
14. LBSC performances under different decision making criteria.....	159
15. Indices used in the case study.....	183
16. Comparison of the deterministic model vs. proposed stochastic model.....	189
17. Transmission capacity of HVAC power lines from $r$ to $j$ .....	190
18. Transmission capacity of HVDC power lines.....	190
19. Generation capacity of wind farms.....	191
20. Generation capacity of BMPPs.....	192
21. Amount of electricity supplied to out-state demand zones.....	192



## LIST OF FIGURES

<u>Figure</u>	<u>Page</u>
1. Major logistics activities in a switchgrass-based bioethanol supply chain (SBSC) .....	12
2. Switchgrass-based bioethanol supply chain .....	16
3. Optimum location of preprocessing facilities and biorefineries in North Dakota .....	28
4. % of land used for switchgrass .....	29
5. Transportation cost as % of total cost .....	29
6. Total SBSC cost .....	30
7. Cost of refined bioethanol .....	30
8. Marginal land used for switchgrass .....	30
9. Storage losses for traditional bales .....	30
10. Total SBSC cost .....	31
11. Refined bioethanol cost .....	31
12. Breakdown of total annual switchgrass-based bioethanol supply chain cost .....	31
13. Total SBSC cost .....	32
14. Total transportation cost .....	32
15. Impact of switchgrass yields on land allocation and bioethanol cost .....	33
16. Major logistics activities in a LBSC .....	46
17. Switchgrass cultivation sites and biorefinery locations (deterministic model) .....	60
18. Switchgrass cultivation sites and biorefinery locations (stochastic model) .....	61
19. Impact of variability on expected profit .....	63
20. Impact on marginal land allocation .....	63
21. Impact on bioethanol production .....	64

22. Impact of ethanol price on profit.....	66
23. Impact of ethanol price on decisions.....	66
24. Impact of ethanol demand on profit.....	68
25. Impact of ethanol demand on decisions.....	68
26. Impact of rainfall level on profit.....	69
27. Impact of crop residue price on profit.....	69
28. Impact of rainfall level on decisions.....	70
29. Impact of residue price on decisions.....	70
30. Impact of penalty cost on profit.....	72
31. Impact of penalty cost on decisions.....	72
32. Lignocellulosic based biomass-to-bioethanol supply chain.....	88
33. Co-operation mode vs. stand-alone mode.....	104
34. Total profit (stand-alone vs. co-op).....	104
35. GHG emissions (stand-alone vs. co-op).....	105
36. Impact of variability on profit.....	107
37. Impact of variability on GHG emissions.....	108
38. Biomass processed by biorefineries.....	109
39. Biomass inventory kept at biorefineries.....	110
40. Biomass processed by biochemical.....	110
41. Biomass processed by thermochemical.....	111
42. Bioethanol production by biorefineries.....	111
43. Bioethanol inventory and demand.....	112
44. Impact on LBSC performance.....	113

45. Impact on type of biorefineries .....	113
46. Impact on LBSC performance .....	114
47. Impact on type of biorefineries .....	115
48. Major logistics activities in a LBSC .....	132
49. Renewable fuel standard (RFS) .....	134
50. Modified application of the SAA method .....	142
51. 3D Pareto optimum sets .....	156
52. Social vs. environmental performance .....	156
53. Economic vs. social objective .....	157
54. Economic vs. environmental objective .....	157
55. Histogram of fixed subsidy policy .....	160
56. Histogram of variable subsidy policy .....	161
57. Major logistics activities in a WBBRESC .....	175
58. Power curve for a wind farm .....	179
59. Capacities and locations of existing wind farms in ND .....	184
60. First-stage decisions (deterministic model) .....	187
61. First-stage decisions (stochastic model) .....	188
62. Impact on expected WBBRESC profit .....	193
63. Impact on generation capacity .....	194
64. Impact on expected WBBRESC profit .....	194
65. Impact on electricity generation capacity .....	195
66. Impact on expected WBBRESC profit .....	195
67. Impact on electricity generation capacity .....	196

## LIST OF APPENDIX TABLES

<u>Table</u>	<u>Page</u>
A1. Values of input parameters ( $A_i, B_i, C_i, M_e^t$ ).....	207
A2. Cumulative rate of switchgrass dry-matter weight loss for harvest methods .....	208
A3. Values of other key input parameters .....	208
A4. Values of key deterministic parameters.....	208
A5. Values of stochastic parameters .....	208
A6. “Mean” values of input parameters $\delta_i, A_i, B_i, C_i, \zeta_i, M_e, a_i, b_i$ .....	209
A7. Values of deterministic parameters .....	210
A8. Values of stochastic parameters .....	210
A9. Discretized levels of independent random variables (IRVs) .....	210
A10. Values of stochastic parameters .....	211
A11. Values of key deterministic parameters.....	211
A12. Values of key deterministic parameters.....	212
A13. Values of stochastic parameters .....	212
A14. Values of input parameters $\zeta_i, B_r, \eta_r, \Delta_r$ .....	212

## CHAPTER 1. INTRODUCTION

### **1.1. Background**

The U.S. is the world's leading energy consumer and utilizes resources in the form of fossil fuels, nuclear, and renewables to meet its energy demand for: 1) refined liquid fuels (e.g. gasoline) for the transportation sector; 2) electricity; and 3) heating/cooling. Fossil fuels (in the form of petroleum, natural gas and coal) account for 83% of the energy supplied to the U.S. economy in 2012. Nuclear power supplied 9% while the various renewable energy sources (including biomass, wind, hydropower, solar, and geothermal) contributed only 8% to the U.S. energy supply.

There is growing public awareness that consumption of fossil fuels in large amounts is contributing to global warming by releasing increasing quantities of greenhouse gas emissions (containing carbon, sulfur and other atmospheric pollutants). In addition, extraction of large quantities of coal, natural gas, and crude oil are leading to faster depletion of the finite reserves of fossil fuels. The depletion of fossil fuels is likely to result in price fluctuations, uncertainties in the energy supply chain, and social upheaval from possible job losses. In order to secure the energy future and protect the environment, the U.S. is looking for renewable resources to meet the increasing demands for its transportation and electricity sectors.

#### **1.1.1. Biofuels**

Biofuels produced from various renewable biomass feedstocks has the potential to cost-effectively satisfy a portion of U.S. energy needs for the transportation sector, while at the same time safeguarding the environment, reducing dependence on fossil fuels, and providing social benefits. Biomass procurement and feedstock quality are the key cost drivers that impact the cost of bioenergy products including biofuels.

Bioethanol is one type of biofuel that is currently widely used in the transportation sector. Although the first generation bioethanol production has been commercialized around the world, it is still debatable about food or energy when the cultivated lands have been used for the production of first generation bioethanol feedstock. Recent research unfavorably evaluates the environmental impact of producing bioethanol from first generation feedstock (such as corn and sugarcane) on the water table, soil acidification, and greenhouse gas emissions.

Therefore, new generation of biomass feedstocks are being studied intensively to develop more viable bioethanol. United States Department of Agriculture (USDA) has highlighted the current and potential availability of 1.3 billion tons per year of lignocellulosic biomass for bioenergy production. The identified biomass production areas include 450 million acres of agricultural land (mostly in the Midwest) which is a quarter of the land area of the U.S., and 670 million acres of forestland (mostly in the Pacific Northwest), representing a third of the total land area of the continental United States.

Bioethanol produced from lignocellulosic feedstock show enormous potential as an economically and environmentally sustainable renewable energy source. Lignocellulosic biomass is mainly composed of cellulose, hemicellulose, and lignin. Switchgrass is one type of lignocellulosic feedstock that is suitable for cultivation on marginal land (with arid soil) without competing for cropland with other agriculture products. Switchgrass fields initially require two years to setup and are productive for a further eight years before requiring reseeding. Switchgrass is considered as one of the best second generation bioethanol feedstock due to the following economic, environmental and social benefits: 1) easy to grow; 2) low cost of production; 3) low soil nutrient requirement; 4) not consuming too much water; 5) high net energy yield per unit of cultivated land; 6) adapted to a wide range of environments including marginal soils and arid climates; 7) improved soil conservation; 8) reduction of greenhouse gas emissions; and 9) economic stimulation of underdeveloped rural areas.

Despite its enormous potential, the cultivation of switchgrass is limited to pilot scale plots in agricultural research stations and has not yet been successfully commercialized. Based on current U.S. availability, two of the most promising sources of lignocellulosic biomass for bioenergy production in general and bioethanol production in particular are: 1) crop residue – including barley straw, corn stover, sorghum stubble, and wheat straw; and 2) woody materials – including urban wood waste, logging and mill residues.

In North American, woody biomass can be procured year round while switchgrass and crop residues can only be harvested in late fall before the first killing frost. However all the available supply of crop residue is not harvestable due to the need to leave significant portion of the residue on the field to prevent soil erosion and to maintain crop yields in the subsequent growing season. Most researchers advise that the percentage of agriculture residue that can be sustainably removed be less than 30%. Although both herbaceous biomass (i.e. switchgrass and crop residues) and woody materials are classified as lignocellulosic but their chemical composition (in terms of percentages of lignin, cellulose and hemicellulose) and the expected yield of bioethanol is not similar. The type of lignocellulosic biomass feedstock (i.e. herbaceous or woody) is not the only determinant of bioethanol yield. Another important factor is the selection of the biomass-to-bioethanol conversion pathway.

Biochemical and thermochemical pathways represent the two main currently available technologies for converting lignocellulosic biomass into bioethanol. For biochemical refineries, the bioethanol yield from herbaceous biomass is greater than that from woody materials. The reverse is true for thermochemical refineries. Typical biochemical conversion technologies include separate hydrolysis and fermentation, simultaneous saccharification and fermentation, and consolidated bioprocessing. After recovery of the primary product (i.e. bioethanol), the residual solids from the refining process (i.e. lignin) are utilized in a fluidized bed combustor to produce electricity as a co-product. The thermochemical pathway typically involves gasification and pyrolysis based conversions.

Thermochemical conversion technology processes wood chips and/or densified herbaceous biomass pellets through a series of phase reactions for the production of bioethanol and other higher alcohols (like butanol and propanol) which can be used as “greener” substitute for heating oil.

### **1.1.2. Renewable electricity**

Renewable electricity is one important type of energy that can provide environmental benefits (i.e. displacement of coal-fired electricity) as well as social benefits (i.e. job creations, economic stimulation of local communities, etc.). Electricity generation consumes the largest share of the U.S. energy resources. Generation of electricity utilizes 40%, refining of liquid transportation fuels consumes 29% while the combined demand for heating/cooling utilizes 31% of the energy supply. Of the total electricity production in the U.S. in 2012, 69% was generated from fossil fuels (mainly coal, natural gas, and other petroleum products), 20% from nuclear power, and 11% was produced from renewables (including wind, solar, geothermal, hydropower, and biomass). Hydropower generated the maximum share of 7% while the contribution of wind and biomass was 2% and 1.4% respectively. The share of hydropower is not expected to increase as the hydroelectric resource has plateaued out with most of the promising large-scale hydropower sites in the U.S. already being tapped for electricity generation. Wind and biomass represent the two highest potential resources currently available for electricity generation in the United States.

Wind energy is one of the highest potential renewable resources currently available for electricity generation in the United States. The estimated onshore wind energy has the annual potential to generate 5 million GWh of electricity. In the U.S. wind power was used to generate 90000 GWh of electricity in 2012, representing 23% of generation from renewables. Even though wind generated electricity currently makes up only 2% of total U.S. electricity generation, wind power has grown at a 25% annual rate (from 2001 to 2010) and represents 35% of all new generating capacity. Onshore wind technology is generally considered to be commercially available in the U.S.



Biofuels are not the only bioenergy product that can be obtained from biomass. In 2012 an estimated 63000 GWh of electricity was generated in the U.S. using biomass as energy feedstock, which represents 16% of generation from renewables. Combustion technologies used to convert biomass to electricity are generally considered commercial. Currently, biomass is the only renewable source that can be used to generate both electricity and produce liquid transportation fuels, as such accurate estimates for bioelectricity generation potential in the United States are difficult to obtain but are estimated to be around 1.4 million GWh.

## **1.2. Research motivation**

In 2012, biofuels (i.e. bioethanol and biodiesel) produced from various biomass renewables was used to meet 7% of the annual U.S. requirement of liquid transportation fuels (i.e. gasoline and diesel). By 2022 the Renewable Fuel Standard (RFS) requires the use of biomass renewables to produce 36 billion gallons per year (BGPY) of biofuels out of which only 15 BGPY can be bioethanol refined from corn starch. Out of the remaining 21 BGPY, a minimum of 16 BGPY is to be bioethanol refined from lignocellulosic feedstocks.

The large-scale use of gasoline and diesel in the transportation sectors has an adverse impact on the environment. The combustion of fossil-fuels releases huge quantities of carbon and other pollutants into the atmosphere. GHG emissions are considered a major contributing cause of global warming. Reduction in carbon emissions (e.g. due to gasoline being substituted by bioethanol) is a major component of the RFS requirements of cellulosic based biofuels. By 2022, the RFS mandates that lignocellulosic-based bioethanol displace 20% of annual gasoline demand on an energy equivalent basis and also achieve a 30% net reduction (on 2005 levels) in emissions from the transportation sector.

Unlike liquid transportation fuels, there is no federal mandate that requires a minimum percentage of electricity to be generated from renewables. However, varying level of mandated support is provided by individual states. As of 2012, twenty eight states have enacted binding renewable

portfolio standards (RPS) that require power utilities to generate a minimum percentage of electricity from renewable resources. With the support provided by the various state level RPSs, projections indicate that renewables can contribute up to 20% of total U.S. electricity generation by 2030.

Design and optimization of sustainable renewable energy supply chains (RESCs) is essential in order to account for government mandates, provide financial viability, reduce environmental damage, and increase social benefits for local communities. Research is needed in two distinct types of RESCs, namely: 1) biomass-to-biofuel; and 2) renewable energy-to-electricity. RESC is a complex system which consists of multiple and jointly occurring uncertainties which include: 1) crop yield and purchase price of biomass feedstock; 2) technological efficiency of converting biomass feedstock into biofuels and/or bioelectricity; 3) wind speeds which impact the power output of wind turbines; 4) sale price and demand of biofuels and electricity; and 5) government incentives for renewable energy products.

The multiple uncertainties if not jointly considered in the decision making process result in non-optimal (or even infeasible) solutions which generate lower profits, increased environmental pollution, and reduced social benefits. This research incorporates multiple uncertainties into the decision making process in order to make optimal decisions such as: 1) site selection and allocation of land for biomass cultivation; 2) biomass harvest and storage methods; 3) amount of biomass feedstock to be procured, stored and processed into biofuels and/or bioelectricity; 4) installation site selection and capacity of bioethanol refineries, biopower plants, and wind turbines; 5) selection of biomass-to-biofuel conversion pathway; 6) portfolio of biomass resources allocated for electricity generation; 7) grid connectivity of renewable electricity generators and the transmission capacity of power lines; and 8) amount and types of renewable energy products to be produced.

Multi-period planning of RESC infrastructure development (i.e. land allocated for biomass cultivation, biorefineries, renewable electricity generators, etc.) is also studied to minimize investment risk by considering the temporal variation in demand for renewable energy products. Optimal strategic

and tactical decisions are therefore implemented to mitigate the effect of spatial and temporal uncertainties in the RESC setting.

Additionally, many models that have been developed only optimize the financial performance of the RESC and disregard other performance criterion. This research provides a framework that simultaneously improves economic, environmental, and social aspects of sustainability. It provides insights about the supply chain decisions that need to be taken under different governmental policies and incentives. In addition, it allows policy makers to develop policies that are feasible and would encourage renewable energy production. Overall, the research outcomes will help U.S. renewable energy industries (especially in the Midwest) to optimally utilize the currently and potentially available wind and biomass resources to sustainably operate in an efficient (and cost effective) manner, boost the regional economy, and protect the environment.

### **1.3. Research contribution and structure**

Research is needed to develop robust RESCs that can sustainably deliver competitive renewable energy products (i.e. bioethanol and/or electricity) to the end-market. The contribution and structure of this research effort is as follows:

Chapter 2 proposes a mixed integer linear programming (MILP) model that minimizes the cost (by optimizing the various logistics aspects) and demonstrates the sustainability of a lignocellulosic-based bioethanol supply chain (LBSC) that uses switchgrass as biomass feedstock. The proposed model considers the impact of switchgrass crop yield, biomass densification, switchgrass dry-matter loss during storage, and economies of scale in biorefinery capacities on the total LBSC cost. Decision variables include switchgrass cultivation site selection and marginal land allocation, biomass inventory level, location of biomass preprocessing facilities, location and capacity of biorefineries, volume of bioethanol produced by biorefineries, and volume of bioethanol shipped to biofuel demand zones.

The research problem in Chapter 2 assumes that the input parameters (i.e. switchgrass yield, bioethanol demand, etc.) are deterministic. However, decisions based on deterministic assumptions will result in non-optimal solutions if uncertainties exist. Therefore there is a need to incorporate the impact of the uncertainties in the LBSC, and propose optimal hedging strategies, such as the use of multiple types of lignocellulosic feedstock in addition to switchgrass to reduce the impact of the disruptions in the supply of biomass feedstock.

Chapter 3 proposes a two-stage stochastic MILP formulation to maximize the expected profit of an integrated LBSC (that uses switchgrass and crop residue as biomass feedstock) under multiple uncertainties in switchgrass supply, crop residue purchase price, bioethanol demand and selling price uncertainties. To maximize the expected profit, the following logistics decisions are optimized: 1) allocation of available marginal land in biomass supply zones for switchgrass cultivation; 2) amount of crop residues to be purchased from biomass supply zones; 3) material flow of biomass feedstock (switchgrass and crop residue) from biomass supply zones to the biorefineries; 5) site selection from potential locations for installation of biorefineries; 6) volume of bioethanol to be produced by the biorefineries; and 7) material flow of bioethanol from the biorefineries to the biofuel demand zones.

The research problem in Chapter 3 considers profit maximization of a LBSC as the sole objective. Economic decision models that are developed without considering other needs of a society (such as environmental) do not show the practical relevance. Biofuel supply chain models that integrate sustainability provide for better decision making and will forecast realistic profits or costs. This will help in better co-ordination for the activities in the entire supply chain. An economic model which promotes environmental needs is crucial for economic and sustainable growth.

Chapter 4 proposes a two-stage stochastic MILP formulation to maximize the expected profit of an integrated LBSC (that uses crop residue and woody material as biomass feedstock) while simultaneously minimizing carbon emissions. Environmental impact is monetized through carbon

credits and directly incorporated into the objective function. Multiple uncertainties in supply/demand and prices are considered jointly. Key decision variables determines the location, choice of conversion technology (i.e. biochemical vs. thermochemical), and biomass processing capacity of biorefineries. Strategies for optimizing the performance of the LBSC are solved simultaneously within the integrated system by using the Sample Average Approximation (SAA) method.

In Chapter 5, a mathematical model that integrates long-term strategic decisions (across all the planning periods) and short-term operational decisions (for each planning period) is developed to optimize the LBSC performance over multiple criteria (including economic, environmental and social impacts) under uncertainties in biomass supply and purchase price, bioethanol demand and sales price. The research effort so far (Chapters 2–4) has assumed that the infrastructure (i.e. amount of land used for biomass cultivation, production capacities of biorefineries, etc.) needed to produce the target volume of biofuels is built in one go. However the Renewable Fuel Standard (RFS) allows for multi-period planning of biorefinery installation with different production levels for each year from 2013 till 2022. Although the environmental impact has been incorporated (see Chapter 4), the social impact has not been addressed. The proposed stochastic model is solved by using a sequential application of a modified SAA method and Benders decomposition.

In Chapter 6, the grid design and optimal allocation of wind and biomass resources for renewable electricity supply chains in the U.S. is studied. Due to wind intermittency, the generation and supply of wind electricity is not uniform and cannot be counted on to be readily available to meet the electricity demand. On the other hand, biomass resource represents a type of “stored” energy and is the only renewable resource that can be used for producing both liquid transportation fuels and generating electricity whenever required. However, amount of biomass resources are finite and might not be sufficient to meet demand for both electricity and biofuels in the U.S. due to the production mandates of the federal Renewable Fuel Standard. Therefore the role of wind and biomass resources is jointly

analyzed for renewable electricity generation. Policies are proposed and evaluated for the optimal allocation of finite biomass resources for electricity generation. A two-stage stochastic MILP model is proposed that optimally balances the electricity demand across the available supply from wind and biomass resources. Results from the proposed model are used to design an optimal grid infrastructure (from power production to transmission) that integrates electricity generated from multiple renewable resources into the power grid under uncertainties in wind speed and electricity sale price. A case study set in the American Midwest is presented to demonstrate the effectiveness of the proposed stochastic model by determining the optimal logistic and supply chain decisions for generation and transmission of renewable electricity. Sensitivity analysis is conducted to study the impact of subsidy level for renewable electricity production on the expected supply chain profit.

## CHAPTER 2. AN INTEGRATED OPTIMIZATION MODEL FOR SWITCHGRASS-BASED BIOETHANOL SUPPLY CHAIN

### **2.1. Abstract**

Bioethanol produced from lignocellulosic feedstock show enormous potential as an economically and environmentally sustainable renewable energy source. Switchgrass (*panicum virgatum*) is considered as one of the best second generation feedstock for bioethanol production. In order to commercialize the production of switchgrass-based bioethanol, it is essential to design an efficient switchgrass-based bioethanol supply chain (SBSC) and effectively manage the logistics operation. This paper proposes an integrated mathematical model to determine the optimal comprehensive supply chain/logistics decisions to minimize the total SBSC cost by considering existing constraints. A case study based on North Dakota state (ND) in the United States illustrates the application of the proposed model. The results demonstrate that by using only 61% of the available marginal land for production of switchgrass feedstock, 100% of the annual gasoline energy equivalent requirement of ND can be economically met from the produced bioethanol. Sensitivity analysis is conducted to provide insights for efficiently managing the entire SBSC and minimizing the cost.

### **2.2. Introduction and literature review**

Due to the energy crisis, environmental and social issues, researchers have been attracted to develop sources of renewable energies to secure the energy consumption, protect the environment, and to promote regional development. Biofuel is one type of the renewable energies that can be used in multiple ways to substitute fossil-fuel based energy. Bioethanol is one type of biofuel that is currently widely used in transportation section [1]. Although the first generation bioethanol production has been commercialized around the world, it is still debatable about food or energy when the cultivated lands have been used for the production of first generation bioethanol feedstock. A study by Carriquiry et al.

[2] unfavorably evaluates the environmental impact of producing first generation bioethanol feedstock (such as corn and sugarcane) on the water table, soil acidification, and greenhouse gas emissions.

Therefore, new generation of lignocellulosic biomass feedstocks are being studied intensively to develop more viable bioethanol. Lignocellulosic biomass is mainly composed of cellulose, hemicellulose, and lignin [3]. Switchgrass is one type of lignocellulosic feedstock that is suitable for cultivation on marginal land (with arid soil) without competing for cropland with other agriculture products [4]. It is considered as one of the best second generation bioethanol feedstock due to the following economic, environmental and social benefits: 1) easy to grow; 2) low cost of production; 3) low soil nutrient requirement; 4) not consuming too much water; 5) high net energy yield per unit of cultivated land; 6) adapted to a wide range of environments including marginal soils and arid climates; 7) improved soil conservation; 8) reduction of greenhouse gas (GHG) emissions; and 9) economic stimulation of underdeveloped rural areas [5].

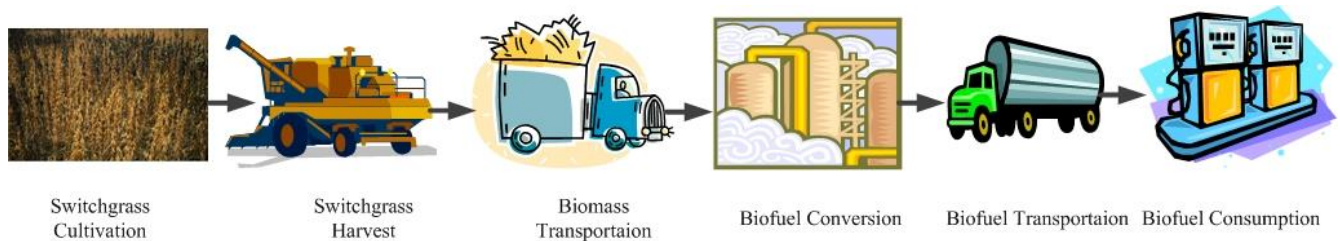


**Fig. 1. Major logistics activities in a switchgrass-based bioethanol supply chain (SBSC)**

The major logistics activities in a switchgrass-based bioethanol supply chain (SBSC) are shown in Fig. 1. They include switchgrass cultivation, harvesting, storage, biomass transportation, bioethanol conversion, bioethanol transportation, and bioethanol consumption. Many decisions in SBSC involve tradeoffs. For example, determining the locations of switchgrass cultivation sites, preprocessing facilities and biorefineries should consider the following tradeoffs. Locating the biorefineries close to bioethanol demand points will reduce the transportation cost of bioethanol, but might increase the switchgrass biomass transportation cost if the biorefineries are far away from the switchgrass cultivation sites. Due to the complex tradeoffs involved, various competing supply chain and logistics



decisions that affect the SBSC cannot be made independently. Therefore, comprehensive management and optimization of all the individual logistical components along the entire supply chain is essential to minimize the total cost or maximize the total profit [6].

Literature review has shown that considerable research has been done on developing models for optimizing various logistical configurations of biomass-based supply chains [7, 8]. Some of the recent and relevant models dealing with the optimization of lignocellulosic biomass-based bioethanol supply chains are reviewed here. Unless otherwise stated, the reviewed models consider switchgrass as a source of lignocellulosic biomass feedstock, and have a one year time horizon.

Eksioglu et al. [9] and Dunnett et al. [10] consider crop residue as the source of lignocellulosic biomass. The models also consider the impact of biomass crop yield, biomass densification, biomass dry-matter loss during storage, and economies of scale in biorefinery capacities on the total supply chain cost. Decision variables include biomass cultivation site selection and land allocation, location and capacity of preprocessing facilities, location and capacity of biorefineries. Zhu et al. [11], Giorola et al. [12], You et al. [13], and An et al. [14] consider the impact of switchgrass crop yield, switchgrass densification, switchgrass dry-matter loss during storage, and economies of scale in biorefinery capacities on the total SBSC cost. Decision variables include switchgrass cultivation site selection and land allocation, location and capacity of preprocessing facilities, location and capacity of biorefineries. The model by Zhu et al. [11] does not consider the impact of bioethanol transportation cost on the total SBSC cost. The model by Giorola et al. [12] has a time horizon of 20 years. The model by An et al [14] considers the use of marginal land for switchgrass cultivation. Marvin et al. [15] and Judd et al. [16] consider the impact of biomass crop yield, harvest method (round bales), biomass dry-matter loss during storage, and economies of scale in biorefinery capacities on the total SBSC cost. Decision variables include land allocation for biomass cultivation, location and capacity of biorefineries. The

model by Marvin et al. [15] considers crop residue as the source of lignocellulosic biomass. The model by Judd et al. [16] does not consider the amount of biofuel produced as a decision variable.

Based on the commonly identified and relevant logistics aspects from the reviewed models, this paper proposes a MILP model that will minimize the entire SBSC cost (by optimizing the various individual logistics aspects of the SBSC) and demonstrate the sustainability. The proposed model will consider the impact of switchgrass crop yield, switchgrass densification, switchgrass dry-matter loss during storage, and economies of scale in biorefinery capacities on the total SBSC cost. Decision variables include switchgrass cultivation site selection and marginal land allocation, switchgrass biomass inventory level, location of preprocessing facilities, location and capacity of biorefineries, volume of bioethanol produced by each biorefinery, and the volume of bioethanol shipped to each biofuel demand zone.

In addition, the proposed MILP model is differentiated (from other efforts in this field) by uniquely contributing to the state-of-the-art by incorporating the following specific characteristics:

- The proposed model exclusively considers marginal land for switchgrass cultivation (while the model by An et al. [14] considers marginal land only as a supplement to cropland). By limiting the potential switchgrass cultivation areas to only marginal lands (i.e. land not suitable for use as cropland or pastureland), competition for land with food grains for human and animal consumption is avoided.
- None of the reviewed literature contains an MILP model that deals with the impact of multiple switchgrass harvest methods on the total SBSC cost. The proposed model considers three different harvest methods (namely round bales, square bales, and loose chop) [17]. Round bale or square bale harvesting method is cheaper in term of cost compared to loose chop method. Round or square bales can be directly used as feedstock for biorefineries, while switchgrass harvested as loose chop needs to be further densified at a preprocessing facility before it can be

used as feedstock. Switchgrass harvested as traditional bales can be stored at the harvest site under tarp storage systems. Harvested round bales and square bales suffer from moderate and high storage losses respectively. Due to biomass degradation of stored square and round bales, more biomass will be required to produce same amount of bioethanol (increasing the production cost) when compared to loose chop (that has been densified). Preprocessing of loose chop has an additional cost component but eliminates dry-matter storage loss and increases biomass density [18]. Due to volumetric restrictions, a standard 23.6 tonne capacity truck can accommodate 8.2 tonne, 11.8 tonne, 14.5 tonne, and 23.6 tonne respectively of loose chop, round bales, square bales, and densified bales of switchgrass [17]. The transportation cost of densified loose chop is significantly lower than that of traditional switchgrass bales [17].

- The spatial nature of rainfall distribution and its impact on switchgrass crop yields is an important determinant in the selection of cultivation sites and allocation of land for switchgrass cultivation. Switchgrass is a perennial crop (requiring two years for crop establishment and harvestable for the next eight years) which requires that cultivation land be committed for 10 years [19]. While annual crops like corn and wheat can be rotated each year at different cultivation sites with different amounts of land under cultivation.

### **2.3. Problem statement**

A list of indices, sets, parameters, and decision variables is given in the Nomenclature section. The research studies a comprehensive switchgrass-based bioethanol supply chain (SBSC) as shown in Fig. 2. Switchgrass can be cultivated in available marginal lands (not used for other agriculture purposes) located in  $i$  supply zones. Then, switchgrass can be collected by harvest method  $j$  into round bales ( $j = 1$ ), square bales ( $j = 2$ ), or loose chop ( $j = 3$ ). If using round bales or square bales method during harvesting, the biomass will be either shipped directly to the  $r$  biorefineries or stored near the  $i$  supply zones. Storage of traditional bales (round or square) will result in increasing degradation of the

biomass material during each time period  $t$ . When using loose chop harvest method, the biomass will be shipped by silage truck to the  $k$  preprocessing facilities for densification and storage. When required, the stored densified bales are transported from the  $k$  preprocessing facilities to the  $r$  biorefineries. The biomass is converted into bioethanol in biorefineries. Finally, bioethanol is transported from the  $r$  biorefineries to  $e$  demand zones.

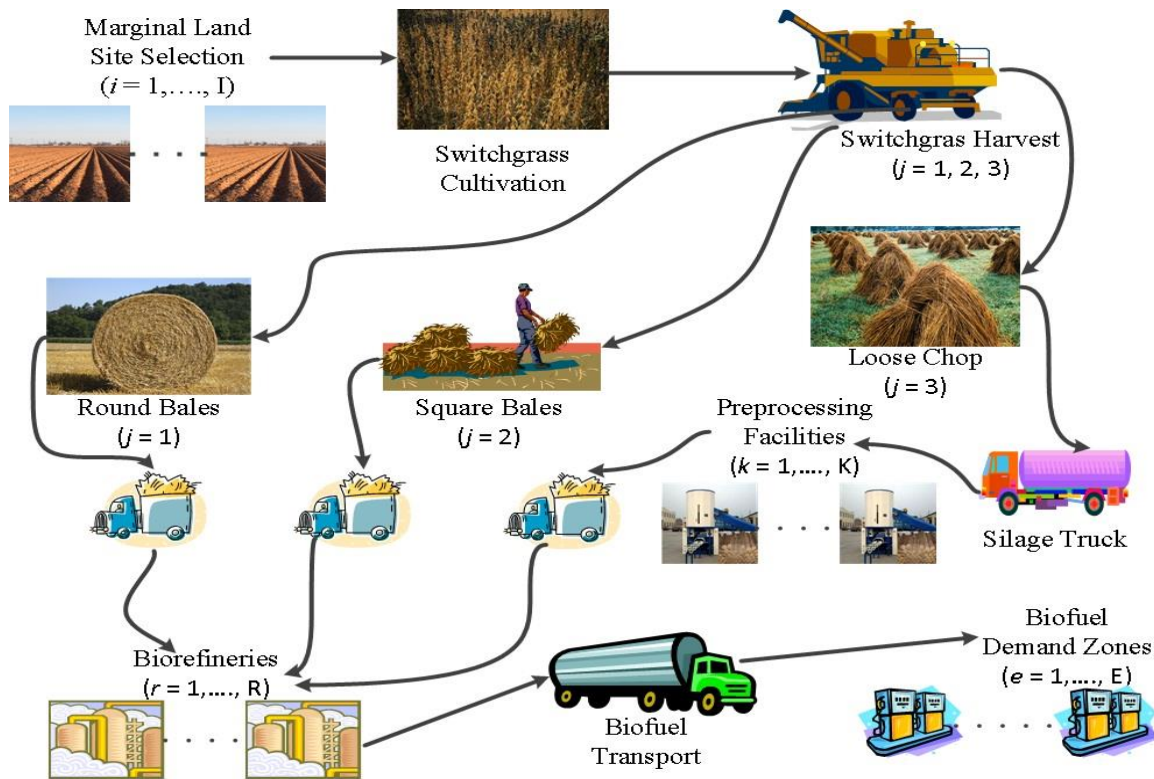


**Fig. 2. Switchgrass-based bioethanol supply chain**

In order to minimize the total SBSC cost, the following supply chain/logistics decisions are optimized in the proposed MILP model: 1) selection of  $i$  cultivation sites and allocation of available marginal land for switchgrass production; 2) selection of switchgrass harvest method  $j$ ; 3) inventory level of harvested switchgrass during time period  $t$ ; 4) site selection for location of  $k$  preprocessing facilities; 5) material flow of loose chop switchgrass from  $i$  supply zones to  $k$  preprocessing facilities; 6) site selection for location of  $r$  biorefineries; 7) capacity level  $q$  for selected  $r$  biorefineries; 8) material flow of switchgrass biomass from  $i$  supply zones (and  $k$  processing facilities) to  $r$

biorefineries; 9) bioethanol production volume of  $r$  biorefineries during time period  $t$ ; 10) material flow of bioethanol from  $r$  biorefineries to  $e$  biofuel demand zones during time period  $t$ .

## 2.4. Assumptions

The various assumptions used in the proposed MILP model are explained below.

- Switchgrass harvest frequency of once a year (after the first killing frost) is used in this model. Research indicates that the timing and frequency of switchgrass harvest are important factors that affect crop yield and harvest cost. Studies by McLaughlin et al. [19], Mulkey et al. [20], Lee et al. [21], and Lewandowski et al. [22] show that harvesting switchgrass once a year after the first killing frost is the most economical and environmentally friendly harvest frequency for biomass production in North America in general and the colder Northern Great Plains region of the United States in particular.
- Since the road haulage (using trucks and tankers) is available in all the area, this research will only consider the road haulage for the transportation of biomass and bioethanol. Different transportation modes will impact the total logistics cost as well. However, it is easy to expand the model to consider different transportation modes. Studies by Mahmudi et al. [23] and Eksioglu et al. [9] compare different transportation modes of delivering switchgrass biomass from farms to the biorefineries (e.g. barge, truck, rail, etc.) and conclude that road transportation using trucks is the most cost effective transportation mode when the travel distance is less than 400 km. Total cost increases linearly with hauling distance, and decreases as truck capacity increases. The National Research Council [24] compares different transportation modes of delivering refined bioethanol from biorefineries to customers (e.g. pipeline, tanker, rail, etc.) and concludes that road transportation using tankers is the most cost effective transportation mode when the travel distance is less than 800 km.

- The per capita bioethanol requirement in each demand zone is assumed to be known. The total bioethanol requirement is assumed to be proportional to the population in each demand zone.

## 2.5. Model formulation

A mixed integer linear programming (MILP) model is proposed to minimize the total switchgrass-based bioethanol supply chain (SBSC) cost by determining the optimal level of the various supply chain logistics decision variables. The formulation (objective function and constraints) of the proposed model are explained in the following sections.

### 2.5.1. Objective function

The objective of the proposed model is to minimize the total annualized SBSC cost. The total SBSC cost includes marginal land rental cost, switchgrass cultivation cost, switchgrass harvest cost, switchgrass storage cost at supply zone, loose chop transportation cost from supply zone to preprocessing facility, densified switchgrass transportation cost from preprocessing facility to biorefinery, preprocessing cost of loose chop, operational cost of biorefinery, traditional bales transportation cost from supply zone to biorefinery, bioethanol transportation cost from biorefinery to bioethanol demand zone, annualized fixed cost of preprocessing facilities and biorefineries. The different cost components of the objective function are explained below.

Eq. 2.1 refers to the marginal land rental cost for all  $i$  supply zones, and is the sum-product of  $C_i$  (rental cost parameter) and  $X_{ij}$  (marginal land area in supply zone  $i$  harvested by method  $j$ ). For each supply zone,  $C_i$  significantly impacts on the cultivation site selection. The rental cost of marginal land, location of cultivation site, and switchgrass yield are heavily dependent on each other. Land located in areas having higher switchgrass yields generally has higher rental cost. However, yield is not the only determinant for high land rent cost. Land located in areas near transportation networks (e.g. highways, railroad stations, and sea/river ports) tend to have higher rental cost due to the comparatively lower cost to transport the switchgrass to the biorefineries. Tradeoff between these factors is necessary to

optimally select one or more of the potential cultivation sites and allocate the optimal amount from the available marginal land in each cultivation site.

$$\sum_{i=1}^I \sum_{j=1}^{J=3} C_i X_{ij} \quad (2.1)$$

Eq. 2.2 refers to the switchgrass cultivation cost for all  $i$  supply zones, and is the sum-product of  $P_i$  (cultivation cost parameter) and  $X_{ij}$  (marginal land area in supply zone  $i$  harvested by method  $j$ ). Cultivation cost includes the cost of seeds, tilling, and fertilizer.  $P_i$  (\$/hectare) is not dependent on the switchgrass harvest method.

$$\sum_{i=1}^I \sum_{j=1}^{J=3} P_i X_{ij} \quad (2.2)$$

Eq. 2.3 refers to the switchgrass harvest cost for all  $i$  supply zones, and is the sum-product of  $H_j$  (cost parameter for harvest method  $j$ ) and  $X_{ij}$  (marginal land area in supply zone  $i$  harvested by method  $j$ ). Apart from the harvesting cost, the choice of harvest method also has a big impact on the switchgrass storage cost, and the cost of transporting the switchgrass biomass to the biorefineries. Tradeoffs between biomass harvest cost (Eq. 2.3), biomass storage cost (Eq. 2.4), and biomass transportation cost (Eqs. 2.5, 2.9) are considered to select the optimal switchgrass harvest method for each cultivation site.

$$\sum_{i=1}^I \sum_{j=1}^{J=3} H_j X_{ij} \quad (2.3)$$

Eq. 2.4 refers to the storage cost of traditional bales (round or square) of switchgrass at all  $i$  supply zones, and is the sum-product of  $\zeta_j$  (storage cost parameter for harvest method  $j \neq 3$ ) and  $S_{ij}^t$  (switchgrass amount stored at supply zone  $i$  by harvest method  $j \neq 3$  during time period  $t$ ). The tradeoffs in harvest costs, biomass storage costs, and dry matter losses during storage (for traditional bales) are considered in determining the optimal multi period inventory levels of the switchgrass bales. The storage cost for switchgrass harvested as loose chop ( $j = 3$ ) is considered in Eq. 2.7.

$$\sum_{i=1}^I \sum_{j=1}^{J=2} \sum_{t=1}^T \xi_j S_{ij}^t \quad (2.4)$$

Eq. 2.5 refers to loose chop transportation cost from all  $i$  supply zones to all  $k$  preprocessing facilities, and is the sum-product of  $\alpha_{ik}$  (loose chop transportation cost parameter from  $i$  to  $k$ ),  $D_{ik}$  (distance between supply zone  $i$  and preprocessing facility  $k$ ), and  $V_{ik}$  (amount of loose chop switchgrass sent from supply zone  $i$  to preprocessing facility  $k$ ).

$$\sum_{i=1}^I \sum_{k=1}^K \alpha_{ik} D_{ik} V_{ik} \quad (2.5)$$

Eq. 2.6 refers to densified bales transportation cost from all  $k$  preprocessing facilities to all  $r$  biorefineries, and is the sum-product of  $\gamma_{kr}$  (densified bales transportation cost parameter from  $k$  to  $r$ ),  $D_{kr}$  (distance between preprocessing facility  $k$  and biorefinery  $r$ ), and  $V_{kr}^t$  (densified bales amount sent from preprocessing facility  $k$  to biorefinery  $r$  during time period  $t$ ).

$$\sum_{k=1}^K \sum_{r=1}^R \sum_{t=1}^T \gamma_{kr} D_{kr} V_{kr}^t \quad (2.6)$$

For Eq. 2.5 and Eq. 2.6, preprocessing facilities need to be optimally located such that the transportation cost of both the loose chop (from the switchgrass supply zones to the preprocessing facilities) and densified bales (from preprocessing facilities to biorefineries) is minimized. In this research, the model will select the optimal location of preprocessing facilities (from predetermined candidate sites) in order to minimize the overall SBSC cost.

Eq. 2.7 refers to the preprocessing cost of loose chop switchgrass, and is the sum-product of  $U_k$  (preprocessing cost parameter of facility  $k$ ) and  $V_{ik}$  (amount of loose chop switchgrass sent from supply zone  $i$  to preprocessing facility  $k$ ). Preprocessing cost parameter  $U_k$  (\$/tonne) includes storage cost of loose chop switchgrass and densified bales.

$$\sum_{i=1}^I \sum_{k=1}^K U_k V_{ik} \quad (2.7)$$



Eq. 2.8 refers to the biorefinery operational cost, and is the sum-product of  $N_r$  (bioethanol production cost parameter for refinery  $r$ ) and  $Z_r^t$  (volume of bioethanol produced by biorefinery in location  $r$  during time period  $t$ ). Bioethanol refining cost parameter  $N_r$  (\$/liter) is not dependent on the capacity of the biorefinery.

$$\sum_{r=1}^R \sum_{t=1}^T N_r Z_r^t \quad (2.8)$$

Eq. 2.9 refers to traditional switchgrass bales ( $j \neq 3$ ) transportation cost from all  $i$  supply zones to all  $r$  biorefineries, and is the sum-product of  $F_{jir}$  (traditional bales transportation cost parameter from  $i$  to  $r$ ),  $D_{ir}$  (distance between supply zone  $i$  and biorefinery  $r$ ), and  $V_{ijr}^t$  (amount of traditional bales from supply zone  $i$  sent to biorefinery  $r$  during time period  $t$ ).

$$\sum_{i=1}^I \sum_{j=1}^{J=2} \sum_{r=1}^R \sum_{t=1}^T F_{jir} D_{ir} V_{ijr}^t \quad (2.9)$$

Eq. 2.10 refers to bioethanol transportation cost from all  $r$  biorefineries to all  $e$  demand zones, and is the sum-product of  $\psi_{re}$  (bioethanol transportation cost parameter from  $r$  to  $e$ ),  $D_{re}$  (distance between biorefinery  $r$  and demand zone  $e$ ), and  $Z_{re}^t$  (volume of bioethanol sent from biorefinery in location  $r$  to demand zone  $e$  during time period  $t$ ).

$$\sum_{e=1}^E \sum_{r=1}^R \sum_{t=1}^T \psi_{re} D_{re} Z_{re}^t \quad (2.10)$$

For Eqs. 2.6, 2.9, 2.10, tradeoff between the higher transportation cost of the lower density switchgrass biomass and the lower transportation cost of the higher density bioethanol is needed to optimally locate the biorefineries in order to minimize the cost of transporting switchgrass biomass (from supply zones and/or preprocessing facilities) to biorefineries along with the cost of transporting the refined bioethanol to the demand zones [25]. In this research, the model will select the optimal location of biorefineries (from predetermined candidate sites) in order to minimize the SBSC cost.

Eq. 2.11 refers to the fixed cost of preprocessing facilities, and is the sum-product of  $W_k$  (annualized fixed cost parameter of facility  $k$ ) and  $Y_k$  (number of preprocessing facilities in all  $k$  locations). In this research, the model will select the optimal number of preprocessing facilities, each with a discrete annual densification capacity [26].

$$\sum_{k=1}^K W_k Y_k \quad (2.11)$$

Eq. 2.12 refers to the fixed cost of biorefineries, and is the sum-product of  $G_{rq}$  (annualized biorefinery fixed cost parameter for capacity level  $q$  at location  $r$ ) and  $Y_{rq}$  (number of biorefineries with capacity level  $q$  in all  $r$  locations). Fixed cost of biorefineries is a major component of the total SBSC cost. Tradeoff between the lower fixed cost (but higher per liter cost) of a smaller capacity biorefinery with the higher fixed cost (but lower per liter cost) of a larger capacity biorefinery are needed to select the optimal biorefinery capacity. In this research, discrete biorefinery capacity levels will be considered [27] and the model will determine the optimal capacity level for each selected biorefinery.

$$\sum_{r=1}^R \sum_{q=1}^Q G_{rq} Y_{rq} \quad (2.12)$$

Considering all the cost elements, the following objective cost function  $\theta$  is obtained (which has to be minimized):

$$\begin{aligned} \theta = & \sum_{i=1}^I \sum_{j=1}^{J=3} C_i X_{ij} + \sum_{i=1}^I \sum_{j=1}^{J=3} P_i X_{ij} + \sum_{i=1}^I \sum_{j=1}^{J=3} H_j X_{ij} + \sum_{i=1}^I \sum_{j=1}^{J=2} \sum_{t=1}^T \xi_j S_{ij}^t + \sum_{i=1}^I \sum_{k=1}^K \alpha_{ik} D_{ik} V_{ik} + \sum_{k=1}^K \sum_{r=1}^R \sum_{t=1}^T \gamma_{kr} D_{kr} V_{kr}^t + \\ & \sum_{i=1}^I \sum_{k=1}^K U_k V_{ik} + \sum_{r=1}^R \sum_{t=1}^T N_r Z_r^t + \sum_{i=1}^I \sum_{j=1}^{J=2} \sum_{r=1}^R \sum_{t=1}^T F_{jir} D_{ir} V_{ijr}^t + \sum_{e=1}^E \sum_{r=1}^R \sum_{t=1}^T \psi_{re} D_{re} Z_{re}^t + \sum_{k=1}^K W_k Y_k + \sum_{r=1}^R \sum_{q=1}^Q G_{rq} Y_{rq} \end{aligned} \quad (2.13)$$

### 2.5.2. Capacity constraints

Eq. 2.14 ensures that in each supply zone  $i$ , the allocated marginal land for switchgrass cultivation does not exceed the marginal land availability.

$$\sum_{j=1}^J X_{ij} \leq B_i \quad \forall i \quad (2.14)$$

Eq. 2.15 ensures that the amount of loose chop (from all supply zones) assigned to a preprocessing facility is within the densification capacity constraints of preprocessing facility  $k$ .

$$\varphi_k \lambda_k Y_k \leq \sum_{i=1}^I V_{ik} \leq \lambda_k Y_k \quad \forall k \quad (2.15)$$

Eq. 2.16 ensures that a maximum of one bioethanol refinery (of all  $q$  capacity levels) is situated at each location  $r$ .

$$\sum_{q=1}^Q Y_{rq} \leq 1 \quad \forall r \quad (2.16)$$

Eq. 2.17 ensures that a biorefinery of capacity level  $q$  (if built at location  $r$ ) cannot produce more bioethanol than its capacity during each time period  $t$ . The proposed model will consider the available amount of biomass, and bioethanol demand to determine the optimal production level of biorefineries.

$$Z_r^t \leq \sum_{q=1}^Q \rho_{rq}^t Y_{rq} \quad \forall r, t \quad (2.17)$$

Eq. 2.18 ensures that during each time period  $t$ , the production capacity of all biorefineries is greater than or equal to the bioethanol requirement in all  $e$  demand zones.

$$\sum_{r=1}^R \sum_{q=1}^Q \rho_{rq}^t Y_{rq} \geq \sum_{e=1}^E M_e^t \quad \forall t \quad (2.18)$$

Eq. 2.19 ensures that the bioethanol production rate is greater than the minimum biorefinery capacity utilization rate.

$$\sum_{r=1}^R \sum_{t=1}^T Z_r^t \geq \sum_{q=1}^Q \sum_{r=1}^R \sum_{t=1}^T O_{rq} \rho_{rq}^t Y_{rq} \quad (2.19)$$

### 2.5.3. Material flow constraints

The level of annual rainfall significantly impacts on  $A_i$  (switchgrass yield in supply zone  $i$ ). Lee and Boe [28] have shown a strong linear relationship (90% correlation) between annual rainfall level and switchgrass yield in South Dakota. Similarly, Muir et al. [29] report a 97% positive correlation between annual rainfall and switchgrass yield. In the proposed model, the switchgrass yield as a linear function of the annual rainfall is modeled in Eq. 2.20 and impacts Eqs. 2.21–2.22.

$$A_i = A (\delta_i / \bar{\delta}) \quad \forall i \quad (2.20)$$

Where

$\delta_i$  average annual rainfall in switchgrass supply zone  $i$

$\bar{\delta}$  average annual rainfall at an observed cultivation site

$A$  average switchgrass yield at an observed cultivation site

Eq. 2.21 ensures that in each supply zone  $i$ , the amount of loose chop sent to all preprocessing facilities  $k$  is not greater than the amount of harvested loose chop. Switchgrass harvested as loose chop ( $j = 3$ ) from each supply zone needs to be assigned to one (or more) preprocessing facilities for densification. The proposed model will consider this constraint to determine the optimal loose chop material flow from each supply zone  $i$  to all preprocessing facilities.

$$\sum_{k=1}^K V_{ik} \leq A_i X_{ij} \quad \forall i \quad \text{and } j=3 \quad (2.21)$$

Eq. 2.22 ensures that in each supply zone  $i$ , the amount of switchgrass produced (by harvest method  $j \neq 3$ ) is equal to the annual amount of switchgrass biomass stored as round or square bales.

$$A_i \sum_{j=1}^{J=2} X_{ij} = \sum_{j=1}^{J=2} \sum_{t=1}^T S_{ij}^t \quad \forall i \quad (2.22)$$

Eq. 2.23 ensures that the amount of switchgrass from each supply zone  $i$  (by harvest method  $j \neq 3$ ) sent to all biorefineries (during each time period  $t$ ) is not more than the “usable” amount of stored traditional switchgrass bales (discounting dry-matter loss during storage). Switchgrass harvested as

traditional bales ( $j \neq 3$ ) from each supply zone  $i$  needs to be assigned to one (or more) of the bioethanol refineries.

$$\sum_{j=1}^{J=2} \sum_{r=1}^R V_{ijr}^t \leq \sum_{j=1}^{J=2} S_{ij}^t (1 - L_j^t) \quad \forall i, t \quad (2.23)$$

Eq. 2.24 ensures that for each preprocessing facility  $k$ , the amount of densified bales sent to all biorefineries (over all time periods  $t$ ) is not greater than the total amount of loose chop ( $j = 3$ ) received from all switchgrass supply zones. Densified bales produced by each preprocessing facility needs to be assigned to one (or more) biorefineries.

$$\sum_{r=1}^R \sum_{t=1}^T V_{kr}^t \leq \sum_{i=1}^I V_{ik} \quad \forall k \quad (2.24)$$

Eq. 2.25 ensures that the cumulative amount of switchgrass (from traditional bales  $j \neq 3$  plus densified bales  $j = 3$ ) received by each biorefinery  $r$  is all converted into bioethanol during each time period  $t$ . The proposed model will determine the optimal biomass material flow from all cultivation sites and all preprocessing facilities to each biorefinery.

$$Z_r^t = \sum_{i=1}^I \sum_{j=1}^{J=2} \beta_r V_{ijr}^t + \sum_{k=1}^K \beta_r V_{kr}^t \quad \forall r, t \quad (2.25)$$

Eq. 2.26 ensures that during any time period  $t$ , the volume of bioethanol (from all biorefineries) assigned to each demand zone  $e$  is not less than the biofuel requirement. Bioethanol produced from individual biorefineries needs to be assigned to one (or more) of the demand zones. The proposed model will consider this constraint to determine the optimal bioethanol flow from all biorefineries to each demand zone  $e$  during each time period  $t$ .

$$\sum_{r=1}^R Z_{re}^t \geq M_e^t \quad \forall e, t \quad (2.26)$$

## 2.6. Case study

This case study will examine a switchgrass-based bioethanol supply chain (SBSC) set in the U.S. state of North Dakota (ND). Muir et al. [29], Casler et al. [30], and Sanderson et al. [31] have evaluated switchgrass for potential as a biomass energy crop in the Northern Great Plains (NGP) of the United States, and have concluded that the environmental and soil conditions in the NGP are ideally suitable for the commercial cultivation of switchgrass. The soil and climate of ND is representative of the NGP region, and hence also ideally suited for the production of biomass feedstock from the cultivation of switchgrass. Graham et al. [32] have also identified estimated potential land area (8.1 million hectares) for switchgrass cultivation in North Dakota. According to the United States Department of Agriculture [33], in 2007, cropland accounted for 69%, pastureland 26% and marginal land 4% of the 16.2 million hectares of total farmland under cultivation in North Dakota. The case study will focus only on the marginal land which totals around 0.7 million hectares.

The MILP model will aim to demonstrate if 100% of the current annual gasoline requirement of ND (1420 MLPY) [34] can be economically and sustainably met by using switchgrass as feedstock for production of 2130 MLPY ( $= 1420 \times 1.5$ ) of bioethanol. In the case study, one liter of gasoline contains the energy equivalent of 1.5 liters of bioethanol [24].

### 2.6.1. Input parameters

The following input assumptions relevant to the case study are also made;

- Modeling horizon of 1 year. Each month of the year will be considered a time period ( $t = 1, \dots, 12$ ).
- All 53 counties of North Dakota are potential switchgrass supply ( $i = 1, \dots, 53$ ) and bioethanol demand zones ( $e = 1, \dots, 53$ ). Switchgrass production and bioethanol demand to be centered at the county “seat” (e.g. Fargo is the seat of Cass county).

- Each of the 53 counties in North Dakota has multiple cities which have basic infrastructure like access to road transportation, harvesting equipment, crop storage, farm labor, etc. This paper has short-listed candidate sites by considering only the 53 county seats (maximum of 1 candidate site in each county). County seats are potential locations for a preprocessing facility ( $k = 1, \dots, 53$ ) and biorefinery ( $r = 1, \dots, 53$ ).
- Biorefineries with capacity of 190 MLPY and 380 MLPY will be considered.
- For all time periods  $t$ , there is no seasonality effect in the demand of bioethanol.

As previously stated in section 2.5.3, the switchgrass yield is assumed to be a linear function of the annual rainfall, and modeled in Eq. 2.20. For this case study, rainfall data from North Dakota State University [35] and observed switchgrass yield from an agriculture research station in South Dakota was used ( $A = 16.3$  tonne/hectare,  $\delta = 449$  mm) [28]. Eq. 2.20 can now be used to estimate the switchgrass yield at any supply zone. For example, at supply zone  $i = 13$  (Griggs county),  $\delta_{13} = 523$  mm and  $A_{13} = 16.3(523/449) = 19.0$  tonne/hectare. The estimated switchgrass yields for the remaining supply zones, along with other input parameters used in this case study are displayed in Tables A1–A3 (Appendix A).

## 2.7. Results and sensitivity analysis

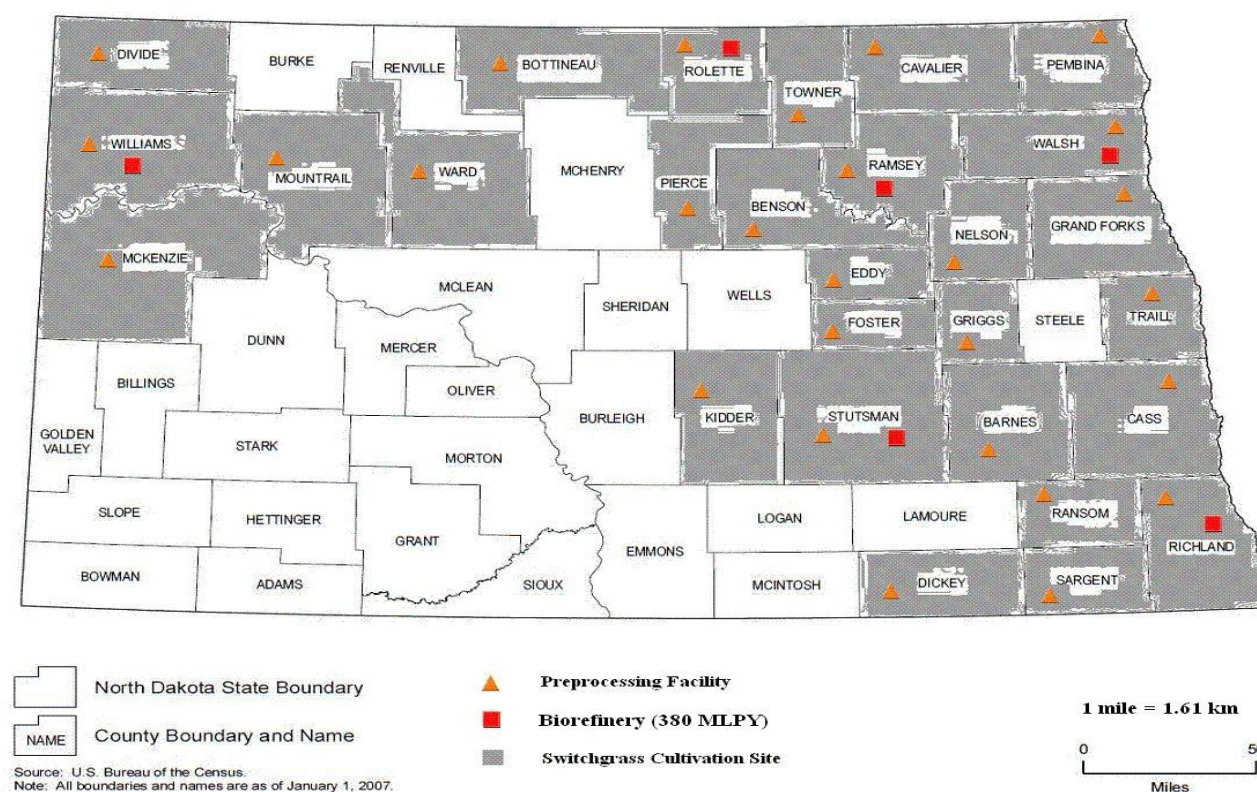
The MILP model (Eq. 2.1 to Eq. 2.26) is solved by the commercial LINGO 10.0 solver of LINDO systems. The model has 655 constraints, 76641 continuous variables, and 159 integer variables. Using an Intel 1.6 GHz processor, the global optimal solution is reached after 5.25 hours of run time (and 17 million iterations). The result shows that loose chop ( $j = 3$ ) is the optimal harvest method for all  $i$  switchgrass supply zones.

Table 1 gives the optimal assignment of biomass preprocessing facilities and bioethanol demand zones to individual biorefineries.

**Table 1. Optimal assignment of bioethanol demand zones to individual biorefineries**

County location and maximum capacity of bioethanol refinery	County location of preprocessing facilities assigned to biorefinery	County location of bioethanol demand zones assigned to biorefinery
Ramsey (380 MLPY)	Benson, Eddy, Nelson, Ramsey, Towner	Barnes, Benson, Burleigh, Dickey, Eddy, Emmons, Foster, Grand Forks, Grant, Griggs, Kidder, LaMoure, Logan, McIntosh, Morton, Mountrail, Nelson, Ramsey, Sheridan, Sioux, Steele, Towner, Wells
Richland (380 MLPY)	Cass, Ransom, Richland, Sargent, Traill	Cass, Ransom, Richland, Sargent
Rolette (380 MLPY)	Bottineau, Cavalier, Pierce, Rolette, Towner	Bottineau, Burke, Cavalier, McHenry, McLean, Mercer, Mountrail, Oliver, Pierce, Renville, Rolette, Ward
Stutsman (380 MLPY)	Barnes, Dickey, Foster, Griggs, Kidder, Stutsman	Barnes, Burleigh, Dickey, Kidder, LaMoure, Logan, McIntosh, Stutsman
Walsh (380 MLPY)	Cavalier, Grand Forks, Pembina, Traill, Walsh	Cass, Grand Forks, Pembina, Traill, Walsh
Williams (380 MLPY)	Divide, McKenzie, Mountrail, Ward, Williams	Adams, Billings, Bowman, Divide, Dunn, Golden Valley, Hettinger, McKenzie, Mountrail, Slope, Stark, Williams

Fig. 3 gives the optimum locations of switchgrass cultivation sites, biorefineries and preprocessing facilities.



**Fig. 3. Optimum location of preprocessing facilities and biorefineries in North Dakota**

The selected switchgrass cultivation sites are located in areas with high switchgrass yield and/or low marginal land rental cost. The model selects 28 preprocessing facilities, along with 6 biorefineries each with a capacity of 380 MLPY. The annualized capital cost (\$ 0.19/liter) for a 380 MLPY



biorefinery is 8.3% lower than the annualized capital cost (\$ 0.21/liter) for a 190 MLPY biorefinery [27]. Due to advantage of the lower per liter cost resulting from the economies of scale, the optimum solution preferentially selects biorefineries with capacity of 380 MLPY over biorefineries with capacity of 190 MLPY.

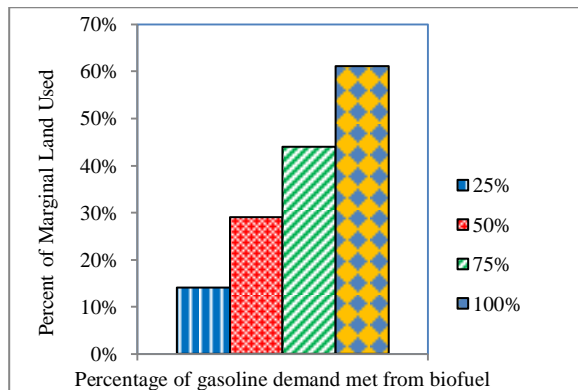
### 2.7.1. Impact of different level of bioethanol demand on the SBSC decisions

In addition to the original scenario of meeting 100% of gasoline demand through bioethanol production, the case study also investigates the effect of meeting 25%, 50%, and 75% of ND's annual demand of gasoline energy equivalent requirement through bioethanol production.

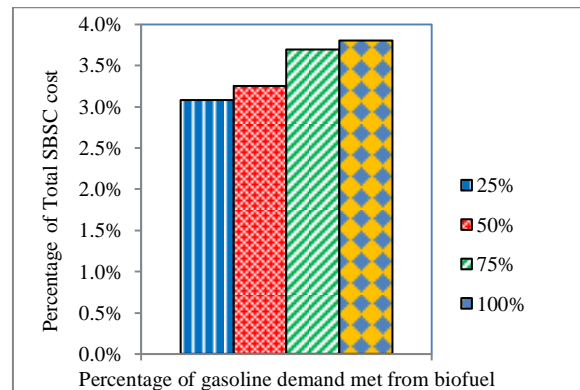
**Table 2. Percentage of gasoline demand met from cellulosic bioethanol (scenario planning)**

SBSC Logistics Decision Variables	Percentage of gasoline demand met from bioethanol			
	25%	50%	75%	100%
Annual production volume of bioethanol (million liters)	535	1,070	1,600	2,130
Production capacity of biorefineries (MLPY)	568	1,135	1,700	2,270
Number of biorefineries with 190 MLPY capacity	1	0	1	0
Number of biorefineries with 380 MLPY capacity	1	3	4	6

The results are summarized in Table 2 and displayed in Figs. 4–7.



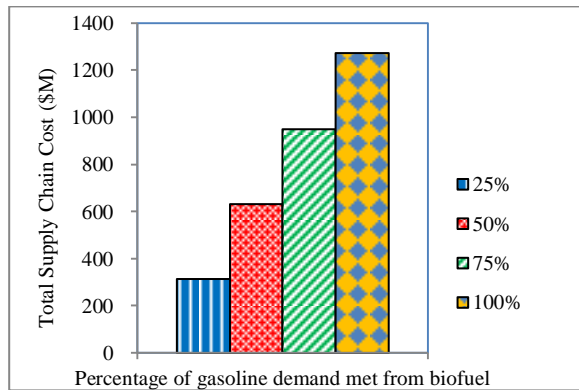
**Fig. 4. % of land used for switchgrass**



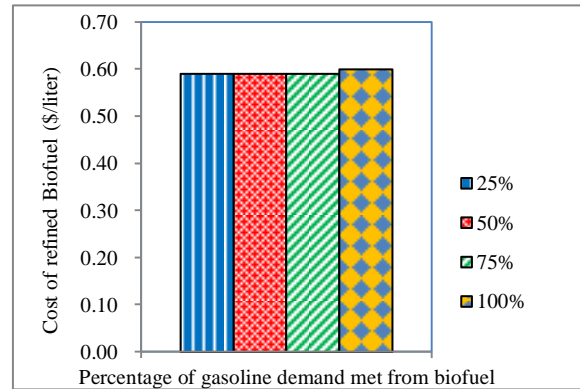
**FIG. 5. Transportation cost as % of total cost**

Fig. 4 and Fig. 6 show that the amount of marginal land used, and the total SBSC cost proportionately increases with the increase in the demand level for bioethanol. Fig. 5 indicates that transportation cost (as percentage of the total SBSC cost) varies in a narrow range between 3% and

3.8% for the varying demand levels for bioethanol. However, the refined bioethanol cost is almost constant at \$0.59/liter and is not affected by the varying demand levels as shown in Fig. 7.



**Fig. 6. Total SBSC cost**



**Fig. 7. Cost of refined bioethanol**

**2.7.2. Effect of different harvest methods on the total SBSC cost**

The impact of the other two harvest methods (round and square bales) on the total SBSC cost is also investigated. By “forcing” the solver to choose each harvest method one at a time, the solver returned the same optimal county locations for the biorefinery irrespective of the harvest method *j*.

The optimum solution for the key decision variables is displayed in Fig. 8 (Land Usage), Fig. 9 (Storage Loss), Fig. 10 (SBSC Cost), and Fig. 11 (Bioethanol Cost).

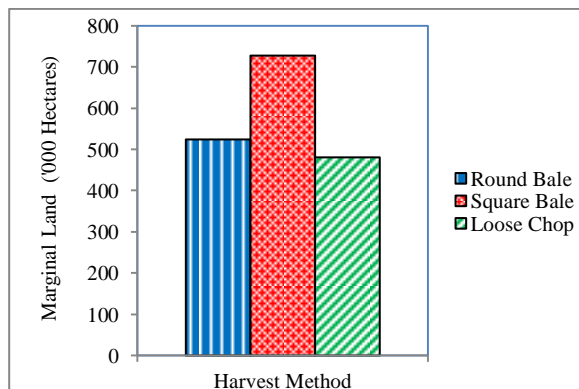


**Fig. 8. Marginal land used for switchgrass**

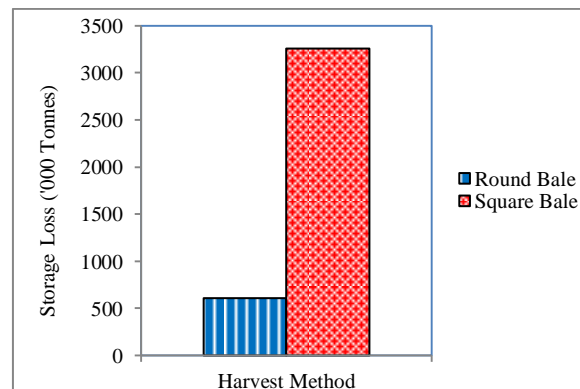


**Fig. 9. Storage losses for traditional bales**

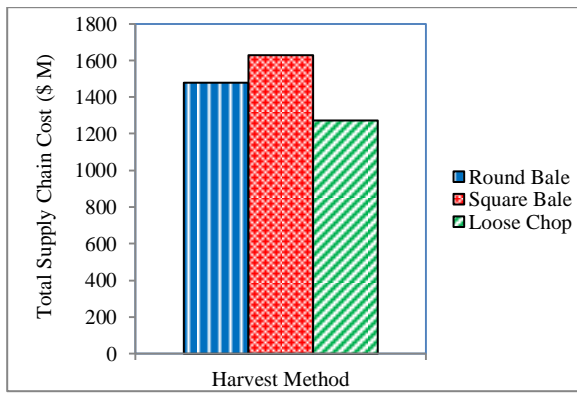


**Fig. 10. Total SBSC cost**

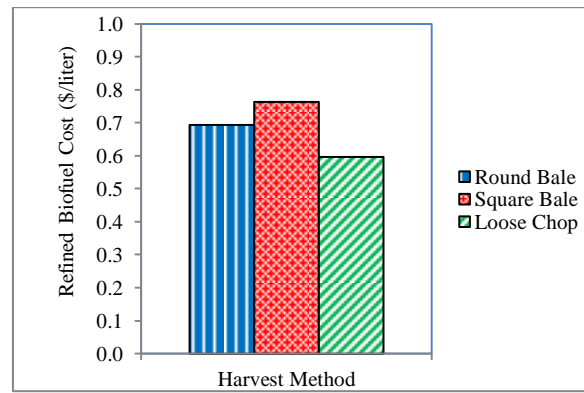


**Fig. 11. Refined bioethanol cost**

### 2.7.3. Impact of biorefinery locations on the transportation and total SBSC costs

The results shows that by using loose chop as the harvest method, the SBSC cost for producing 2130 MLPY of bioethanol is \$0.6/liter (including \$0.004/liter transportation cost of shipping refined bioethanol to the demand zones). The bioethanol cost compares very favorably with the current benchmark refinery gate cost of \$0.59/liter of bioethanol as highlighted by Brechbill et al. [27].

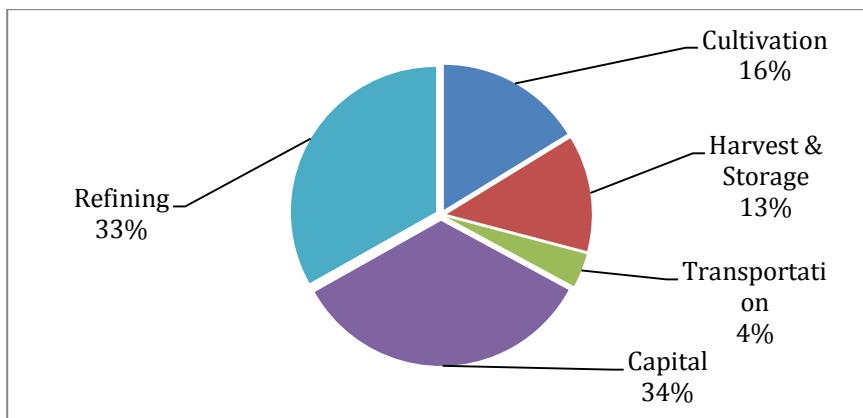


**Fig. 12. Breakdown of total annual switchgrass-based bioethanol supply chain cost**

The total SBSC cost breakdown for the optimum harvest method ( $j = 3$ ) is given in Fig. 12, and shows that transportation accounts for 4% of the total SBSC cost. However, in absolute terms the transportation cost is quite large and amounts to \$50 million. A non-optimal scenario was run, arbitrarily locating the six 380 MLPY biorefineries. The resulting total SBSC cost amounted to \$1491 million while transportation cost was \$250 million (16% of total SBSC cost). Although the total SBSC

cost increased by 17% but the resulting transportation cost increased by 400%. The comparisons between the optimal and a non-optimal solution are displayed in Fig. 13 and Fig. 14.

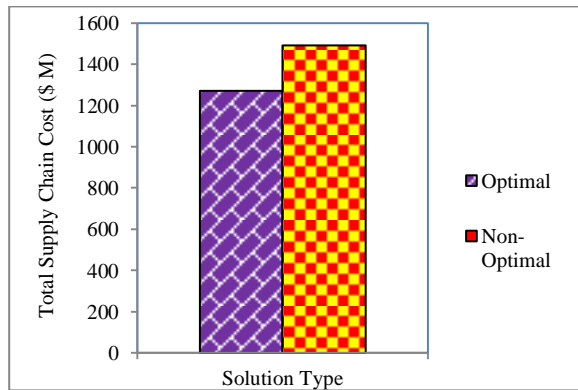


**Fig. 13. Total SBSC cost**

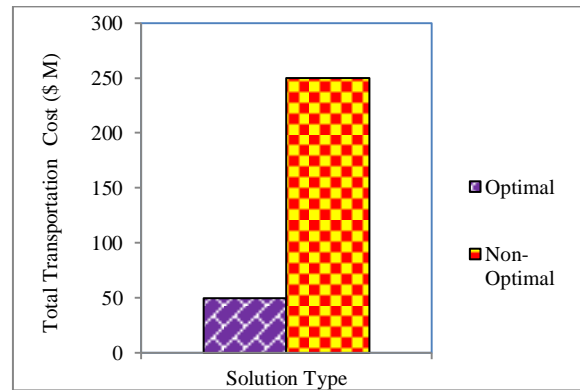


**Fig. 14. Total transportation cost**

#### 2.7.4. Impact of different levels of switchgrass yield on the SBSC decision variables

Rainfall is not deterministic and fluctuates on an annual basis. This will also result in the variation of switchgrass yields at each cultivation site. Historical rainfall records from the past 117 years (1895 to 2011) for North Dakota (ND) indicate that the highest annual rainfall level of 621 mm was recorded in 2010 while the lowest annual rainfall level of 219 mm was recorded in 1936 [35]. Drought defined as less than 75% of average annual rainfall [37], occurred in 7 out of 117 years. While more than 125% of average annual rainfall occurred in only 5 out of the 117 years [35]. 94% of the time, the annual rainfall was greater than 0.75 times the average level.

Scenario analysis is conducted whereby, the optimal level of the key decision variables (e.g. location of cultivation sites, marginal land allocated for cultivation, location and capacity of biorefineries, etc.) are obtained for a wide range of switchgrass yield scenarios. In all scenarios, the minimum volume of bioethanol to be produced is 2130 MLPY (annual requirement for ND). Sensitivity analysis is conducted to help decision makers in planning and efficiently managing a SBSC over a wide range of switchgrass yields (resulting from varying levels of rainfall). Yield levels ranging

from 0.75 to 1.25 times the average switchgrass yield are considered. Low yield level corresponds to low rainfall level and vice versa.

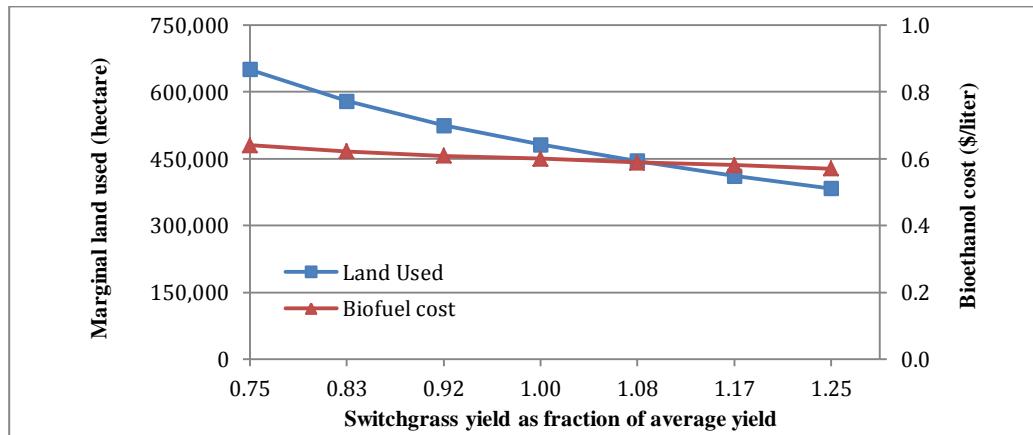


**Fig. 15. Impact of switchgrass yields on land allocation and bioethanol cost**

The results show that the location and capacity of biorefineries is independent of the level of switchgrass yield. All scenarios returned an optimal solution where six 380 MLPY biorefineries are located in the same counties as were obtained using 100% of average yield level (section 2.7, Fig. 3). Fig. 15 shows that the amount of marginal land allocated for switchgrass cultivation is influenced by the level of switchgrass yield. However, the cost of refined bioethanol fluctuates in a narrow band (between \$0.57/liter and \$0.64/liter) over the switchgrass yield range.

## 2.8. Conclusions

This paper proposes a mixed integer linear programming (MILP) model which integrates all the supply chain and logistics decisions thereby minimizing the total annualized switchgrass-based bioethanol supply chain (SBSC) cost. The case study shows that it is cost effective and sustainable to meet 100% of ND's annual demand of gasoline energy equivalent requirement using current bioethanol conversion technology. The MILP model shows that it is optimal to harvest switchgrass as loose chop and build biorefineries with total capacity of 2270 MLPY of bioethanol (or 1514 MLPY of gasoline energy equivalent) in ND. Once switchgrass starts to be cultivated on a commercial basis as part of the second generation of lignocellulosic biomass feedstock, it is expected that the SBSC cost will be

substantially reduced due to the resulting technological advances in switchgrass cultivation, harvesting, storage, preprocessing, and bioethanol conversion.

The proposed model (with a time horizon of one year) has led to important insights about the various logistics components of the SBSC and how they interact with each other. These insights include but are not limited to: 1) harvesting switchgrass as loose chop is shown to be the optimal harvest method as compared to traditional round or square baling methods, 2) in order to produce a given amount of bioethanol, the location of biorefineries is insensitive to the annual variation in switchgrass yield, 3) total amount of marginal land (used for switchgrass cultivation) is influenced by the level of switchgrass yield, and 4) total transportation cost is sensitive to the location of biorefineries and their distance from the switchgrass supply zones (and bioethanol demand zones). If the biorefineries are not optimally located, the SBSC cost can increase by 17% while the transport cost can increase by 400%.

Chapter 3 will incorporate the impact of the uncertainties in the SBSC (such as fluctuation of rainfall level and the resulting switchgrass yield), and propose optimal hedging strategies, such as the use of multiple types of lignocellulosic feedstock (e.g. corn stover and wheat straw) in addition to switchgrass to reduce the impact of the disruptions in biomass supply.

## 2.9. Nomenclature

### 2.9.1. Indices

$e$	Bioethanol demand zones ( $e = 1, \dots, E$ )
$i$	Switchgrass supply zones ( $i = 1, \dots, I$ )
$j$	Switchgrass harvest methods $j = 1$ (Round Bales); $j = 2$ (Square Bales); $j = 3$ (Loose Chop)
$k$	Switchgrass preprocessing facility locations ( $k = 1, \dots, K$ )
$q$	Capacity levels of biorefineries ( $q = 1, \dots, Q$ )
$r$	Biorefinery locations ( $r = 1, \dots, R$ )
$t$	Modeling horizon of 1 year with time periods ( $t = 1, \dots, T$ )

### 2.9.2. Binary decision variables

$Y_k$  {1, if preprocessing facility setup in location  $k$ ; Else 0}

$Y_{rq}$  {1, if biorefinery of capacity level  $q$  setup in location  $r$ ; Else 0}

### 2.9.3. Continuous decision variables

$S_{ij}^t$  Amount of switchgrass stored at supply zone  $i$  by harvest method  $j \neq 3$  during time period  $t$   
(tonne)

$V_{ik}$  Amount of loose chop switchgrass from supply zone  $i$  sent to preprocessing facility  $k$  (tonne)

$V_{ijr}^t$  Amount of switchgrass from  $i$  by harvest method  $j \neq 3$  sent to biorefinery  $r$  during time period  $t$   
(tonne)

$V_{kr}^t$  Amount of densified switchgrass from preprocessing facility  $k$  sent to biorefinery  $r$  during time period  $t$  (tonne)

$X_{ij}$  Marginal land area in supply zone  $i$  harvested by method  $j$  (hectare)

$Z_{re}^t$  Volume of bioethanol from biorefinery in location  $r$  sent to demand zone  $e$  during time period  $t$   
(liter)

$Z_r^t$  Volume of bioethanol produced by biorefinery in location  $r$  during time period  $t$  (liter)

### 2.9.4. Parameters

$A_i$  Switchgrass yield from marginal land in supply zone  $i$  (tonne/hectare)

$B_i$  Maximum marginal land area available for switchgrass cultivation in supply zone  $i$  (hectare)

$C_i$  Annual rental cost of marginal land in supply zone  $i$  (\$/hectare)

$D_{ik}$  Distance between supply zone  $i$  and preprocessing facility  $k$  (km)

$D_{ir}$  Distance between supply zone  $i$  and biorefinery  $r$  (km)

$D_{kr}$  Distance between preprocessing facility  $k$  and biorefinery  $r$  (km)

$D_{re}$  Distance between biorefinery  $r$  and demand zone  $e$  (km)

$F_{jir}$	Transportation cost of switchgrass (harvest method $j \neq 3$ ) from supply zone $i$ to biorefinery $r$ (\$/tonne x km)
$G_{rq}$	Annualized fixed cost of biorefinery $r$ with capacity level $q$ (\$)
$H_j$	Switchgrass harvest cost by method $j$ (\$/hectare)
$L_j^t$	Cumulative rate of switchgrass dry weight loss for harvest method $j \neq 3$ during time period $t$
$M_e^t$	Volume requirement of bioethanol in demand zone $e$ during each time period $t$ (liter)
$N_r$	Processing cost of refined bioethanol at biorefinery $r$ (\$/liter)
$O_{rq}$	Minimum capacity utilization rate of biorefinery $r$ with capacity level $q$
$P_i$	Switchgrass cultivation cost in supply zone $i$ (\$/hectare)
$U_k$	Preprocessing cost (including storage cost) of loose chop switchgrass at facility $k$ (\$/tonne)
$W_k$	Annualized fixed cost of preprocessing facility $k$ (\$)
$\alpha_{ik}$	Transportation cost of loose chop switchgrass from supply zone $i$ to preprocessing facility $k$ (\$/tonne x km)
$\beta_r$	Bioethanol yield (from switchgrass biomass) for biorefinery $r$ (liter/tonne)
$\gamma_{kr}$	Transportation cost of densified switchgrass bales from preprocessing facility $k$ to biorefinery $r$ (\$/tonne x km)
$\delta_i$	Annual rainfall level in supply zone $i$ (mm)
$\lambda_k$	Maximum annual switchgrass densification capacity of preprocessing facility $k$ (tonne)
$\xi_j$	Switchgrass storage cost for harvest method $j \neq 3$ (\$/tonne)
$\rho_{rq}^t$	Maximum bioethanol production volume of biorefinery $r$ with capacity level $q$ during time period $t$ (liter)
$\varphi_k$	Minimum capacity utilization rate of preprocessing facility $k$ (tonne)
$\psi_{re}$	Transportation cost of bioethanol from biorefinery $r$ to demand zone $e$ (\$/liter x km)



## 2.10. References

- [1] Schnepf, R. Cellulosic Ethanol: Feedstocks, Conversion Technologies, Economics, and Policy Options. United States Congressional Research Service 2010: R41460.
- [2] Carriquiry M, Du X, Timilsina G. Second generation biofuels: Economics & policies. *Energy Policy* 2011;39:4222–34.
- [3] Murphy J, McCarthy K. Ethanol production from energy crops and wastes for use as a transportation fuel in Ireland. *Applied Energy* 2005;82:148-166.
- [4] Sokhansanj S, Mani S, Turhollow, Kumar A, Bransby D, Lynd L, Laser M. Large-scale production, harvest and logistics of switchgrass – current technology and envisioning a mature technology. *Biofuels, Bioprod. Bioref.* 2009;3:124–41.
- [5] McLaughlin S, Walsh M. Evaluating environmental consequences of producing herbaceous crops for bioenergy. *Biomass and Bioenergy* 1998;14:317–24.
- [6] Gold S, Seuring S. Supply chain and logistics issues of bio-energy production. *Journal of Cleaner Prod.* 2011;19:32–42.
- [7] Sultana A, Kumar A. Optimal siting and size of bioenergy facilities using geographic information system. *Applied Energy* 2012;94:192–201.
- [8] Mobini M, Sowlati T, Sokhansanj S. Forest biomass supply logistics for a power plant using the discrete-event simulation approach. *Applied Energy* 2011;88:1241–1250.
- [9] Eksioglu S, Acharya A, Leightley L, Arora S. Analyzing the design and management of biomass-to-biorefinery supply chain. *Computers & Industrial Engineering* 2009;57:1342–52.
- [10] Dunnett A, Adjiman C, Shah N. A spatially explicit whole-system model of the lignocellulosic bioethanol supply chain: an assessment of decentralised processing potential. *Biotechnology for Biofuels* 2008;1:13.

- [11] Zhu X, Yaq Q. Logistics system design for biomass-to-bioenergy industry with multiple types of feedstocks. *Bioresource Technology* 2011;102:10936–10945.
- [12] Giarola S, Shah N, Bezzo F. A comprehensive approach to the design of ethanol supply chains including carbon trading effects. *Bioresource Technology* 2012;107:175–185.
- [13] You F, Tao L, Graziano D, Snyder S. Optimal Design of Sustainable Cellulosic Biofuel Supply Chains: Multiobjective Optimization Coupled with Life Cycle Assessment and Input–Output Analysis. *AIChE Journal* 2012;58(4):1157–1180.
- [14] An H, Wilhelm W, Searcy S. A mathematical model to design a lignocellulosic biofuel supply chain system with a case study based on a region in Central Texas. *Bioresource Technology* 2011;102:7860–7870.
- [15] Marvin W, Schmidt L, Benjaafar S, Tiffany D, Daoutidis P. Economic Optimization of a Lignocellulosic Biomass-to Ethanol Supply Chain. *Chemical Engineering Science* 2011.
- [16] Judd J, Sarin S, Cundiff J. Design, modeling, and analysis of a feedstock logistics system. *Bioresource Technology* 2012;103:209–218.
- [17] Larson J, Mooney D, English B, Tyler D. Cost evaluation of alternative switchgrass producing, harvesting, storing, and transporting systems and their logistics in the Southeastern USA. *Agricultural Finance Review* 2010;70:184–200.
- [18] Mani S, Sokhansanj S, Bi X, Turhollow A. Economics of producing fuel pellets from biomass. *Applied Engineering in Agriculture* 2006;22:421–26.
- [19] McLaughlin S, Kszos L. Development of switchgrass (*panicum virgatum*) as a bioenergy feedstock in the United States. *Biomass and Bioenergy* 2005;28:515–35.
- [20] Mulkey V, Owens V, Lee D. Management of switchgrass-dominated conservation reserve program lands for biomass production in South Dakota. *Crop Science* 2006;46:712–20.

- [21] Lee D, Owens V, Doolittle J. Switchgrass and soil carbon sequestration response to ammonium nitrate, manure, and harvest frequency on conservative reserve program land. *Agron J* 2007;99:462–68.
- [22] Lewandowski I, Kicherer A. Combustion quality of biomass: Practical relevance and experiments to modify the biomass quality of *Miscanthus x giganteus*. *Eur J Agron* 1997;6:163–77.
- [23] Mahmudi H, Flynn P. Rail vs. truck transportation of biomass. *Applied Biochemistry and Biotechnology* 2005:1–16.
- [24] America's Energy Future Panel on Alternative Liquid Transportation Fuels. *Liquid Transportation Fuels from Coal and Biomass: Technological Status, Costs, and Environmental Impacts*. National Academy of Sciences; National Academy of Engineering; NRC; 2009:228–30.
- [25] Leduc S, Lundgren J, Franklin O, Dotzauer E. Location of a biomass based methanol production plant: A dynamic problem in northern Sweden. *Applied Energy* 2010;87:68-75.
- [26] Bransby D, Smith A, Taylor R, Duffy P. Switchgrass budget model: an interactive budget model for producing and delivering switchgrass to a bioprocessing plant. *Industrial Biotechnology* 2005;1:122–25.
- [27] Brechbill S, Tyner W. *The Economics of Biomass Collection, Transportation, & Supply to Indiana Cellulosic & Electrical Utility Facilities*. Purdue University, Dept of Agricultural Economics, Working Paper 08-03;2008.
- [28] Lee D, Boe A. Biomass Production of Switchgrass in Central South Dakota. *Crop Science* 2005;45:2583–90.
- [29] Muir J, Sanderson J, Ocumpaugh W, Jones R, Reed R. Biomass production of ‘Alamo’ switchgrass in response to nitrogen, phosphorus, and row spacing. *Agron J* 2001;93:896–901.
- [30] Casler M, Boe A. Cultivar x environment interactions in switchgrass. *Crop Science* 2003;43:2226–2233.

- [31] Sanderson M, Read J, Reed R. Harvest management of switchgrass for biomass feedstock and forage production. *Agron J* 1999;91:5–10.
- [32] Graham R, Walsh M. A National Assessment of Promising Areas for Switchgrass, Hybrid Poplar, or Willow Energy Crop Production. Oak Ridge National Laboratory, ORNL – 6944;1999.
- [33] United States Department of Agriculture (USDA), National Agricultural Statistics Service: 2007 Census of Agriculture.
- [34] U.S. Energy Information Administration, State Energy Data 2009.
- [35] North Dakota Annual 1981-2010 Precipitation (mm). <http://www.ndsu.edu/ndsco/precip/monthly/>
- [36] United States Bureau of the Census: 2007 County Map of North Dakota.
- [37] Smart A, Dunn B, Gates R. Historical weather patterns: A guide for drought planning. *Rangelands* 2005;27:10–12.
- [38] United States Census Bureau: 2010 County Population within North Dakota.  
[http://www.ndsu.edu/sdc/data/census/ND\\_CntyRace2010.pdf](http://www.ndsu.edu/sdc/data/census/ND_CntyRace2010.pdf)
- [39] United States Department of Agriculture (USDA), National Agricultural Statistics Service: 2011 County Rents & Values.
- [40] Leistriz F. Supply price for switchgrass in south central North Dakota. Growing the Bioeconomy Conference. Ames, Iowa. September 7-10, 2008.
- [41] Duffy M. Estimated Costs for Production, Storage & Transportation of Switchgrass. Iowa State Univ., PM2042;2007.
- [42] Rand McNally. <http://www.randmcnally.com/kmage-calculator.do>

## CHAPTER 3. OPTIMIZATION OF A MULTI FEEDSTOCK LIGNOCELLULOSIC-BASED BIOETHANOL SUPPLY CHAIN UNDER MULTIPLE UNCERTAINTIES

### 3.1. Abstract

An integrated multi feedstock (i.e. switchgrass and crop residue) lignocellulosic-based bioethanol supply chain is studied under jointly occurring uncertainties in switchgrass yield, crop residue purchase price, bioethanol demand and sales price. A two-stage stochastic mathematical model is proposed to maximize expected profit by optimizing the strategic and tactical decisions. A case study based on North Dakota (ND) state in the U.S. demonstrates that in a stochastic environment it is cost effective to meet 100% of ND's annual gasoline demand from bioethanol by using switchgrass as primary and crop residue as secondary biomass feedstock. Although results show that the financial performance is degraded as variability of the uncertain parameters increases, the proposed stochastic model increasingly outperforms the deterministic model under uncertainties. The locations of biorefineries (i.e. first-stage integer variables) are insensitive to the uncertainties. Sensitivity analysis shows that “mean” value of stochastic parameters have a significant impact on the expected profit and optimal values of first-stage continuous variables. Increase in level of mean ethanol demand and mean sale price results in higher bioethanol production. When mean switchgrass yield is at low level and mean crop residue price is at high level, all the available marginal land is used for switchgrass cultivation.

### 3.2. Introduction and literature review

In 2010, the total gasoline requirement for the U.S. transportation sector was 507000 million liters per year (MLPY) [1]. Out of which 49000 MLPY of bioethanol was supplied from various biomass renewables to meet 6% of the annual gasoline requirement [2]. One liter of gasoline contains the energy equivalent of 1.5 liters of bioethanol. By 2022 the U.S. Renewable Fuel Standard (RFS) requires production of 136000 MLPY of biofuels, out of which only 57000 MLPY can be bioethanol

refined from corn starch. Out of the remaining 79000 MLPY, a minimum of 61000 MLPY are to be bioethanol refined from lignocellulosic feedstock including perennial grasses like switchgrass, crop residue, short rotation woody crops, forest residue, and municipal waste [3–5].

In North America, one of the most promising primary sources of lignocellulosic biomass is switchgrass (*panicum virgatum*) [3, 6]. Agriculture residues like corn stover and wheat straw left on the field after crop harvest also show great potential as a source of lignocellulosic biomass feedstock [7]. As of 2012, the production of bioethanol from lignocellulosic feedstock is limited to pilot scale projects and has not been successfully commercialized [3]. To encourage investment in bioethanol refineries, it is imperative that an economically viable supply of lignocellulosic biomass [3] is guaranteed. This allows biorefineries to operate at a sufficiently high utilization level to achieve economies of scale [8]. The production of switchgrass is largely driven by the annual level of rainfall. Adverse weather conditions (i.e. drought or floods) can cause massive disruption in the supply of switchgrass biomass [6]. A strategy for mitigating risk in biomass feedstock supply is to use multiple sources of lignocellulosic biomass [9, 10] in addition to switchgrass. In the upper Midwest region of the United States, all three crops (i.e. corn, wheat, and switchgrass) are harvested once a year in early autumn after the first killing frost [6, 11, 12]. The chemical composition of corn stover and wheat straw is very similar to switchgrass in terms of percentages of lignin, cellulose and hemicellulose [13, 14]. A biorefinery utilizing lignocellulosic biomass as feedstock can interchangeably utilize any of the three feedstocks with minimal effect on biorefinery operating costs or bioethanol yields [15]. Any negative cost (or efficiency) effects will be more than compensated by the increased reliability in biomass supply from multiple feedstock sources, and will allow the biorefinery to operate at or near optimal levels under a range of biomass supply chain disruption scenarios [16].

Most work done so far in literature regarding optimization of integrated lignocellulosic-based bioethanol supply chain (LBSC) has been confined to using the “deterministic” parameters to obtain

the optimal production capacity and locations of biorefineries [6, 17], biomass preprocessing facilities [6, 18], site selection and allocation of marginal land for biomass cultivation [6, 19]. However, there are uncertainties inherent in a LBSC [20]. These uncertainties introduce significant risk in the decision making process. Literature review has highlighted some of the key uncertainties inherent in the life cycle of a LBSC [16, 20], namely: 1) switchgrass yield due to unpredictable weather conditions; 2) purchase price of available crop residues; 3) demand for bioethanol; and 4) sale price for bioethanol.

In recent literature, two-stage stochastic programming is found to be the dominant approach to deal with optimization under uncertainty [21–23]. Two-stage stochastic mathematical models involve two types of decisions: first stage decisions that must be made before the realization of the uncertain parameters, and second stage (i.e. recourse) decisions that are taken once the uncertainty is unveiled. The objective is to choose the first-stage decision variables in such a way that the expected value of the objective function is maximized (or minimized) over all the scenarios.

In the LBSC stochastic optimization problem, the planning decisions, such as site selection and allocation of available marginal land for switchgrass cultivation, biorefinery locations and bioethanol production capacities are “strategic” decisions that need to be taken before the uncertainty unveils [24–28]. A farmer cannot cultivate perennial crops like switchgrass at one site for a given year and then change over to a different site for the next year as can be done for annual crops like corn and wheat [28]. As such, farmers need to set aside a fixed amount of land for switchgrass cultivation over a 10 year period as switchgrass fields require two years to setup and are productive for a further eight years before requiring reseeding [28]. Similarly, facility planning decisions (i.e. biorefinery site selection and production capacity) are capital intensive and cannot be easily adjusted once implemented [25].

As such, the structure of the problem lends itself to be modeled as a two-stage stochastic optimization problem where the first-stage decisions (i.e. allocation of land for switchgrass cultivation, bioethanol production capacity for each biorefinery, and locations of biorefineries) are taken before the

uncertainty in switchgrass yield, purchase price of crop residues, bioethanol demand and biofuel sale price unfolds. Second-stage decisions are taken once the uncertainty is materialized. Tactical recourse decisions include but are not limited to the: amount of pre-processed switchgrass to be transported from each biomass supply zone to each biorefinery, amount of pre-processed switchgrass to be directly sold from each biomass supply zone, amount of crop residues to be purchased from each biomass supply zone and transported to each biorefinery, volume of bioethanol to be shipped from each biorefinery to each bioethanol demand zone, volume of bioethanol to be directly sold from each biorefinery, and volume of unmet bioethanol requirement in each demand zone, to mitigate the impact of each uncertain scenario. These operational decisions can be adjusted with a recourse cost depending on the actual realization of uncertain parameters [22].

Most of the preliminary work on stochastic optimization of bioethanol supply chains only considers one type of uncertainty (such as uncertain bioethanol demand, or bioethanol sale price uncertainty) [24–26]. Work by [27] considers an LBSC where the supply and demand uncertainties are considered separately but not jointly. The first-stage decision variables include biorefinery location and capacity. Biomass procurement is considered as a second stage variable.

This article proposes a two-stage stochastic mixed integer linear programming (MILP) formulation to maximize the expected profit of an integrated LBSC under multiple uncertainties with the following unique contributions to literature: 1) Switchgrass supply, crop residue purchase price, bioethanol demand and selling price uncertainties are considered jointly; 2) First-stage decisions include both integer and continuous variables. The integer variable determines the location of biorefineries. The continuous variables include bioethanol production capacity for each biorefinery, and allocation of marginal land. To the best of our knowledge this is the first effort to study the allocation of marginal land for switchgrass cultivation in a stochastic environment; 3) The second stage decision variables include amount of pre-processed switchgrass to be directly sold from biomass supply zones,



amount of crop residues to be purchased from biomass supply zones, amount of biomass feedstock to be transported from the biomass supply zones to the biorefineries, volume of bioethanol to be directly sold from biorefineries, volume of bioethanol to be transported from the biorefineries to the biofuel demand zones, and the volume of unmet bioethanol requirement for each demand zone; 4) The optimal strategies on location of biorefineries, bioethanol production capacity of each biorefinery, site selection and allocation of marginal land, are solved simultaneously within the integrated system; and 5) A case study based in the U.S. is used to demonstrate the effectiveness of the stochastic model and to provide managerial insights about the various logistical aspects of the LBSC.

### **3.3. Problem statement**

This research studies a comprehensive LBSC. A list of indices, parameters, and decision variables is given in the Nomenclature section.

Based on previous work by [6], this paper assumes that: 1) switchgrass is harvested as loose chop, once a year after the first killing frost; 2) only road haulage for the transportation of lignocellulosic biomass and bioethanol is considered; and 3) the total bioethanol requirement is proportional to the population in each demand zone.

The major logistics activities in a LBSC are shown in Fig. 16. Switchgrass can be cultivated in available marginal lands [28] located in  $i$  biomass supply zones and harvested as loose chop [6]. The harvested loose chop is then pre-processed on-site using mobile densification equipment [29]. The densified switchgrass is then transported from  $i$  biomass supply zones to the  $r$  biorefineries. After satisfying the biomass requirement for the biorefineries, any excess amount of densified switchgrass is directly sold from  $i$  biomass supply zones. In case the total amount of harvested switchgrass is not sufficient (e.g. low crop yield due to adverse climatic conditions, or insufficient amount of land under cultivation, etc.), the remaining biomass requirement for the biorefineries is made up by procuring crop

residues in the form of traditional bales of corn stover and wheat straw from  $i$  biomass supply zones and transporting them to the  $r$  biorefineries.

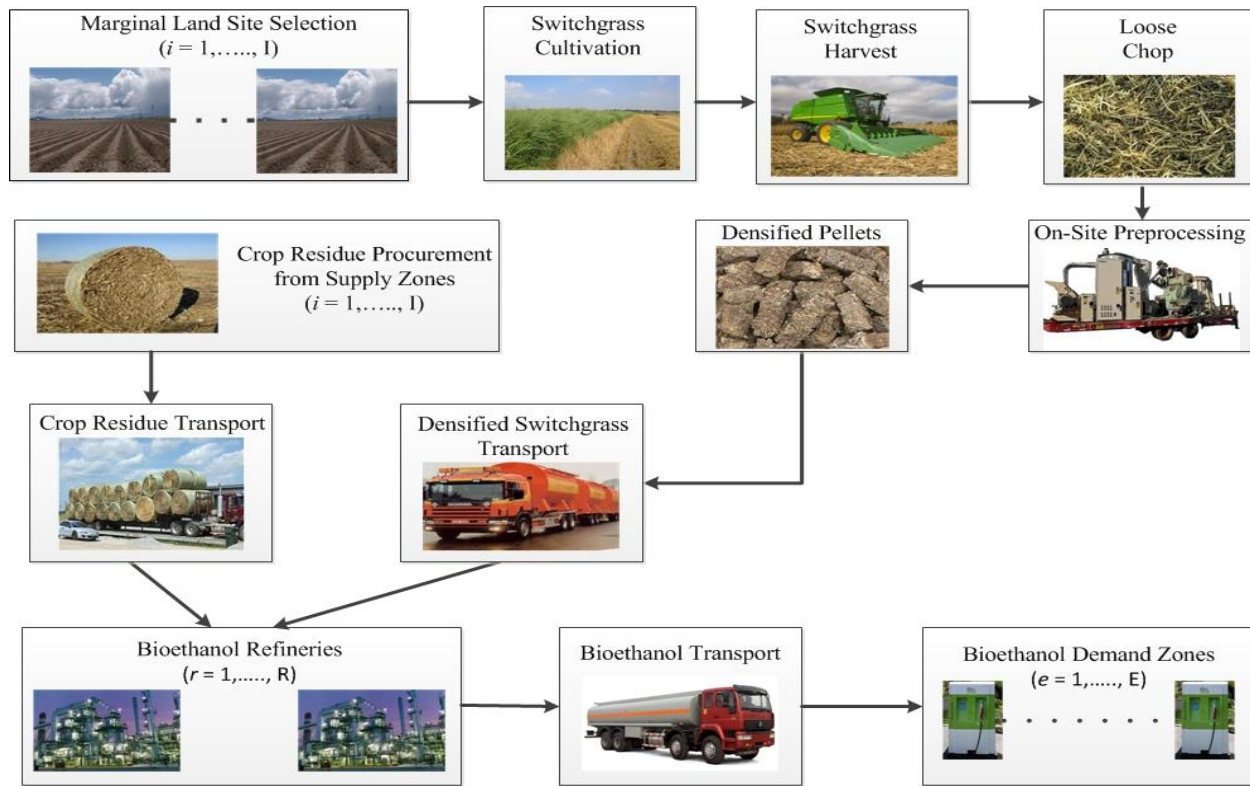


**Fig. 16. Major logistics activities in a LBSC**

The biomass is converted into ethanol in the biorefineries. The volume of bioethanol produced is driven by the maximum production capacity of each biorefinery. Finally, the produced bioethanol is transported from the  $r$  biorefineries to  $e$  biofuel demand zones. After satisfying the total bioethanol requirement, any excess volume of bioethanol is directly sold from  $r$  biorefineries. In case the total volume of bioethanol produced is not sufficient to meet the total bioethanol demand, the shortfall in bioethanol requirement is made up by “importing” bioethanol by paying a penalty cost (\$/liter).

To maximize the annualized LBSC profit, the following logistics decisions need to be optimized: 1) cultivation sites selection from the  $i$  biomass supply zones and allocation of available marginal land for switchgrass production; 2) amount of crop residues to be purchased from the  $i$  biomass supply zones; 3) amount of densified switchgrass to be directly sold from the  $i$  biomass supply zones; 4) material flow

of lignocellulosic feedstock (densified switchgrass and crop residue) from the  $i$  biomass supply zones to the  $r$  biorefineries; 5) sites selection from  $r$  biorefinery locations; 6) volume of bioethanol to be produced by the  $r$  biorefineries; 7) volume of bioethanol to be directly sold from the  $r$  biorefineries; 8) material flow of bioethanol from the  $r$  biorefineries to the  $e$  biofuel demand zones; and 9) volume of unmet bioethanol requirement for the  $e$  biofuel demand zones.

Literature review has highlighted some of the key uncertainties inherent in the life cycle of a LBSC [6, 16, 20]. The following sections present the multiple uncertainties that are jointly considered in the proposed stochastic MILP model.

### **3.3.1. Stochastic nature of the LBSC**

This study jointly considers four of the major sources of uncertainties [6, 16, 20], namely: i) uncertainty in switchgrass yield due to unpredictable weather conditions; ii) uncertainty in the purchase price of available crop residues; iii) uncertainty in the demand for bioethanol; and iv) uncertainty in the sale price for bioethanol.

Uncertainty in commodity/energy prices and their supply/demand is commonly modeled using known probability distributions which are based on statistical analysis of historical data [30].

- **Uncertainty in switchgrass yield:** Literature review has indicated that switchgrass yields exhibit a great range of variations on an annual basis. 90% of the yield variations are caused by the variation in rainfall level at the cultivation site during a given year [31]. This randomness in switchgrass yield has a major impact in deciding how much of the available marginal land to allocate for switchgrass cultivation in each supply zone. The challenge is to determine the amount of land to be cultivated that is the best possible combination under all possible yield scenarios. Therefore, there is a need to develop modeling tools that can predict switchgrass yields at different cultivation sites under a range of rainfall scenarios. A proposed approach is

presented (see section 3.6.1 for details) to model the switchgrass yield (under any scenario) before the actual harvesting has taken place.

- **Uncertainty in the purchase price of available crop residues:** Crop residue is a harvesting by-product of the primary crop [32–34]. The farm-gate price of crop residue is only partly influenced by the cultivation and harvesting cost of the primary crop [14, 32]. The market price of crop residue is largely dictated by its demand from various competing sectors (e.g. use as animal feed and bedding, use as an energy supplement in co-firing with coal, and use as a biomass feedstock for biofuel production) [7, 11, 34]. The demand for crop residue is not deterministic and this in turn causes the purchase cost of crop residue to fluctuate on an annual basis [35]. In this paper the crop residue purchase price is modeled as a correlated function of its demand (see section 3.6.2 for details).
- **Uncertainty in the demand for bioethanol:** The RFS requires biofuels to satisfy at least 20% of the demand for liquid transportation fuels by 2022 [4, 5]. However, demand for gasoline (and hence ethanol) is not deterministic and fluctuates on an annual basis [36]. A probability function is used to model the uncertainty in bioethanol demand by analyzing historical demand data (see section 3.6.3).
- **Uncertainty in the sale price for bioethanol:** The sale price of bioethanol fluctuates in a random manner and is influenced by several factors that include but are not limited to the following [37]: 1) demand for gasoline; 2) sale price of crude oil; and 3) government incentives for the production and sale of biofuels. A probability function is used to model the uncertainty in bioethanol sale price by analyzing historical sale price of ethanol (see section 3.6.4 for details).

### **3.4. Model formulation**

A two-stage stochastic MILP model is proposed to maximize the expected LBSC profit by determining the optimal level of the various logistics decision variables. The formulation (objective

function and constraints) of the model are explained in the following sections. All continuous decision variables are non-negative, while all integer variables have 0–1 (i.e. binary) restriction.

### 3.4.1. Objective function of the LBSC

The objective function of the proposed model is to maximize the expected annualized LBSC profit. The expected profit equals the expected revenue minus the expected cost. The expected LBSC revenue includes income from sale of densified switchgrass, bioethanol sales, and tax credit from sale of subsidized biofuel. The expected LBSC cost includes marginal land rental cost, switchgrass cultivation cost, switchgrass harvest cost, operational cost of biorefinery, annualized capital cost of biorefineries, penalty cost of unmet bioethanol demand, preprocessing cost of switchgrass, densified switchgrass transportation cost from supply zone to biorefinery, crop residue purchase cost, crop residue transportation cost from supply zone to biorefinery, and bioethanol transportation cost from biorefinery to biofuel demand zone.

Eq. 3.1 gives the objective function  $\theta$  (i.e. expected LBSC profit) which needs to be maximized.

$$\text{Max } \theta = -F1 - F2 - F3 - F4 - F5 + E_{\omega} [R1(\omega) + R2(\omega) + R3(\omega) - C1(\omega) - C2(\omega) - C3(\omega) - C4(\omega) - C5(\omega) - C6(\omega)] \quad (3.1)$$

The different components of the objective function are explained below.

$$F1 = \sum_{i=1}^I C_i X_i \quad (3.2)$$

$$F2 = \sum_{i=1}^I \kappa_i X_i \quad (3.3)$$

$$F3 = \sum_{i=1}^I H_i X_i \quad (3.4)$$

$$F4 = \sum_{r=1}^R N_r Z_r \quad (3.5)$$

$$F5 = \sum_{r=1}^R (GY_r + TZ_r) \quad (3.6)$$

$$R1(\omega) = \chi \sum_{i=1}^I J_i(\omega) \quad (3.7)$$

$$R2(\omega) = \sum_{r=1}^R t(\omega) Z_r \quad (3.8)$$

$$R3(\omega) = \tau \sum_{r=1}^R \sum_{e=1}^E S_{re}(\omega) \quad (3.9)$$

$$C1(\omega) = \varphi \sum_{e=1}^E O_e(\omega) \quad (3.10)$$

$$C2(\omega) = \sum_{i=1}^I U_i K_i(\omega) \quad (3.11)$$

$$C3(\omega) = \sum_{i=1}^I \sum_{r=1}^R \gamma_{ir} D_{ir} V_{ir}(\omega) \quad (3.12)$$

$$C4(\omega) = \sum_{i=1}^I \sum_{r=1}^R \varepsilon(\omega) F_{ir}(\omega) \quad (3.13)$$

$$C5(\omega) = \sum_{i=1}^I \sum_{r=1}^R \eta_{ir} D_{ir} F_{ir}(\omega) \quad (3.14)$$

$$C6(\omega) = \sum_{r=1}^R \sum_{e=1}^E \psi_{re} D_{re} S_{re}(\omega) \quad (3.15)$$

Eq. 3.2 refers to the rental cost of marginal land for switchgrass cultivation. Eq. 3.3 refers to the switchgrass cultivation cost. Eq. 3.4 refers to the harvesting cost of switchgrass. Eq. 3.5 refers to the operational cost of biorefineries. Eq. 3.6 refers to the fixed and variable cost of installed biorefineries. Eq. 3.7 refers to the revenue from sale of densified switchgrass. Eq. 3.8 refers to the revenue from the sale of bioethanol. Eq. 3.9 refers to the tax credit accrued from the sale of subsidized bioethanol. Eq. 3.10 refers to the penalty cost incurred due to unmet bioethanol demand. Eq. 3.11 refers to the preprocessing cost of loose chop into densified biomass. Preprocessing cost includes storage cost of loose chop and the resulting densified switchgrass. Eq. 3.12 refers to transport cost of densified

switchgrass from biomass supply zones to biorefineries. Eq. 3.13 refers to the purchase cost of crop residue. Eq. 3.14 refers to transport cost of crop residue from biomass supply zones to biorefineries. Eq. 3.15 refers to transport cost of subsidized bioethanol from biorefineries to biofuel demand zones.

### 3.4.2. Capacity constraints

$$X_i \leq B_i \quad \forall i \quad (3.16)$$

$$\sum_{r=1}^R F_{ir}(\omega) \leq \mu_i \zeta_i \quad \forall i, \omega \quad (3.17)$$

$$\rho_{\min} Y_r \leq Z_r \leq \rho_{\max} Y_r \quad \forall r \quad (3.18)$$

The capacity constraints are given by Eqs. 3.16–3.18. Eq. 3.16 ensures that in each biomass supply zone  $i$ , the allocated marginal land for switchgrass cultivation do not exceed the marginal land availability. Eq. 3.17 ensures that in each supply zone  $i$ , the amount of crop residue sent to all biorefineries is less than the maximum allowable amount of crop residue that can be removed. Eq. 3.18 ensures that a biorefinery if built at location  $r$  must have a bioethanol production capacity more than  $\rho_{\min}$  “minimum capacity” and cannot have a bioethanol production capacity more than  $\rho_{\max}$  “maximum capacity”.

### 3.4.3. Material flow constraints

$$K_i(\omega) \leq A_i(\omega) X_i \quad \forall i, \omega \quad (3.19)$$

$$J_i(\omega) + \sum_{r=1}^R V_{ir}(\omega) \leq K_i(\omega) \quad \forall i, \omega \quad (3.20)$$

$$\sum_{i=1}^I \beta_r [V_{ir}(\omega) + F_{ir}(\omega)] = Z_r \quad \forall r, \omega \quad (3.21)$$

$$Z_r = L_r(\omega) + \sum_{e=1}^E S_{re}(\omega) \quad \forall r, \omega \quad (3.22)$$

$$O_e(\omega) + \sum_{r=1}^R S_{re}(\omega) = M_e(\omega) \quad \forall e, \omega \quad (3.23)$$

The material flow constraints are given by Eqs. 3.19–3.23. In each biomass supply zone, Eq. 3.19 and 3.20 respectively ensure that the amount of loose chop that is pre-processed, and the amount of densified switchgrass sold plus the amount sent to all biorefineries, is not greater than the total amount of loose chop harvested. Eq. 3.21 ensures that the cumulative amount of biomass (from densified switchgrass plus crop residue) received by each biorefinery is all converted into bioethanol. Eq. 3.22 ensures that for each biorefinery, the volume of bioethanol produced is equal to the volume of unsubsidized bioethanol sold from the refinery-gate plus the volume of subsidized bioethanol sent to all demand zones. Eq. 3.23 ensures that the volume of unmet bioethanol requirement plus the volume of subsidized bioethanol transported from all biorefineries is equal to the biofuel requirement in each bioethanol demand zone.

### 3.5. Case study setup

This case study examines a LBSC in the U.S. state of North Dakota (ND). Switchgrass is only cultivated in the available marginal lands and is considered as the primary biomass feedstock. Crop residues consisting of corn stover and wheat straw are considered as the secondary biomass feedstock. The proposed stochastic MILP model will determine the optimal level of the key logistics decision variables that maximize the expected profit of the LBSC. In addition, the performance of the proposed stochastic model is compared with that of the traditional deterministic model under uncertainties to demonstrate the effectiveness of the proposed stochastic model. Sensitivity analysis is also conducted to highlight the impact of different input parameters on the optimal logistics decisions and the expected LBSC profit.

Input parameters used in this case study are displayed in Tables A4–A6 (Appendix A).



### 3.5.1. Model assumptions

The various assumptions used in the proposed stochastic MILP model are explained below. In addition, the conversion factors from the metric units (SI) to the United States customary units are given in Appendix B.

- All 53 counties of ND are potential biorefinery locations, biomass supply and bioethanol demand zones. Biomass availability and bioethanol demand are centered at the county “seat” (e.g. Fargo is the seat of Cass county) [6, 38].
- Lignocellulosic-based biorefineries with a production capacity of less than 190 MLPY are not economically viable [9] while those with a production capacity of more than 380 MLPY have not yet been commercialized [16]. Therefore in this work an installed biorefinery has a production capacity ( $Z_r$ ) between 190 MLPY and 380 MLPY.
- Expected annualized LBSC profit to be maximized. Revenues and costs are considered on an annual basis. Eq. 3.24 is used to annualize the initial investment of a biorefinery with life  $n$  years and interest rate of  $q\%$  [16]. For example, a 190 MLPY biorefinery requires an initial investment of \$523 Million. With biorefinery life ( $n$ ) of 20 years and interest rate ( $q$ ) of 5%, the annualized cost is \$42 Million obtained from Eq. 3.24 [6, 16].

$$\text{Annualized Cost} = [q(\text{Initial Investment})] / [1 - (1 + q)^{-n}] \quad (3.24)$$

- In Eq. 3.6, annual fixed cost of biorefinery ( $G$ ) and annual variable cost of biorefinery ( $T$ ) are obtained by the following approximation. As shown in literature, Eq. 3.25 is used to calculate the total annual cost ( $Q_r$ ) of a biorefinery with capacity  $Z_r$  [39], where  $\alpha$  is a scaling factor,  $Z_0$  is a reference capacity, and  $Q_0$  is the annualized cost of a biorefinery with capacity of  $Z_0$ . In this work,  $\alpha$  is set to 0.8 [39]. Using Eq. 3.25,  $Q_r$  of a 380 MLPY biorefinery is calculated as \$73.1 Million for a reference capacity of 190 MLPY with annualized cost of \$42 Million.

$$Q_r = Q_0(Z_r / Z_0)^\alpha \quad \forall r \quad (3.25)$$

In this work,  $Z_r$  is set in the interval of (190, 380) MLPY. For this interval Eq. 3.25 is linearized and approximated by Eq. 3.26 in order to avoid non-linear term in the proposed stochastic model. The best value of  $G$  is \$8883500 and  $T$  is \$0.17/liter. Using Eq. 3.26 the annualized cost ( $Q_r$ ) of a 380 MLPY biorefinery is estimated at \$73.4 Million which compares favorably to the value obtained using Eq. 3.25.

$$Q_r = G + TZ_r \quad \forall r \quad (3.26)$$

- For each installed biorefinery, the bioethanol production volume is equal to the bioethanol production capacity. The production capacity is a first-stage decision variable representing substantial investment. It is economically effective that the entire capacity is fully utilized for bioethanol production in each scenario.
- Total bioethanol production volume of all biorefineries should not be greater than 2280 MLPY, which is the maximum annual bioethanol demand for ND under any scenario.
- In any scenario if there is excess bioethanol volume leftover after meeting 100% of ND's bioethanol requirements, it can be sold outside the state. However, out-of-state sale of bioethanol will not qualify for the tax credit [4].
- Not all the crop residue is available for bioethanol production, since significant portion of the residue should be kept on the field to prevent soil erosion [34] and higher operating cost [35]. Most researchers advise that the percentage of agriculture residue that can be sustainably removed from the field be less than 30% [35]. Therefore, in this work only 30% of the total amount of crop residue ( $\zeta_i$ ) in biomass supply zone  $i$  can be sustainably removed.
- The proposed stochastic model has “full recourse”. Any resulting shortage in the amount of switchgrass biomass produced due to lower than average annual rainfall is fully offset by procuring the remaining lignocellulosic biomass requirement in the form of expensive crop

residue. Similarly, any shortfall in meeting the in-state bioethanol demand is fully offset by incurring penalty cost ( $\varphi$ ) for each liter of unmet bioethanol demand [27].

### 3.6. Modeling the uncertainties in the LBSC

In this work, all stochastic scenarios are governed by three independent random variables (IRVs) which are not correlated. The first IRV,  $\delta(\omega)$  refers to the annual rainfall level for the state of ND and is used to obtain the switchgrass yield ( $A_i(\omega)$ ) in each biomass supply zone, and the purchase price for crop residue ( $\varepsilon(\omega)$ ). The second IRV,  $M(\omega)$  is used to model the annual bioethanol demand for the entire state of ND. The third IRV,  $\iota(\omega)$  is used to model the unsubsidized sale price for bioethanol.

#### 3.6.1. Modeling switchgrass yield

Switchgrass yield is highly correlated to the annual rainfall level [6, 31]. Rainfall records [40] from the past 117 years (1895 to 2011) for the state of ND indicate that annual rainfall level is a Normally distributed random variable with a mean of 449 mm and standard deviation of 73 mm. The Normal probability distribution used to model annual rainfall level is truncated on the interval (218, 620). For large number of scenarios ( $\Omega > 10000$ ), a Normal distribution can generate extremely high rainfall level or even negative rainfall levels. The truncation ensures that the values never exceed 620 mm or fall below 218 mm, so as to better mimic the actual extreme rainfall levels in ND.

For the same time period (1895 to 2011), rainfall patterns for each of the 53 counties in ND are also analyzed and show a high degree of correlation ( $> 0.85$ ) between the state-wide average rainfall  $\delta$  and the rainfall  $\delta_i$  in each county of ND. However, the degree of correlation between the state-wide rainfall and county-level rainfall is not uniform for each of the 53 counties in ND. As such, 53 separate linear regression models are developed for predicting annual rainfall  $\delta_i(\omega)$  in county  $i$  given a specific level of state-wide rainfall  $\delta(\omega)$  for each stochastic scenario  $\omega$ . The generic linear regression rainfall model for county  $i$  is given in Eq. 3.27, where  $a_i$  represents the regression coefficient, and  $b_i$  is the y-

intercept when  $\delta(\omega) = 0$ . Values of  $a_i$  and  $b_i$  along with the “mean” value of  $\delta_i(\omega)$  for all 53 counties of ND are given in Table A6 in Appendix A.

$$\delta_i(\omega) = a_i\delta(\omega) + b_i \quad \forall i, \omega \quad (3.27)$$

The described linear relationship between switchgrass yield and rainfall [6] is modified and displayed in Eq. 3.28. The average values of  $\delta_i$  and  $A_i$  (in Table A6 in Appendix A) are then used to predict the switchgrass yield ( $A_i(\omega)$ ) for county  $i$  during scenario  $\omega$ .

$$A_i(\omega) = A_i[\delta_i(\omega) / \delta_i] \quad \forall i, \omega \quad (3.28)$$

Where

$\delta_i$  average annual rainfall in switchgrass supply zone  $i$

$\delta_i(\omega)$  predicted annual rainfall in switchgrass supply zone  $i$  during scenario  $\omega$

$A_i$  average switchgrass yield in supply zone  $i$

$A_i(\omega)$  predicted switchgrass yield in supply zone  $i$  during scenario  $\omega$

### 3.6.2. Modeling the purchase price for crop residues

In this work the purchase price of crop residue is assumed to be correlated to its demand [7, 11, 34]. Scenarios with high annual rainfall will result in bumper harvest of switchgrass, and the farm-gate price of crop residue will be at the low level (and vice versa) as there will be less demand to buy crop residue to meet the biomass feedstock requirement for a biorefinery. The random variable  $\delta(\omega)$ , together with Eq. 3.29 is used to model the crop residue purchase price ( $\varepsilon(\omega)$ ) for each scenario  $\omega$ . In the U.S. the average farm-gate price of crop residue is \$83/tonne and ranges from \$51/tonne to \$125/tonne [32]. Therefore, in all scenarios  $\varepsilon(\omega)$  is truncated on the interval (51, 125).

$$\varepsilon(\omega) = 165 - 118.71\delta(\omega) \quad \forall \omega \quad (3.29)$$

### 3.6.3. Modeling the demand for bioethanol

In 2009 the total gasoline consumption in ND was 1422 MLPY [36] or 2133 MLPY of bioethanol on an energy equivalent basis. However, the demand for gasoline (and hence ethanol) is not deterministic and fluctuates on an annual basis [36]. Historical data (1981 to 2005) shows that the annual gasoline energy equivalent demand ( $M(\omega)$ ) in ND is a Normally distributed random variable with mean of 2133 MLPY and standard deviation of 64 MLPY. The Normal probability distribution used to model ethanol demand is truncated on the interval (2006, 2280).

### 3.6.4. Modeling the sale price for bioethanol

The U.S. RFS [4] does not guarantee a fixed biofuel sale price. The most common biofuel is bioethanol, whose market price over the last 10 years has fluctuated between \$0.26/liter to \$0.79/liter with a mean price of \$0.53/liter [37]. The only subsidy provided is the \$0.13 tax credit accrued for each liter of biofuel [4] sold to meet the annual demand.

Gasoline price is considered as a surrogate for ethanol price as there is 83% positive correlation between the per liter price of gasoline and ethanol [37]. Researchers have previously modeled ethanol price as a Normal distribution with a standard deviation equal to 15% of the mean [33]. As such, this work models the ethanol sale price ( $\iota(\omega)$ ) as a Normally distributed random variable with mean of \$0.53/liter and standard deviation of \$0.08/liter. The Normal probability distribution used to model ethanol sale price is truncated on the interval (0.26, 0.79).

### 3.7. Solution procedure for the proposed stochastic MILP model

Modeling the uncertainties as continuous probability distributions is likely to result in an infinite number of stochastic scenarios [20]. To reduce the computational burden and to make the optimization problem tractable, a set of discrete scenarios are instead used to describe the random events. In the proposed stochastic MILP model, each IRV is discretized into 10 levels (see Table 3).

The number of discretized levels used is sufficient to ensure that the probability distribution is accurately captured. Since there are three independent random variables, the total number of scenarios is  $10^3$ . Each scenario  $\omega$  (where  $\omega = 1, \dots, 1000$ ) is equally likely to happen with probability  $P(\omega) = 1/1000$ . The 1000 discrete scenarios are used to convert the stochastic MILP model into the Deterministic Equivalent Model (DEM) which contains 239069 constraints, 1135053 continuous variables, and 53 binary variables. The DEM (Eqs. 3.1–3.23) is coded in GAMS and executed by the XpressMP solver (with the optimality tolerance gap set at  $< 1\%$ ) using the parallel computing platform of NEOS (network enabled optimization solution) server [41] hosted at [www.neos-server.org/neos](http://www.neos-server.org/neos).

**Table 3. Discretized levels of independent random variables (IRVs)**

Ethanol sale price " $\iota$ " (\$/liter)			Annual rainfall level " $\delta$ " (mm)			In-state ethanol demand " $M$ " (MLPY)		
Level	Range	Mean	Level	Range	Mean	Level	Range	Mean
L_ $\iota$ <sub>01</sub>	$0.26 \leq \iota < 0.43$	0.39	L_ $\delta$ <sub>01</sub>	$219 \leq \delta < 356$	322	L_ $M$ <sub>01</sub>	$2006 \leq M < 2052$	2023
L_ $\iota$ <sub>02</sub>	$0.43 \leq \iota < 0.47$	0.45	L_ $\delta$ <sub>02</sub>	$356 \leq \delta < 387$	373	L_ $M$ <sub>02</sub>	$2052 \leq M < 2082$	2068
L_ $\iota$ <sub>03</sub>	$0.47 \leq \iota < 0.49$	0.48	L_ $\delta$ <sub>03</sub>	$387 \leq \delta < 410$	400	L_ $M$ <sub>03</sub>	$2082 \leq M < 2097$	2091
L_ $\iota$ <sub>04</sub>	$0.49 \leq \iota < 0.51$	0.50	L_ $\delta$ <sub>04</sub>	$410 \leq \delta < 430$	420	L_ $M$ <sub>04</sub>	$2097 \leq M < 2120$	2106
L_ $\iota$ <sub>05</sub>	$0.51 \leq \iota < 0.53$	0.52	L_ $\delta$ <sub>05</sub>	$430 \leq \delta < 448$	440	L_ $M$ <sub>05</sub>	$2120 \leq M < 2139$	2125
L_ $\iota$ <sub>06</sub>	$0.53 \leq \iota < 0.55$	0.54	L_ $\delta$ <sub>06</sub>	$448 \leq \delta < 467$	458	L_ $M$ <sub>06</sub>	$2139 \leq M < 2150$	2140
L_ $\iota$ <sub>07</sub>	$0.55 \leq \iota < 0.57$	0.56	L_ $\delta$ <sub>07</sub>	$467 \leq \delta < 486$	476	L_ $M$ <sub>07</sub>	$2150 \leq M < 2165$	2155
L_ $\iota$ <sub>08</sub>	$0.57 \leq \iota < 0.59$	0.58	L_ $\delta$ <sub>08</sub>	$486 \leq \delta < 509$	498	L_ $M$ <sub>08</sub>	$2165 \leq M < 2184$	2174
L_ $\iota$ <sub>09</sub>	$0.59 \leq \iota < 0.63$	0.61	L_ $\delta$ <sub>09</sub>	$509 \leq \delta < 540$	526	L_ $M$ <sub>09</sub>	$2184 \leq M < 2210$	2197
L_ $\iota$ <sub>10</sub>	$0.63 \leq \iota < 0.83$	0.67	L_ $\delta$ <sub>10</sub>	$540 \leq \delta < 621$	578	L_ $M$ <sub>10</sub>	$2210 \leq M < 2267$	2239

### 3.8. Comparison of the deterministic model vs. proposed stochastic model

In this work, the base-case models the stochastic parameters by fitting historical data to known probability distributions (see Table A5 in Appendix A). Co-efficient of variance (CV) is used to measure the level of variability of stochastic parameters. CV is defined as the ratio of standard deviation over the mean value [22]. For the base-case, CV for the stochastic parameters annual rainfall level ( $\delta$ ), in-state bioethanol demand ( $M$ ), crop residue purchase price ( $\epsilon$ ), bioethanol sale price ( $\iota$ ) is 0.16, 0.03, 0.16, and 0.15 respectively (see section 3.6).

### 3.8.1. For the base-case

This section compares the performance of the proposed stochastic model with traditional deterministic model. Value of stochastic solution (VSS) is used to compare the results. VSS is defined as the difference between the expected profit of the stochastic model vs. the deterministic model under uncertainties [22]. For the stochastic model, the optimal values of first-stage decision variables and the expected profit (along with the values of second-stage decision variables) is obtained by solving its DEM counterpart. For the deterministic model, the optimal values of the first-stage decision variables obtained by solving the problem for a single scenario using the “mean” values of the input parameters are used in the stochastic model to calculate the expected profit (and the values of second-stage decision variables).

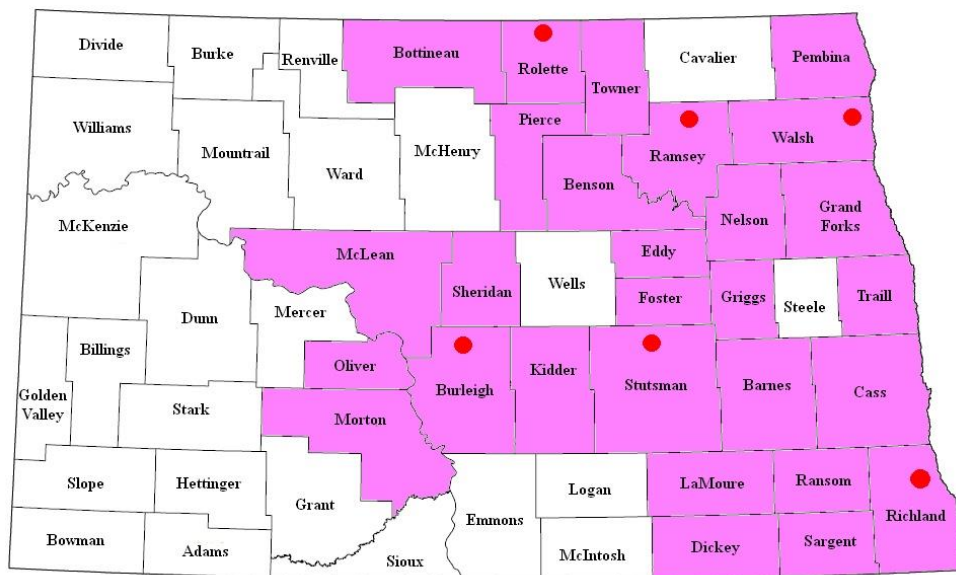
Table 4 summarizes the performance of the stochastic model vs. the deterministic model for the base-case. The proposed stochastic model gives robust decisions that lead to VSS of \$34 M and 34% ( $= 100 \cdot (138 - 103) / 103$ ) higher expected profit for the LBSC than that of the deterministic model. The deterministic model incurs more costs for purchasing crop residue and higher penalty for unmet bioethanol demand. The stochastic model maximizes the expected profit by increasing bioethanol production volume to take advantage of scenarios with high bioethanol demand and/or high sale price.

Switchgrass cultivation footprint obtained from the deterministic and stochastic models is displayed in Fig. 17 and Fig. 18 respectively. The western part of ND is relatively arid (compared to the eastern part) and annually receives 391 mm of rainfall while the state-wide level is 449 mm [40], and is therefore shown to not be selected as cultivation sites by both models. The stochastic model utilizes 27% ( $= 100 \cdot (3689 - 2906) / 2906$ ) more marginal land than the deterministic model. The amount of marginal land allocated for switchgrass cultivation (i.e. first-stage continuous variable) is shown to be extremely sensitive to the inherent uncertainty in switchgrass yield. To reduce the impact of the expensive purchase cost of crop residue needed to meet the shortfall in biomass requirement due to



below average switchgrass yields, the stochastic model prefers to cultivate switchgrass over a larger area of marginal land when compared to the deterministic model. Both the deterministic model and the proposed stochastic model select the same optimum number (i.e. six) and location of biorefineries.

**Table 4. Comparison of deterministic model vs. proposed stochastic model for the base-case**

Expected annualized values	Results	
	Deterministic model	Stochastic model
Expected LBSC profit (\$ M)	103	138
Expected LBSC revenue (\$ M)	1427	1541
Expected LBSC cost (\$ M)	1324	1403
Expected purchase cost of crop residue (\$ M)	49	12
Expected penalty cost of unmet bioethanol demand (\$ M)	25	0
<b>First-stage decision variables</b>		
Total marginal land used for switchgrass cultivation ('000 Hectare)	476	604
Total marginal land used as % of available marginal land	60%	76%
Total volume of bioethanol production (MLPY) in North Dakota	2131	2237
Production volume (MLPY) for biorefinery at Burleigh county	380	380
Production volume (MLPY) for biorefinery at Ramsey county	380	380
Production volume (MLPY) for biorefinery at Walsh county	380	380
Production volume (MLPY) for biorefinery at Stutsman county	337	380
Production volume (MLPY) for biorefinery at Rolette county	299	380
Production volume (MLPY) for biorefinery at Richland county	360	344



 North Dakota State Boundary  
 County Boundary and Name

 Biorefinery  
 Switchgrass Cultivation Sites

1 mile = 1.61 km  
 0 50  
 Miles

**Fig. 17. Switchgrass cultivation sites and biorefinery locations (deterministic model)**



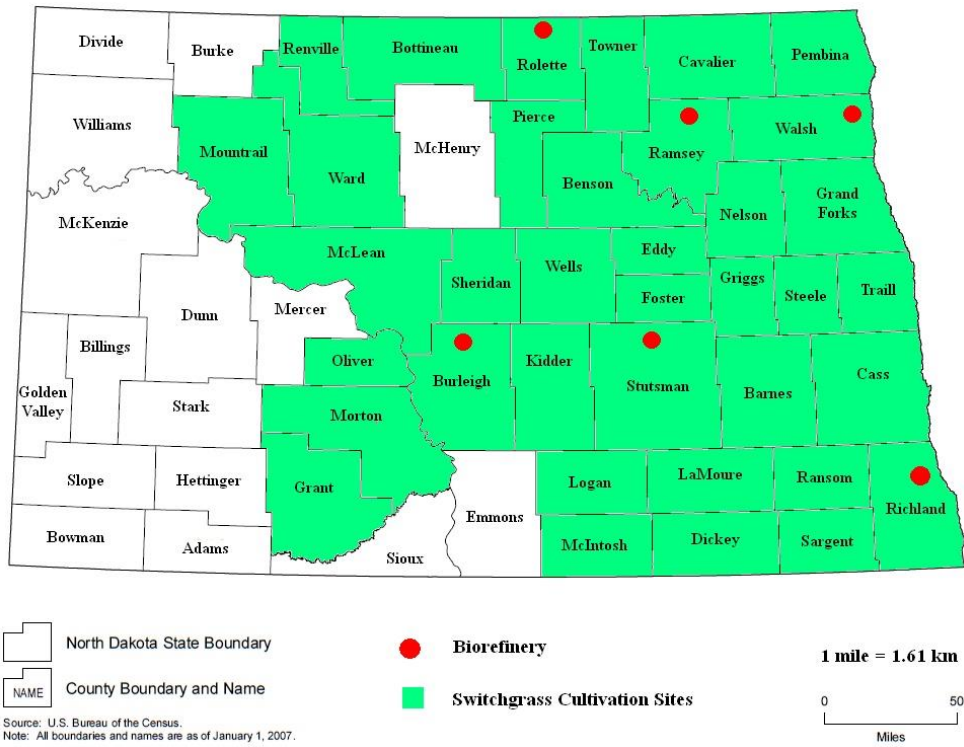


**Fig. 18. Switchgrass cultivation sites and biorefinery locations (stochastic model)**

The optimum location of biorefineries is invariably near switchgrass supply zones with high biomass yields [34]. Historical data analysis shows that the annual rainfall level in each county is highly correlated ( $> 0.85$ ) due to the small geographical scale of the LBSC (i.e. only a single state is considered). Therefore, although the switchgrass yield for an individual supply zone varies considerably (mainly based on the level of annual rainfall), but it is correlated with the switchgrass yield of other supply zones in ND. This leads to the first-stage integer variables being insensitive to the inherent uncertainty in switchgrass yield.

The deterministic and stochastic models select different total bioethanol production volumes. The stochastic model produces 5% ( $= 100 \cdot (2237 - 2131) / 2131$ ) more bioethanol volume than the deterministic model. Bioethanol production volume for each biorefinery (i.e. first-stage continuous variable) is shown to be extremely sensitive to the in-state bioethanol demand uncertainty. To minimize the impact of the high penalty cost for unmet in-state bioethanol demand, the proposed stochastic model shows that it is optimal to produce more bioethanol compared to the deterministic model.

The proposed stochastic model is shown to be more effective than the counterpart deterministic model. However, the computational burden of the proposed stochastic model is significant with the optimal solution being reached after 16.25 hours of CPU run time. While the optimal solution of the deterministic model (run over a single scenario using the “mean” values of the input parameters) is trivial (i.e. < 1 min of CPU run time). Using the optimal values of the first-stage integer decision variables (i.e. locations of bioethanol refineries) obtained from the deterministic model as a surrogate solution for the uncertain environment, the computational burden of the stochastic model is considerably reduced (i.e. only the optimal values for marginal land allocation and production capacities of biorefineries need to be determined). The optimum solution for the reduced stochastic linear programming model (with only continuous first-stage decision variables) is reached after only 0.2 hours of CPU run time while maintaining the overall accuracy of the results.

### 3.8.2. Under different levels of variability

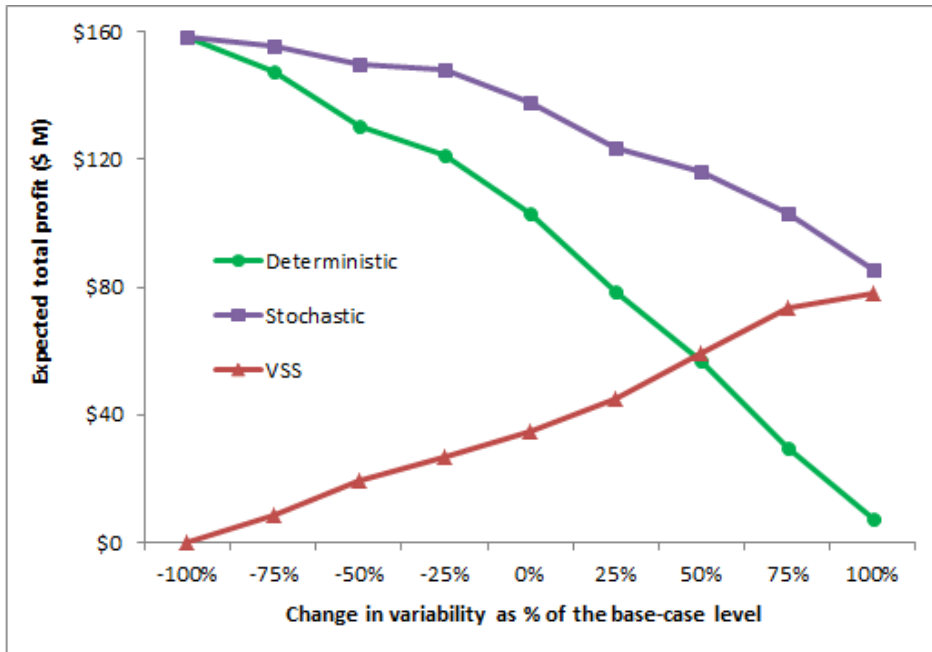
The variability level of each stochastic parameter is changed as a specific percentage of the base-case level. Table 5 displays a number of “cases” that are used to evaluate the impact of variability level on financial performance of both models. In case 1 there is no variability while in case 8 the variability level of each stochastic parameter is double that of the base-case level.

**Table 5. Different levels of variability**

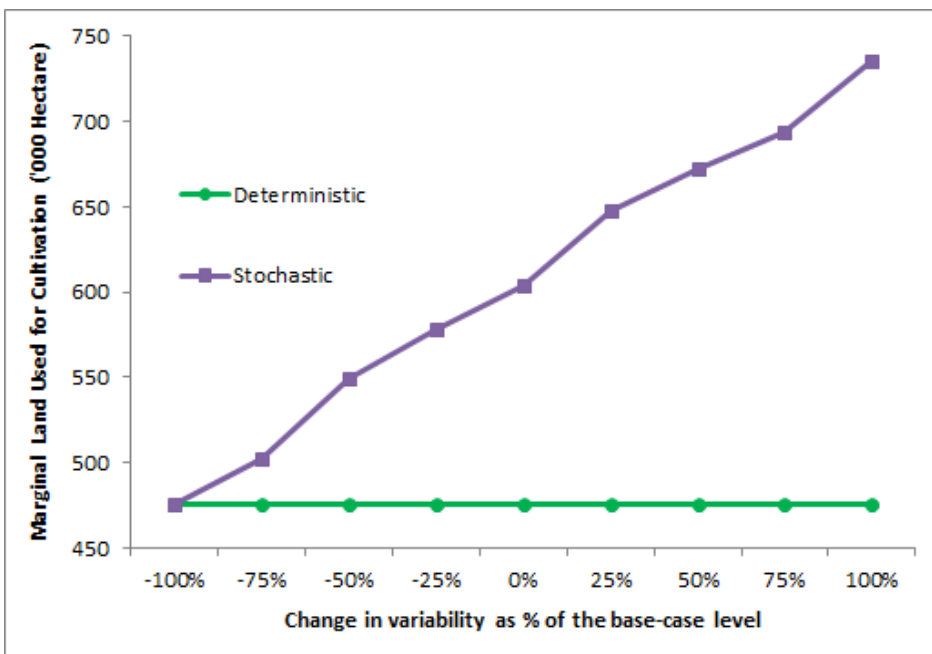
Variability case	% change from base-case	CV of stochastic parameters			
		$\delta$	$M$	$\varepsilon$	$t$
case1	-100%	0.00	0.00	0.00	0.00
case2	-75%	0.04	0.01	0.04	0.04
case3	-50%	0.08	0.02	0.08	0.08
case4	-25%	0.12	0.02	0.12	0.11
base-case	0%	0.16	0.03	0.16	0.15
case5	25%	0.20	0.04	0.20	0.19
case6	50%	0.24	0.05	0.24	0.23
case7	75%	0.28	0.05	0.28	0.26
case8	100%	0.32	0.06	0.32	0.30

Fig. 19 shows that as variability increases the financial performances of both the deterministic and the proposed stochastic model are degraded. However, the proposed stochastic model increasingly outperforms the deterministic model under uncertainties, and the VSS increases with rising variance.

Fig. 20 shows the impact of variability on marginal land allocation for switchgrass cultivation.



**Fig. 19. Impact of variability on expected profit**



**Fig. 20. Impact on marginal land allocation**

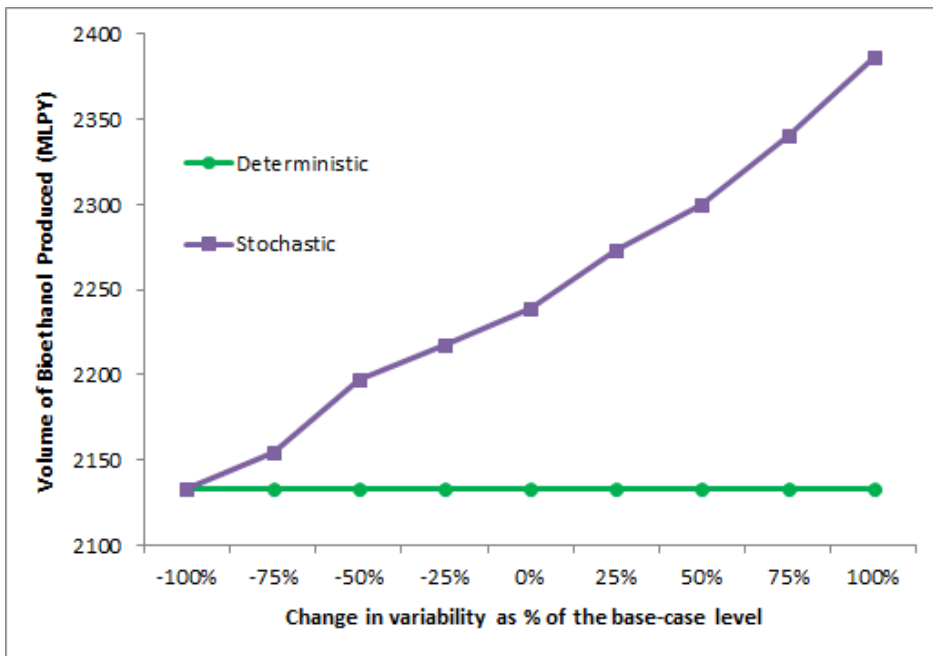


**Fig. 21. Impact on bioethanol production**

Fig. 20 and Fig. 21 show that as variability increases the deterministic model increasingly underestimates the marginal land allocation for switchgrass cultivation and the volume of bioethanol production, respectively. This demonstrates the effectiveness of the proposed stochastic model compared to the deterministic model under all levels of variability in an uncertain environment.

### 3.8.3. For different levels of recourse parameters

Table 6 summarizes the performance of the proposed stochastic model vs. the deterministic model for different levels of the recourse parameters of crop residue purchase price ( $\varepsilon$ ) and penalty cost for unmet bioethanol demand ( $\varphi$ ).

The stochastic parameter  $\varepsilon(\omega)$  has a “mean” value of \$83/tonne and a minimum value of \$50/tonne. The value of the deterministic parameter  $\varphi$  is set at \$1.06/liter (i.e. double the “mean” ethanol sale price) and the minimum possible value is \$0/liter (i.e. no penalty resulting from unmet demand). Only when both  $\varepsilon$  and  $\varphi$  are simultaneously at their lowest level,  $VSS \approx 0$ . Otherwise VSS is significant even when  $\varepsilon$  and  $\varphi$  are separately (but not jointly) at the minimum possible level.

**Table 6. VSS at different levels of crop residue price ( $\varepsilon$ ) and penalty for unmet demand ( $\varphi$ )**

Crop residue purchase price " $\varepsilon$ " (\$/tonne)	Penalty cost for unmet ethanol demand " $\varphi$ " (\$/liter)	Expected LBSC profit (\$ M)		VSS (\$ M)
		Deterministic model	Stochastic model	
83	1.06	103	138	35
50	1.06	126	149	23
83	0.00	129	142	13
50	0.00	151	152	1

### 3.9. Sensitivity analysis

The analysis so far using the base-case has considered the “mean” values of the stochastic parameters that are obtained from historical data analysis and current literature. However the mean values of the stochastic parameters might be different from the base-case when logistic decisions are made. Sensitivity analysis is conducted to evaluate the impact of different mean values of the following stochastic parameters on the expected profit and major LBSC logistic decision variables: 1) sale price of ethanol; 2) in-state demand for bioethanol; 3) annual rainfall level and crop residue purchase price (inversely correlated to rainfall level).

Sensitivity analysis is also conducted to measure the impact of different levels of penalty for unmet bioethanol demand (i.e. deterministic parameter) on the major LBSC logistic decision variables.

#### 3.9.1. Impact of mean value of ethanol sale price on the LBSC logistic decisions

In the base-case the mean value of bioethanol sale price ( $\iota(\omega)$ ) is \$0.53/liter. For sensitivity analysis the mean value of  $\iota(\omega)$  is varied from \$0.26/liter to \$0.79/liter.

Fig. 22 indicates that level of mean value of  $\iota(\omega)$  significantly impacts the expected profit in a step-wise linear function. The break-even point is achieved once mean value of  $\iota(\omega)$  exceeds \$0.4/liter. When mean value of  $\iota(\omega)$  is between \$0.4/liter and \$0.53/liter, the expected profit is flat at \$138 M as the difference between expected revenue and cost is static. As mean value of  $\iota(\omega)$  exceeds \$0.53/liter, the expected profit increases linearly as the expected costs remain static.

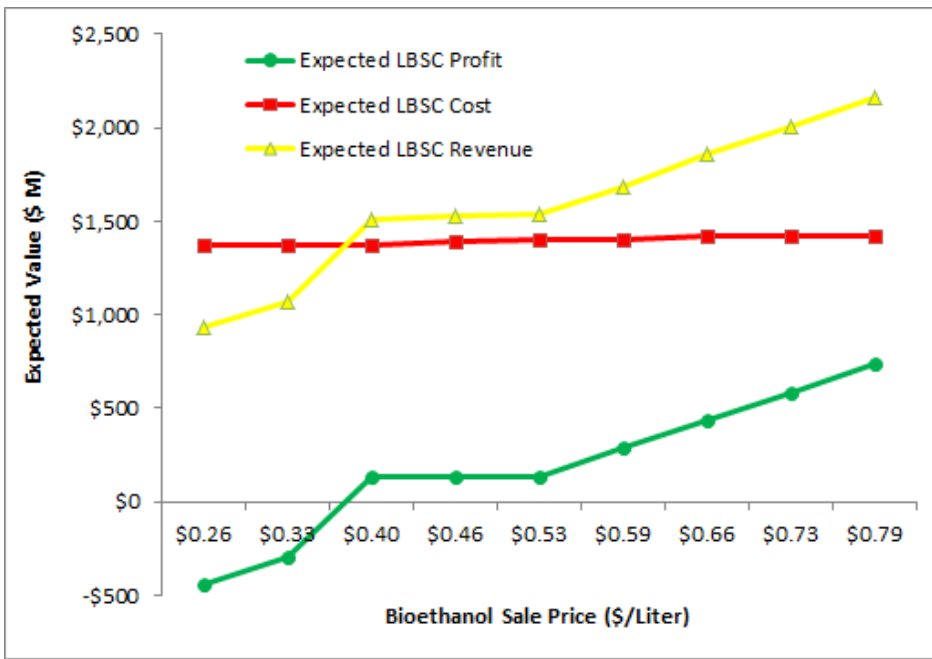


Fig. 22. Impact of ethanol price on profit

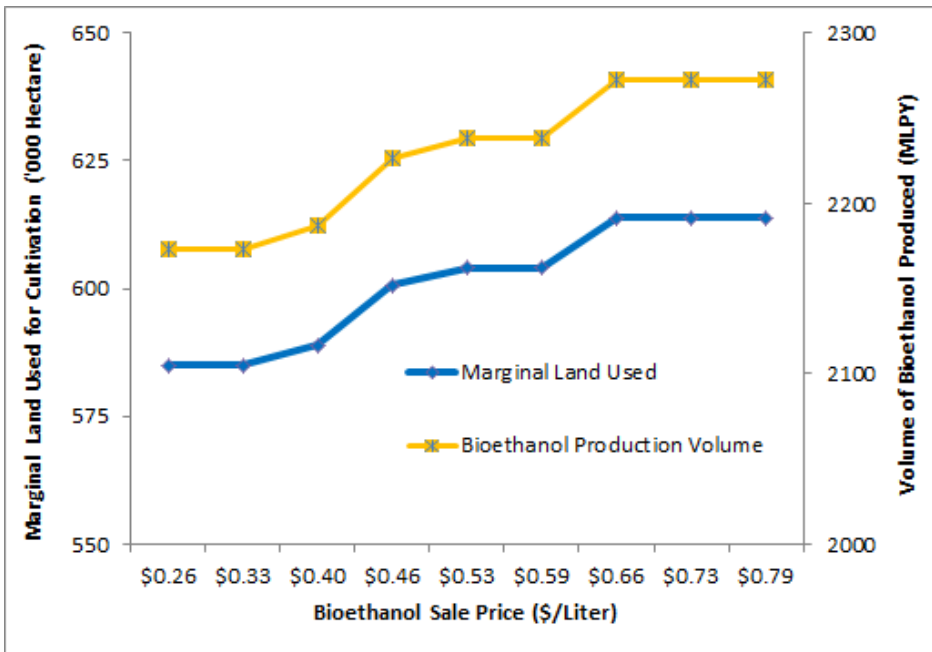


Fig. 23. Impact of ethanol price on decisions

Fig. 23 indicates that the amount of marginal land used for switchgrass cultivation is static at its lowest value until mean value of  $i(\omega)$  reaches the break-even point of \$0.4/liter. The amount of marginal land used linearly increases with the increase in mean value of  $i(\omega)$  from \$0.4/liter to \$0.66/liter. As mean value of  $i(\omega)$  exceeds \$0.66/liter, the demand for biomass plateaus and no extra

marginal land is needed for switchgrass cultivation. Fig. 23 also indicate that mean value of  $\iota(\omega)$  significantly impacts the total volume of bioethanol produced. The bioethanol production volume jumps from 2173 MLPY to 2237 MLPY once mean value of  $\iota(\omega)$  exceeds \$0.46/liter. As mean value of  $\iota(\omega)$  increases further to \$0.66/liter, the volume of bioethanol produced increases until it reaches its maximum production level of 2280 MLPY. Increase in mean value of  $\iota(\omega)$  acts as an incentive for higher bioethanol production. The increased demand for biomass feedstock requires more marginal land for switchgrass cultivation.

### **3.9.2. Impact of mean value of in-state ethanol demand on the LBSC logistic variables**

In the base-case mean value of in-state ethanol demand ( $M(\omega)$ ) is 2133 MLPY. For sensitivity analysis the mean value of  $M(\omega)$  is varied between 2006 MLPY and 2280 MLPY.

Fig. 24 indicate that mean value of  $M(\omega)$  significantly impacts the expected profit. As mean value of  $M(\omega)$  increases from 2006 MLPY to 2158 MLPY, the expected profit is relatively flat. The highest amount of profit is expected when mean value of  $M(\omega)$  is between 2158 MLPY to 2195 MLPY. However, the expected LBSC profit starts to decrease once mean value of  $M(\omega)$  exceeds 2233 MLPY. Biomass requirements needed to satisfy mean value of  $M(\omega)$  greater than 2195 MLPY invariably leads to switchgrass being cultivated on marginal lands with high rental cost and/or low switchgrass yields that are located further away from biorefineries, thus incurring substantial transportation costs that reduce the expected profit.

Fig. 25 indicate that amount of marginal land used for switchgrass cultivation is static at its lowest value until mean value of  $M(\omega)$  reaches 2044 MLPY. Amount of marginal land used linearly increases with increase in mean value of  $M(\omega)$  from 2082 MLPY to 2158 MLPY. As mean value of  $M(\omega)$  exceeds 2158 MLPY, demand for biomass plateaus and no extra marginal land is needed for switchgrass cultivation. Fig. 25 also indicate that mean value of  $M(\omega)$  significantly impacts the volume of bioethanol produced. Bioethanol production volume linearly increases from 2105 MLPY to 2280

MLPY as mean value of  $M(\omega)$  increases from 2006 MLPY to 2158 MLPY. As mean value of  $M(\omega)$  exceeds 2158 MLPY it has no effect on the volume of bioethanol produced which has already plateaued out as its maximum production volume of 2280 MLPY.

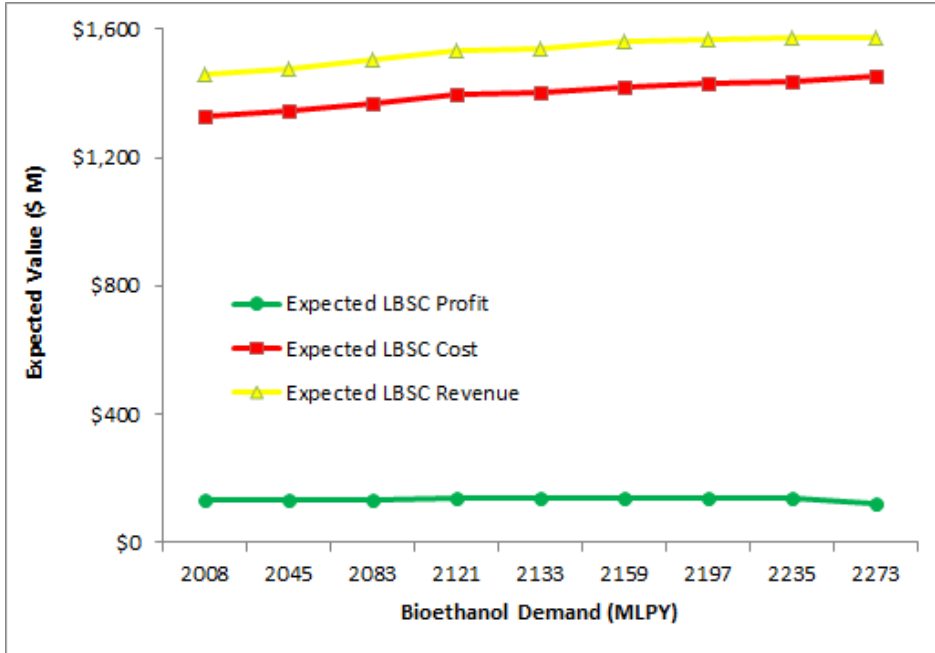


Fig. 24. Impact of ethanol demand on profit

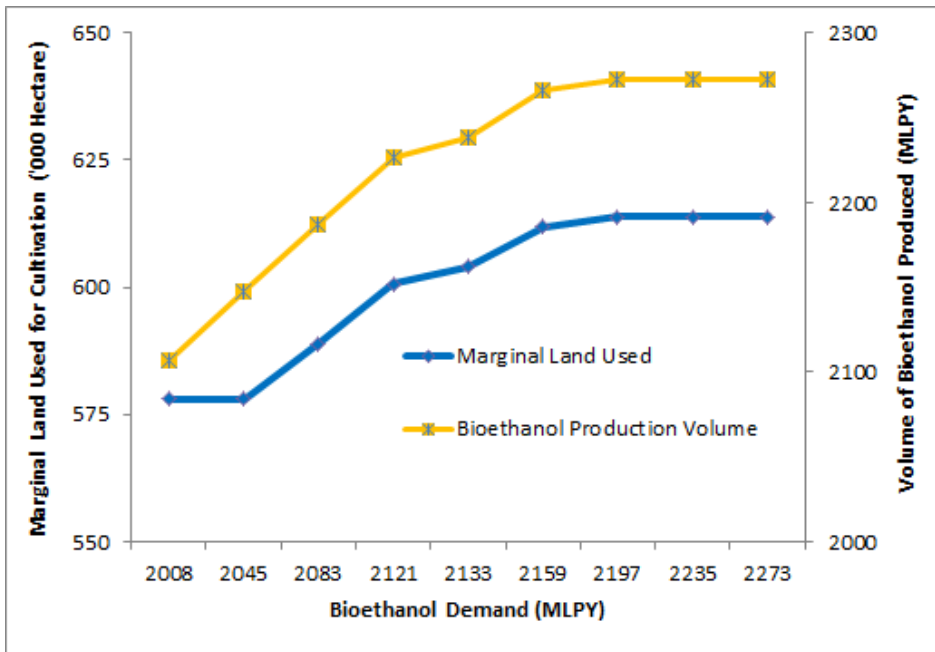


Fig. 25. Impact of ethanol demand on decisions



### 3.9.3. Impact of mean value of rainfall (and crop residue price) on LBSC logistic variables

Mean value of annual rainfall level ( $\delta(\omega)$ ) is 449 mm. For sensitivity analysis the mean value of  $\delta(\omega)$  is varied between 218 mm to 620 mm. Crop residue purchase price ( $\varepsilon(\omega)$ ) is inversely correlated to rainfall level. Mean value of  $\varepsilon(\omega)$  is \$83/tonne and is varied between \$51/tonne to \$125/tonne.

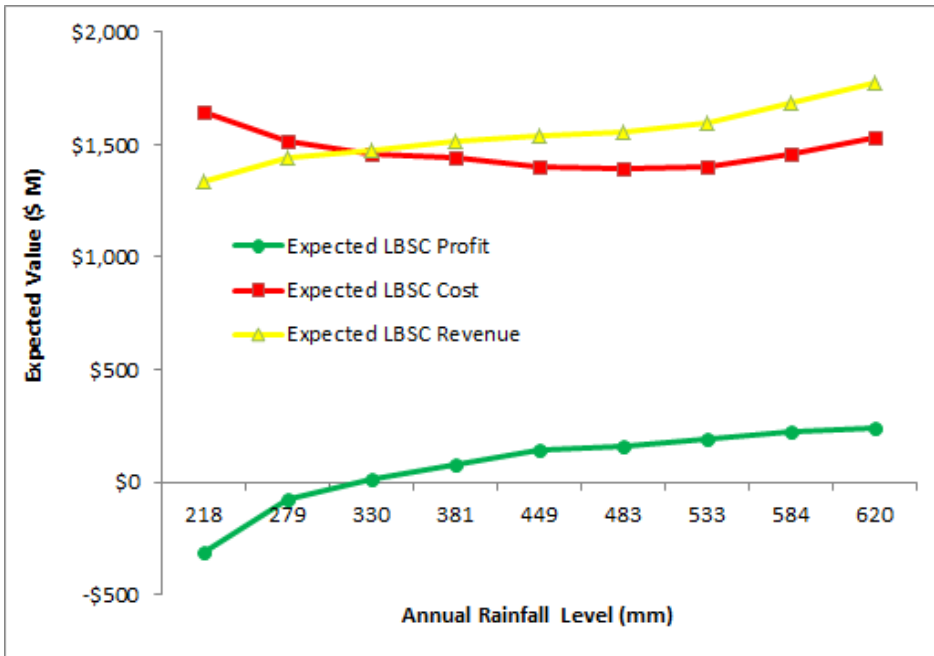


Fig. 26. Impact of rainfall level on profit

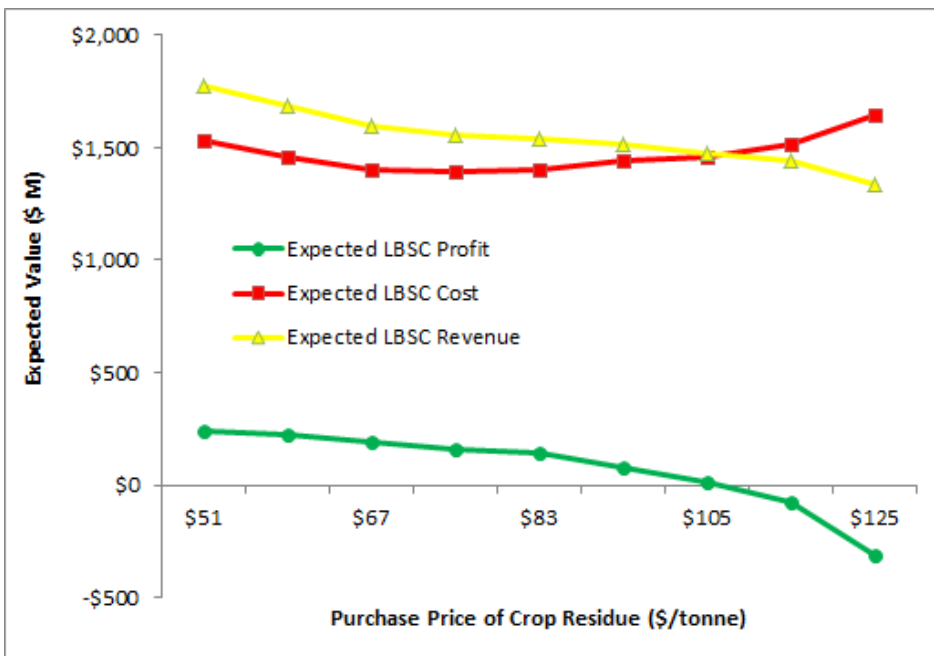
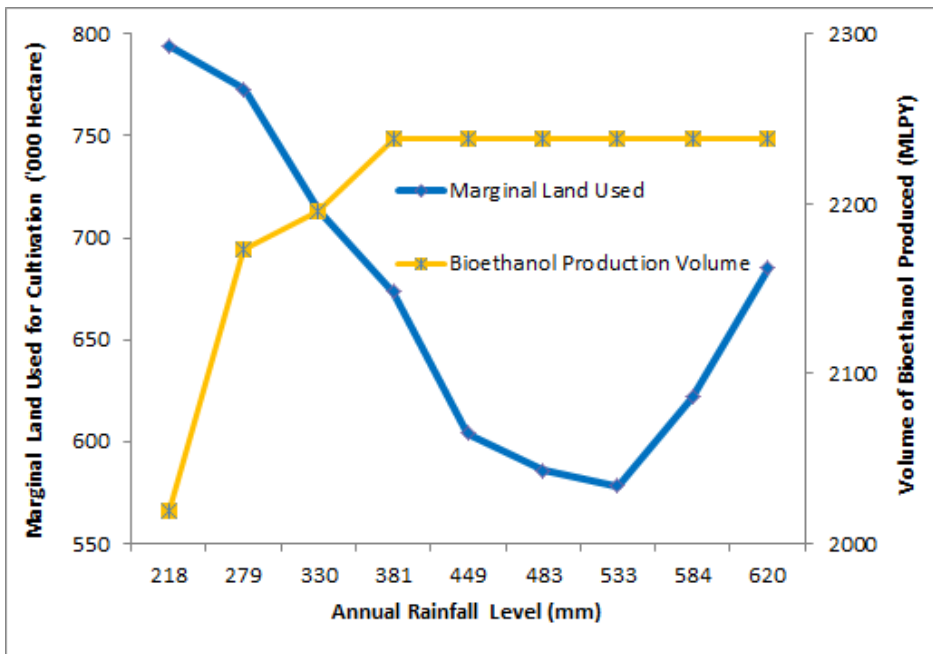
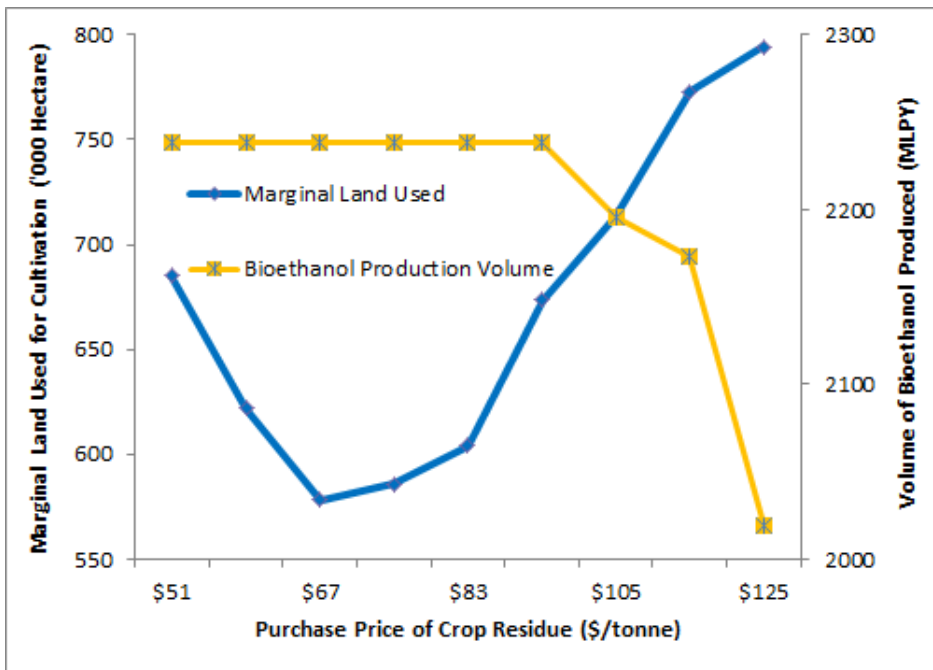


Fig. 27. Impact of crop residue price on profit



**Fig. 28. Impact of rainfall level on decisions**



**Fig. 29. Impact of residue price on decisions**

Figs. 26 and 27 indicate that mean value of  $\delta(\omega)$  and  $\varepsilon(\omega)$  significantly impacts the expected profit in a curvilinear manner. The break-even point is achieved once mean value of  $\delta(\omega) > 330$  mm and mean value of  $\varepsilon(\omega)$  is  $< \$105$ /tonne.

Figs. 28 and 29 indicate that mean values of  $\delta(\omega)$  and  $\varepsilon(\omega)$  significantly impacts the amount of marginal land used for switchgrass cultivation. When mean value of  $\delta(\omega)$  is less than 280 mm and mean value of  $\varepsilon(\omega)$  exceeds \$113/tonne, all of the available marginal land is used for switchgrass cultivation. As mean value of  $\delta(\omega)$  increases to 508 mm and mean value of  $\varepsilon(\omega)$  falls below \$72/tonne, only three-fourths of the available marginal land is used (i.e. lowest level). As mean value of  $\delta(\omega)$  exceeds 533 mm and mean value of  $\varepsilon(\omega)$  is less than \$67/tonne, the amount of marginal land used starts to increase again. This results in higher switchgrass production and the excess amount is sold for additional profit.

Figs. 28 and 29 also indicate that mean values of  $\delta(\omega)$  and  $\varepsilon(\omega)$  significantly impacts the volume of bioethanol produced. Bioethanol production volume linearly increases from 2033 MLPY to 2237 MLPY as mean value of  $\delta(\omega)$  increases from 218 mm to 381 mm and mean value of  $\varepsilon(\omega)$  decreases from \$116/tonne to \$95/tonne. As mean value of  $\delta(\omega)$  exceeds 381 mm and mean value of  $\varepsilon(\omega)$  is less than \$95/tonne, the volume of bioethanol produced is unaffected (i.e. already plateaued out at a production volume of 2237 MLPY). Even the highest (i.e. 620mm) mean value of  $\delta(\omega)$  and the lowest (i.e. \$50/tonne) mean value of  $\varepsilon(\omega)$  does not offer sufficient inducement to increase bioethanol production volume above 2237 MLPY. Similar results are also displayed in Fig. 24 which show that the expected profit starts to decrease once the bioethanol production volume exceeds 2195 MLPY.

#### **3.9.4. Impact of penalty cost of unmet bioethanol demand on the LBSC logistic variables**

Penalty cost for unmet bioethanol demand ( $\varphi$ ) is a deterministic parameter and is varied between \$0/liter (i.e. there is no penalty) and \$1.06/liter (i.e. severe penalty equal to double the “mean” sale price of ethanol) [27].

Fig. 30 indicates that penalty cost for unmet ethanol demand marginally impacts the expected LBSC profit. As  $\varphi$  increases from \$0/liter to \$1.06/liter, the expected LBSC profit decreases in a very narrow band from \$138 M to \$142 M.

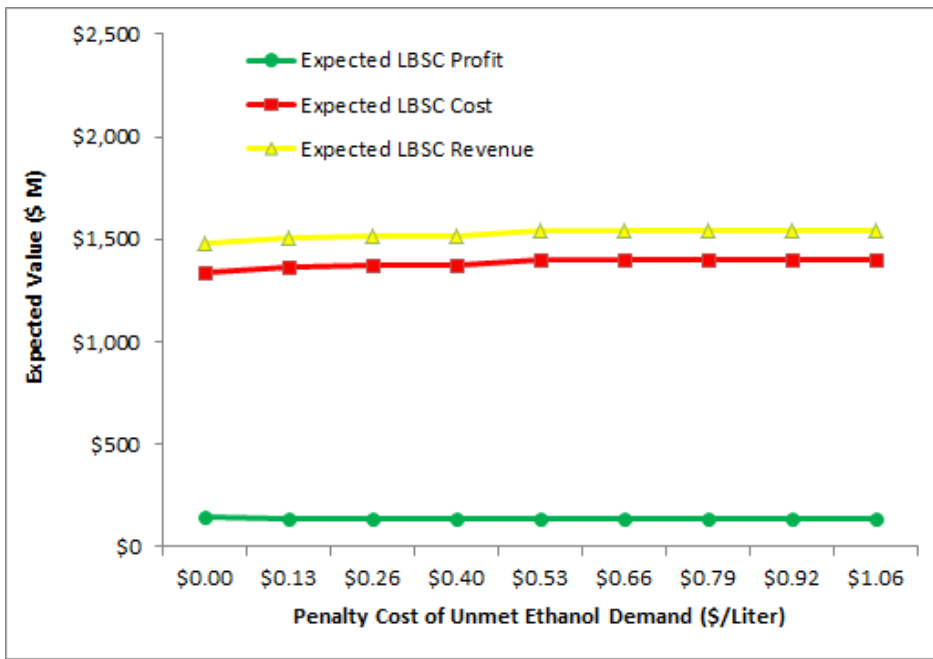


**Fig. 30. Impact of penalty cost on profit**

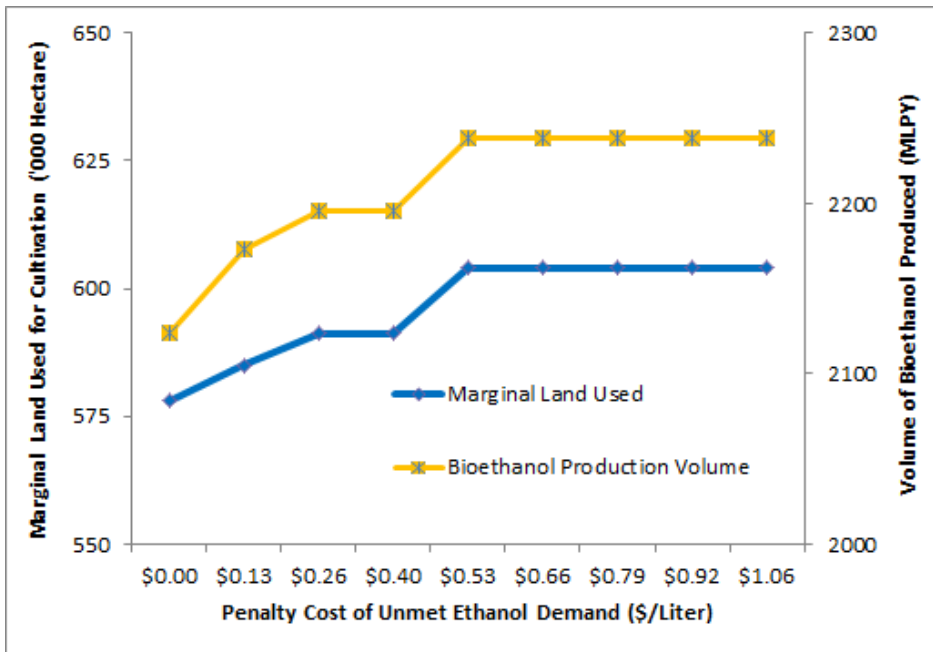


**Fig. 31. Impact of penalty cost on decisions**

Fig. 31 indicates that the bioethanol production volume generally increases in a linear manner from 2123 MLPY to 2237 MLPY as penalty cost for unmet ethanol demand increases from \$0/liter to \$0.53/liter. As penalty cost for unmet ethanol demand exceeds \$0.53/liter (i.e. equal to the “mean” price of ethanol), the volume of bioethanol produced is unaffected (i.e. already plateaued out at a production

volume of 2237 MLPY). Even when  $\varphi = \$0/\text{liter}$ , the volume of bioethanol produced is significant at 2123 MLPY. Bioethanol production level is influenced more by the opportunity to generate higher sales of ethanol due to increase in bioethanol demand rather than by trying to avoid high penalty cost for unmet ethanol demand. Fig. 31 also indicates that the amount of marginal land used increases linearly as penalty cost for unmet ethanol demand increases from  $\$0/\text{liter}$  to  $\$0.53/\text{liter}$ . As penalty cost for unmet ethanol demand exceeds  $\$0.53/\text{liter}$ , the amount of marginal land used is unaffected (i.e. already plateaued out).

### **3.10. Conclusion**

This paper studies a multi feedstock LBSC under multiple and jointly occurring uncertainties in switchgrass yield, crop residue purchase price, bioethanol demand, and bioethanol sale price. A two-stage stochastic MILP model is proposed to maximize the expected LBSC profit by determining the optimal values of the first-stage decisions that include both integer (i.e. locations of biorefineries) and continuous variables (i.e. allocation of marginal land for switchgrass cultivation, and bioethanol production capacity for each biorefinery).

A case study based on ND state in the U.S. illustrates the application of the proposed stochastic model. The results demonstrate that the proposed stochastic model outperforms the counterpart deterministic model (under uncertainties) across different variability and recourse parameter levels. The deterministic model underestimates the marginal land allocation for switchgrass cultivation and the volume of bioethanol production. As variability of the stochastic parameters increases, the financial performance of both the deterministic and stochastic models is degraded. However, the proposed stochastic model increasingly outperforms the deterministic model under uncertainties, and the VSS increases with rising variance. Results shows that across all levels of variability in a stochastic environment, it is cost effective to meet 100% of ND's annual gasoline demand from locally produced

bioethanol by using switchgrass as the primary (on account of lower cost) and crop residue as the secondary biomass feedstock.

The main computational burden of the stochastic model is due to the first-stage integer decision variable (i.e. location of biorefineries). Both the deterministic model and the proposed stochastic model select the same locations of biorefineries due to the highly correlated switchgrass yield among the biomass supply zones. Using the first-stage binary decisions (i.e. locations of biorefineries) obtained from the deterministic model as a surrogate solution for the stochastic environment considerably reduces the computational time while preserving the overall accuracy of the stochastic model.

Sensitivity analyses are conducted to evaluate the impact of different level of “mean” values of the four stochastic parameters: ethanol sale price, in-state ethanol demand, annual rainfall level and crop residue purchase price (inversely correlated to annual rainfall level). The results show: 1) Increase in mean ethanol sale price stimulates higher bioethanol production volume. This requires more marginal land for switchgrass cultivation. In order to maintain a profitable LBSC the mean ethanol sale price should exceed a threshold; 2) When the mean ethanol demand increases, the bioethanol production volume increases as well to obtain higher profit and prevent higher penalty cost due to unmet bioethanol demand; 3) When mean rainfall level increases, the bioethanol production volume increases as well. As mean rainfall level exceeds a minimum value the bioethanol production volume is unchanged; and 4) When mean crop residue purchase price exceeds a minimum value, all of the available marginal land is used for switchgrass cultivation. As mean crop residue purchase price falls below a maximum value, minimum amount of available marginal land is used.

Sensitivity analysis also indicates that as penalty cost of unmet bioethanol demand (i.e. deterministic parameter) increases, a greater area of marginal land is allocated for switchgrass cultivation and a larger ethanol production capacity is assigned to biorefineries (i.e. first-stage continuous decision variables) to prevent high penalty due to unmet demand for bioethanol. As penalty

cost exceeds a threshold the optimal values of first-stage continuous decision variables are unchanged as demand for bioethanol is fully satisfied.

This work optimizes LBSC by considering single objective of economic performance. Chapter 4 will optimize LBSC by considering multiple criteria such as economic and environmental performances [38, 42]. For example, environmental performance is evaluated by the reduction in greenhouse gas emissions [39, 43, 44] through imposition of a carbon tax [45, 46]. Additional lignocellulosic-based biomass resources such as short rotation woody crops, forest residue, and municipal solid waste will also be considered as feedstock in Chapter 4 [47].

### 3.11. Nomenclature

#### 3.11.1. Indices

- $e$  Bioethanol demand zones ( $e = 1, \dots, E$ )
- $i$  Lignocellulosic biomass supply zones ( $i = 1, \dots, I$ )
- $r$  Biorefinery locations ( $r = 1, \dots, R$ )
- $\omega$  Stochastic scenarios ( $\omega = 1, \dots, \Omega$ )

#### 3.11.2. First stage continuous decision variables

- $F1$  Rental cost of marginal land (\$)
- $F2$  Cultivation cost of switchgrass (\$)
- $F3$  Harvesting cost of switchgrass (\$)
- $F4$  Operational cost of biorefineries (\$)
- $F5$  Cost of installed biorefineries (\$)
- $X_i$  Marginal land area in supply zone  $i$  used for switchgrass cultivation (hectare)
- $Z_r$  Volume of bioethanol produced by biorefinery in location  $r$  (liter)

### 3.11.3. First stage binary decision variables

$Y_r$  1 if biorefinery setup in location  $r$ , 0 otherwise

### 3.11.4. Second stage decision variables

$C1(\omega)$  Penalty cost of unmet bioethanol demand during scenario  $\omega$  (\$)

$C2(\omega)$  Preprocessing cost of loose chop switchgrass during scenario  $\omega$  (\$)

$C3(\omega)$  Transportation cost of densified switchgrass during scenario  $\omega$  (\$)

$C4(\omega)$  Purchase cost of crop residue during scenario  $\omega$  (\$)

$C5(\omega)$  Transportation cost of crop residue during scenario  $\omega$  (\$)

$C6(\omega)$  Transportation cost of bioethanol during scenario  $\omega$  (\$)

$F_{ir}(\omega)$  Amount of crop residue sent from biomass supply zone  $i$  to biorefinery  $r$  during scenario  $\omega$   
(tonne)

$J_i(\omega)$  Amount of densified switchgrass directly sold from biomass supply zone  $i$  during scenario  $\omega$   
(tonne)

$K_i(\omega)$  Amount of loose chop switchgrass harvested from biomass supply zone  $i$  during scenario  $\omega$   
(tonne)

$L_r(\omega)$  Volume of unsubsidized bioethanol directly sold from biorefinery  $r$  during scenario  $\omega$  (liter)

$O_e(\omega)$  Volume of unmet bioethanol requirement in biofuel demand zone  $e$  during scenario  $\omega$  (liter)

$R1(\omega)$  Revenue from the sale of densified switchgrass during scenario  $\omega$  (\$)

$R2(\omega)$  Revenue from the sale of bioethanol during scenario  $\omega$  (\$)

$R3(\omega)$  Tax credit accrued from the sale of subsidized bioethanol during scenario  $\omega$  (\$)

$S_{re}(\omega)$  Volume of subsidized ethanol from refinery in location  $r$  sent to biofuel demand zone  $e$  during  
scenario  $\omega$  (liter)

$V_{ir}(\omega)$  Amount of densified switchgrass from biomass supply zone  $i$  sent to biorefinery  $r$  during  
scenario  $\omega$  (tonne)



### 3.11.5. Deterministic parameters

$B_i$	Marginal land area available for switchgrass cultivation in biomass supply zone $i$ (hectare)
$C_i$	Rental cost parameter of marginal land in biomass supply zone $i$ (\$/hectare)
$D_{ir}$	Distance between biomass supply zone $i$ and biorefinery $r$ (km)
$D_{re}$	Distance between biorefinery $r$ and biofuel demand zone $e$ (km)
$G$	Annualized fixed cost of biorefinery (\$)
$H_i$	Switchgrass harvesting cost parameter in biomass supply zone $i$ (\$/hectare)
$N_r$	Operational cost parameter of biorefinery $r$ (\$/liter)
$T$	Annualized variable cost of biorefinery (\$/liter)
$U_i$	Pre-processing cost (including storage cost) parameter of loose chop switchgrass at biomass supply zone $i$ (\$/tonne)
$\chi$	Sale price of densified switchgrass (\$/tonne)
$\beta_r$	Bioethanol yield (from lignocellulosic biomass) parameter for biorefinery $r$ (liter/tonne)
$\gamma_{ir}$	Transportation cost parameter of densified switchgrass from biomass supply zone $i$ to biorefinery $r$ (\$/tonne x km)
$\zeta_i$	Amount of crop residue in biomass supply zone $i$ (tonne)
$\eta_{ir}$	Transport cost parameter of crop residue from supply zone $i$ to biorefinery $r$ (\$/tonne x km)
$\kappa_i$	Switchgrass cultivation cost parameter in biomass supply zone $i$ (\$/hectare)
$\mu_i$	Maximum percentage of available crop residue that can be removed from biomass supply zone $i$
$\rho_{max}$	Maximum bioethanol production capacity of biorefinery (liter)
$\rho_{min}$	Minimum bioethanol production capacity of biorefinery (liter)
$\tau$	Tax credit for subsidized bioethanol production (\$/liter)
$\varphi$	Penalty cost parameter for unmet bioethanol demand (\$/liter)
$\psi_{re}$	Transport cost parameter of ethanol from biorefinery $r$ to biofuel demand zone $e$ (\$/liter x km)

### 3.11.6. Stochastic parameters

$A_i(\omega)$  Switchgrass yield parameter from marginal land in biomass supply zone  $i$  during scenario  $\omega$   
(tonne/hectare)

$M_e(\omega)$  Volumetric requirement of subsidized bioethanol in biofuel demand zone  $e$  during scenario  $\omega$   
(liter)

$\delta_i(\omega)$  Rainfall level in biomass supply zone  $i$  during scenario  $\omega$  (mm)

$\varepsilon(\omega)$  Purchase price of crop residue during scenario  $\omega$  (\$/tonne)

$\iota(\omega)$  Sale price of bioethanol during scenario  $\omega$  (\$/liter)

$P(\omega)$  Probability that scenario  $\omega$  will happen

### 3.12. References

- [1] Energy Information Administration, “Annual Energy Outlook 2011,” Report Number: DOE/EIA-0383(2011). [http://www.eia.gov/forecasts/aeo/pdf/0383\(2011\).pdf](http://www.eia.gov/forecasts/aeo/pdf/0383(2011).pdf)
- [2] CRS adaptation of Energy Information Administration, Annual Energy Review 2009. [http://www.eia.doe.gov/totalenergy/data/annual/pdf/pecss\\_diagram\\_2009.pdf](http://www.eia.doe.gov/totalenergy/data/annual/pdf/pecss_diagram_2009.pdf)
- [3] Sokhansanj S, Mani S, Turhollow, Kumar A, Bransby D, Lynd L, Laser M. Large-scale production, harvest and logistics of switchgrass – current technology and envisioning a mature technology. *Biofuels, Bioprod. Bioref.* 2009;3:124–41.
- [4] U.S. Energy Independence and Security Act of 2007 (EISA).
- [5] Carriquiry M, Du X, Timilsina G. Second generation biofuels: Economics & policies. *Energy Policy* 2011;39:4222–34.
- [6] Zhang J, Osmani A, Awudu I, Gonela V. An integrated optimization model for switchgrass-based bioethanol supply chain. *Applied Energy* 2013;102:1205–1217.
- [7] Cherubini F, Ulgiati S. Crop residues as raw materials for biorefinery systems – A LCA case study. *Appl Energy* 2010;87(1):47–57.

- [8] Parker N, Tittmann P, Hart Q, Nelson R, Skog K, Schmidt A, Gray E, Jenkins B. Development of a biorefinery optimized biofuel supply curve for the Western United States. *Biomass and Bioenergy* 2010;34: 1597–1607.
- [9] Kou N, Zhao F. Effect of multiple-feedstock strategy on the economic and environmental performance of thermochemical ethanol production under extreme weather conditions. *Biomass and Bioenergy* 2011;35: 608–16.
- [10] Zhu X, Yao Q. Logistics system design for biomass-to-bioenergy industry with multiple types of feedstocks. *Bioresour. Technol* 2011;102:10936–10945.
- [11] Morey R, Kaliyan N, Tiffany D, Schmidt D. A corn stover supply logistics system. *Applied Engineering in Agriculture* 2010;26(3):455–61.
- [12] Adapaa P, Tabila L, Schoenau G. Compaction characteristics of barley, canola, oat and wheat straw. *Biosystems Engineering* 2009;104:335–44.
- [13] Murphy J, McCarthy K. Ethanol production from energy crops and wastes for use as a transport fuel in Ireland. *Appl Energy* 2005;82(2):148–166.
- [14] Gallagher M, Hockaday W, Masiello C, Snapp S, McSwiney C, Baldock J. Biochemical Suitability of Crop Residues for Cellulosic Ethanol: Disincentives to Nitrogen Fertilization in Corn Agriculture. *Environ. Sci. Technol.* 2011;45:2013–20.
- [15] Li Z, Liu Y, Liao W, Chen S, Zemetra R. Bioethanol production using genetically modified and mutant wheat and barley straws. *Biomass and Bioenergy* 2011;35: 542–48.
- [16] Kou N, Zhao F. Techno-economical analysis of a thermo-chemical biofuel plant with feedstock and product flexibility under external disturbances. *Energy* 2011;36:6745–52.
- [17] Leduc S, Starfelt F, Dotzauer E, Kindermann G, McCallum I, Obersteiner M, Lundgren J. Optimal location of lignocellulosic ethanol refineries with polygeneration in Sweden. *Energy* 2010;35:2709–2716.

- [18] Van Dyken S, Bakken B, Skjelbred H. Linear mixed-integer models for biomass supply chains with transport, storage and processing. *Energy* 2010;35:1338–1350.
- [19] Papapostolou C, Kondili E, Kaldellis J. Development and implementation of an optimisation model for biofuels supply chain. *Energy* 2011;36:6019–6026.
- [20] Awudu I, Zhang J. Uncertainties and sustainability concepts in biofuel supply chain management: A review. *Renewable and Sustainable Energy Reviews* 2012;16:1359–1368.
- [21] Sahinidis N. Optimization under uncertainty: State-of-the-art and opportunities, *Computers & Chemical Engineering* 2004;28:971–983.
- [22] Birge J, Louveaux F. *Introduction to Stochastic Programming*, first ed. Springer, New York.
- [23] Liu L, Sahinidis N. Optimization in process planning under uncertainty. *Industrial & Engineering Chemistry Research*, 1996;35:4154–4165.
- [24] Kostin A, Guillen-Gosalbez G, Mele F, Bagajewicz M, Jimenez L. Design and planning of infrastructures for bioethanol and sugar production under demand uncertainty. *Chemical Engineering Research and Design* 2012;90:359–376.
- [25] Dal-Mas M, Giarola S, Zamboni A, Bezzo F. Strategic design and investment capacity planning of the ethanol supply chain under price uncertainty. *Biomass and Bioenergy* 2011;35: 2059–71.
- [26] Kim J, Realff M, Lee J. Optimal design and global sensitivity analysis of biomass supply chain networks for biofuels under uncertainty. *Computers and Chemical Engineering* 2011;35:1738– 51.
- [27] Chen C, Fan Y. Bioethanol supply chain system planning under supply and demand uncertainties. *Transportation Research Part E* 2010;48:150–164.
- [28] McLaughlin S, Kszos L. Development of switchgrass (*panicum virgatum*) as a bioenergy feedstock in the United States. *Biomass and Bioenergy* 2005;28:515–35.
- [29] Judd J, Sarin S, Cundiff J. Design, modeling, and analysis of feedstock logistics system. *Bioresour. Technol* 2012;103:209–218.

- [30] Spatari S, Maclean H. Characterizing Model Uncertainties in the Life Cycle of Lignocellulose-Based Ethanol Fuels. *Environ. Sci. Technol.* 2010;44:8773–80.
- [31] Lee D, Boe A. Biomass Production of Switchgrass in Central South Dakota. *Crop Science* 2005;45:2583–90.
- [32] Tyndall J, Berg E, Colletti J. Corn stover as a biofuel feedstock in Iowa’s bio-economy: An Iowa farmer survey. *Biomass and Bioenergy* 2011;35: 1485–95.
- [33] Sharma P, Sarker B, Romagnoli J. A Decision Support Tool for Strategic Analysis of Sustainable Biorefineries. *Computers and Chemical Engineering* 2011;35:1767– 1781.
- [34] Cosic B, Stanic Z, Duic N. Geographic distribution of economic potential of agricultural and forest biomass residual for energy use: Case study Croatia. *Energy* 2011;36:2017–2028.
- [35] Cruse R, Herndl C. Balancing corn stover harvest for biofuels with soil and water conservation. *Journal of Soil and Water Conservation* 2009;64(4):286–291.
- [36] U.S. Energy Information Administration, State Energy Data 2009: Consumption.  
[http://205.254.135.24/state/seds/sep\\_use/total/pdf/use\\_ND.pdf](http://205.254.135.24/state/seds/sep_use/total/pdf/use_ND.pdf)
- [37] O’Brien D, Woolverton M. The Relationship of Ethanol, Gasoline and Oil Prices. Kansas State University 2009.
- [38] You F, Tao L, Graziano D, Snyder S. Optimal Design of Sustainable Cellulosic Biofuel Supply Chains: Multiobjective Optimization Coupled with Life Cycle Assessment and Input–Output Analysis. *AIChE Journal* 2012;58(4):1157–1180.
- [39] Dunnett A, Adjiman C, Shah N. A spatially explicit whole-system model of the lignocellulosic bioethanol supply chain: an assessment of decentralised processing potential. *Biotechnology for Biofuels* 2008;1:13.
- [40] North Dakota Annual 1981-2010 Precipitation.  
<http://www.ndsu.edu/ndsco/precip/monthly/2011.html>

- [41] Czyzyk J, Mesnier M, More J. The NEOS Server. *IEEE J. on Computational Science and Engineering* 1998;5:68–75.
- [42] Palander T. Modelling renewable supply chain for electricity generation with forest, fossil, and wood-waste fuels. *Energy* 2011;36:5984–5993.
- [43] Scott J, Ho W, Dey P. A review of multi-criteria decision-making methods for bioenergy systems. *Energy* 2012;42:146–156.
- [44] Houwing M, Ajah A, Heijnen P, Bouwmans I, Herder P. Uncertainties in the design and operation of distributed energy resources: The case of micro-CHP systems. *Energy* 2008;33:1518–1536.
- [45] Ren H, Zhou W, Nakagami K, Gao W. Integrated design and evaluation of biomass energy system taking into consideration demand side characteristics. *Energy* 2010;35:2210–2222.
- [46] Cucek L, Varbanov P, Klemes J, Kravanja Z. Total footprints-based multi-criteria optimisation of regional biomass energy supply chains. *Energy* 2012;44:135–145.
- [47] Sarkar S, Kumar A, Sultana A. Biofuels and biochemicals production from forest biomass in Western Canada. *Energy* 2011;36:6251–6262.
- [48] United States Census Bureau: 2010 County Population within ND.  
[http://www.ndsu.edu/sdc/data/census/ND\\_CntyRace2010.pdf](http://www.ndsu.edu/sdc/data/census/ND_CntyRace2010.pdf)
- [49] United States Department of Agriculture (USDA), National Agricultural Statistics Service: 2007 Census of Agriculture.
- [50] USDA, National Agricultural Statistics Service: 2011 County Rents & Values.
- [51] Rand McNally. <http://www.randmcnally.com/milage-calculator.do>

## CHAPTER 4. ECONOMIC AND ENVIRONMENTAL OPTIMIZATION OF A LARGE SCALE SUSTAINABLE DUAL FEEDSTOCK LIGNOCELLULOSIC-BASED BIOETHANOL SUPPLY CHAIN IN A STOCHASTIC ENVIRONMENT

### 4.1. Abstract

This work proposes a two-stage stochastic optimization model to maximize the expected profit and simultaneously minimize carbon emissions of a dual-feedstock lignocellulosic-based bioethanol supply chain (LBSC) under uncertainties in supply, demand and prices. The model decides the optimal first-stage decisions and the expected values of the second-stage decisions. A case study based on a 4-state Midwestern region in the U.S. demonstrates the effectiveness of the proposed stochastic model over a deterministic model under uncertainties. Two regional modes are considered for the geographic scale of the LBSC. Under co-operation mode the 4 states are considered as a combined region while under stand-alone mode each of the 4 states is considered as an individual region. Each state under co-operation mode gives better financial and environmental outcomes when compared to stand-alone mode. Uncertainty has a significant impact on the biomass processing capacity of biorefineries. While the location and the choice of conversion technology for biorefineries i.e. biochemical vs. thermochemical, are insensitive to the stochastic environment. As variability of the stochastic parameters increases, the financial and environmental performance is degraded. Sensitivity analysis shows that levels of tax credit and carbon price have a major impact on the choice of conversion technology for a selected biorefinery. Biochemical pathway is preferred over the thermochemical as carbon price increases. Thermochemical pathway is preferred over the biochemical as the level of tax credit increases. In addition, bioethanol production in the U.S. is shown to be unviable without adequate governmental subsidy in the form of tax credits.

## 4.2. Introduction and literature review

In order to secure the energy supply and to safeguard the environment, the U.S. federal government in 2007 enacted the Renewable Fuel Standard (RFS) [1, 2]. In 2022 the annual gasoline demand for the U.S. is projected to be 120000 million gallons (MG). The RFS requires by 2022 the use of bioethanol to displace 20% of the annual gasoline demand on an energy equivalent basis. One gallon of gasoline contains the energy equivalent of 1.5 gallons of ethanol [3]. By 2022 the RFS mandates the production of 36000 million gallons per year (MGPY) of bioethanol, whose energy equivalence is 24000 MGPY of gasoline. Out of this 36000 MGPY only 15000 MGPY can be bioethanol refined from corn starch. Of the remaining 21000 MGPY, a minimum of 16000 MGPY is to be bioethanol refined from lignocellulosic feedstocks including crop residue, woody biomass, and dedicated energy crops [3]. In 2012, corn starch was used to produce 13000 MGPY of bioethanol and is fast approaching its ceiling limit of 16000 MGPY. Until now the production of bioethanol from lignocellulosic feedstock has not been commercialized and is limited to pilot scale projects [3].

The large-scale use of gasoline in the transportation sectors also has an adverse impact on the environment. The combustion of fossil-fuels releases huge quantities of carbon and other pollutants into the atmosphere. Greenhouse gas emissions (GHG) emissions are considered a major contributing cause of global warming [2]. Reduction in GHG emissions due to gasoline being substituted by bioethanol is a major component of the RFS requirements. By 2022, the RFS mandates that bioethanol not only displace 20% of annual gasoline demand on an energy equivalent basis but also achieve a 30% net reduction on 2005 levels in carbon emissions from the transportation sector [2]. In 2005 the total carbon emissions from the transportation sector were 1100 million tons (MT) [1].

In order to encourage investment in cellulosic bioethanol refineries it is imperative that an economically and environmentally viable supply of lignocellulosic biomass is guaranteed [4]. This allows biorefineries to operate at a sufficiently high utilization level needed to exploit the economies of



scale inherent in large refineries [5]. Dedicated energy crops like switchgrass [6] show great potential but their cultivation has not yet been commercialized [3]. A strategy for mitigating risk in biomass supply is to use multiple existing sources of lignocellulosic feedstocks for risk pooling [5, 7]. Therefore, a portfolio approach to biomass feedstock procurement is needed [8]. Based on current U.S. availability [9], two of the most promising sources of lignocellulosic biomass for the production of bioethanol are: 1) crop residue – including barley straw, corn stover, sorghum stubble, and wheat straw [10]; and 2) woody materials – including urban wood waste, logging and mill residues [11].

Currently the price of fossil-fuel based energy products does not take into account the cost of carbon emissions resulting from their use [12]. National governments can play a role in accomplishing a sustainable shift towards renewable bioenergy products by imposing a tax on carbon emissions [13], thereby increasing the cost of energy produced from fossil fuel. Bioenergy produced from lignocellulosic feedstock is considered as carbon neutral, since the carbon emissions resulting from their use release CO<sub>2</sub> that crops and trees captured during photosynthesis [14]. Emissions trading schemes by way of the Regional GHG Initiative of “carbon tax” adopted by 9 Northeastern states in the U.S. have been effective in reducing annual carbon emissions [15]. Studies show that a national level tax of \$40/ton of carbon emissions would raise \$2.5 trillion in the U.S. over a 10-year period [16]. Revenue from such a carbon tax could be used to promote and establish renewable-energy projects in general and biofuel plants in particular.

A comprehensive optimization of the various logistical components along the entire lignocellulosic-based bioethanol supply chain (LBSC) is essential to maximize total profit [3] and minimize carbon emissions. The key logistics variables include the biomass processing capacity, optimal location, and choice of conversion technology of biorefineries. The choice of the conversion pathway i.e. biochemical vs. thermochemical is likely to greatly impact on the financial and environmental performance of the LBSC [7].

Recently, a number of authors [17–19] have presented research on deterministic optimization of LBSC that consider the financial objective and also take into account the environmental impact. Work by [20] presents a linear optimization model. The decision variables include biorefinery location, capacity and choice of conversion pathway. Research by [21] presents a mixed integer linear programming (MILP) optimization model that is solved using *k*-means clustering. The decision variables include biorefinery location and capacity. Work by [12] presents a MILP model along with Pareto optimal curves. The decision variables include biorefinery location, capacity and choice of conversion pathway.

However, there is a great deal of uncertainty relating to prices and supply/demand inherent in a LBSC [3, 12]. These uncertainties introduce significant risk in the decision making process, making it imperative that robust decisions are made concerning the key logistics variables in a stochastic environment.

Most work on the stochastic optimization of biomass-to- bioethanol supply chains only consider the financial objective [22, 23] and do not take into account the environmental impact. Research by [24] presents a 2-stage MILP optimization model that considers uncertainty in biomass supply and purchase price, biofuel demand and sale price. The first-stage decision variables include biorefinery location, capacity and choice of conversion pathway.

Only a few authors have presented research on stochastic optimization of biomass-to-biofuel supply chains that consider the financial objective and also take into account the environmental impact. Research by [25] presents a MILP model for a methanol supply chain that considers uncertainty over four scenarios in biofuel demand. The first-stage decision variables include biorefinery location and capacity. Work by [26] presents a 2-stage MILP model that considers uncertainty over 1000 scenarios in biomass supply and biofuel demand. The first-stage decision variables include biorefinery location, capacity and choice of conversion pathway. The model is solved using Bender’s decomposition.

Research by [27] presents a MILP model for a bioethanol supply chain that considers uncertainty over 100 scenarios in biomass purchase price. The first-stage decision variables include biorefinery capacity and choice of conversion technology.

To the best of our knowledge, no comprehensive work has been carried out on the stochastic multi-period optimization of dual-feedstock biomass-to-bioethanol supply chains under multiple uncertainties where the financial objective is optimized by also taking into account the environmental impact. The closest work has been done by [25–27]. However, the work by [25] does not deal with bioethanol and the biofuel under study is methanol, and the number of stochastic scenarios is limited to 4. While the work by [26] does not take into account the environmental impact and instead considers downside profit risk as the secondary objective. The work by [27] does not consider uncertainty in biomass supply, bioethanol demand, and sale price of bioethanol. The proposed model considers a single bioethanol refinery and site selection is not a decision variable.

This work proposes a two-stage stochastic MILP formulation to maximize the annualized profit of an integrated dual-feedstock LBSC while simultaneously minimizing carbon emissions. The work is differentiated from other efforts in this field by incorporating the following specific LBSC characteristics: 1) environmental impact is monetized through carbon credits and directly incorporated into the objective function, rather than being traded-off using Pareto optimal curves; 2) uncertainties in lignocellulosic-biomass supply, biomass purchase price, bioethanol demand, and bioethanol selling price are considered; 3) first-stage decision variables include both integer and continuous variables. The integer variable determines the location and conversion technology of biorefineries. While the continuous variables determines the biomass processing capacity of biorefineries; 4) second-stage decision variables include amount of each biomass type to be procured from supply zones, amount of biomass feedstock to be transported from the supply zones to the biorefineries, volume of bioethanol to be directly sold from biorefineries, volume of bioethanol to be transported from the biorefineries to the

biofuel demand zones, volume of unmet bioethanol requirement for each demand zone, and the inventory of biomass and bioethanol to be kept by biorefineries; 5) optimal strategies on location of biorefineries, conversion technology selection, and biomass processing capacity of each biorefinery are solved simultaneously within the integrated system by using the Sample Average Approximation (SAA) method; and 6) effectiveness of the proposed model is demonstrated through a case-study with a multi-period time horizon set in a 4-state Midwestern region of the United States.

### 4.3. Problem statement

This research studies a comprehensive dual-feedstock LBSC as shown in Fig. 32.

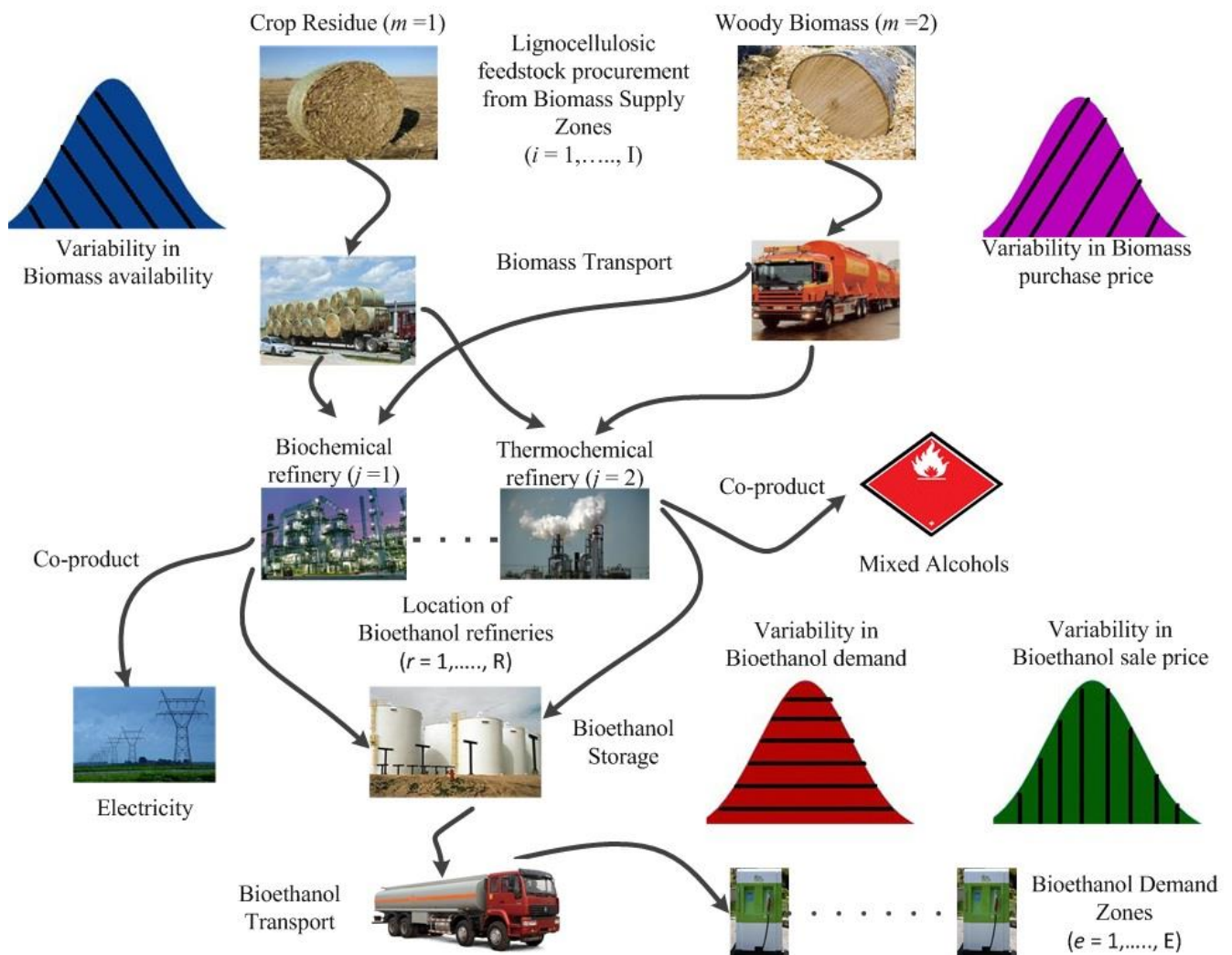


**Fig. 32. Lignocellulosic based biomass-to-bioethanol supply chain**

A list of indices, parameters, and decision variables is given in the Nomenclature section. The conversion factors from the U.S. customary units to the metric units (SI) are given in Appendix C. Based on work by [3], this paper assumes that: 1) only road haulage is considered for the transportation of biomass and bioethanol; and 2) the total bioethanol requirement is proportional to the population in each demand zone.

The major logistics activities in a LBSC are shown in Fig. 32. Feedstock of type  $m$  including crop residue and/or woody materials can be procured from biomass supply zone  $i$ . The biomass feedstock  $m$  is then transported from supply zone  $i$  to biorefinery  $r$  that uses conversion technology  $j$ , i.e. biochemical or thermochemical [28, 29]. The supplied biomass feedstock is converted into bioethanol and co-products, or kept as inventory by biorefinery  $j$ . The volume of bioethanol produced is driven by the ethanol demand and limited by the maximum biomass processing capacity of the biorefinery. The bioethanol is transported from biorefinery  $r$  to biofuel demand zone  $e$ . After satisfying the bioethanol requirement, any excess volume of bioethanol is directly sold from biorefinery  $r$  or kept as inventory. If the volume of ethanol produced is not sufficient to meet the biofuel demand, shortfall in bioethanol requirement incurs a high penalty cost.

In order to maximize the total LBSC profit and the net reduction in carbon emissions, the following logistics decisions need to be optimized:

- Material flow of procured lignocellulosic feedstock  $m$  from biomass supply zone  $i$  to biorefinery  $r$  during time period  $t$ . In the American Midwest, woody biomass can be procured year round [12, 26]. However, crop residues can only be harvested in late fall before the first killing frost [3]. A biorefinery utilizing lignocellulosic biomass can interchangeably utilize both crop residue and/or woody biomass as feedstock [5]. This increased reliability in biomass supply from multiple feedstock sources allows a biorefinery to operate at or near optimal production levels under a range of biomass supply disruption scenarios [8]. Although both crop

residue and woody materials are classified as lignocellulosic biomass [30] but their chemical composition in terms of percentages of lignin, cellulose and hemicellulose, and the expected yield of bioethanol [28, 29] is not similar.

- Biorefinery sites selection from  $r$  potential locations.
- Choice of conversion technology  $j$  to be used by each selected bioethanol refinery. The type of biomass feedstock is not the only determinant of bioethanol yield. Another important factor is the selection of the biomass-to-biofuel conversion pathway [31]. Biochemical and thermochemical pathways represent the two main currently available technologies for converting lignocellulosic biomass into bioethanol. From a financial standpoint the expected revenue (per unit of energy content) from mixed alcohols i.e. co-product from a thermochemical process, is higher than those from electricity i.e. co-product from a biochemical process. While from an environmental standpoint, the expected reduction in carbon emissions (per unit of energy content) from mixed alcohols due to substitution for heating oil is lower than those from bioelectricity due to substitution for coal as the traditional fuel for electricity generation in the United States [28, 29].
- Annual biomass processing capacity of an established biorefinery.
- Amount of biomass type  $m$  to be processed by biorefinery  $r$  during time period  $t$ .
- Amount of biomass type  $m$  to be kept as inventory by biorefinery  $r$  during time period  $t$ .
- Volume of bioethanol to be produced by biorefinery  $r$  during time period  $t$ .
- Volume of bioethanol to be kept as inventory by biorefinery  $r$  during time period  $t$ .
- Volume of unsubsidized bioethanol to be directly sold from biorefinery  $r$  during time period  $t$ .
- Material flow of ethanol from the  $r$  refineries to the  $e$  demand zones during time period  $t$ .
- Volume of unmet subsidized ethanol requirement for the  $e$  demand zones during period  $t$ .

#### **4.4. Stochastic nature of the LBSC**

Literature review [32] has highlighted some of the key uncertainties inherent in the life cycle of a LBSC. As such the logistics decisions taken need to be optimized over the entire range of the stochastic scenarios [33–36].

Commodity prices are usually governed by the available supply and the market demand [36]. However in the case of biomass, the relationship between feedstock purchase price and supply/demand level is not well established [32]. For example, the price of crop residue is only partly influenced by the cultivation and harvesting cost of the primary crop. The purchase price of crop residue is largely dictated by its demand for use as animal feed and bedding, rather than demand as feedstock for biofuel production [32]. Similarly in the case of bioethanol, the relationship between sale price and supply/demand is distorted by government action via the RFS mandate [32]. The “forced” nature of the RFS [2] necessitates production of a certain “mean” volume of bioethanol and distorts the free-market demand for ethanol. The sale price of ethanol is only partly influenced by the production cost and is mainly dictated by the price of diesel and government incentives for cellulosic ethanol production [32].

The development of statistical models to correlate biomass (and bioethanol) price with supply/demand is outside the scope of this work. This work assumes that all the uncertainties are independent variables. As a result, scenarios might arise where the biomass supply level is low but the biomass price is also low. However, the probability of the occurrence of such extreme scenarios is small [32]. Uncertainty in commodity/energy prices and their level of supply/demand is commonly modeled using known probability distributions which are based on statistical analysis of historical data [30, 35]. The following sections present the multiple uncertainties considered in the proposed model.

##### **4.4.1. Uncertainty in supply of biomass feedstock**

The supply of lignocellulosic biomass is not deterministic and fluctuates on an annual basis due to variation in temperature, rainfall [3], and forest fire incidents [36]. This work assumes that if the

biomass supply level for the entire supply chain region is high, then each individual supply zone also have a high biomass supply level [33]. A probability function is used to model the uncertainty in biomass supply level by analyzing historical biomass availability data.  $o(\omega)$ , the biomass supply level is defined as follows:

$$o(\omega) = [\text{Amount of biomass available}(\omega)/\text{Average amount of biomass available}]$$

#### **4.4.2. Uncertainty in the demand for bioethanol**

Demand for gasoline and hence ethanol is not deterministic and fluctuates on an annual basis [1, 37]. This work assumes that if the bioethanol demand level for the entire supply chain region is high, then each individual demand zone also have a high bioethanol demand level [33]. A probability function is used to model the uncertainty in bioethanol demand level by analyzing historical gasoline demand data.  $\pi(\omega)$ , the bioethanol demand level is defined as follows:

$$\pi(\omega) = [\text{Bioethanol demand}(\omega)/\text{Average bioethanol demand}]$$

#### **4.4.3. Uncertainty in the purchase prices for biomass feedstocks**

The purchase price of biomass feedstocks depends on the inherent energy content and is largely influenced by hay price [30]. A probability function is used to model the uncertainty in biomass price level by analyzing historical hay prices.  $v(\omega)$ , the biomass price level is defined as follows:

$$v(\omega) = [\text{Price of hay}(\omega)/\text{Average price of hay}]$$

#### **4.4.4. Uncertainty in the sale prices for bioenergy products**

The sale price of bioenergy products depends on the inherent energy content and is largely influenced by diesel price [38]. A probability function is used to model the uncertainty in energy price level by analyzing historical diesel prices.  $\sigma(\omega)$ , the energy price level is defined as follows:

$$\sigma(\omega) = [\text{Price of diesel}(\omega)/\text{Average price of diesel}]$$



## 4.5. Model formulation

The goal of the study is to determine the optimal configuration of the LBSC along with the associated operational decisions that maximizes its economic and environmental performance under uncertainties. A stochastic MILP model is proposed to maximize the expected LBSC profit by determining the optimal values of the first-stage and second-stage decision variables. The formulation including the objective function and constraints of the model is explained in the following sections. All continuous decision variables are non-negative, while all integer variables have binary restriction.

### 4.5.1. Objective function of the LBSC

The objective function of the proposed stochastic model is to maximize the expected annualized LBSC profit (revenue – cost) subject to meeting the RFS mandates relating to ethanol production and reduction in GHG emissions. Eq. 4.1 refers to the expected profit ( $\theta$ ) which needs to be maximized.

$$\begin{aligned}
 \theta = & - \sum_{r=1}^R \sum_{j=1}^J G_{rj} Y_{rj} - \sum_{r=1}^R \sum_{j=1}^J H_{rj} K_{rj} \\
 & + E_{\omega} \left[ \begin{aligned}
 & \sum_{r=1}^R \sum_{j=1}^J \sum_{e=1}^E \sum_{t=1}^T t_{rt} \sigma(\omega) [L_{rjt}(\omega) + P_{rjet}(\omega)] + \sum_{r=1}^R \sum_{j=1}^J \sum_{t=1}^T \delta_r \sigma(\omega) X_{rjt}(\omega) + \sum_{r=1}^R \sum_{j=1}^J \sum_{t=1}^T \chi_{rt} \sigma(\omega) S_{rjt}(\omega) \\
 & + \sum_{r=1}^R \sum_{j=1}^J \sum_{e=1}^E \sum_{t=1}^T \tau_{re} P_{rjet}(\omega) + \sum_{r=1}^R \sum_{j=1}^J \sum_{t=1}^T \Theta_r X_{rjt}(\omega) + \sum_{r=1}^R \Xi_r [NR_r(\omega) - Cap_r] \\
 & - \sum_{m=1}^M \sum_{i=1}^I \sum_{r=1}^R \sum_{j=1}^J \sum_{t=1}^T \lambda_{mit} \nu(\omega) F_{mirjt}(\omega) - \sum_{m=1}^M \sum_{i=1}^I \sum_{r=1}^R \sum_{j=1}^J \sum_{t=1}^T \eta_{mir} D_{ir} F_{mirjt}(\omega) - \sum_{r=1}^R \sum_{j=1}^J \sum_{e=1}^E \sum_{t=1}^T \psi_{re} D_{re} P_{rjet}(\omega) \\
 & - \sum_{m=1}^M \sum_{r=1}^R \sum_{j=1}^J \sum_{t=1}^T \varsigma_{mt} W_{mrjt}(\omega) - \sum_{r=1}^R \sum_{j=1}^J \sum_{t=1}^T \Delta_t V_{rjt}(\omega) - \sum_{r=1}^R \sum_{j=1}^J \sum_{t=1}^T U_{rj} Z_{rjt}(\omega) - \sum_{e=1}^E \sum_{t=1}^T \varphi_e O_{et}(\omega)
 \end{aligned} \right] \quad (4.1)
 \end{aligned}$$

In Eq. 4.1 the different components of  $\theta$  respectively represent the: 1) fixed cost of bioethanol refineries; 2) variable cost of bioethanol refineries; 3) revenue from the sale of bioethanol; 4) revenue from the sale of renewable electricity; 5) revenue from the sale of mixed alcohol; 6) tax credit accrued from bioethanol production; 7) tax credit accrued from renewable electricity generation; 8) revenue from the sale of carbon credits accrued due to net reduction in GHG emissions; 9) procurement cost of crop residue and woody biomass; 10) biomass transportation cost; 11) bioethanol transportation cost;

12) biomass inventory cost; 13) bioethanol inventory cost; 14) bioethanol production cost; and 15) penalty cost of unmet bioethanol demand.

$$NR_r(\omega) = \left[ \begin{aligned} & N_{Eth} \sum_{r=1}^R \sum_{j=1}^J \sum_{t=1}^T Z_{rjt}(\omega) + N_{Elt} \sum_{r=1}^R \sum_{j=1}^J \sum_{t=1}^T X_{rjt}(\omega) + N_{MA} \sum_{r=1}^R \sum_{j=1}^J \sum_{t=1}^T S_{rjt}(\omega) - \sum_{m=1}^M \sum_{i=1}^I \sum_{r=1}^R \sum_{j=1}^J \sum_{t=1}^T \Lambda_m F_{mirjt}(\omega) \\ & - \sum_{m=1}^M \sum_{r=1}^R \sum_{j=1}^J \sum_{t=1}^T \alpha_{mj} Q_{mrjt}(\omega) - \sum_{m=1}^M \sum_{i=1}^I \sum_{r=1}^R \sum_{j=1}^J \sum_{t=1}^T \beta_m D_{ir} F_{mirjt}(\omega) - \sum_{r=1}^R \sum_{j=1}^J \sum_{e=1}^E \sum_{t=1}^T \gamma D_{re} P_{rjet}(\omega) \end{aligned} \right] \quad (4.2)$$

In Eq. 4.1 the term  $NR_r(\omega)$  refers to the annual reduction in GHG emissions in location  $r$  during scenario  $\omega$ . In Eq. 4.2 the different components of  $NR_r(\omega)$  respectively refer to the: 1) reduction in carbon emissions due to gasoline being substituted by bioethanol; 2) reduction in carbon emissions due to conventional electricity being substituted by bioelectricity; 3) reduction in carbon emissions due to heating oil being substituted by mixed alcohol; 4) increase in carbon emissions from biomass harvesting; 5) increase in carbon emissions from converting biomass into bioethanol; 6) increase in carbon emissions from biomass transport; and 7) increase in carbon emissions from ethanol transport.

#### 4.5.2. Capacity constraints

$$\sum_{r=1}^R \sum_{j=1}^J \sum_{t=1}^T F_{mirjt}(\omega) \leq \zeta_{mi} o(\omega) \quad \forall m, i, \omega \quad (4.3)$$

$$\sum_{r=1}^R \sum_{j=1}^J \sum_{t=2}^T F_{virjt}(\omega) = 0 \quad \forall i, \omega \quad (4.4)$$

$$\sum_{r=1}^R \sum_{j=1}^J Y_{rj} \leq 1 \quad \forall r \quad (4.5)$$

$$\rho_j^{\min} Y_{rj} \leq K_{rj} \leq \rho_j^{\max} Y_{rj} \quad \forall r, j \quad (4.6)$$

$$\sum_{m=1}^M Q_{mrjt}(\omega) \leq (K_{rj}/T) \quad \forall r, j, t \quad (4.7)$$

Eq. 4.3 ensures that in supply zone  $i$ , the amount of biomass type  $m$  sent to all biorefineries over all time periods is not more than the amount of biomass type  $m$  available during scenario  $\omega$ . Crop residue is only available during the first time period. Eq. 4.4 ensures that in supply zone  $i$ , crop residue

is not available for shipment to any biorefinery during any other time period during scenario  $\omega$ . Eq. 4.5 ensures that maximum of one biorefinery is established at location  $r$ . Eq. 4.6 represents the maximum and minimum limits on the annual biomass processing capacity of an established biorefinery. While Eq. 4.7 ensures that a biorefinery does not process more biomass than its capacity in time period  $t$ .

### 4.5.3. Material balance constraints

$$W_{mrj0}(\omega) = W_{mrjT}(\omega) = 0 \quad \forall m, r, j, \omega \quad (4.8)$$

$$(1 - \Pi_t)W_{mrjt-1}(\omega) + \sum_{i=1}^I F_{mirjt}(\omega) = Q_{mrjt}(\omega) + W_{mrjt}(\omega) \quad \forall m, r, j, t, \omega \quad (4.9)$$

$$\sum_{m=1}^M \kappa_{mj} Q_{mrjt}(\omega) = Z_{rjt}(\omega) \quad \forall r, j, t, \omega \quad (4.10)$$

$$\sum_{m=1}^M C_{mj} Q_{mrjt}(\omega) = X_{rjt}(\omega) \quad \forall r, j, t, \omega \quad (4.11)$$

$$\sum_{m=1}^M \mu_{mj} Q_{mrjt}(\omega) = S_{rjt}(\omega) \quad \forall r, j, t, \omega \quad (4.12)$$

$$V_{rj0}(\omega) = V_{rjT}(\omega) = 0 \quad \forall r, j, \omega \quad (4.13)$$

$$V_{rjt-1}(\omega) + Z_{rjt}(\omega) = V_{rjt}(\omega) + L_{rjt}(\omega) + \sum_{e=1}^E P_{rjet}(\omega) \quad \forall r, j, t, \omega \quad (4.14)$$

$$O_{et}(\omega) + \sum_{r=1}^R \sum_{j=1}^J P_{rjet}(\omega) = \Gamma V_{et} \pi(\omega) \quad \forall e, t, \omega \quad (4.15)$$

Eq. 4.8 ensures that no biomass inventory is kept at the start of first time period and at the end of last time period. Eq. 4.9 ensures that in time period  $t$  the available amount of biomass is used to produce bioethanol and/or stored as inventory for the next time period. The available amount of biomass includes feedstock shipped by all  $i$  supply zones during the current time period plus existing biomass inventory from previous time period, discounting for storage loss. Eq. 4.10, Eq. 4.11 and Eq. 4.12 respectively ensure that in time period  $t$  during scenario  $\omega$ , the cumulative amount of biomass used by biorefinery  $r$  is converted into bioethanol, electricity and mixed alcohols. Eq. 4.13 ensures that no bioethanol inventory is kept at the start of first time period and at the end of last time period. Eq. 4.14 ensures that in time period  $t$  the available volume of bioethanol is either shipped to the demand

zones, sold from the refinery-gate, or stored as inventory for the next time period. The available volume of bioethanol includes the bioethanol produced during the current time period plus existing bioethanol inventory from previous time period. Eq. 4.15 ensures that in time period  $t$  during scenario  $\omega$ , the volume of unmet bioethanol requirement plus the volume of bioethanol transported to demand zone  $e$ , is equal to the bioethanol requirement in the biofuel demand zone.

#### 4.6. Solution procedure for the proposed stochastic MILP model

The proposed stochastic MILP model is required to optimally select the: 1) biorefinery installation sites; 2) bioethanol conversion technology for each selected refinery; and 3) biomass processing capacity for each selected refinery.

The main computational burden is imposed by the binary decision variables [26] i.e. selection of biorefinery installation sites and conversion technology, which need to be optimized over all the scenarios. For non-trivial scenarios, the proposed stochastic model (Eqs. 4.1–4.15) cannot be accurately solved within reasonable computational time using traditional algorithms [33]. The application of decomposition techniques is required to make the problem computationally tractable and to obtain optimal solutions within reasonable time frame [39–41]. The SAA algorithm is applied to solve the proposed stochastic MILP model [42]. The algorithm details are described in the following section.

##### 4.6.1. SAA algorithm

For stochastic models with a non-trivial set of scenarios, a number of sampling based approaches have been proposed to estimate objective function values. In the SAA algorithm, a sample set  $\{\omega^1, \omega^2, \dots, \omega^B\}$  of  $B$  scenarios is randomly generated from  $\Omega$  total scenarios, and then a deterministic optimization problem specified by the generated sample set is solved [40]. The expected value of the objective function  $E[Q(x, \zeta(\omega))]$  is approximated by Eq. 4.16.

$$\sum_{b=1}^B Q(x, \zeta(\omega^b)) / B \quad (4.16)$$

The SAA problem (given by Eq. 4.17) corresponding to the original two-stage stochastic model is then solved using traditional deterministic MILP optimization algorithms. The optimal objective value  $z_B$  and an optimal solution  $\hat{x}$  to the SAA problem provide estimates of their true counterparts in the stochastic model.

$$z_B = \max_{x \in X} c^T x + \sum_{b=1}^B Q(x, \xi(\omega^b)) / B \quad (4.17)$$

By generating  $A$  independent sample sets, each containing  $B$  scenarios, and solving the associated SAA problems, objective values  $z_B^1, z_B^2, \dots, z_B^A$  and candidate solutions  $\hat{x}^1, \hat{x}^2, \dots, \hat{x}^A$  are obtained. Eq. 4.18 denotes the average of the  $A$  optimal values of the SAA problems.

$$\bar{z}_B = (1/A) \sum_{a=1}^A z_B^a \quad (4.18)$$

It is universally acknowledged that  $E[\bar{z}_B] \leq z^*$ . Therefore for a maximization problem,  $\bar{z}_B$  provides a statistical estimate for an upper bound on  $z^*$ , the optimal value of the true stochastic problem. For any feasible solution  $\hat{x} \in X$ , the objective value given by  $c^T \hat{x} + E[Q(\hat{x}, \xi(\omega))]$  is clearly a lower bound for  $z^*$ . This lower bound can be estimated by Eq. 4.19 where  $\{\omega^1, \omega^2, \dots, \omega^\Omega\}$  contains the full set of  $\Omega$  scenarios.

$$z_\Omega(\hat{x}) = c^T \hat{x} + \sum_{b=1}^{\Omega} Q(\hat{x}, \xi(\omega^b)) / \Omega \quad (4.19)$$

The above procedure produces up to  $A$  different candidate solutions, one for each sample set. It is logical to take  $\hat{x}^*$  as one of the optimal solutions  $\hat{x}^1, \hat{x}^2, \dots, \hat{x}^A$  of the  $A$  problems which has the largest estimated objective value (for a maximization problem) over the full set of  $\Omega$  scenarios, as given by Eq. 4.20.

$$\hat{x}^* \in \arg \max \{z_\Omega(\hat{x}) \mid \hat{x} \in [\hat{x}^1, \hat{x}^2, \dots, \hat{x}^A]\} \quad (4.20)$$

The quality of the solution  $\hat{x}^*$  is evaluated by computing the optimality gap (as given by Eq. 4.21) for the full set of  $\Omega$  scenarios and comparing it against  $\varepsilon$ , a pre-set criteria.

$$[\bar{z}_B - \hat{z}_\Omega(\hat{x}^*)]/\bar{z}_B \quad (4.21)$$

The use of the SAA algorithm to solve the stochastic problems proposed in this work is demonstrated below:

*Step 1:* Create  $A$  sample sets  $\{A = \Omega, \Omega/B_1, \Omega/B_2, \dots, 1\}$  with each set populated with  $B$  scenarios  $\{B = 1, B_1, B_2, \dots, \Omega\}$  randomly drawn without replacement from the total  $\Omega$  scenarios, such that  $A = \Omega/B$ . In addition,  $\Omega$  must be divisible by the selected value of  $B$ . If say  $\Omega = 10000$ , than  $B$  can only take on values of;

$$B = \{1, 2, 4, 5, 8, 10, 20, 25, 40, 50, 80, 100, 125, 200, 250, 400, 500, 1000, 1250, 2000, 2500, 5000, 10000\}.$$

*Step 2:* Start with the largest value of  $A$  (10000 when  $\Omega = 10000$ ) and create  $A = 10000$  sample sets with each set populated with  $B = 1$  scenario randomly drawn without replacement from the total  $\Omega$  scenarios.

*Step 3:* Solve the SAA problem (Eqs. 4.17–4.20) for the  $A = \Omega$  sets, and compute the optimality gap (Eq. 4.21). The SAA algorithm terminates if the computed optimality gap is less than  $\varepsilon$ , a pre-set criteria. Otherwise go to Step 4.

*Step 4:* If the desired optimality gap is not achieved, then the next largest value of  $A$  ( $= \Omega/B_1 = 10000/2$ ) is used to create a new sample of  $A = 5000$  sets with each set populated with  $B = 2$  scenarios randomly drawn without replacement from the total  $\Omega$  scenarios. The values of the upper bound (given by Eq. 4.18), lower bound (given by Eq. 4.19), and the optimality gap (given by Eq. 4.21) are updated. If the desired optimality gap  $\varepsilon$  is not achieved, than Step 4 is repeated using the next largest value of  $A$  until the computed optimality gap is less than  $\varepsilon$ .

#### 4.7. Case study set-up

Parameters used in this case study are displayed in Tables A7–A9 (see Appendix A). This case study examines a dual-feedstock LBSC. Woody biomass and crop residue are both considered as feedstock. The case study is set in the American Midwest comprising the states of Illinois (IL), Iowa (IA), Minnesota (MN), and Wisconsin (WI). The choice of the 4 states is deliberate as not only the climatic and soil conditions are similar [43], but each state also represents distinct sources of lignocellulosic biomass that is abundantly available. For example crop residue is the primary feedstock in Illinois and Iowa, while woody material is the primary feedstock in Wisconsin. In Minnesota both crop residue and woody biomass is abundantly available [43, 44].

The proposed stochastic MILP model is used to determine the optimal values of the key logistics decision variables so as to maximize the expected total LBSC profit from the sale of bioenergy products and carbon credits accrued from net reduction in GHG emissions.

##### 4.7.1. Model assumptions

The various indices and assumptions used in the proposed stochastic MILP model are given in Table 7 and also explained below:

**Table 7. Indices used in the case study**

$e$	Bioethanol demand zones ( $e = 1, 2, \dots, 360$ )
$i$	Lignocellulosic biomass supply zones ( $i = 1, 2, \dots, 360$ )
$j$	Bioethanol conversion technologies $j = 1$ (Biochemical); $j = 2$ (Thermochemical)
$m$	Lignocellulosic biomass feedstocks $m = 1$ (Crop Residue); $m = 2$ (Woody Biomass)
$r$	Biorefinery locations ( $r = 1, 2, \dots, 360$ )
$t$	Modeling horizon of 1 year with time periods ( $t = 1, 2, 3, 4$ )
$\omega$	Stochastic scenarios ( $\omega = 1, 2, \dots, 10000$ )

- Total planning horizon is 1 year, with 4 time periods ( $t = 1, 2, 3, 4$ ). Each period comprises of 3 months as follows:

$t = 1$ : Comprises of Sept, Oct and Nov

$t = 2$ : Comprises of Dec, Jan and Feb

$t = 3$ : Comprises of Mar, Apr and May

$t = 4$ : Comprises of June, July and Aug

- All 360 counties of the 4-state region are potential biorefinery locations, biomass supply zones, and bioethanol demand zones. Biomass availability and bioethanol demand are centered at the county seat. For example, Chicago is seat of Cook County.
- Demand for co-products i.e. electricity and mixed alcohols, is assumed to be always greater than supply.
- Biorefineries with a biomass processing capacity of less than 1 million tons per year (MTPY) are not economically viable while those with a production capacity of more than 3 MTPY have not yet been commercialized [3]. Therefore in this work an installed biorefinery has a processing capacity ( $K_{rj}$ ) between 1 MTPY and 3 MTPY.
- Revenues and costs are considered on an annual basis. Eq. 4.22 is used to annualize the initial investment of a biorefinery with life  $n$  years and interest rate of  $q\%$  [32]. For example, a 1 MTPY biochemical refinery requires an initial investment of \$835 M [3]. With biorefinery life ( $n$ ) of 20 years and interest rate ( $q$ ) of 5%, the annualized cost is \$67 M obtained from Eq.22.

$$\text{Annualized Cost} = [q(\text{Initial Investment})]/[1 - (1 + q)^{-n}] \quad (4.22)$$

- In Eq. 4.1, annual fixed cost of biorefinery ( $G_{rj}$ ) and annual variable cost of biorefinery ( $H_{rj}$ ) are obtained by the following approximation. As shown in literature, Eq. 4.23 is used to calculate the total annual cost ( $Q_{rj}$ ) of a biorefinery with capacity  $K_{rj}$  [32], where  $\alpha$  is a scaling factor,  $K_{rj}0$  is a reference capacity, and  $Q_{rj}0$  is the annualized cost of a biorefinery with capacity of  $K_{rj}0$ . In this work,  $\alpha = 0.8$  [32]. Using Eq. 4.23,  $Q_{rj}$  of a 3 MTPY biochemical refinery is calculated as \$160.4 M for a reference capacity of 1 MTPY with annualized cost of \$67 M.

$$Q_{rj} = Q_{rj}0(K_{rj} / K_{rj}0)^\alpha \quad \forall j, r \quad (4.23)$$

In this work,  $K_{rj}$  is set in the interval of (1, 3) MTPY. For this interval Eq. 4.23 is linearized and approximated by Eq. 4.24 in order to avoid non-linear term in the proposed stochastic model.

For a biochemical refinery ( $j = 1$ ) the best value of  $G_{rj}$  is \$21.3 Million and  $H_{rj}$  is \$46/ton. Using



Eq. 4.24 the annualized cost ( $Q_{rj}$ ) of a 3 MTPY biochemical refinery is estimated at \$160 M which compares favorably to the value obtained using Eq. 4.23.

$$Q_{rj} = G_{rj} + H_{rj}K_{rj} \quad \forall j, r \quad (4.24)$$

#### 4.7.2. Modeling the uncertainties in a LBSC

In this work, all stochastic scenarios are governed by four independent random variables (IRVs) which are not correlated. The first IRV,  $o(\omega)$  is used to model the supply level of biomass. The second IRV,  $\pi(\omega)$  is used to model the demand level of bioethanol. The third IRV,  $v(\omega)$  is used to model the price level of hay, which acts as a surrogate for the price level of crop residue and woody biomass. The fourth IRV,  $\sigma(\omega)$  is used to model the price level of diesel, which acts as a surrogate for the price level of ethanol, electricity and mixed alcohols. The four IRVs are assumed to follow Normal probability distributions (see Table A8 in Appendix A).

#### 4.7.3. Discretization of continuous stochastic parameters

A set of possible scenarios with a given probability of occurrence are used to describe the random events. The use of continuous probability distributions to model the uncertainty is likely to result in an infinite number of stochastic scenarios [32]. In order to make the problem computationally tractable, each IRV is discretized into 10 levels (see Table A9 in Appendix A).

The number of discretized levels used is sufficient to ensure that the entire range of the normal probability distribution is captured. The resulting total number of scenarios  $\Omega = 10^4 = 10000$ . For example a scenario might have biomass supply at level  $L_{o03}$ , ethanol demand at level  $L_{\pi09}$ , biomass price at level  $L_{v02}$ , and energy price at level  $L_{\sigma06}$ . Each scenario  $\omega$  (where  $\omega = 1, 2, \dots, 10000$ ) is equally likely to happen.

The  $\Omega = 10000$  discrete scenarios are used to convert the stochastic MILP model into the Deterministic Equivalent Model (DEM) which is coded in GAMS and has 720 binary variables. The

SAA algorithm is used to solve the DEM, with 1% as the pre-set criteria for the optimality gap. For this work an optimality gap of 0.94% is achieved from a sample of 100 sets, with each set populated with 100 scenarios randomly drawn without replacement from the 10000 scenarios.

#### **4.8. Case study results**

Two regional modes of co-operation and stand-alone are considered for the geographic scale of the LBSC. Under co-operation mode the 4 states are considered as a combined region, inter-state exchange of biomass and bioethanol is allowed. Biorefineries can procure biomass from any zone within the 4-state region. Bioethanol produced within a state that is used to meet in-state demand qualifies for an in-state tax credit of \$0.5/gallon [3], while bioethanol that is used to meet out-state demand within the 4-state region qualifies for a reduced out-state tax credit of \$0.25/gallon. Bioethanol surplus to requirement of the entire 4-state region can be sold at prevailing market rates and does not qualify for any type of tax credit, while unmet bioethanol demand within the 4-state region incurs a high penalty cost.

Under stand-alone mode each of the 4 states is considered as an individual region and the stochastic MILP model is solved individually for each state. Biorefineries located in a state can only procure biomass from supply zones within that state. Only bioethanol produced within a state can be used to meet in-state demand and qualifies for a tax credit of \$0.5/gallon [3]. Bioethanol surplus to requirement of an individual state can be sold at prevailing market rates and does not qualify for a tax credit, while unmet demand for bioethanol within a state incurs a penalty cost.

##### **4.8.1. Comparison of outcomes in stand-alone vs. co-operation mode under uncertainties**

In this section the results in a stochastic environment for each state are compared under stand-alone and co-operation modes. Biorefinery locations under co-operation and stand-alone modes are displayed in Fig. 33. The depicted size of the biorefinery icons (Triangle or Square) is correlated to its biomass processing capacity. Under both modes the total number of biorefineries and choice of

conversion technology in the 4-state region remains the same but the locations and biomass processing capacities of biorefineries are different. Under the stand-alone mode, some of the states do not have enough biomass feedstock to produce bioethanol that can substitute 20% of the annual gasoline demand. For example Illinois has a bioethanol shortfall of 334 MGPY. While states like Minnesota and Wisconsin have substantial biomass leftover even after satisfying internal demand for bioethanol. Finally there are states like Iowa that can cost-effectively meet their bioethanol requirement but do not have any surplus biomass leftover.

Under co-operation mode the locations of biorefineries in biomass-deficit states like Illinois is “pushed-out” from the geographic center towards the state-line of neighboring biomass-surplus states. For biomass surplus-states like Minnesota and Wisconsin the locations of biorefineries are “pulled-in” towards the geographic center away from the state-line of neighboring biomass-deficit states. Biorefineries in biomass-surplus states are able to procure biomass from northern supply zones located away from the center. Vacating of areas near the boundary of biomass-deficit states by biorefineries in biomass-surplus states allows biorefineries in biomass-deficit states to cost-effectively procure biomass from the “vacated” supply zones in biomass-surplus states. The biorefinery locations remain unchanged for states like Iowa with enough biomass for internal needs but no exportable surplus.

Co-operation mode allows inter-state exchange of bioethanol and/or biomass from surplus to deficit states. This allows greater utilization of available biomass resources within the 4-state region. As a result, the total biomass processing capacity of biorefineries is 15% greater compared to stand-alone mode. The greater processing capacity under co-operation mode leads to production of larger volume of bioethanol. Each state under co-operation mode gives better financial (see Fig. 34) and environmental (see Fig. 35) outcomes compared to stand-alone mode. For example, IL is the main financial beneficiary under co-operation mode when compared to stand-alone mode. This is due to the huge penalty cost associated with unmet bioethanol demand incurred under stand-alone mode, while

under co-operation mode the shortfall is met by increased bioethanol production within IL by using biomass procured from out-state supply zones, and the supply of cheaper bioethanol from MN and WI.

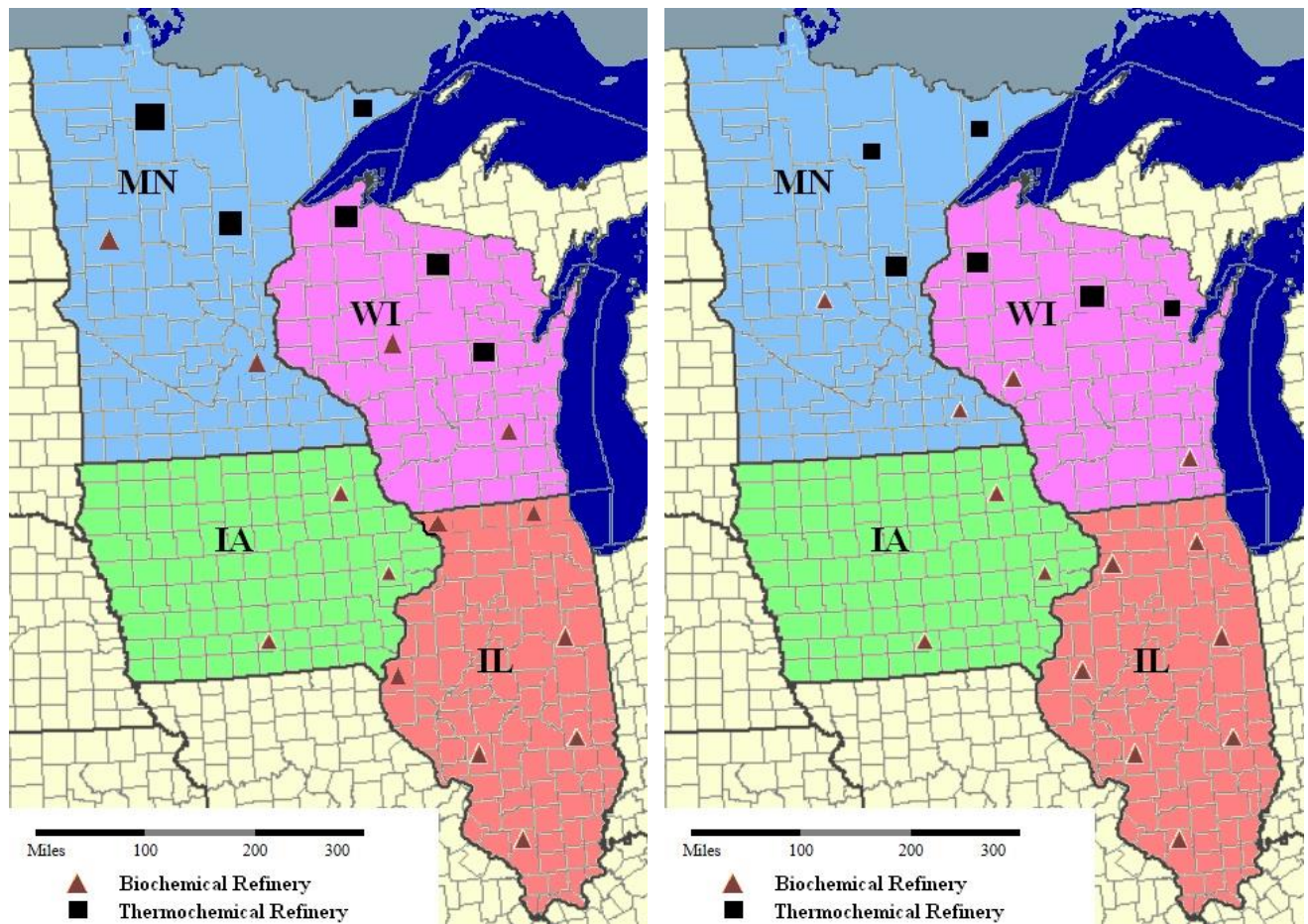


**Fig. 33. Co-operation mode vs. stand-alone mode**

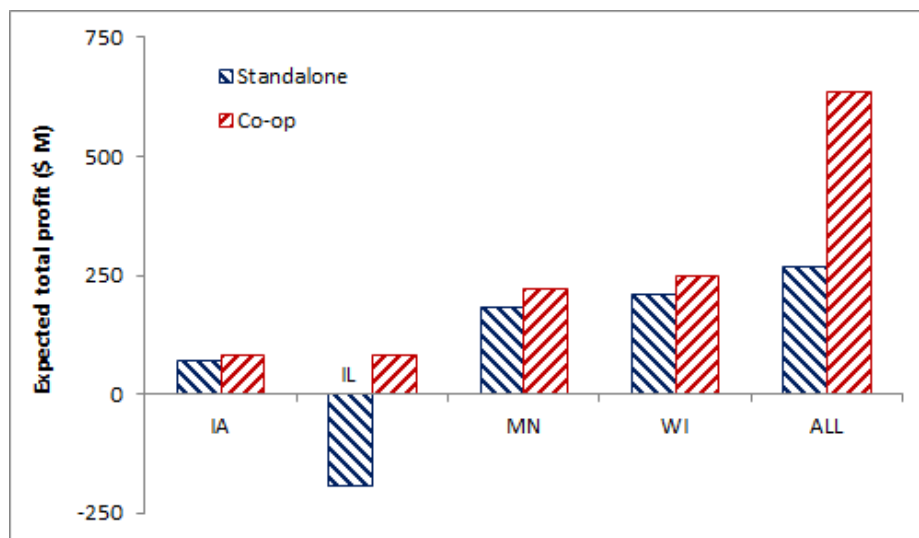


**Fig. 34. Total profit (stand-alone vs. co-op)**

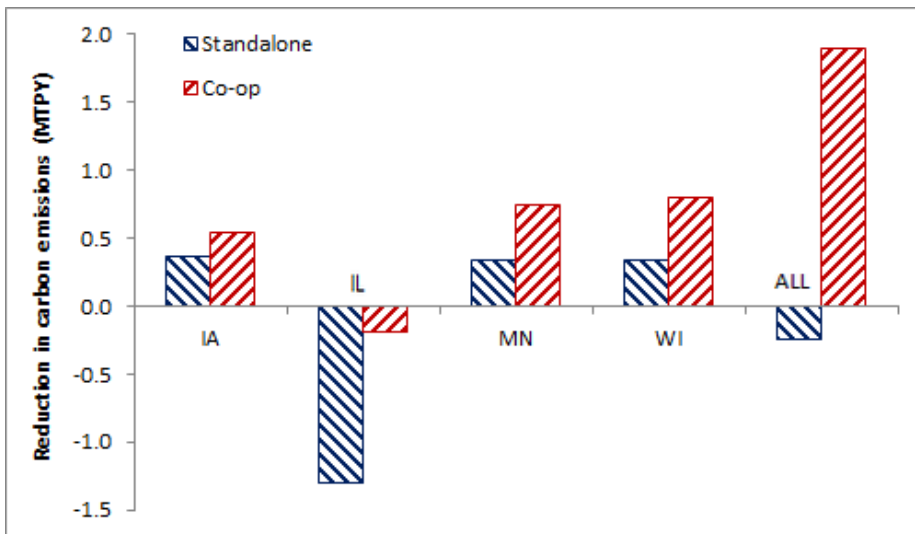


**Fig. 35. GHG emissions (stand-alone vs. co-op)**

Table 8 shows that under co-operation mode, 7% of biomass procured within a state is transported out-state to other regions within the 4-state area. Another advantage of the co-operation mode over the standalone mode is the permissibility of bioethanol exchange within the 4-state region. As a result, more than 13% of bioethanol produced by biorefineries within a state is transported out-state. Within the 4-state region, a greater proportion of bioethanol is exchanged compared to biomass. Bioethanol is of high density and incurs lower transport cost, while biomass is of low density and incurs substantial transport cost over large distances [3].

**Table 8. Inter-state exchange of biomass and bioethanol under co-operation mode**

Expected values	Iowa	Illinois	Minnesota	Wisconsin
Biomass processed by in-state biorefineries (MTPY)	6.9	15.1	11.1	11.4
Biomass procured from in-state supply zones (MTPY)	6.0	13.0	11.1	11.4
Biomass procured from out-state supply zones (MTPY)	0.9	2.1	0.0	0.0
Biomass sent to out-state biorefineries (MTPY)	0.9	0.0	0.9	1.2
Bioethanol production (MGPY)	615	1,330	921	940
Bioethanol consumed in-state (MGPY)	510	1,330	726	727
Bioethanol sent out-state (MGPY)	105	0	195	213

#### 4.8.2. Under co-operation mode

The performance of the stochastic model is compared with a traditional deterministic model (under uncertainties) that uses the “mean” values of the stochastic input parameters. Value of stochastic

solution (VSS) is used to compare the performance of the stochastic model to the deterministic model. VSS is defined as the difference between the expected profits of the stochastic model vs. the deterministic model under uncertainties [45]. The optimal output values of the first-stage decision variables obtained from the deterministic model are fixed and used as parametric inputs to the stochastic model to calculate the expected profit of the deterministic model under uncertainties [45].

In an uncertain environment, the stochastic model gives robust decisions that lead to better financial and environmental outcomes compared to the deterministic model (for details see Table 9).

**Table 9. Comparison of stochastic vs. deterministic model in co-op mode under uncertainty**

Expected profit values	Results	
	Deterministic	Stochastic
Total annualized profit (\$ M) = a) + b)	523	637
a) Annualized profit from bioethanol and co-products (\$ M)	506	561
b) Annualized profit from carbon credits (\$ M)	17	76
<b>First-stage decision variables</b>		
Number of biorefineries = c) + d)	20	20
c) Number of biochemical refineries	14	14
d) Number of thermochemical refineries	6	6
Biomass processing capacity of biorefineries (MTPY) = e) + f)	40.0	44.5
e) Processing capacity of biochemical refineries (MTPY)	30.5	32.2
f) Processing capacity of thermochemical refineries (MTPY)	9.5	12.3
<b>Second-stage decision variables</b>		
Crop residue processed by biorefineries (MTPY) = g) + h)	26.0	29.6
g) Crop residue processed by biochemical refineries (MTPY)	25.2	26.5
h) Crop residue processed by thermochemical refineries (MTPY)	0.8	3.1
Woody biomass processed by biorefineries (MTPY) = i) + j)	14.0	14.9
i) Woody biomass processed by biochemical refineries (MTPY)	5.3	5.7
j) Woody biomass processed by thermochemical refineries (MTPY)	8.7	9.2
Bioethanol produced by biorefineries (MGPY) = k) + l)	3,456	3,806
k) Bioethanol produced by biochemical refineries (MGPY)	2,700	2,849
l) Bioethanol produced by thermochemical refineries (MGPY)	756	957
Electricity produced by biochemical refineries (GWh/year)	6,060	6,396
Mixed Alcohols produced by thermochemical refineries (MGPY)	132	167
Unmet demand for bioethanol (MGPY)	114	1
*Net reduction in carbon emissions (MTPY)	0.427	1.894

The stochastic model more than quadruples the net reduction in carbon emissions. The stochastic model increases expected profit by 22% =  $[(637-523)/523]$  over the deterministic model in an uncertain environment. Co-efficient of variance (CV) is defined as the ratio of standard deviation over the mean value [45]. In this work the four stochastic parameters are assumed to have low variability, i.e.  $0.11 < CV < 0.16$  (Table A8 in Appendix A). As the CV of all the stochastic parameters increases, the financial (see Fig. 36) and environmental (see Fig. 37) performance of both deterministic and stochastic models is degraded. However, the stochastic model increasingly outperforms the deterministic model under uncertainties, and the VSS increases with rising variance (see Fig. 36). This demonstrates the effectiveness of the stochastic model over all levels of variability.

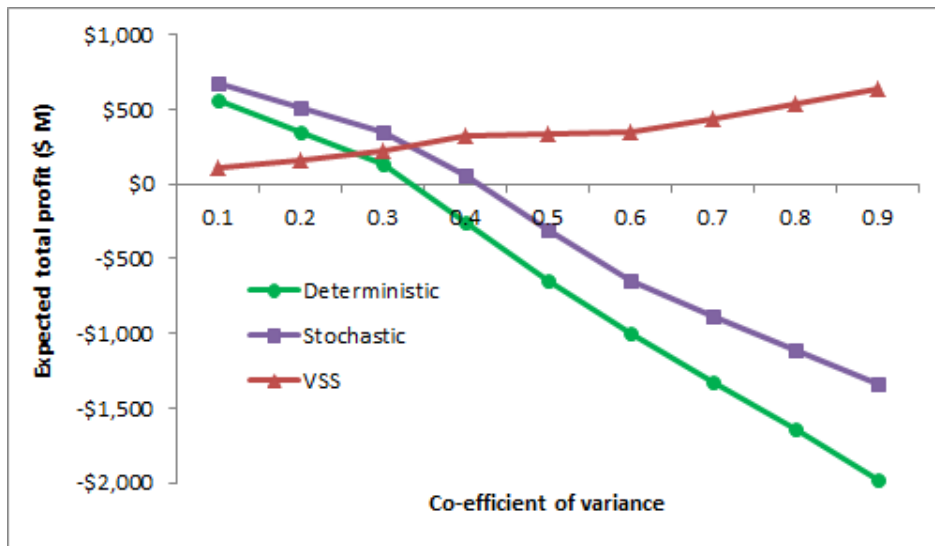


**Fig. 36. Impact of variability on profit**

The deterministic model incurs higher penalty for unmet bioethanol demand. The stochastic model aims to minimize the penalty cost by allocating a larger biomass processing capacity to biorefineries, while simultaneously maximizing the expected revenue in order to obtain the optimal decision variables that result in the highest expected profit. Biomass processing capacities of biorefineries obtained from the deterministic and stochastic models are different. The stochastic model processes significantly more biomass than the deterministic model (see Table 9) to hedge against the

impact of the high penalty cost for unmet bioethanol demand. Biomass processing capacity for each biorefinery is shown to be extremely sensitive to the uncertainties.

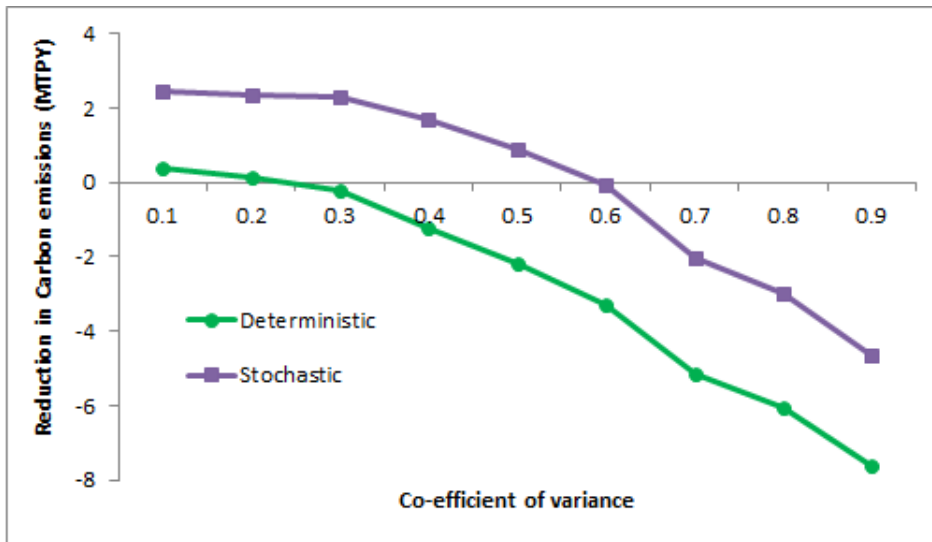


**Fig. 37. Impact of variability on GHG emissions**

The results of location and conversion technology selection of biorefineries are the same in deterministic and stochastic models. Fig. 33 shows that the optimum location of biorefineries is invariably near supply zones with high biomass availability and/or high bioethanol demand [3]. For example, McHenry County (IL) with an abundant supply of crop residue is selected as location for a biochemical refinery which is less than 40 miles from Chicago (representing 18% of total ethanol demand within the 4-state region). Although the biomass availability level for an individual supply zone varies considerably, but it is correlated with the availability level of other zones in the region. Similarly, the bioethanol requirement level for an individual demand zone varies considerably, but it is correlated with the demand level of other zones in the region. The selection of biorefinery installation sites is therefore insensitive to the inherent uncertainty in biomass availability and bioethanol demand.

In the Midwestern states, forest and logging residue can be harvested year round [12, 26] and no inventory needs to be kept as woody biomass is available on demand. However, crop residues can only be harvested in late fall before the first killing frost [3] during the first time period. As a result,



biorefineries need to keep appropriate inventory of crop residue and incur holding cost to ensure that biomass requirement in each time period is met [46]. Thermochemical refineries mainly rely on woody biomass as feedstock to produce bioethanol [28, 29] and as such have limited need of crop residue as biomass feedstock or keeping inventory of biomass. Biochemical refineries prefer crop residue [28, 29] as biomass feedstock and are willing to incur holding cost to keep appropriate inventory of crop residue and only require woody biomass if crop residue is not available for procurement [28, 29].

Fig. 38 shows that during each time period the amount of biomass processed by biochemical and thermochemical refineries is uniform. This indicates that the biorefineries are able to offset the effect of seasonality in crop residue availability by keeping appropriate inventory to ensure that the same amount of biomass is processed in each time period. However, the composition of the types of biomass processed in each time period is not uniform.

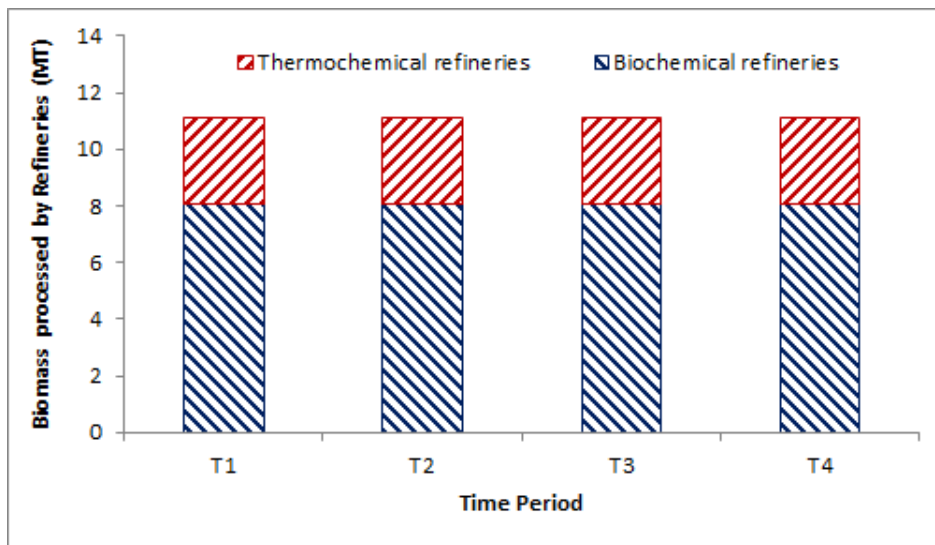


**Fig. 38. Biomass processed by biorefineries**

Figs. 39 and 40 shows that biochemical refineries procure crop residue once a year at the beginning of time period 1. The inventory level is determined by the inventory cost and the bioethanol yield. If a biochemical refinery exclusively processes woody materials as feedstock, the resulting bioethanol yield will be substantially lower [28, 29]. As a result, a biochemical refinery prefers to keep

inventory of crop residue even at the end of period 3 so that woody materials are not exclusively processed during the last period. The entire inventory is consumed before the end of the last period.

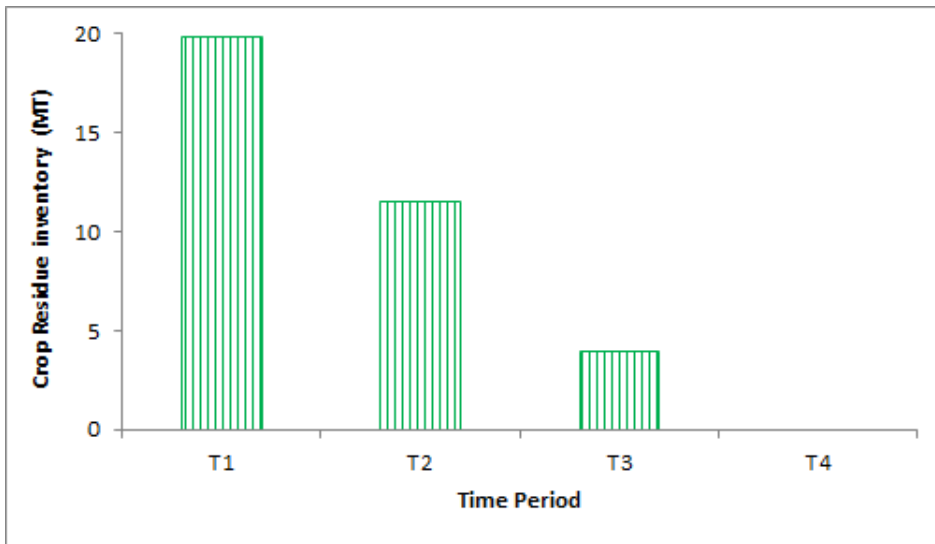


**Fig. 39. Biomass inventory kept at biorefineries**

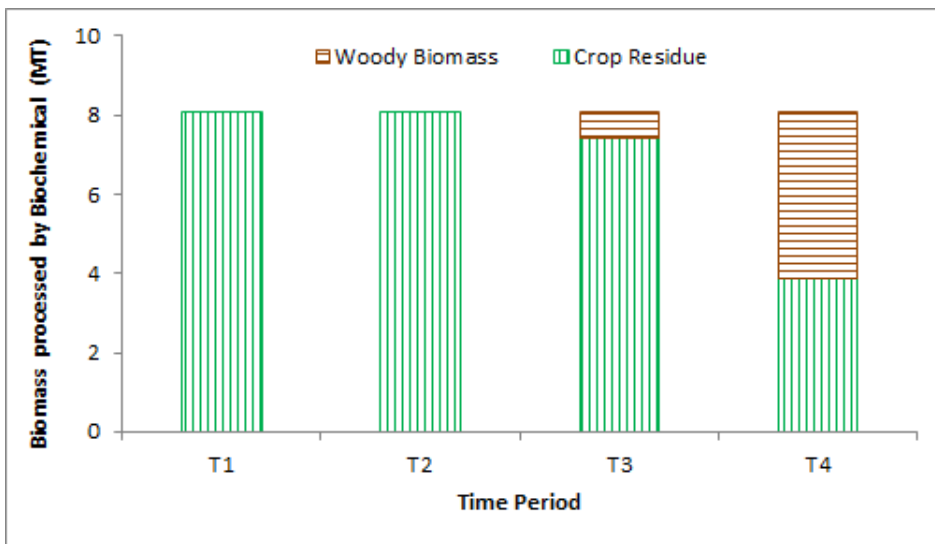


**Fig. 40. Biomass processed by biochemical**

Fig. 41 shows that for thermochemical refineries, only during time period 1 is crop residue used as feedstock (as it is readily available) and represents 70% of the amount of biomass processed while the share of woody biomass is 30%. In the remaining time periods ( $t = 2, 3$  and 4), woody materials are exclusively used as biomass feedstock.



**Fig. 41. Biomass processed by thermochemical**

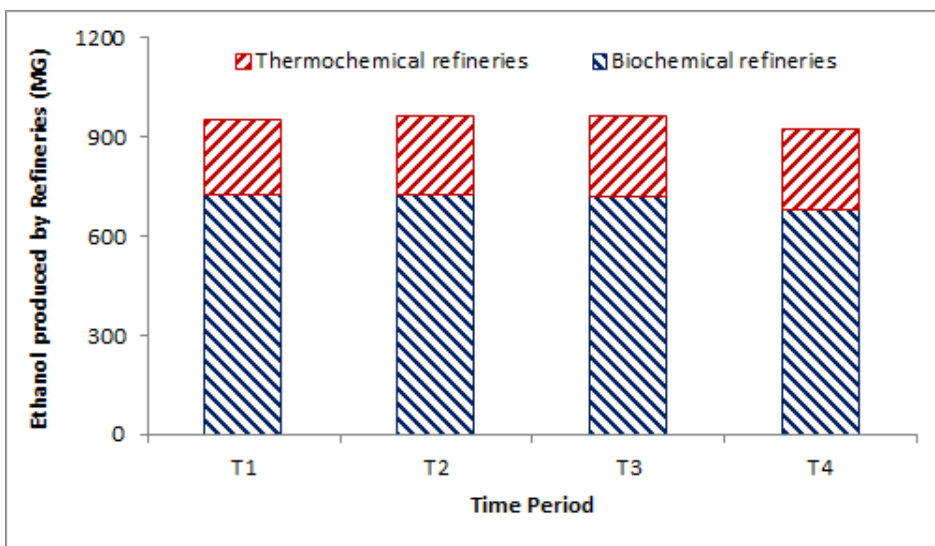


**Fig. 42. Bioethanol production by biorefineries**

Same amount of biomass is processed by biorefineries in each time period (see Fig. 38).

However, Fig. 42 shows that the volume of bioethanol produced by refineries is not uniform across all the 4 time periods. The volume of bioethanol produced by a biorefinery is largely dependent on the type of biomass used. For biochemical refineries, the bioethanol yield from crop residue is greater than that from woody biomass. The reverse is true for thermochemical refineries [28, 29].

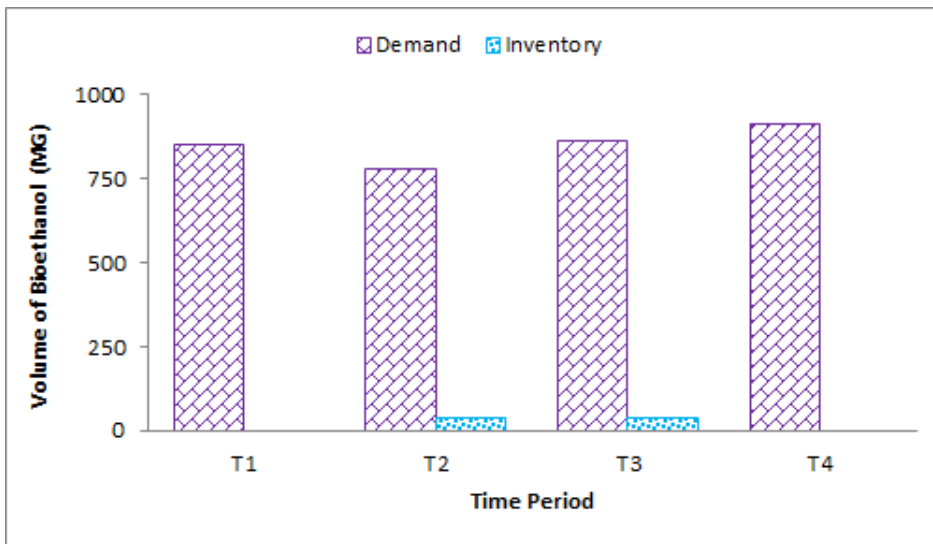


**Fig. 43. Bioethanol inventory and demand**

Fig. 43 shows that the demand for bioethanol exhibits slight seasonality whose magnitude is not the same as the seasonality in the supply of crop residue. Time period 2 has the lowest demand for bioethanol while time period 4 has the highest demand for bioethanol. Biorefineries take advantage of the higher bioethanol production during the first 3 time periods to build up the inventory of bioethanol. During period 4, the lowest volume of bioethanol is produced while the highest demand for bioethanol is experienced. The gap between supply and demand is met from the inventory of bioethanol available at the beginning of period 4. The entire inventory of bioethanol is depleted by the end of period 4.

#### 4.9. Sensitivity analysis

Section 4.8.1 has shown that the results for each individual state under co-operation mode results in higher profit and bigger reduction in carbon emissions when compared to results under stand-alone mode. While section 4.8.2 has shown that the proposed stochastic model is superior to a traditional deterministic model in terms of better financial and environmental outcomes when uncertainty exists. In this section sensitivity analysis is therefore carried out on the stochastic model under co-operation mode. Sensitivity analysis is conducted to measure the impact of the following key deterministic parameters, namely: 1) carbon price; and 2) bioethanol production tax credit.

### 4.9.1. Impact of carbon price

The deterministic input parameter value used in this case study is \$40/ton of carbon-equivalent emissions[16], while the price level of carbon emissions is varied from \$0/ton to \$100/ton [27, 47].

Fig. 44 indicates that the carbon price significantly impacts on the net reduction in carbon emissions and the expected total profit in an increasing manner. However, the rate of increase in the total profit is smaller than the rate of increase in the net reduction in carbon emissions. This is due to the fact that profit from the sale of carbon credits constitute less than 2% of the total (see Table 9).

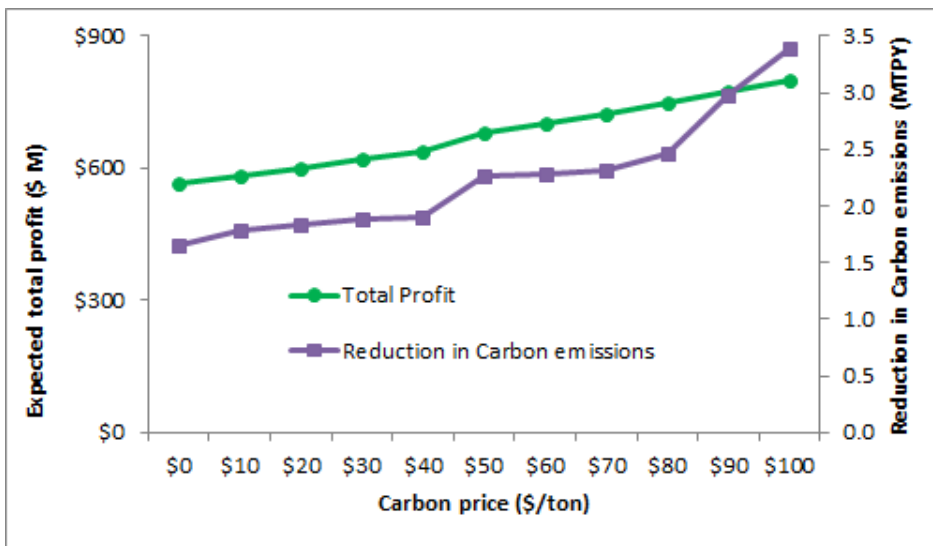


Fig. 44. Impact on LBSC performance

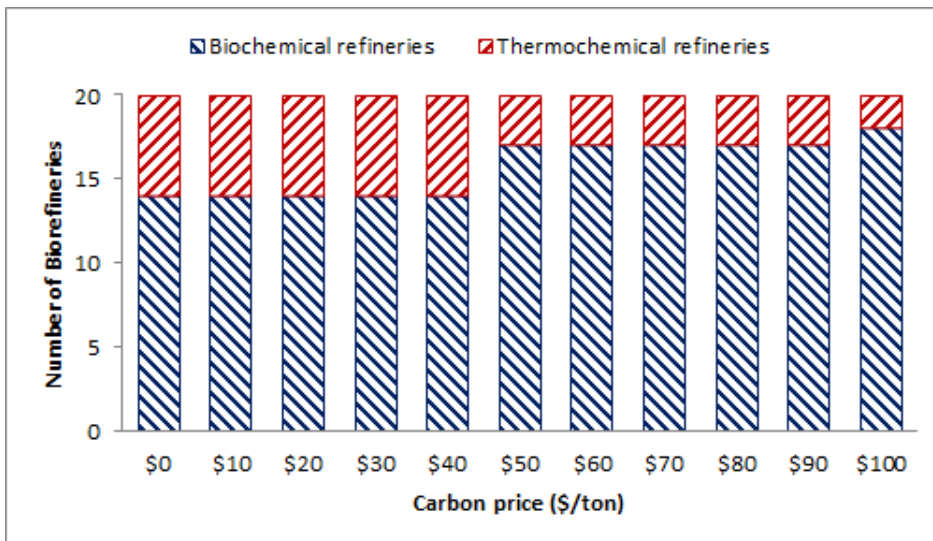


Fig. 45. Impact on type of biorefineries

Fig. 45 indicates that the carbon price significantly impacts on the composition of the biorefineries. As the carbon price exceeds \$40/ton, the number of thermochemical refineries decreases while the number of biochemical refineries increases. At the maximum carbon price of \$100/ton, the largest number of biochemical and smallest number of thermochemical refineries are installed.

#### 4.9.2. Impact of bioethanol tax credit

The deterministic input parameter value used in this case study is \$0.5/gallon [3], while the level of bioethanol tax credit is varied from \$0/gallon to \$1/gallon [37].

Fig. 46 indicates that the bioethanol tax credit significantly impacts on the expected profit in an increasing manner. Low level of tax credit (less than \$0.3/gallon) results in a huge financial loss due to the LBSC being “forced” to produce bioethanol under threat of penalty associated with unmet bioethanol demand. The profit break-even point is achieved once tax credit exceeds \$0.3/gallon. Tax credit acts as an incentive to produce enough bioethanol in order to meet the demand. Once the bioethanol demand is met, increasing the tax credit only increases the profit and does not increase the production of bioethanol. As such, the net reduction in carbon emissions plateaus out once the tax credit exceeds \$0.4/gallon.

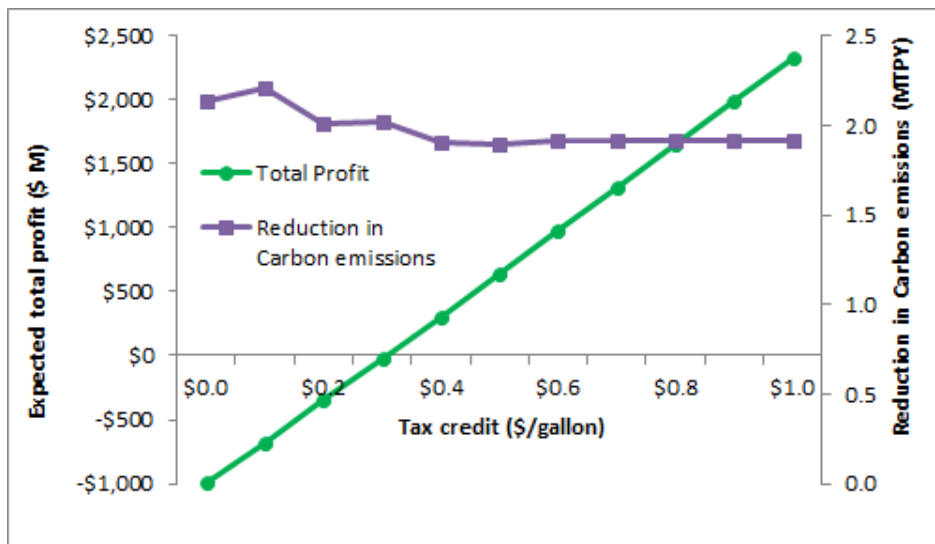
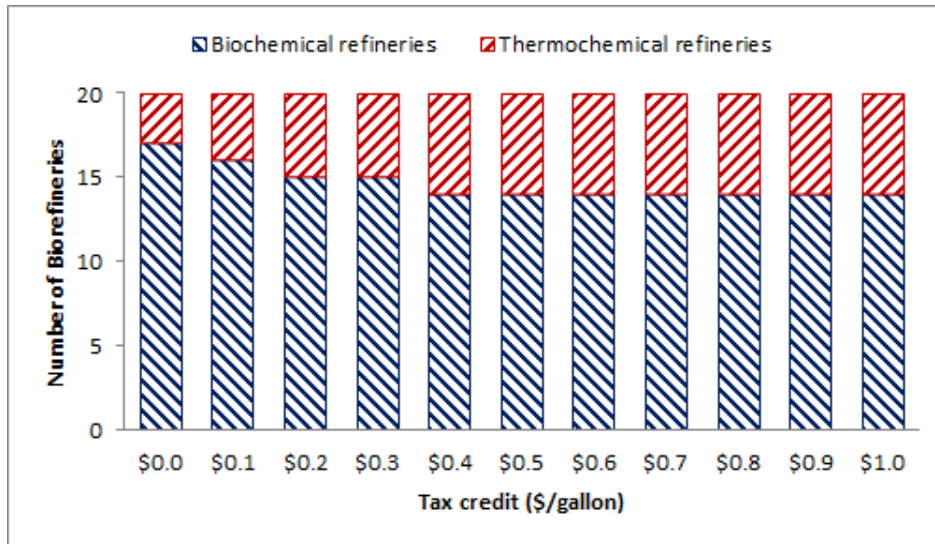


Fig. 46. Impact on LBSC performance

Fig. 47 indicates that the tax credit significantly impacts on the composition of the biorefineries. As the tax credit increases, the number of biochemical refineries starts to decrease while the number of thermochemical refineries increases. As the tax credit exceeds \$0.30/gallon, the largest number of thermochemical and smallest number of biochemical refineries are selected for installation.



**Fig. 47. Impact on type of biorefineries**

#### 4.10. Conclusion

This paper proposes a multi-period two-stage stochastic MILP model for simultaneously maximizing the expected profit and the net reduction in carbon emissions of a dual-feedstock LBSC. The model integrates all the supply chain logistics to arrive at optimal decisions that include both continuous and integer variables.

First, a case study based on a 4-state Midwestern region in the U.S. demonstrates the impact of the geographic scale of the supply chain on the financial and environmental performance. Two regional modes are considered for the geographic scale of the supply chain. Results show that each state under co-operation mode gives better financial and environmental outcomes when compared to stand-alone mode. The main advantage of the co-operation mode over the standalone mode is the permissibility of biomass and bioethanol exchange within the 4-state region. This allows biomass-deficit states like

Illinois to cost-effectively meet shortfall in bioethanol demand by importing biomass and bioethanol from surplus states like Minnesota and Wisconsin. The co-operation mode allows greater utilization of biomass resources within the 4-state region and higher production of bioethanol.

Second, the case study results show that the expected annualized LBSC profit and the net reduction in carbon emissions obtained using the proposed stochastic model is significantly higher than the traditional deterministic model under uncertainties. As variability of the stochastic parameters increases, the financial and environmental performance of both the deterministic and stochastic models is degraded. However, the stochastic model increasingly outperforms the deterministic model under uncertainties, and the VSS increases with rising variance. Results shows that in a stochastic environment with low to medium variability (CV less than 0.4), it is cost effective and sustainable to meet up to 20% of a 4-state Midwestern region's annual demand of gasoline energy equivalent requirement from locally produced bioethanol by using crop residue and woody materials as lignocellulosic biomass feedstock. Compared to the stochastic model, the deterministic model underestimates the biomass processing capacity of biorefineries resulting in incurring huge penalty cost related to unmet bioethanol demand. However, the location and type of conversion technology used by biorefineries are shown to be insensitive to the stochastic environment.

Finally, sensitivity analysis is conducted to provide insights for efficiently managing the entire LBSC. Location and biomass processing capacity of biorefineries is found to be insensitive to the level of carbon price and bioethanol tax credit. Both the carbon price and tax credit have a major impact on the selection of biomass-to-biofuel conversion technology. Biochemical pathway is increasingly preferred over the thermochemical as carbon price increases. Thermochemical pathway is increasingly preferred over the biochemical as the level of tax credit increases. In addition, U.S. bioethanol production using currently available conversion technologies is shown to be financially unprofitable without substantial governmental subsidy of at least \$0.3/gallon tax credit. On the other hand,



governmental subsidy greater than \$0.4/gallon only inflates profit and does not further improve the environmental performance. The per gallon production cost of bioethanol and the bioethanol yield (per ton of biomass processed) of both biochemical and thermochemical technologies will need to significantly improve before the production of lignocellulosic-based bioethanol becomes commercially viable in the U.S. without needing governmental subsidies.

This work has considered optimization of the financial and environmental performance as the dual-objective. Chapter 5 will include social benefits in achieving multi-objective optimization under uncertainties. This work has assumed that uncertainties are uncorrelated. Future work can also consider development of statistical models to correlate biomass (and bioethanol) price with its supply/demand level. Such an approach will avoid extreme scenarios where for example the bioethanol demand level is high but the bioethanol sale price is low.

## 4.11. Nomenclature

### 4.11.1. Indices

- $e$  Bioethanol demand zones ( $e = 1, \dots, E$ )
- $i$  Lignocellulosic biomass supply zones ( $i = 1, \dots, I$ )
- $j$  Bioethanol conversion technologies ( $j = 1, \dots, J$ )
- $m$  Lignocellulosic biomass feedstocks ( $m = 1, \dots, M$ )
- $r$  Biorefinery locations ( $r = 1, \dots, R$ )
- $t$  Modeling horizon of 1 year with time periods ( $t = 1, \dots, T$ )
- $\omega$  Stochastic scenarios ( $\omega = 1, \dots, \Omega$ )

### 4.11.2. First stage decision variables

- $K_{rj}$  Biomass processing capacity of biorefinery at location  $r$  with technology  $j$  (tons/year)
- $Y_{rj}$  {1, if biorefinery with conversion technology  $j$  setup in location  $r$ ; Else 0}

### 4.11.3. Second stage decision variables

$F_{mirjt}(\omega)$  Amount of biomass  $m$  sent from zone  $i$  to biorefinery  $r$  (with technology  $j$ ) in time period  $t$  during scenario  $\omega$  (tons)

$L_{rjt}(\omega)$  Volume of unsubsidized ethanol sold from refinery  $r$  (with technology  $j$ ) in period  $t$  during scenario  $\omega$  (gallons)

$NR_r(\omega)$  Net reduction in carbon emissions in location  $r$  during scenario  $\omega$  (tons)

$O_{et}(\omega)$  Volume of unmet subsidized ethanol demand in zone  $e$  in period  $t$  during scenario  $\omega$  (gallons)

$P_{rjet}(\omega)$  Volume of subsidized ethanol from refinery  $r$  (with technology  $j$ ) to zone  $e$  in period  $t$  during scenario  $\omega$  (gallons)

$Q_{mrjt}(\omega)$  Amount of biomass  $m$  for ethanol production at refinery  $r$  (with technology  $j$ ) in period  $t$  during scenario  $\omega$  (tons)

$S_{rjt}(\omega)$  Volume of mixed alcohol produced by biorefinery  $r$  (with technology  $j$ ) in time period  $t$  during scenario  $\omega$  (gallons)

$V_{rjt}(\omega)$  Volume of bioethanol stored as inventory at refinery  $r$  (with technology  $j$ ) in period  $t$  during scenario  $\omega$  (gallons)

$W_{mrjt}(\omega)$  Amount of biomass  $m$  stored as inventory at refinery  $r$  (with technology  $j$ ) in time period  $t$  during scenario  $\omega$  (tons)

$X_{rjt}(\omega)$  Amount of electricity generated by biorefinery  $r$  (with technology  $j$ ) in time period  $t$  during scenario  $\omega$  (MWh)

$Z_{rjt}(\omega)$  Volume of bioethanol produced by biorefinery  $r$  (with technology  $j$ ) in time period  $t$  during scenario  $\omega$  (gallons)

### 4.11.4. Deterministic parameters

$\Xi_r$  Price of carbon emissions in location  $r$  (\$/ton CO<sub>2</sub> equiv.)

$\Theta_r$  Renewable electricity generation tax credit in location  $r$  (\$/MWh)

$Cap_r$	Carbon emission reduction target in location $r$ (tons CO <sub>2</sub> equiv.)
$C_{mj}$	Electricity generation parameter for biomass type $m$ from conversion technology $j$ (MWh/ton)
$D_{ir}$	Distance between biomass supply zone $i$ and biorefinery $r$ (miles)
$D_{re}$	Distance between biorefinery $r$ and bioethanol demand zone $e$ (miles)
$G_{rj}$	Annualized fixed cost of biorefinery at location $r$ with conversion technology $j$ (\$)
$H_{rj}$	Variable cost parameter of biorefinery at location $r$ with conversion technology $j$ (\$/ton)
$N_{EIt}$	Reduction in carbon emissions from renewable electricity (tons CO <sub>2</sub> -equiv./MWh)
$N_{MA}$	Reduction in carbon emissions from mixed alcohols (tons CO <sub>2</sub> -equiv./gallon)
$N_{Eth}$	Reduction in carbon emissions from bioethanol (tons CO <sub>2</sub> -equiv./gallon)
$U_{rj}$	Ethanol production cost parameter of biorefinery at location $r$ with conversion technology $j$ (\$/gallon)
$\alpha_{mj}$	Carbon emission of processing biomass type $m$ with technology $j$ (tons CO <sub>2</sub> -equiv./ton)
$\beta_m$	Carbon emission of transporting biomass type $m$ (tons CO <sub>2</sub> -equiv./ton x mile)
$\gamma$	Carbon emission of transporting bioethanol (tons CO <sub>2</sub> -equiv./gallon x mile)
$\delta_r$	Average sale price of renewable electricity generated at location $r$ (\$/MWh)
$\Pi_t$	Ratio of biomass storage loss in time period $t$
$\Lambda_m$	Carbon emission of harvesting biomass type $m$ (tons CO <sub>2</sub> -equiv./ton)
$\zeta_{mi}$	Average amount of biomass type $m$ available in supply zone $i$ (tons)
$\eta_{mir}$	Transport cost parameter of biomass $m$ from supply zone $i$ to biorefinery $r$ (\$/ton x mile)
$\iota_{rt}$	Average sale price of unsubsidized bioethanol at location $r$ in time period $t$ (\$/gallon)
$\kappa_{mj}$	Bioethanol yield parameter for biomass type $m$ from conversion technology $j$ (gallons/ton)
$\lambda_{mit}$	Average purchase price of biomass type $m$ at supply zone $i$ in time period $t$ (\$/ton)
$\mu_{mj}$	Mixed alcohol yield parameter for biomass type $m$ from conversion technology $j$ (gallons/ton)

$v_{et}$	Avg. bioethanol demand (energy equivalent to 100% of gasoline requirement) in zone $e$ during period $t$ (gallons)
$\Delta_t$	Bioethanol inventory cost parameter in time period $t$ (\$/gallon)
$\rho_j^{max}$	Maximum amount of biomass that can be processed by biorefinery $r$ with conversion technology $j$ (tons/year)
$\rho_j^{min}$	Minimum amount of biomass that must be processed by biorefinery $r$ with conversion technology $j$ (tons/year)
$\zeta_{mt}$	Inventory cost parameter for biomass type $m$ in time period $t$ (\$/ton)
$\tau_{re}$	Tax credit for bioethanol production in location $r$ for consumption in demand zone $e$ (\$/gallon)
$\varphi_e$	Penalty cost parameter for unmet bioethanol requirement at biofuel demand zone $e$ (\$/gallon)
$\chi_{rt}$	Average sale price of mixed alcohol at location $r$ in time period $t$ (\$/gallon)
$\psi_{re}$	Transport cost parameter of ethanol from refinery $r$ to biofuel demand zone $e$ (\$/gallon x mile)
$\Gamma$	Ratio of annual gasoline demand to be satisfied from subsidized bioethanol

#### 4.11.5. Stochastic parameters

$v(\omega)$	Purchase price level of biomass during scenario $\omega$
$o(\omega)$	Supply level of biomass during scenario $\omega$
$\pi(\omega)$	Demand level of bioethanol during scenario $\omega$
$\sigma(\omega)$	Sale price level of energy during scenario $\omega$

#### 4.12. References

- [1] U.S. Energy Information Administration (EIA). <http://www.eia.gov/petroleum>
- [2] U.S. Energy Independence and Security Act of 2007 (EISA).
- [3] Zhang J, Osmani A, Awudu I, Gonela V. An integrated optimization model for switchgrass-based bioethanol supply chain. *Applied Energy* 2013;102:1205–17.

- [4] Zhu X, Li X, Yao Q, Chen Y. Challenges and models in supporting logistics system design for dedicated-biomass-based bioenergy industry. *Bioresource Technology* 2011;102:1344–1351.
- [5] Zhu X, Yao Q. Logistics system design for biomass-to-bioenergy industry with multiple types of feedstocks. *Bioresource Technology* 2011;102:10936–45.
- [6] Cherubini F, Jungmeier G. LCA of a biorefinery concept producing bioethanol, bioenergy, and chemicals from switchgrass. *Int J Life Cycle Assess* 2010;15:53–66.
- [7] Mabee W, McFarlane P, Saddler J. Biomass availability for lignocellulosic ethanol production. *Biomass Bioenergy* 2011;35:4519–4529.
- [8] Kou N, Zhao F. Effect of multiple-feedstock strategy on the economic and environmental performance of thermochemical ethanol production under extreme weather conditions. *Biomass Bioenergy* 2011;35:608–616.
- [9] Perlack R, et al. 2012. Biomass as a feedstock for a bioenergy and bioproducts industry: The technical feasibility of a billion-ton annual supply. ORNL, Oak Ridge, TN.
- [10] Cherubini F, Ulgiati S. Crop residues as raw materials for biorefinery systems – A LCA case study. *Applied Energy* 2010;87:47–57.
- [11] Wu J, Sperow M, Wang J. Economic Feasibility of a Woody Biomass-Based Ethanol Plant in Central Appalachia. *Journal of Agricultural and Resource Economics* 2010;35:522–544.
- [12] You F, Tao L, Graziano D, Snyder S. Optimal design of sustainable cellulosic biofuel supply chains: Multiobjective optimization coupled with life cycle assessment and input–output analysis. *AIChE Journal* 2012;58(4):1157–1180.
- [13] Tol R. The Social Cost of Carbon: Trends, Outliers and Catastrophes. *Economics: The Open Access, Open-Assessment E-Journal* 2008;2:25.
- [14] Shabani N, Sowlati T. A mixed integer non-linear programming model for tactical value chain optimization of a wood biomass power plant. *Applied Energy* 2013;104: 353–61.

- [15] Regional Greenhouse Gas Initiative (RGGI). <http://www.rggi.org>
- [16] Tang A, Chiara N, Taylor J. Financing renewable energy infrastructure: Formulation, pricing and impact of a carbon revenue bond. *Energy Policy* 2012;45:691–703.
- [17] Cucek L, Varbanov P, Klemes J, Kravanja Z. Total footprints-based multi-criteria optimisation of regional biomass energy supply chains. *Energy* 2012;44:135–145.
- [18] Giarola S, Zamboni A, Bezzo F. Spatially explicit multi-objective optimisation for design and planning of hybrid first and second generation biorefineries. *Computers and Chemical Engineering* 2011;35:1782– 1797.
- [19] Zamboni A, Shah N, Bezzo F. Spatially explicit static model for the strategic design of future bioethanol production systems. 2. Multi-objective environmental optimization. *Energy Fuels* 2009;23:5134–5143.
- [20] Frombo F, Minciardi R, Robba M, Rosso F, Sacile R. Planning woody biomass logistics for energy production: A strategic decision model. *Biomass Bioenergy* 2009;33:372–383.
- [21] Kocoloski M, Griffin W, Matthews H. Estimating national costs, benefits, and potential for cellulosic ethanol production from forest thinnings. *Biomass Bioenergy* 2011;35:2133–2142.
- [22] An H, Wilhelm W, Searcy S. A mathematical model to design a lignocellulosic biofuel supply chain system with a case study based on a region in Central Texas. *Bioresour Technol* 2011;102:7860–7870.
- [23] Dal-Mas M, Giarola S, Zamboni A, Bezzo F. Strategic design and investment capacity planning of the ethanol supply chain under price uncertainty. *Biomass Bioenergy* 2011;35:2059–2071.
- [24] Kim J, Realff M, Lee J. Optimal design and global sensitivity analysis of biomass supply chain networks for biofuels under uncertainty. *Computers and Chemical Engineering* 2011;35:1738–51.
- [25] Leduc S, Lundgren J, Franklin O, Dotzauer E. Location of a biomass based methanol production plant: A dynamic problem in northern Sweden. *Appl Energy* 2010;87:68–75.

- [26] Gebreslassie B, Yao Y, You F. Design under uncertainty of hydrocarbon biorefinery supply chains: Multiobjective stochastic programming models, decomposition algorithm, and a comparison between CVaR and downside risk. *AIChE Journal* 2012;58:2155–2179.
- [27] Giarola S, Shah N, Bezzo F. A comprehensive approach to the design of ethanol supply chains including carbon trading effects. *Bioresour Technol* 2012;107:175–185.
- [28] Foust T, Aden A, Dutta A, Phillips S. An economic and environmental comparison of a biochemical and a thermochemical lignocellulosic ethanol conversion processes. *Cellulose* 2009;16:547–565.
- [29] Mu D, Seager T, Rao P, Zhao F. Comparative Life Cycle Assessment of Lignocellulosic Ethanol Production: Biochemical Versus Thermochemical Conversion. *Environmental Management* 2010;46:565–578.
- [30] Diersen M. 2008. Hay Price Forecasts at the State Level. Proceedings of the NCCC-134 Conference on Applied Commodity Price Analysis, Forecasting, and Market Risk Management. St. Louis, MO.
- [31] Spatari S, Bagley D, MacLean H. Life cycle evaluation of emerging lignocellulosic ethanol conversion technologies. *Bioresource Technology* 2010;101:654–667.
- [32] Osmani A, Zhang J. Stochastic optimization of a multi feedstock lignocellulosic-based bioethanol supply chain under multiple uncertainties. *Energy* 2013;59:157–172.
- [33] Awudu I, Zhang J. Stochastic production planning for a biofuel supply chain under demand and price uncertainties. *Applied Energy* 2013;103:189–96.
- [34] Chen C, Fan Y. Bioethanol supply chain system planning under supply and demand uncertainties. *Transportation Research Part E* 2010;48:150–164.
- [35] Spatari S, MacLean H. Characterizing Model Uncertainties in the Life Cycle of Lignocellulose-Based Ethanol Fuels. *Environ Sci Technol* 2010;44:8773–8780.

- [36] Parker N, Tittmann P, Hart Q, Nelson R, Ken K, Schmidt A, Gray E, Jenkins B. Development of a biorefinery optimized biofuel supply curve for the Western United States. *Biomass Bioenergy* 2010;34:1597–1607.
- [37] Carriquiry M, Du X, Timilsina G. Second generation biofuels: Economics and policies. *Energy Policy* 2011;39:4222–4234.
- [38] O’Brien D, Woolverton M. *The Relationship of Ethanol, Gasoline and Oil Prices*. 2009 Kansas State University. Kansas, USA.
- [39] Lam H, Klemes J, Kravanja Z. Model-size reduction techniques for large-scale-biomass production and supply networks. *Energy* 2011;36:4599–4608.
- [40] Kleywegt A, Shapiro A, Homem-De-Mello T. The sample average approximation method for Stochastic discrete optimization. *SIAM J. Optim.* 2001;12:479–502.
- [41] Escudero L, Garin M, Merino M, Perez G. An exact algorithm for solving large-scale two-stage stochastic mixed-integer problems: Some theoretical and experimental aspects. *European Journal of Operational Research* 2010;204:105–116.
- [42] Kostin A, Guillen-Gosalbez G, Mele F, Bagajewicz M, Jimenez L. Design and planning of infrastructures for bioethanol and sugar production under demand uncertainty. *Chemical Engineering Research and Design* 2012;90:359–376.
- [43] Tyndall J, Schulte L, Hall R, Grubh K. Woody biomass in the U.S. Cornbelt? Constraints and opportunities in the supply. *Biomass Bioenergy* 2011;35:1561–1571.
- [44] Petrolia D. The economics of harvesting and transporting corn stover for conversion to fuel ethanol: a case study for Minnesota. *Biomass Bioenergy* 2008;32:603–612.
- [45] Birge J, Louveaux F. *Introduction to Stochastic Programming*, first ed. Springer, New York.
- [46] Eksioglu S, Acharya A, Leightley L, Arora S. Analyzing the design and management of biomass-to-biorefinery supply chain. *Computers Industrial Engineering* 2009;57:1342–1352.



- [47] Wetterlund E, Leduc S, Dotzauer E, Kindermann G. Optimal localisation of biofuel production on a European scale. *Energy* 2012;41:462–472.
- [48] You F, Wang B. Life cycle optimization of biomass-to-liquid supply chains with distributed-centralized processing networks. *Ind Eng Chem Res* 2011;50:10102–10127.
- [49] Database for State Incentives for Renewables and Efficiency. <http://www.dsireusa.org>
- [50] Osmani A, Zhang J, Gonela V, Awudu I. Electricity generation from renewables in the United States: Resource potential, current usage, technical status, challenges, strategies, policies, and future directions. *Renewable and Sustainable Energy Reviews* 2013;24:454–472.
- [51] Oak Ridge National Laboratory (ORNL). <http://webmap.ornl.gov/biomass/biomass.html>
- [52] USDA, National Agricultural Statistics Service. <http://www.nass.usda.gov>
- [53] National Renewable Energy Laboratory (NREL). <http://www.nrel.gov/gis/biomass.html>
- [54] Rand McNally. <http://www.randmcnally.com/milage-calculator.do>

## CHAPTER 5. MULTI-PERIOD STOCHASTIC OPTIMIZATION OF A SUSTAINABLE MULTI FEEDSTOCK SECOND GENERATION BIOETHANOL SUPPLY CHAIN

### 5.1. Abstract

Second generation bioethanol has been promoted by many nations as a sustainable substitute for gasoline. Until now the production of second generation bioethanol has not been commercialized due to high total logistic cost. Hence, this work proposes a comprehensive stochastic optimization model to design a sustainable and robust second generation bioethanol supply chain under multiple uncertainties. Multi-period planning is carried out to minimize investment risk by considering temporal variation in bioethanol demand. The objective is to simultaneously maximize financial profit, reduce GHG emissions, and increase jobs creation over the entire planning horizon, while satisfying bioethanol demand and GHG emission constraints in each planning period. The  $\epsilon$ -constraint method is used to trade-off among the competing objectives and a goal programming framework is provided to ensure that a set of feasible solutions is obtained that achieves specified levels of economic, environmental, and social performances. In order to solve the proposed large-scale stochastic MILP model efficiently and effectively, this work utilizes a two-step solution approach involving sequential application of a modified Sample Average Approximation method and Benders decomposition. A case study is presented to demonstrate the effectiveness of the proposed stochastic model by determining strategic decisions over all the planning periods and operational decisions within each planning period for sustainable second generation bioethanol production from multiple biomass feedstocks in a Midwestern U.S. region over a 10 year planning horizon. The research effort also assesses different renewable energy subsidy policies by comparing the resulting economic performance.

### 5.2. Introduction

Due to the energy crisis (i.e. depletion of fossil-fuels), environmental issues (i.e. increase in carbon emissions), and social issues (i.e. job losses due to global recession), researchers have been

attracted to develop sources of renewable energies to secure the energy consumption, protect the environment, and to promote social development of economically depressed areas. Biofuel is one type of the renewable energies that can be used in multiple ways to substitute fossil-fuel energy. Bioethanol is one type of biofuel that is currently widely used in transportation section as a gasoline substitute [1].

Although the first generation bioethanol production from food crops such as corn and sugarcane has been commercialized around the world, it is still debatable about food or energy when the cultivated lands have been used for the production of bioethanol feedstock. Work by [2] unfavorably evaluates the environmental impact of producing first generation bioethanol feedstock on the water table, soil acidification, and GHG emissions. Therefore, second generation of non-food lignocellulosic biomass feedstock is being studied intensively to develop more viable bioethanol.

In North America one of the most promising primary sources of lignocellulosic biomass is switchgrass, a perennial native grass [3]. Switchgrass (*panicum virgatum*) is suitable for cultivation on marginal land (with arid soil) without competing for cropland with other agriculture products [4]. Crop residue and woody materials also show potential as a secondary source of lignocellulosic biomass feedstock [5, 6].

In order to improve various aspects of sustainability in a lignocellulosic-based bioethanol supply chain (LBSC), the U.S. government is promoting policies that: 1) mandate and incentivize production of bioethanol from lignocellulosic biomass feedstocks; 2) aim to reduce GHG emissions by displacing gasoline with environmentally friendly bioethanol; and 3) improve social benefits to local communities through job creation via biomass cultivation and bioethanol production.

The U.S. government has enacted legislation to cap the production of bioethanol from corn starch [1]. The U.S. Renewable Fuel Standard (RFS) requires by 2022 production of 36000 million gallons per year (MGPY) of biofuels [7], out of which only 15000 MGPY can be bioethanol refined from corn

starch. Out of the remaining 21000 MGPY, a minimum of 16000 MGPY are to be ethanol refined from lignocellulosic biomass [2].

Reduction in GHG emissions due to gasoline being substituted by bioethanol is also a major component of the RFS requirements of cellulosic based biofuels. The RFS mandates by 2022 that lignocellulosic-based bioethanol also achieve a 60% net reduction on 2005 levels in GHG emissions from the transportation sector [1].

Until now the production of bioethanol from lignocellulosic feedstock has not been commercialized [3]. The decisions made regarding the key logistics variables are likely to greatly impact on the financial, environmental and social performances of the LBSC [8]. In order to sustainably meet the RFS target for lignocellulosic-bioethanol production, a comprehensive optimization of the various logistical components along the entire supply chain is essential by taking into account: 1) staggered nature of the RFS; 2) multiple optimization criteria; and 3) stochastic nature of the LBSC. The reasons are elaborated below.

To produce the target volume of bioethanol for the year 2022 (when the RFS target of satisfying 20% annual demand of transportation fuels from biofuels becomes binding) requires substantial upfront investment in: 1) cultivating agricultural land for biomass production; and 2) installation of bioethanol refineries of required production capacities. Committing billions of dollars at once significantly increases the investment risk and discourages participation by potential investors in bioethanol production. Even if the required capital funds are made available (e.g. government investment credits, low-interest loans, etc.), the massive infrastructure needed to produce 16000 MGPY of lignocellulosic-bioethanol by 2022 cannot be developed within a single year. The required upfront investment and the financial risk can be substantially reduced if the infrastructure development is staggered across multiple years as allowed by the RFS [1, 7].

In developing sustainable biofuel supply chains, the challenge is to simultaneously maintain financial viability, reduce environmental damage, and provide greater social benefits. In the face of these seemingly competing factors, multi-objective decision making allows generation of best alternatives based on realistic assumption on decision variables, contribution of each decision variable to the objectives, and constraints. Single objective optimization aims to yield a single best design that is superior to the rest. In multi-objective optimization there generally exists a set of designs in the solution space, which are superior to all other designs. However, within this set, no design is superior to another in all criteria. These designs constitute a Pareto optimum set [9], and no improvement can be made with respect to one objective without worsening the other objective(s).

In addition, there are a number of uncertainties relating to supply/demand and prices inherent to a LBSC [10]. These uncertainties introduce significant risk in the decision making process, making it imperative that robust decisions are made concerning the key logistics variables in a stochastic environment. This increases the complexity and consequently the solution space of the problem as “deterministic” parameters cannot be exclusively used to obtain the optimal values of the decision variables.

This work is the first research work that incorporates economic, environmental, and social sustainability in multi-period optimization of a LBSC while considering multiple uncertainties in supply, demand, and prices. The work is differentiated from other efforts in this field by incorporating the following specific LBSC characteristics: 1) environmental impact is quantified through net reduction in carbon emissions; 2) social impact is quantified through number of full-time jobs created during the infrastructure set-up (i.e. installation of bioethanol refineries) and operational phase (i.e. biomass cultivation, bioethanol production, etc.); 3) environmental and social impacts are traded-off against the financial objective (i.e. profit maximization) using the  $\epsilon$ -constraint method; 4) uncertainties in lignocellulosic-biomass supply, bioethanol demand, and bioethanol selling price are considered

jointly; and 5) to demonstrate the effectiveness of the research, the proposed stochastic mathematical model is used to determine the multi-period long-term (i.e. 10 years) infrastructure and operational requirements for sustainable lignocellulosic-bioethanol production from switchgrass, crop residue, and woody materials in the Midwestern state of Wisconsin.

In solving stochastic MILP optimization problems the main computational burden is imposed by the binary/integer decision variables [11] which need to be optimized over all the scenarios. Although stochastic modeling approaches provide more reliable results when compared to traditional deterministic models [12], the resulting heavier computational burden means that stochastic MILP models cannot be accurately solved using traditional algorithms employed by commercial solvers [10]. The application of heuristics and/or decomposition techniques is required to obtain optimal solutions within reasonable time frame [13, 14]. In this work a two-step solution approach involving sequential application of the Sample Average Approximation (SAA) method followed by Benders decomposition is used to make the optimization problem computationally tractable.

The rest of the paper is structured as follows. Section 5.3 provides literature review on LBSC optimization and highlights the research significance. Section 5.4 gives a summary of the problem statement and evaluates the uncertain parameters. Section 5.5 presents the proposed stochastic optimization model. Section 5.6 proposes a two-step decision making framework for LBSC optimization. Section 5.7 presents the case study and provides the numerical experimental design. Section 5.8 summarizes the results and policy analyses. Final conclusions and further research are outlined in section 5.9.

### **5.3. Literature review and research significance**

Literature review has shown that considerable research has been done on developing mathematical models for optimizing various logistical configurations of biomass-based supply chains [15, 16]. However most work done so far regarding optimization of integrated LBSC has been confined

to using the “deterministic” parameters to obtain the optimal production capacity, choice of conversion technology, and locations of biorefineries [17, 18], site selection and allocation of marginal land for biomass cultivation [3]. Most work on the deterministic optimization of LBSC only considers the financial objective. Recently, a number of authors [19–23] have presented research that also takes into account the environmental impact.

The preliminary work on stochastic optimization of bioethanol supply chains only considers one type of uncertainty such as uncertain bioethanol demand, or bioethanol sale price uncertainty [24–26]. Work by [27] considers an LBSC where the supply and demand uncertainties are considered separately but not jointly. Only a few recent works [12] jointly consider the multiple uncertainties in biomass supply, biomass purchase price, bioethanol demand, and bioethanol sales price. The literature on multi-objective stochastic optimization of LBSC is sparse with most work only considering the financial objective [25, 26, 28]. Only a few recent works have incorporated the environmental impact of GHG emissions [18, 20, 29, 30] and social impact of job creation for stimulation of economically depressed areas [31]. Work by [32] presents a MILP model along with Pareto optimal curves that trade-off among the economic, environmental and social performances while developing sustainable biofuel supply chains. However the research is conducted for a single planning period and parametric uncertainty is not considered.

Similarly, the literature on multi-period LBSC optimization is limited. The research so far has assumed that the infrastructure needed to produce the target volume of bioethanol for the year 2022 is developed in one go. Till date only a few efforts [33] have considered multi-period optimization of biofuel supply chains. However the research only considers the single-objective of profit maximization in a deterministic environment and does not specifically incorporate uncertainties.

To the best of our knowledge, no comprehensive work has been carried out on the stochastic multi-period optimization of multi-feedstock biomass-to-bioethanol supply chains under multiple

uncertainties where the financial objective is optimized by also taking into account the environmental and social impacts. To fill the identified gap in current literature and to advance the state-of-art in LBSC optimization, this work proposes a two-stage stochastic MILP formulation to maximize the expected profit of a multi-period long-term multi-feedstock LBSC while simultaneously minimizing carbon emissions and maximizing jobs creation.

#### 5.4. Problem statement

This research studies a comprehensive multi-period long-term (i.e. 10 year period) multi-feedstock LBSC under multiple uncertainties (see Fig. 48). A list of indices, parameters, and decision variables is given in the Nomenclature section. The conversion factors from the U.S. customary units to the metric units (SI) are given in Appendix C.

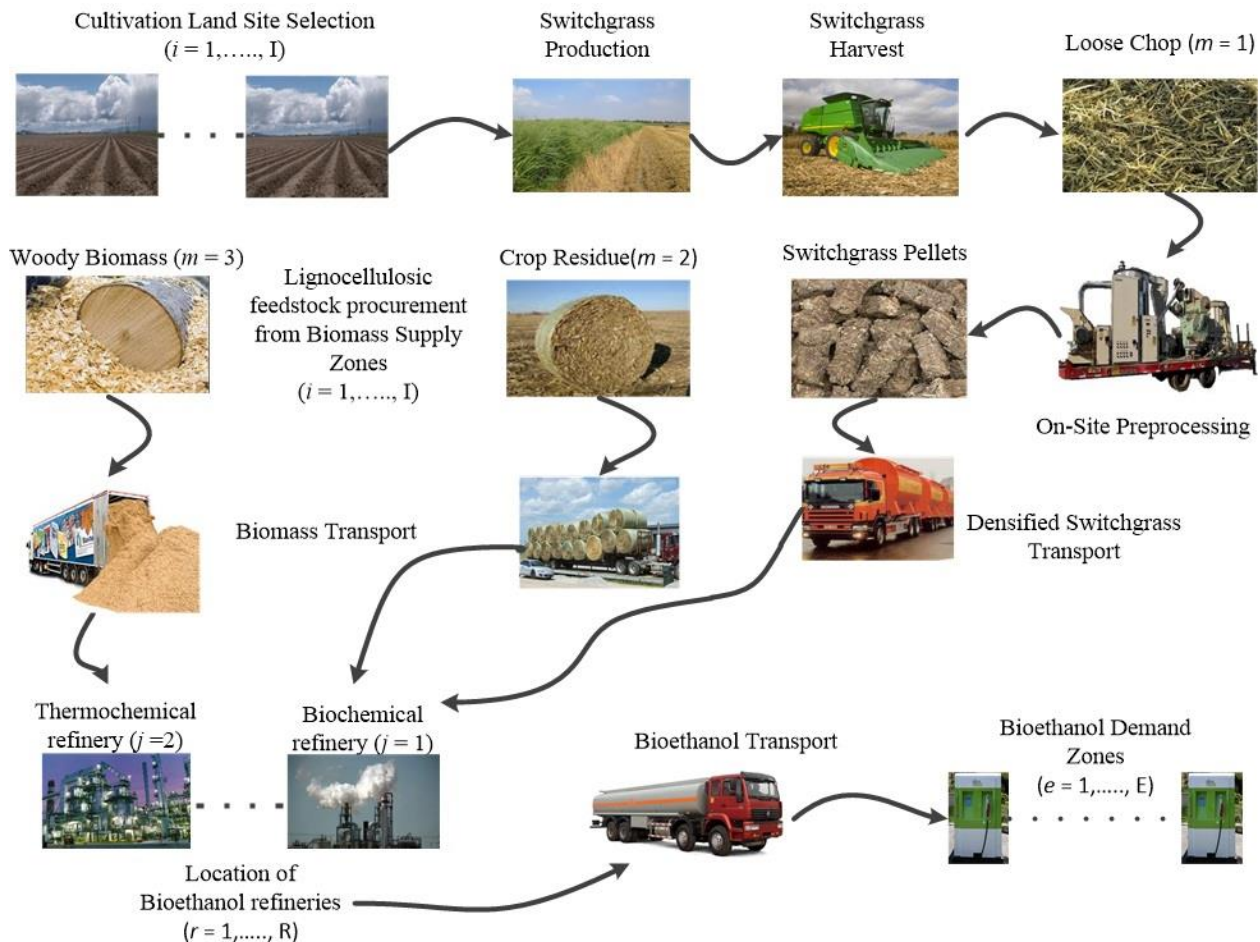


**Fig. 48. Major logistics activities in a LBSC**



Dedicated energy crops like switchgrass [34] show great potential but the crop yield is variable. The production of switchgrass is largely driven by the annual level of rainfall [35]. Adverse weather conditions (i.e. drought or floods) can cause massive disruption in the supply of switchgrass biomass [3]. A strategy for mitigating risk (i.e. risk pooling) in biomass supply is to use multiple existing sources of lignocellulosic feedstocks like crop residue and/or woody biomass [8, 36] in addition to switchgrass.

The major logistics activities in a LBSC are shown in Fig. 48. Feedstock of type  $m$  (i.e. switchgrass, crop residue or woody materials) can be harvested and/or procured from biomass supply zone  $i$ . The biomass feedstock  $m$  is then transported from supply zone  $i$  to biorefinery  $r$  that uses conversion technology  $j$  (i.e. biochemical or thermochemical). The supplied biomass feedstock is converted into bioethanol and co-products by biorefinery  $r$  using conversion technology  $j$ . The volume of bioethanol produced is driven by the ethanol demand and limited by the maximum biomass processing capacity of biorefinery  $r$ . The bioethanol is transported from biorefinery  $r$  to biofuel demand zone  $e$ . After satisfying the total bioethanol requirement, any excess volume of bioethanol is directly sold from biorefinery  $r$ . If the volume of bioethanol produced is not sufficient to meet the demand, shortfall in bioethanol requirement incurs a high penalty cost.

Based on work by [12] this research will assume that: 1) switchgrass and crop residues are harvested once a year after the first killing frost in late autumn; 2) woody materials can be harvested year round; 3) only road haulage for the transportation of lignocellulosic biomass and bioethanol is considered; and 4) the total bioethanol requirement during a planning period is proportional to the population in each demand zone.

The RFS allows for multi-period planning of biomass production and biorefinery installation, with different production levels for each year till 2022 [1, 7]. The timing and volumetric lignocellulosic-bioethanol quantities of the RFS are illustrated in Fig. 49. A 10 year time horizon can be

divided into a number of planning periods e.g. each planning period covers 2 years. Decision makers have to arrive at optimal long-term (i.e. across all the planning periods) and short-term (i.e. for each planning period) decisions to optimize the performance of the LBSC. Long-term and short-term decisions in a LBSC are related and impact one-another. As a result the optimal logistic decisions for each planning period cannot be arrived at independently of the subsequent planning periods (see Fig. 49). Coordinating decisions, while a challenging problem, has the potential to improve the long-term performance of a LBSC across multiple criteria.

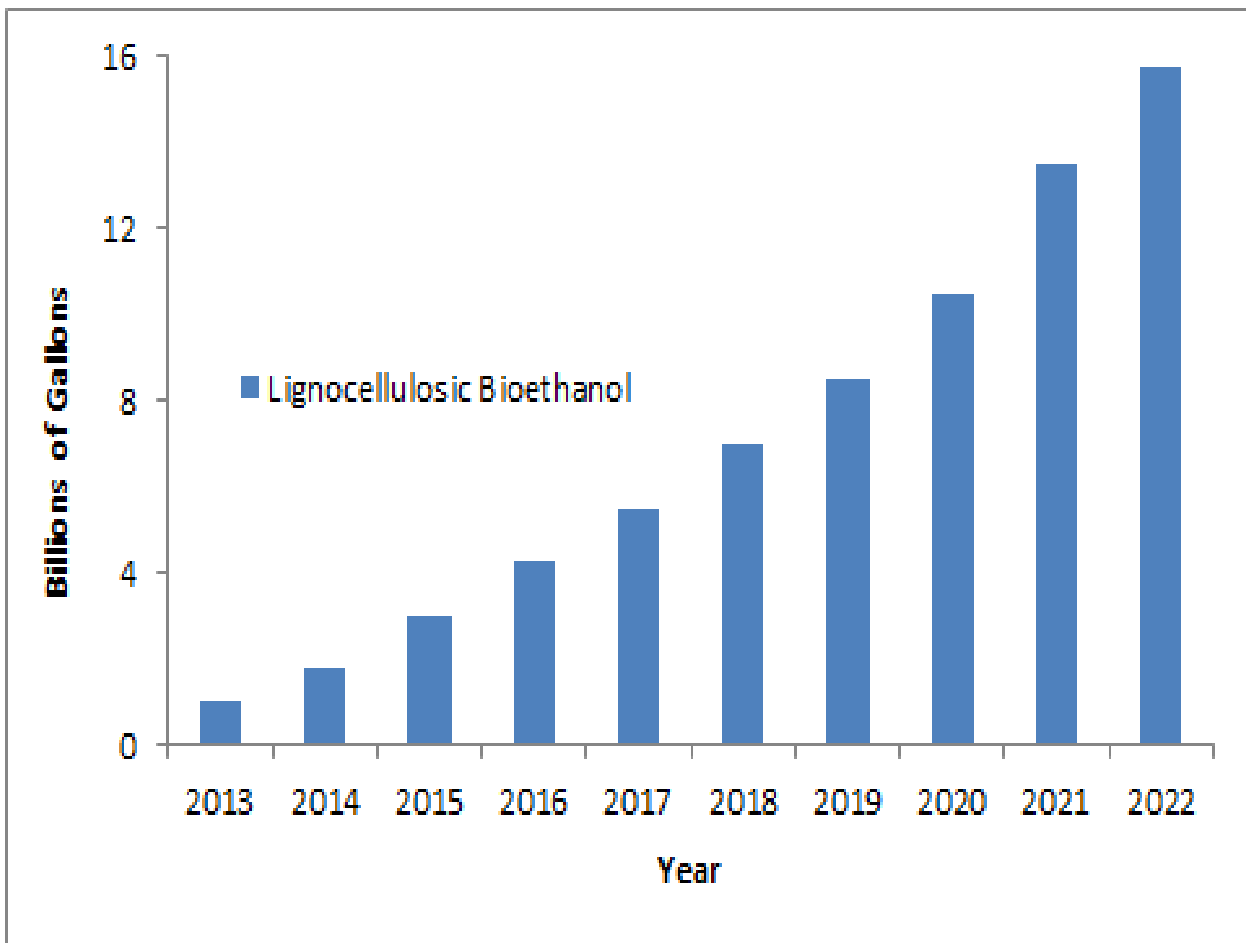


**Fig. 49. Renewable fuel standard (RFS)**

In order to maximize the expected LBSC profit, reduction in GHG emissions, and social benefits, the following strategic (i.e. first-stage) decisions need to be optimized for each planning period across all the stochastic scenarios:

- Cultivation sites selection from  $i$  supply zones and allocation of available marginal land for switchgrass production.
- Bioethanol refinery sites selection from  $r$  potential locations.
- Choice of conversion technology  $j$  to be used by each selected biorefinery. Biochemical and thermochemical pathways represent the two main current technologies for converting lignocellulosic biomass into bioethanol.
- Annual biomass processing capacity of each selected biorefinery.

For a given planning period, the following second stage decisions also need to be optimized for each stochastic scenario:

- Amount of switchgrass to be harvested and densified from biomass supply zones.
- Amount of crop residues and/or woody materials to be procured from biomass supply zones.
- Material flow of procured lignocellulosic feedstock  $m$  from supply zone  $i$  to biorefinery  $r$ .
- Amount of biomass type  $m$  to be processed by each biorefinery  $r$ .
- Volume of bioethanol to be produced by the  $r$  biorefineries.
- Material flow of bioethanol from the  $r$  refineries to the  $e$  biofuel demand zones.
- Volume of unmet bioethanol requirement for the  $e$  biofuel demand zones.

#### **5.4.1. Modeling the stochastic nature of the LBSC**

Literature review [12] has highlighted some of the key uncertainties inherent in the life cycle of a LBSC. This study jointly considers three of the major sources of uncertainties in each planning period, namely: 1) switchgrass yield due to unpredictable weather conditions; 2) demand for bioethanol; and 3) sale price for bioethanol.

In each planning period the “mean” value of the stochastic parameters are fixed. While across different planning periods the “mean” values can shift. The temporal dimension arises in long-term

LBSC planning when biomass cultivation and bioethanol production infrastructure needs to be expanded over time in response to the growing demand imposed by government mandates. Probability functions are used to model the uncertainties by analyzing historical data [37]. The following uncertainties are jointly considered in this work:

- The supply of switchgrass is not deterministic and fluctuates due to variation in annual rainfall [3]. The switchgrass supply level,  $o(\omega) = [\text{Switchgrass yield}(\omega)/\text{Average Switchgrass yield}]$
- Demand for ethanol is not deterministic and fluctuates on an annual basis [2]. The bioethanol demand level,  $\pi(\omega) = [\text{Bioethanol demand}(\omega)/\text{Average bioethanol demand}]$
- The price of bioenergy products depends on the inherent energy content and is influenced by gasoline price [12]. Energy price level,  $\sigma(\omega) = [\text{Price of gasoline}(\omega)/\text{Average price of gasoline}]$

## 5.5. Model formulation

The goal of the study is to determine for each planning period the optimal configuration of the LBSC (i.e. first-stage decisions) along with the associated operational decisions (i.e. second-stage) under uncertainties. A stochastic MILP model with multiple objectives is proposed to respectively maximize the economic, environmental, and social performances. The formulation including the objective functions and constraints of the model is explained in the following sections. All continuous decision variables are non-negative, while all integer variables have 0–1 (i.e. binary) restriction.

### 5.5.1. Objective functions of the LBSC

The proposed model is solved to optimality for each individual objective function (e.g. financial performance), while the values of the remaining objective functions (e.g. environmental and social performances) are computed based on the decisions obtained from the single-objective optimization. The proposed model has three distinct objective functions, namely: maximization of profit; maximization of reduction in GHG emissions; and maximization of jobs creation.

The financial objective of the LBSC is profit maximization (i.e. revenue – cost) subject to meeting the RFS mandates relating to bioethanol production and reduction in GHG emissions. Eq. 5.1 refers to the expected profit ( $\theta$ ) which needs to be maximized.

The different components of  $\theta$  (for each scenario  $\omega$ ) respectively refer to: fixed cost of biorefineries; variable cost of biorefineries; switchgrass production cost; revenue from the sale of bioethanol; revenue from the sale of renewable electricity; revenue from the sale of mixed alcohol; tax credit accrued from bioethanol production; tax credit accrued from renewable electricity generation; procurement cost of crop residue and woody biomass; biomass transportation cost; bioethanol transportation cost; harvest cost of switchgrass; preprocessing cost of switchgrass; bioethanol production cost; and penalty cost of unmet bioethanol demand.

$$\begin{aligned}
\theta = & - \sum_{r=1}^R \sum_{j=1}^J \sum_{t=1}^T G_{rj} Y_{rjt} - \sum_{r=1}^R \sum_{j=1}^J \sum_{t=1}^T H_{rj} K_{rjt} - \sum_{i=1}^I \sum_{t=1}^T \Xi_i M G_{it} \\
& + E_{\omega} \left[ \begin{aligned}
& \sum_{r=1}^R \sum_{j=1}^J \sum_{e=1}^E \sum_{t=1}^T t_{rt} \sigma_t(\omega) [L_{rjt}(\omega) + P_{rjet}(\omega)] + \sum_{r=1}^R \sum_{j=1}^J \sum_{t=1}^T \delta_{rt} \sigma_t(\omega) X_{rjt}(\omega) + \sum_{r=1}^R \sum_{j=1}^J \sum_{t=1}^T \chi_{rt} \sigma_t(\omega) S_{rjt}(\omega) + \\
& \sum_{r=1}^R \sum_{j=1}^J \sum_{e=1}^E \sum_{t=1}^T \tau_{re} P_{rjet}(\omega) + \sum_{r=1}^R \sum_{j=1}^J \sum_{t=1}^T \Theta_r X_{rjt}(\omega) - \sum_{m=2}^M \sum_{i=1}^I \sum_{r=1}^R \sum_{j=1}^J \sum_{t=1}^T \lambda_{mit} F_{mirjt}(\omega) - \sum_{m=1}^M \sum_{i=1}^I \sum_{r=1}^R \sum_{j=1}^J \sum_{t=1}^T \eta_{mir} D_{ir} F_{mirjt}(\omega) \\
& - \sum_{r=1}^R \sum_{j=1}^J \sum_{e=1}^E \sum_{t=1}^T \psi_{re} D_{re} P_{rjet}(\omega) - \sum_{i=1}^I \sum_{t=1}^T l c_i H V_{it}(\omega) - \sum_{i=1}^I \sum_{r=1}^R \sum_{j=1}^J \sum_{t=1}^T p p_i F_{lirjt}(\omega) - \sum_{r=1}^R \sum_{j=1}^J \sum_{t=1}^T U_{rj} Z_{rjt}(\omega) - \sum_{e=1}^E \sum_{t=1}^T \varphi_e O_{et}(\omega)
\end{aligned} \right] \tag{5.1}
\end{aligned}$$

The environmental objective of the LBSC is maximization of reduction in GHG emissions subject to meeting the RFS mandates relating to bioethanol production. Eq. 5.2 refers to the expected net reduction in GHG emissions ( $NR$ ) which needs to be maximized.

The different components of  $NR$  (for each scenario  $\omega$ ) respectively refer to: reduction in carbon emissions due to gasoline being substituted by bioethanol; reduction in carbon emissions due to conventional electricity being substituted by bioelectricity; reduction in carbon emissions due to heating oil being substituted by mixed alcohol; increase in carbon emissions from biomass harvesting;

increase in carbon emissions from converting biomass into biofuel; increase in carbon emissions from biomass transport; and increase in carbon emissions from biofuel transport.

$$NR = E_{\omega} \left[ \begin{aligned} & Q_{Eth} \sum_{r=1}^R \sum_{j=1}^J \sum_{t=1}^T Z_{rjt}(\omega) + Q_{Elt} \sum_{r=1}^R \sum_{j=1}^J \sum_{t=1}^T X_{rjt}(\omega) + Q_{MA} \sum_{r=1}^R \sum_{j=1}^J \sum_{t=1}^T S_{rjt}(\omega) - \sum_{m=1}^M \sum_{i=1}^I \sum_{r=1}^R \sum_{j=1}^J \sum_{t=1}^T \Lambda_m F_{mirjt}(\omega) \\ & - \sum_{m=1}^M \sum_{i=1}^I \sum_{r=1}^R \sum_{j=1}^J \sum_{t=1}^T \alpha_{mj} F_{mirjt}(\omega) - \sum_{m=1}^M \sum_{i=1}^I \sum_{r=1}^R \sum_{j=1}^J \sum_{t=1}^T \beta_m D_{ir} F_{mirjt}(\omega) - \sum_{r=1}^R \sum_{j=1}^J \sum_{e=1}^E \sum_{t=1}^T \gamma D_{re} P_{rjet}(\omega) \end{aligned} \right] \quad (5.2)$$

The social objective of the LBSC is maximization of job creation subject to meeting the RFS mandates relating to bioethanol production and reduction in GHG emissions. Eq. 5.3 refers to the expected number of jobs created ( $JB$ ) which needs to be maximized.

$$JB = \sum_{r=1}^R \sum_{j=1}^J \sum_{t=1}^T fb_{rj} K_{rjt} + E_{\omega} \left[ \sum_{i=1}^I \sum_{t=1}^T fm_i HV_{it}(\omega) \right] \quad (5.3)$$

The different components of  $JB$  (for each scenario  $\omega$ ) respectively refer to: number of jobs created during the installation and operation of a bioethanol refinery; and number of jobs created during switchgrass harvest.

### 5.5.2. Environmental performance constraint

Eq. 5.4 ensures that the expected reduction in carbon emissions is not less than the total carbon emission reduction target for the entire supply chain over all the planning periods.

$$NR \geq \sum_{r=1}^R \sum_{t=1}^T Cap_{rt} \quad (5.4)$$

### 5.5.3. Capacity constraints

$$MG_{it} \leq B_i \quad \forall i, t \quad (5.5)$$

$$HV_{it}(\omega) \leq MG_{it} \quad \forall i, t, \omega \quad (5.6)$$

$$\sum_{r=1}^R \sum_{j=1}^J F_{virjt}(\omega) \leq o_t(\omega) v_i HV_{it}(\omega) \quad \forall m, i, \omega, t \quad (5.7)$$

$$\sum_{r=1}^R \sum_{j=1}^J F_{mirjt}(\omega) \leq \zeta_{mi} \quad \forall i, \omega, t, m = 2, 3 \quad (5.8)$$

$$\sum_{j=1}^J Y_{rjt} \leq 1 \quad \forall r, t \quad (5.9)$$

$$\rho_j^{\min} Y_{rjt} \leq K_{rjt} \leq \rho_j^{\max} Y_{rjt} \quad \forall r, j, t \quad (5.10)$$

$$\sum_{m=1}^M \sum_{i=1}^I F_{mirjt}(\omega) \leq K_{rjt} \quad \forall r, j, t \quad (5.11)$$

The capacity constraints are given by Eq. 5.5 – 5.11. Eq. 5.5 ensures that in biomass supply zone  $i$ , the allocated marginal land for switchgrass cultivation do not exceed the marginal land availability. Eq. 5.6 ensures that in biomass supply zone  $i$ , the harvested land do not exceed the allocated marginal land for switchgrass cultivation. Eq. 5.7 ensures that in biomass supply zone  $i$ , the amount of biomass type  $m = 1$  sent to all biorefineries is not more than the amount of available densified switchgrass during scenario  $\omega$ . Eq. 5.8 ensures that in biomass supply zone  $i$ , the amount of biomass type  $m \neq 1$  sent to all biorefineries during scenario  $\omega$  is not more than the amount of available biomass type  $m$ . Eq. 5.9 ensures that maximum of one biorefinery is situated at location  $r$ . Eq. 5.10 ensures that a biorefinery (if built at location  $r$  with conversion technology  $j$ ) must annually process more biomass than minimum design capacity ( $\rho_j^{\min}$ ) and cannot process more biomass than maximum design capacity ( $\rho_j^{\max}$ ). Eq. 5.11 ensures that during scenario  $\omega$  a biorefinery does not process more biomass than its processing capacity.

#### 5.5.4. Material balance constraints

$$\sum_{m=1}^M \sum_{i=1}^I \kappa_{mj} F_{mirjt}(\omega) = Z_{rjt}(\omega) \quad \forall r, j, t, \omega \quad (5.12)$$

$$Z_{rjt}(\omega) = L_{rjt}(\omega) + \sum_{e=1}^E P_{rjet}(\omega) \quad \forall r, j, t, \omega \quad (5.13)$$

$$\sum_{m=1}^M \sum_{i=1}^I C_{mj} F_{mirjt}(\omega) = X_{rjt}(\omega) \quad \forall r, j, t, \omega \quad (5.14)$$

$$\sum_{m=1}^M \sum_{i=1}^I \mu_{mj} F_{mirjt}(\omega) = S_{rjt}(\omega) \quad \forall r, j, t, \omega \quad (5.15)$$

$$O_{et}(\omega) + \sum_{r=1}^R \sum_{j=1}^J P_{rjet}(\omega) = \Gamma v_{et} \pi_{et}(\omega) \quad \forall e, t, \omega \quad (5.16)$$

The material balance constraints are given by Eqs. 5.12 – 5.16. Eq. 5.12 ensures that in planning period  $t$  the cumulative amount of biomass (from all type  $m$  feedstocks) used by biorefinery  $r$  is converted into bioethanol (i.e. primary product) during scenario  $\omega$ . Eq. 5.13 ensures that in planning period  $t$  the volume of bioethanol produced by biorefinery  $r$  is either sold as unsubsidized bioethanol from the refinery-gate, or sent as subsidized biofuel to demand zones. Eq. 5.14 ensures that in planning period  $t$  the cumulative amount of biomass (from all type  $m$  feedstocks) used by biorefinery  $r$  is also converted into electricity (i.e. co-product) during scenario  $\omega$ . Eq. 5.15 ensures that in planning period  $t$  the cumulative amount of biomass (from all type  $m$  feedstocks) used by biorefinery  $r$  is also converted into mixed alcohol (i.e. co-product) during scenario  $\omega$ . Eq. 5.16 ensures that in each planning period  $t$  during scenario  $\omega$ , the volume of unmet bioethanol requirement plus the volume of bioethanol transported to demand zone  $e$ , is equal to the bioethanol requirement in biofuel demand zone.

#### 5.5.5. Link constraints

$$MG_{i(t-1)} \leq MG_{it} \quad \forall i, t \quad (5.17)$$

$$Y_{rj(t-1)} \leq Y_{rjt} \quad \forall r, j, t \quad (5.18)$$

$$K_{rj(t-1)} \leq K_{rjt} \quad \forall r, j, t \quad (5.19)$$

Constraints represented by Eqs. 5.17 – 5.19 link the various planning periods. As a result the optimal logistic decisions for each planning period cannot be arrived at independently of the subsequent planning periods. To achieve an overall effectiveness of the LBSC expansion, the dynamics of such an evolving process needs to be taken into consideration. Eq. 5.17 ensures that once a supply zone is selected as a biomass cultivation site, the allocated marginal land for switchgrass production can be increased but not decreased in subsequent planning period(s). Eq. 5.18 ensures that a biorefinery will not shut down once it opens. Eq. 5.19 ensures that the production capacity of an installed biorefinery can be increased but not decreased in subsequent planning period(s).



## 5.6. Two-step solution methodology for the proposed stochastic multi-period MILP model

For stochastic models with a non-trivial number of scenarios (greater than 1000), a number of sampling based approaches like SAA have been proposed to estimate objective function values. For large number of scenarios (greater than 10000), the desired optimality gap for reasonable accuracy might not be achievable using the traditional SAA method.

Benders decomposition is also found to be useful in solving stochastic models (with a non-trivial set of scenarios) within reasonable computation time using a small number of iterations, generally less than 100 [10]. However, Benders decomposition is extremely slow to converge when binary/integer variables are present in the first-stage e.g. the capacitated facility location problems which are NP-hard [38, 39]. For large number of scenarios (greater than 10000), Benders decomposition may not obtain an optimal solution (of desired accuracy even after more than 500 iterations) for the full stochastic problem involving both binary and continuous first-stage decisions.

In order to solve the proposed stochastic model with greater accuracy within reasonable computational time, this work utilizes a 2-step solution approach involving sequential application of a modified SAA method and Benders decomposition. The modified SAA method is first applied to only solve the binary variables present in the stochastic model. Using the optimal values of the first-stage binary decision variables obtained from the application of the modified SAA method as a surrogate solution for the complete stochastic problem, the computational burden of the stochastic model is considerably reduced i.e. only the optimal values for the continuous decision variables need to be determined. For large number of scenarios (greater than 10000), even the reduced stochastic linear programming (LP) model can still be too big to be directly solved using commercial solvers without running out of memory. Therefore, Benders decomposition is then used to obtain the optimum solution for the reduced stochastic LP model using a small number of iterations (i.e. less than 100).

### 5.6.1. Modified SAA method

Details regarding application of SAA method for the stochastic optimization of biomass-to-biofuel supply chain are provided by [29]. During the traditional use of the SAA method, the algorithm terminates when the desired optimality gap is achieved [40]. However, for large number of scenarios (say 16000), the desired optimality gap for reasonable accuracy (i.e. less than 0.5%) is not achievable using the traditional SAA method.

In order to solve the proposed large-scale stochastic model within reasonable computational time, a modified SAA method is proposed where the aim is to arrive at a solution (irrespective of the desired optimality gap) where each sample set gives the same values for the binary variables. The use of the “modified” SAA algorithm is displayed in Fig. 50.

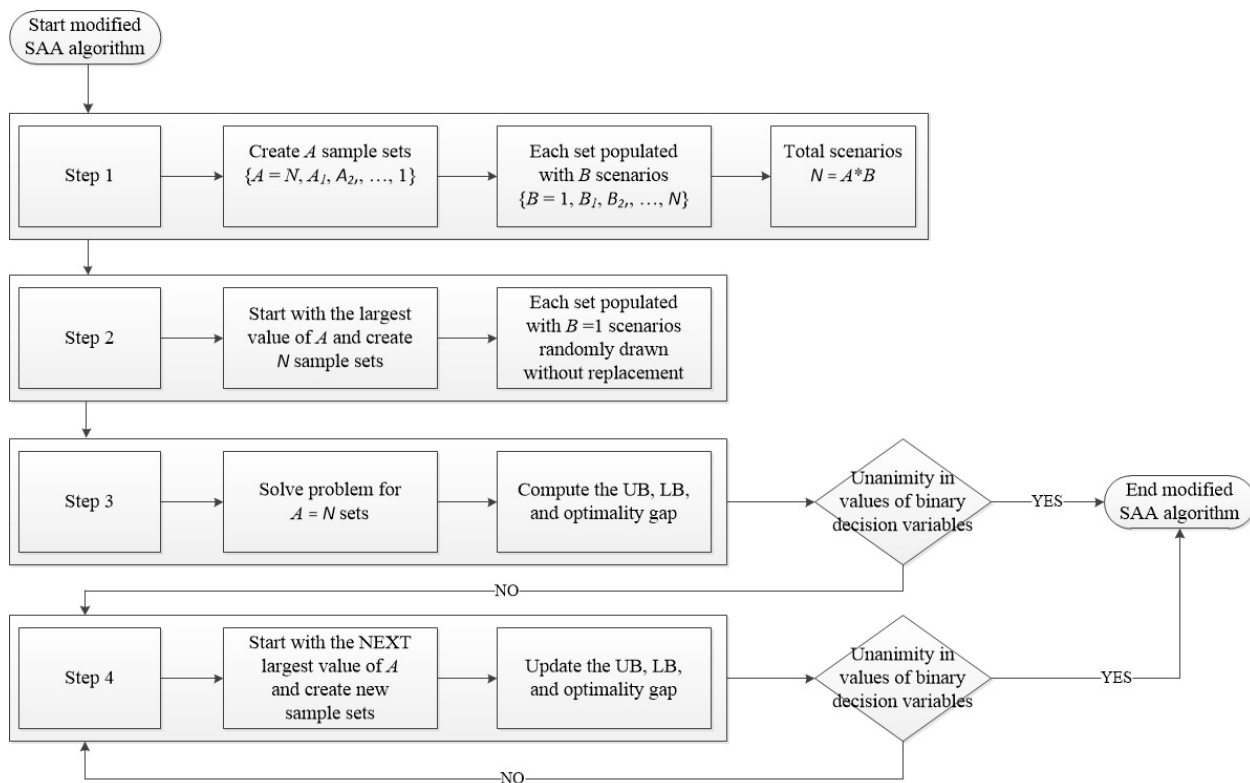


**Fig. 50. Modified application of the SAA method**

## 5.6.2. Benders decomposition

Having determined the optimal values of the first-stage binary decision variables using the modified SAA method, Benders decomposition is used to determine the first-stage continuous decision variables for each planning period i.e. allocation of marginal land for switchgrass cultivation and biomass processing capacity of biorefineries. The problem is divided into master and sub-problem, where the master problem contains the deterministic part, and the sub-problem has the stochastic part. Details regarding application of Benders decomposition for the stochastic optimization of biomass-to-biofuel supply chain are provided by [10]. In order not to have redundancy in equations, we introduce the general two-stage stochastic problem (see Eq. 5.20) to make reference to the algorithm easy and for clearer explanation.

### Two-stage stochastic problem

$$\begin{aligned}
 \text{Max} \quad & z = c^T x + E_{\omega}[\max q(\omega)^T y(\omega)] \\
 \text{s.t.} \quad & Ax \leq b \\
 & T(\omega)x + Wy(\omega) = h(\omega) \\
 & x \geq 0, y(\omega) \geq 0
 \end{aligned} \tag{5.20}$$

### Master problem

$$\begin{aligned}
 \text{Min} \quad & z_1 = c^T x + \eta \\
 \text{s.t.} \quad & Ax = b, \\
 & \eta \geq \frac{1}{N} \sum_{\omega=1}^N \pi_{\omega}(h_{\omega} - B_{\omega}z_{j,k}) \\
 & x \geq 0, z_{j,k} \geq 0.
 \end{aligned} \tag{5.21}$$

### Sub problem

$$\begin{aligned}
 \text{Min} \quad & z_2 = d_{\omega}^T y_{\omega}(\omega) \\
 \text{s.t.} \quad & W_{\omega}y_{\omega}(\omega) = h_{\omega}(\omega) - T_{\omega}xbar \\
 & x \geq 0, y(\omega) \geq 0
 \end{aligned} \tag{5.22}$$

Where  $xbar$  is the optimal solution of  $x$  in the first stage

In Eq. 5.21,  $\eta$  is the optimality cut. The Benders decomposition algorithm is as follows:

*Step 1:* Set  $l = 1$ , where  $l$  is the iteration counter, and  $UB_l = \infty$ , that is, upper bound is set to positive infinity, and the lower bound is set to zero,  $LB_l = 0$ . Solve problem Eqs. 5.21 and let  $\eta = 0$  to obtain the optimal decision values of the master problem without cut.

- Step 2:* Solve the sub problem, i.e. Eq. 5.22 by using  $z_{j,k}$  as a constant to obtain the optimal first-stage decisions, i.e.  $xbar$
- Step 3:* Determine the dual of the sub problem, and represent them by the dual variables, in this case  $\pi_\omega$
- Step 4:* Update the upper bound by setting:  $UB_{l+1} = \min \{UB_l, z_1 + z_2\}$  where  $z_1$  and  $z_2$  are the objective function value of the master and sub problems respectively
- Step 5:* Update the lower bound by setting:  $LB_{l+1} = z_1$
- Step 6:* Add cut  $\eta$  to the master problem
- Step 7:* Proceed to test if  $(UB_l - LB_l) < Tolerance$ , return the optimal solution, otherwise, set the iteration counter to  $l = l + 1$ . Here Tolerance is a pre-determined small value (i.e.  $< 0.5\%$ ) to determine the stopping criterion
- Step 8:* Solve the updated master problem Eq. 5.21 and add the updated cut  $\eta$  and go back to step 2.

In the master problem the individual LBSC performances represent the optimization objectives. For optimizing the financial performance, Eq. 5.1 represents the objective function (i.e. cost minimization). Similarly, Eq. 5.2 and Eq. 5.3 respectively represent the objective functions of carbon emission minimization and job loss minimization. Constraints represented by Eqs. 5.4, 5.5, 5.9–5.11, 5.17–5.19 become part of the master problem while constraints represented by Eqs. 5.6–5.8, 5.12–5.16 become part of the sub problem.

### **5.6.3. Trade-off among different performance criteria**

In developing sustainable LBSC, the challenge is to simultaneously maintain financial viability, reduce environmental damage, and provide greater social benefits. In the face of these competing objectives, no improvement can be made with respect to one objective without worsening the other objective(s). In this work the  $\varepsilon$ -constraint method [32] is used for conducting trade-off analysis among

different performance criteria. The following example details how the  $\varepsilon$ -constraint method is applied for trade-off between financial and environmental performance.

The proposed stochastic model is optimized for economic performance with Eq. 5.1 representing the objective function and the value of environmental performance (represented by Eq. 5.2) calculated based on the decisions obtained from economic optimization. This is referred to as the “base case” where the financial and environmental performances are respectively represented by  $\theta_{\text{base}}$  and  $NR_{\text{base}}$ . The value of the environmental performance is increased by an amount ( $\varepsilon$ ) and added as a new constraint to the optimization model as Eq. 5.23. The optimization model is rerun and the new value of the economic performance ( $\theta_{\text{New}}$ ) is calculated. The value of the environmental performance is incrementally increased and the corresponding value of economic performance is recalculated until the model becomes infeasible i.e. the required environmental performance cannot be achieved.

$$NR_{\text{New}} \geq NR_{\text{Base}} + \varepsilon \quad (5.23)$$

Similar methodology can be used for conducting the following trade-offs: 1) financial vs. social performance; and 2) social vs. environmental performance.

## 5.7. Case study set-up

Parameters used in this case study are displayed in Tables A10 and A11 (see Appendix A). The case study is set in the Midwestern state of Wisconsin (WI) and aims to show if 20% of the annual demand for gasoline (by the year 2022) can be met by the production of bioethanol from multiple lignocellulosic biomass feedstocks (i.e. switchgrass, crop residue, and woody materials) while satisfying the mandated reduction in GHG emissions.

### 5.7.1. Model assumptions

The various indices and assumptions used in the stochastic MILP model are displayed in Table 10 and also explained below.

**Table 10. Indices used in the case study**

$e$	Bioethanol demand zones ( $e = 1, 2, \dots, 72$ )
$i$	Lignocellulosic biomass supply zones ( $i = 1, 2, \dots, 72$ )
$j$	Bioethanol conversion technologies $j = 1$ (Biochemical); $j = 2$ (Thermochemical)
$m$	Lignocellulosic feedstocks $m = 1$ (Switchgrass); $m = 2$ (Crop Residue); $m = 3$ (Woody Biomass)
$r$	Biorefinery locations ( $r = 1, 2, \dots, 72$ )
$t$	Planning periods ( $t = 1, 2, 3, 4, 5$ )
$\omega$	Stochastic scenarios ( $\omega = 1, 2, \dots, N$ )

- Total planning horizon is 10 year, with 5 planning periods ( $t = 1, 2, 3, 4, 5$ ). Each planning period comprises of 2 years.
- All 72 counties of Wisconsin are potential biorefinery locations, biomass supply zones, and bioethanol demand zones. Biomass availability and bioethanol demand are centered at the county seat (e.g. Hurley is seat of Iron County).
- Demand for co-products (i.e. electricity and mixed alcohols) is assumed to be always greater than supply.
- Work by [12, 29] has shown that stochastic models outperform deterministic models under uncertainties. This work therefore focuses on the results and analysis of the stochastic model.

### 5.7.2. Modeling the uncertainties in a LBSC

In this work, all stochastic scenarios are governed by 3 independent random variables (IRVs) which are not correlated. The first IRV,  $\alpha_t(\omega)$  is used to model switchgrass supply level. The second IRV,  $\pi_t(\omega)$  is used to model bioethanol demand level. The third IRV,  $\sigma_t(\omega)$  is used to model gasoline price level, which acts as a surrogate for price level of bioethanol, electricity and mixed alcohols. The three IRVs are assumed to follow Normal probability distributions.

### 5.7.3. Discretization of continuous stochastic parameters

A set of possible scenarios with a given probability of occurrence are used to describe the random events. The use of continuous probability distributions to model the uncertainty is likely to result in an infinite number of stochastic scenarios [12, 29]. In order to make the problem

computationally tractable, each IRV is discretized into 10 levels (see Table 11). The number of discretized levels used is sufficient to ensure that the entire range of the probability distribution is captured. The resulting total number of stochastic scenarios =  $(10^3)^5 = 10^{15}$ .

**Table 11. Discretized levels of independent random variables (IRVs)**

Supply level of switchgrass		Demand level of bioethanol		Price level of bioenergy	
Level	Mean Value	Level	Mean Value	Level	Mean Value
L_o01	0.68	L_π01	0.84	L_σ01	0.75
L_o02	0.80	L_π02	0.90	L_σ02	0.86
L_o03	0.87	L_π03	0.94	L_σ03	0.91
L_o04	0.93	L_π04	0.96	L_σ04	0.95
L_o05	0.97	L_π05	0.99	L_σ05	0.98
L_o06	1.03	L_π06	1.01	L_σ06	1.02
L_o07	1.07	L_π07	1.04	L_σ07	1.05
L_o08	1.13	L_π08	1.06	L_σ08	1.09
L_o09	1.20	L_π09	1.10	L_σ09	1.14
L_o10	1.32	L_π10	1.16	L_σ10	1.25

A large number of scenarios (i.e.  $10^{15}$ ) are required because the problem includes a very large number of uncertain parameters as a result of the multi-period nature of the model and the large size of the LBSC network. The number of stochastic scenarios need to be reduced (while maintaining the overall accuracy of the results) in order to ensure solution within reasonable computation time. To reduce the model size and the number of scenarios, a Monte Carlo sampling approach is used to generate a sample of  $N$  scenarios [41, 42], with each scenario  $\omega$  (where  $\omega = 1, 2, \dots, N$ ) equally likely to happen. The number of scenarios is determined by using a statistical method [32] to obtain solutions within specific confidence intervals for a desired level of accuracy. Eq. 5.24 depicts the method which is effective for scenario reduction, particularly for large-scale problems with infinite scenarios. Where  $Z = z$ -value (e.g. 2.58 for 99% confidence level) and  $c =$  confidence interval, expressed as decimal (e.g.  $\pm 1\% = 0.01$ ).

$$N = (Z / 2c)^2 \tag{5.24}$$

For a problem with almost infinite number of scenarios (i.e.  $10^{15}$ ), a sample size of  $N = 16000$  can find the true optimal solution with 99% probability with an accuracy of  $\pm 1\%$ .

#### **5.7.4. Sequential application of modified SAA method and benders decomposition**

The  $N = 16000$  discrete scenarios are used to convert the proposed stochastic MILP model into the Deterministic Equivalent Model (DEM) which is coded in GAMS and has 720 binary variables. The DEM is executed by the XpressMP solver using the platform of NEOS server hosted at [www.neos-server.org/neos](http://www.neos-server.org/neos).

The modified SAA algorithm is used to solve the binary decision variables in the DEM, with 0.5% as the pre-set criteria for the optimality gap ( $\epsilon$ ). For this work unanimity in the values of the binary variables is achieved from a sample of 16 sets, with each set populated with 1000 scenarios randomly drawn without replacement from the 16000 scenarios. The Upper Bound (UB) on the expected profit is \$846 Million while the Lower Bound is \$836 Million. The achieved optimality gap =  $[(UB - LB)/UB] = [(846 - 836)/846] = 0.012$  (or 1.2%). Further reduction in the optimality gap is not possible as subsequent iterations of the SAA method (i.e. sample of 8 sets, with each set populated with 2000 scenarios) are not solvable by the commercial XpressMP solver due to the large number of stochastic scenarios in each sample set.

Using the optimal values of the first-stage integer decision variables obtained from the application of the modified SAA method as a surrogate solution for the complete stochastic problem, the computational burden of the stochastic model is considerably reduced. The optimum solution for the reduced stochastic LP model with only continuous first-stage decision variables is reached after 75 iterations of the Benders algorithm coded in GAMS and executed by the commercial XpressMP solver. The expected profit is \$842 Million and the achieved optimality gap =  $[(UB - \text{expected profit})/UB] = [(846 - 842)/846] = 0.0047$  (or 0.47%).



Using the modified SAA method, the optimal solution for the binary variables (for each of the 16 sample sets with each set populated with 1000 scenarios) is reached after 27000 sec of CPU run time. While using the Benders algorithm, the optimum solution for the continuous variables (over all the 16000 scenarios) is reached after 1800 seconds of CPU run time. Table 12 shows that compared to using only the SAA method, the two-step approach (i.e. sequential application of the modified SAA method and Benders decomposition) to solve the stochastic model gives a higher expected LBSC profit (i.e. \$842 Million vs. \$836 Million) with greater accuracy (i.e. optimality gap of 0.47% vs. 1.2%).

**Table 12. Modified SAA method vs. 2-step approach**

Comparison Criteria	Modified SAA	2-step approach
Expected Profit (\$ Million)	836	842
Optimality Gap	1.20%	0.47%

## 5.8. Case study results

### 5.8.1. First-stage decisions during each planning period

The first-stage decisions (i.e. allocation of marginal land for switchgrass cultivation, site selection, conversion technology, and biomass processing capacity of bioethanol refineries) reached under different optimization objectives are discussed in the following sections. Prior to the first planning period, it is assumed that marginal land is not allocated for switchgrass cultivation and no bioethanol refinery (of any conversion technology) is installed.

The financial performance is optimized by maximizing  $\theta$  (see Eq. 5.1) while subject to constraints represented by Eqs. 5.4 – 5.19. The values for the environmental performance (see Eq. 5.2) and social performance (see Eq. 5.3) are computed based on the decisions obtained from financial optimization.

The eastern part of Wisconsin is relatively arid (compared to the western part) and is therefore shown to not be selected as switchgrass cultivation site during any planning period. However, the eastern counties have abundant woody biomass resources. Switchgrass is preferred as the main source

of biomass feedstock as it has the lowest production cost. Increasing amounts of woody biomass (comprising up to 37% of the total feedstock consumption) is procured once the best sites for switchgrass cultivation (i.e. marginal land with high crop yield and/or low land rental cost) are exhausted. Due to high purchase price of crop residue it only comprises a maximum of 8% of the total amount of feedstock consumed.

During the first planning period, a single biochemical refinery with biomass processing capacity of 1.05 million tons per year (MTPY) is installed in Trempealeau county. 152000 acres of marginal land are allocated for switchgrass cultivation. This represents 8% of the total marginal land in the state of WI. The average amount of feedstock procured as switchgrass, crop residue and woody materials are 0.87 MTPY (82%), 0.05 MTPY (5%), and 0.13 MTPY (13%) respectively. The figures in parenthesis represent the percentage contribution of each source of feedstock. Herbaceous biomass (preferred by biochemical refineries) comprising of switchgrass and crop residue represents the bulk of the procured feedstock (= 87%).

During the second planning period, 349000 acres of marginal land are allocated for switchgrass cultivation. This represents 18% of the total marginal land in the state of WI. The average amount of feedstock procured as switchgrass, crop residue and woody materials are 2.01 MTPY (83%), 0.25 MTPY (6%), and 0.13 MTPY (11%) respectively. Herbaceous biomass still represents the bulk of the procured feedstock (= 89%). Biomass processing capacity of the existing biochemical refinery (in Trempealeau county) is increased to 2.41 MTPY.

During the third planning period, 568000 acres of marginal land are allocated for switchgrass cultivation. This represents 29% of the total marginal land in the state of WI. The average amount of feedstock procured as switchgrass, crop residue and woody materials are 3.33 MTPY (84%), 0.27 MTPY (7%), and 0.38 MTPY (9%) respectively. Herbaceous biomass still represents the bulk of the procured feedstock (= 91%). Biomass processing capacity (of the existing biochemical refinery in

Trempealeau county) is increased to 2.56 MTPY, and a new biochemical refinery (with biomass processing capacity of 1.41 MTPY) is installed in Richland county.

During the fourth planning period, 847000 acres of marginal land are allocated for switchgrass cultivation. This represents 43% of the total marginal land in the state of WI. The average amount of feedstock procured as switchgrass, crop residue and woody materials are 4.97 MTPY (83%), 0.45 MTPY (8%), and 0.53 MTPY (9%) respectively. Herbaceous biomass still represents the bulk of the procured feedstock (= 91%). Biomass processing capacities of the existing biochemical refineries in Richland and Trempealeau county are both increased to 3 MTPY.

During the fifth planning period, 948000 acres of marginal land are allocated for switchgrass cultivation. This represents 48% of the total marginal land in the state of WI. The average amount of feedstock procured as switchgrass, crop residue and woody materials are 5.51 MTPY (58%), 0.45 MTPY (5%), and 3.55 MTPY (37%) respectively. Herbaceous biomass still represents the bulk of the procured feedstock (= 63%) but the contribution of woody biomass is also significant (= 37%). In addition to the existing biochemical refineries, new thermochemical refineries respectively installed in Marathon and Oconto county. Bioethanol produced from thermochemical refineries now account for one-third of the total bioethanol production in the LBSC.

The environmental performance is optimized by maximizing  $NR$  (see Eq. 5.2) while subject to constraints represented by Eqs. 5.4 – 5.19. Values for financial performance (see Eq. 5.1) and social performance (see Eq. 5.3) are computed based on decisions obtained from environmental optimization.

The eastern part of Wisconsin has an abundant supply of crop residue (compared to the western part). Crop residue is preferred as the main source of biomass as it has the lowest GHG emissions (compared to switchgrass or woody biomass) during feedstock procurement. Small amounts of woody biomass (comprising less than 9% of the total feedstock consumption) is procured once the best supply zones for crop residue procurement are exhausted.

Due to relatively high GHG emissions associated with switchgrass cultivation, marginal land is not allocated for switchgrass cultivation during any planning period. Biochemical refineries are exclusively selected and the trend is towards installing a larger number of widely spread small biorefineries (with biomass processing capacities less than 1.6 MTPY) to reduce the transportation distance from supply zones. This in turn reduces the GHG emissions during biomass transportation.

During the first planning period, crop residue is exclusively used as the biomass feedstock. A single biochemical refinery (with biomass processing capacity of 1.29 MTPY) is installed in Calumet county. During the second planning period, crop residue is still exclusively used as the biomass feedstock. A new biochemical refinery (with biomass processing capacity of 1.25 MTPY) is also installed in Trempealeau county. During the third planning period, crop residue is still exclusively used as the biomass feedstock. A new biochemical refinery (with biomass processing capacity of 1.43 MTPY) is also installed in Lincoln county. During the fourth planning period, the average amount of feedstock procured as crop residue and woody materials are 5.67 MTPY (95%), and 0.32 MTPY (5%) respectively. The figures in parenthesis represent the percentage contribution of each source of feedstock. Crop residue still represents the bulk of the procured feedstock. New biochemical refineries (with biomass processing capacities of 1.57 MTPY and 1.11 MTPY) are also installed in Waushara and Waukesha county respectively. During the fifth planning period, the average amount of feedstock procured as crop residue and woody biomass are 5.67 MTPY (91%), and 0.32 MTPY (9%) respectively. Crop residue still represents the bulk of the procured feedstock. New biochemical refineries are also installed in Washburn and Dane county respectively.

The social performance is optimized by maximizing  $JB$  (see Eq. 5.3) while subject to constraints represented by Eqs. 5.4 – 5.19. The values for the financial performance (see Eq. 5.1) and environmental performance (see Eq. 5.2) are computed based on the decisions obtained from social optimization.

The eastern part of Wisconsin has relatively low switchgrass yields (compared to the western part) but has abundant woody biomass resources. Switchgrass is preferred as the main source of biomass feedstock as it creates the largest number of jobs during biomass procurement (compared to crop residue and/or woody biomass). Small amounts of woody biomass (comprising less than 8% of the total feedstock consumption) is procured once the best sites for switchgrass cultivation (i.e. marginal land with high crop yield and/or low land rental cost) are exhausted and/or when no more marginal land is available for switchgrass cultivation. Thermochemical refineries are exclusively selected as they create more jobs when compared to biochemical refineries (of similar biomass processing capacity). As such, negligible amount ( $\approx 0\%$ ) of crop residue is procured as biomass feedstock during any period.

During the first planning period, 275000 acres of marginal land are allocated for switchgrass cultivation in 4 south western counties. This represents 14% of the total marginal land in the state of WI. Switchgrass is exclusively used as the biomass feedstock. A single thermochemical refinery (with biomass processing capacity of 1.31 MTPY) is installed in Richland county.

During the second planning period, 608000 acres of marginal land are allocated for switchgrass cultivation in 7 south western counties. This represents 31% of the marginal land in the state of WI. Switchgrass is still exclusively used as biomass feedstock. Biomass processing capacity (of existing thermochemical refinery in Richland county) is increased to 3 MTPY (i.e. max capacity limit).

During the third planning period, 1053000 acres of marginal land are allocated for switchgrass cultivation in the central, north central, north eastern, and south western counties. This represents 53% of the marginal land in the state of WI. Switchgrass is still exclusively used as biomass feedstock. In addition to the existing thermochemical refinery (in Richland county), a new thermochemical refinery (with processing capacity of 1.96 MTPY) is installed in Oconto county.

During the fourth planning period, 1434000 acres of marginal land are allocated for switchgrass cultivation in the central, east central, north central, north eastern, north western, and south western

counties. This represents 72% of the total marginal land in the state of WI. The average amount of feedstock procured as switchgrass, and woody materials are 7.10 MTPY (95%), and 0.35 MTPY (5%) respectively. The figures in parenthesis represent the percentage contribution of each source of feedstock. Switchgrass still represents the bulk of the procured feedstock. Biomass processing capacity (of the existing thermochemical refinery in Oconto county) is increased to 3 MTPY (i.e. max capacity limit), and a new thermochemical refinery (with biomass processing capacity of 1.44 MTPY) is installed in Washburn county.

During the fifth planning period, 1984000 acres are allocated for switchgrass cultivation. This represents 100% of the marginal land. Amount of feedstock procured as switchgrass, and woody materials are 10.50 MTPY (93%), and 0.84 MTPY (7%) respectively. Switchgrass still represents bulk of the procured feedstock. Processing capacity (of existing thermochemical refinery in Washburn county) is increased to 3 MTPY (i.e. max capacity limit), and a new thermochemical refinery (with processing capacity of 2.34 MTPY) is installed in Waushara county.

LBSC performances under different optimization objectives are displayed in Table 13 and discussed below. Profit maximization (i.e. economic performance) favors switchgrass as the main feedstock (as long as it is cheaper to procure than crop residue and/or woody biomass) produced from the cultivation of switchgrass on marginal land.

**Table 13. LBSC performances under different optimization objectives**

<b>Optimization Objective</b>	<b>Profit (\$ Million)</b>	<b>Reduction in GHG emissions (Million Tons)</b>	<b>Jobs Created</b>
Maximize Financial Performance	842	8.68	8444
Maximize Environmental Performance	50	9.55	6908
Maximize Social Performance	253	6.46	12582

From a financial standpoint the expected revenue (per unit of energy content) provided by the co-product (i.e. mixed alcohols) from a thermochemical refinery is higher than those from co-product (i.e. bioelectricity) from a biochemical refinery.

Reduction in GHG emissions favors procurement of crop residue and/or woody biomass rather than switchgrass. In life-cycle analysis (LCA), the GHG emissions are largely credited to the primary crop (e.g. corn) or activity (e.g. harvesting of timber for commercial logging). The residual biomass is only credited with carbon emissions during the collection and transporting phases. In the case of switchgrass, LCA also include emissions during the crop cultivation phase.

From an environmental standpoint, the reduction in carbon emissions (per unit of energy content) provided by mixed alcohols (i.e. due to substitution for heating oil) produced by a thermochemical refinery is lower than those from bioelectricity (i.e. due to substitution for coal as the fuel for electricity generation in the U.S.) produced by a biochemical refinery.

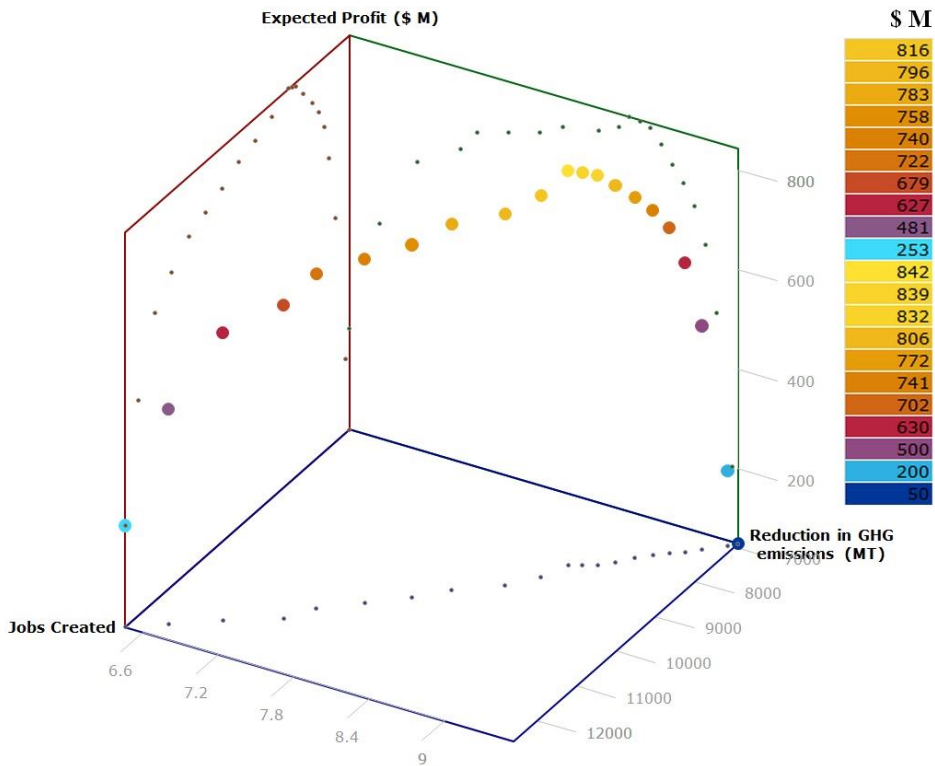
Increase in job creation favors switchgrass as the main feedstock. More jobs are created during switchgrass cultivation compared to collection of agricultural residue.

From a social standpoint, installation and operation of a thermochemical refinery creates more jobs than those from a biochemical refinery of similar processing capacity. This is due to the fact that the installation and operation of a thermochemical refinery is much more capital and labor intensive.

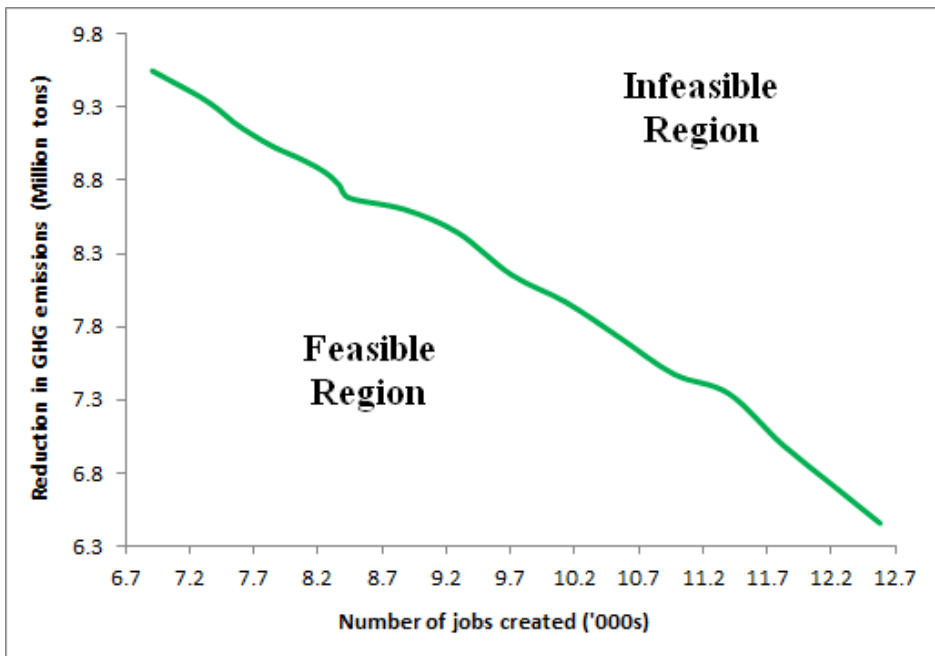
### **5.8.2. Trade-off among economic, environmental and social performance criteria**

Fig. 51 displays the 3D (three dimensional) Pareto optimum sets. Expected profit (in \$ Million) is plotted on the  $z$ -axis, reduction in carbon emissions (in Million Tons) on the  $x$ -axis, and number of jobs created on the  $y$ -axis. Fig. 51 shows that there is no single solution set which simultaneously maximizes all 3 performance criteria. Maximization of job creation results in the smallest reduction in carbon emissions and vice versa. Similarly, profit is maximized (i.e. base-case) when both the environmental and social performance are not at their highest levels.

For more clarity, trade-offs between the key performance criteria (i.e. environmental vs. social, economic vs. social, and economic vs. environmental) using the  $\epsilon$ -constraint method is analyzed.



**Fig. 51. 3D Pareto optimum sets**



**Fig. 52. Social vs. environmental performance**

Fig. 52 shows that the objective of maximizing reduction in GHG emissions is contradictory to the objective of maximizing job creations (and vice versa). Best environmental performance is



achieved by exclusively using crop residue as the feedstock for biochemical refineries while the best social performance is achieved by exclusively using switchgrass as the feedstock for thermochemical refineries. For a given reduction in GHG emissions, the number of jobs created (as shown by the Pareto curve in Fig. 52) cannot be increased by further reducing the financial profit.

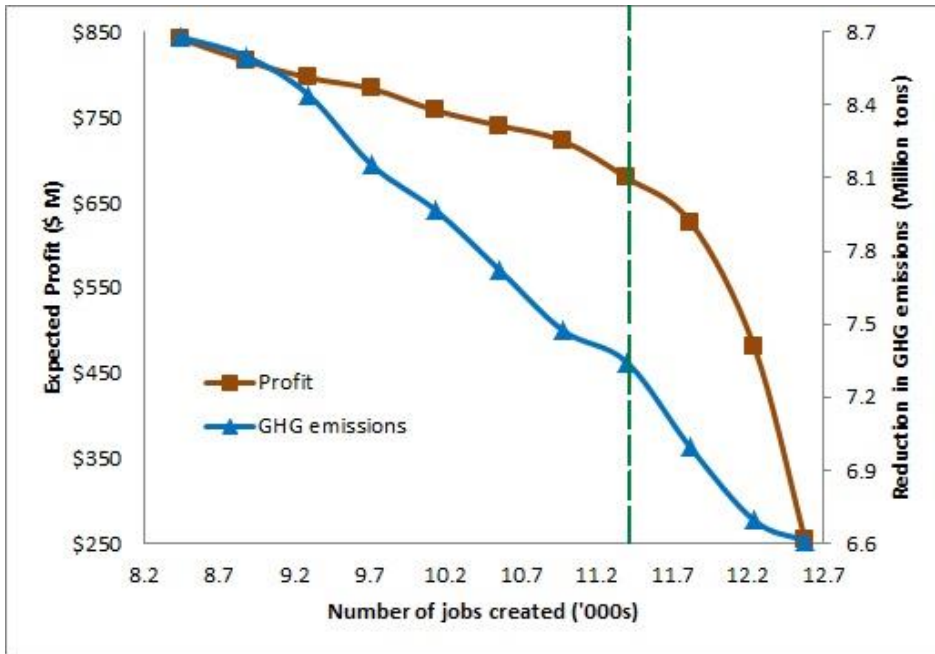


**Fig. 53. Economic vs. social objective**

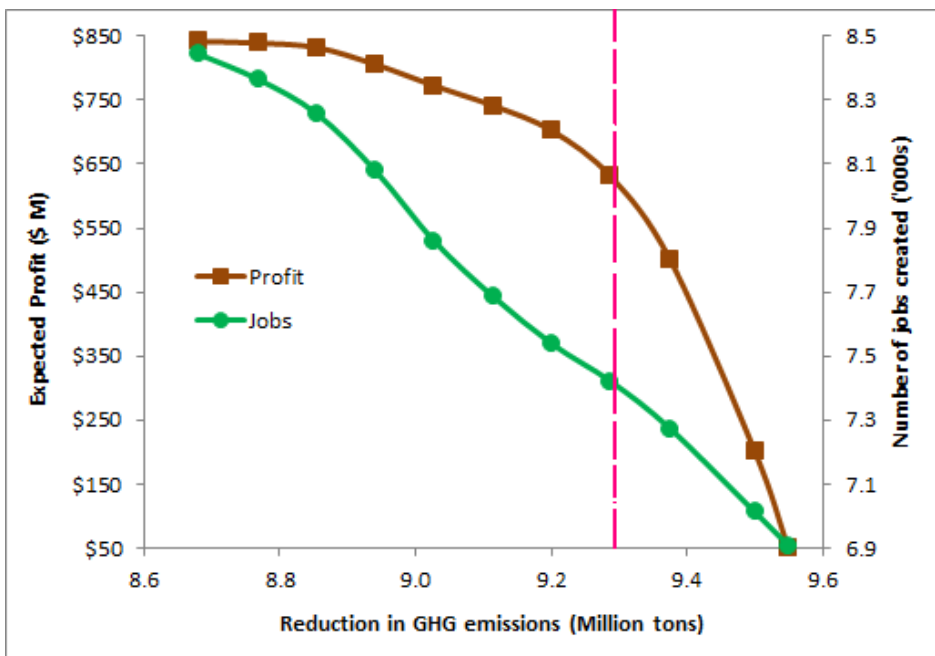


**Fig. 54. Economic vs. environmental objective**

Fig. 53 displays the trade-off between economic and social performance. Compared to the base-case, 35% increase in job creations result in 20% reduction in expected profit and 15% increase in carbon emissions. A further 15% increase in job creations results in a staggering 50% reduction in expected profit. Areas on the left and right sides of the dotted line respectively refer to the “recommended” and “not recommended” regions. The point where the dotted line meets the profit curve represents a suitable trade-off between the economic and social performances when environmental performance is of secondary importance.

Fig. 54 displays the trade-off between economic and environmental performance. Compared to the base-case, 7% increase in emission reduction results in 25% reduction in expected profit and 12% decrease in job creations. A further 3% increase in emission reduction results in a staggering 70% reduction in expected profit. Areas on the left and right sides of the dotted line respectively refer to the “recommended” and “not recommended” regions. The point where the dotted line meets the profit curve represents a suitable trade-off between the economic and environmental performances when social performance is of secondary importance.

From the above sections, the maximum achievable values of financial profit, reduction in GHG emissions, and job creations are obtained and are respectively referred to as  $\theta_{Max}$ ,  $NR_{Max}$ , and  $JB_{Max}$ . Decision makers can add the following constraints (Eq. 5.25 to Eq. 5.28) to the stochastic model. This ensure that an optimal solution (or a set of feasible solutions) is obtained that achieves a specified level of performances desired by the decision makers. Parameters  $a$ ,  $b$ , and  $c$  respectively refer to the ratio of the maximum achievable values of economic, environmental, and social performances to be achieved.

$$\theta \geq a\theta_{Max} \quad (5.25)$$

$$NR \geq bNR_{Max} \quad (5.26)$$

$$JB \geq cNB_{Max} \quad (5.27)$$

$$0 \leq a, b, c \leq 1 \quad (5.28)$$

Using the goal-programming approach, the expected values of the different LBSC objectives for a number of decision making criteria are displayed in Table 14.

**Table 14. LBSC performances under different decision making criteria**

Decision criteria	Profit (\$ Million)	Reduction in GHG emissions (Million Tons)	Jobs created
$a \geq 0.95; b \geq 0.90; c \geq 0.65$	806	8.94	8080
$a \geq 0.90; b \geq 0.85; c \geq 0.80$	758	7.97	10100
$a \geq 0.80; b \geq 0.75; c \geq 0.90$	679	7.34	11400
$a \geq 0.75; b \geq 0.95; c \geq 0.60$	630	9.29	7420

### 5.8.3. Fixed vs. variable bioethanol production tax credit

Literature review [12] shows that bioethanol production in the U.S. is unviable without adequate governmental subsidy in the form of production tax credits. The prevailing federal policy is to subsidize cellulosic bioethanol production by providing a tax credit of \$0.5/gallon. This policy is reflected in the base-case and is named as the fixed subsidy policy. Irrespective of the prevailing market price of ethanol, the fixed subsidy policy provides for a constant subsidy. A potential drawback of the fixed subsidy policy is that in scenarios with low ethanol sale price (and/or low switchgrass yield) the bioethanol producers are likely to make a small profit (or even a loss). Conversely scenarios are equally likely with high ethanol sale price. The fixed subsidy policy is likely to inflate the LBSC profit in those scenarios. This “boom” and “bust” cycle introduces unneeded uncertainty for LBSC planners as the expected profit is likely to exhibit volatility with a greater spread. In this work the ethanol market price follows a Normal distribution with a mean of \$2/gallon. The expected value of the revenue/gallon is therefore \$2.5/gallon and is a stochastic parameter. Under this policy, subsidy is a deterministic parameter (equal to \$0.5/gallon) and revenue/gallon is a stochastic parameter given by Eq. 5.29. For example if in a scenario the ethanol sale price is \$1.4/gallon then; revenue/gallon = 1.4 + 0.5 = \$1.9/gallon.

$$Revenue_F(\omega) = Ethanol\ price(\omega) + Fixed\ subsidy \quad (5.29)$$

This work proposes an alternate governmental policy which is named as the variable subsidy policy. Under this policy the tax credit is no longer a fixed \$0.5/gallon but fluctuates according to the

prevailing market price of ethanol. It is postulated that a variable subsidy is likely reduce the volatility and spread of the expected profit, thereby reducing risk for potential investors in LBSC. Under this policy, revenue/gallon is a deterministic parameter (equal to \$2.5/gallon) and subsidy is a stochastic parameter given by Eq. 5.30. For example if in a scenario the ethanol sale price is \$1.7/gallon then; variable subsidy =  $2.5 - 1.7 = \$0.8/\text{gallon}$ .

$$\text{Variable subsidy}(\omega) = \text{Revenue}_V - \text{Ethanol price}(\omega) \quad (5.30)$$

The fixed and variable subsidy policies are assessed based on the resulting economic performance of the LBSC. Figs. 55 and 56 display the volatility in expected LBSC profit for each subsidy policy. For both subsidy policies, mean value of expected profit is \$842 Million and the governmental outlay on tax credit is \$917 Million. The variable subsidy policy does not result in a drop in expected profit nor increases the total amount of subsidies. Under fixed subsidy policy, expected profit is a normally distributed random variable with standard deviation of \$307 Million and 0.37 as co-efficient of variance. Under variable subsidy policy, expected profit is a normally distributed random variable with standard deviation of \$92 Million and 0.11 as co-efficient of variance.

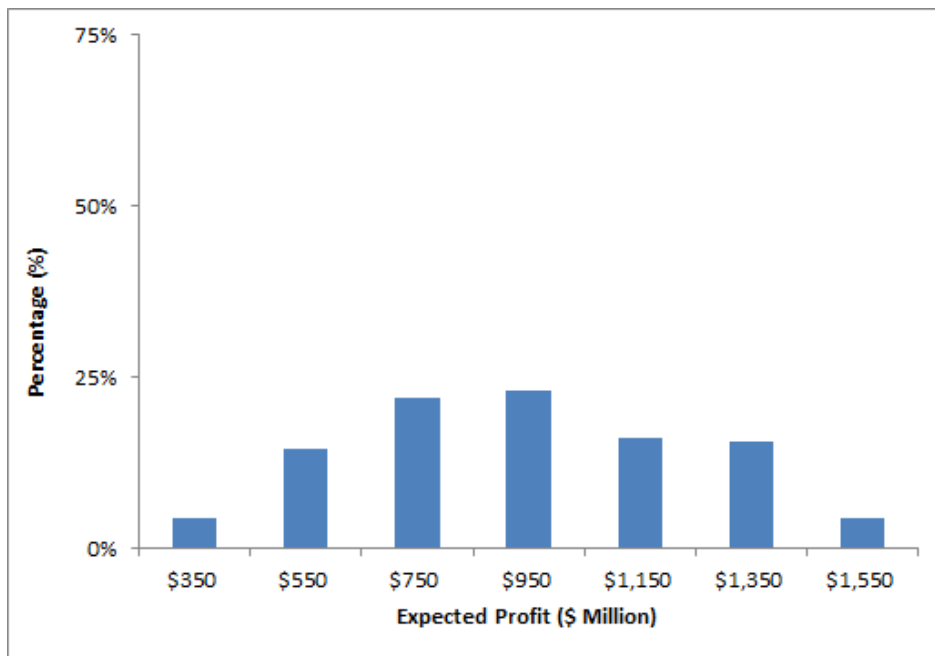


**Fig. 55. Histogram of fixed subsidy policy**

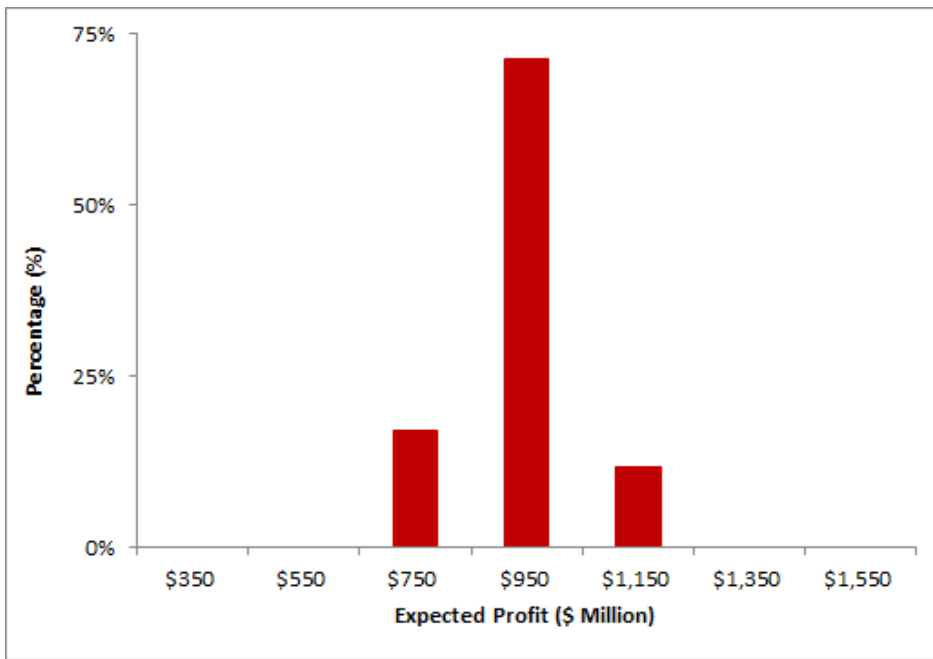


**Fig. 56. Histogram of variable subsidy policy**

For both subsidy policies, the median value of expected profit is \$950 Million but the frequency of occurrence is 25% and 70% respectively for the fixed and variable subsidy policies. Varying the subsidy (depending on the market price of ethanol) greatly reduces the investment risk by not letting expected profit fall below \$750 Million (i.e. a maximum drop of 10% compared to the mean), while in the fixed subsidy policy expected profit can fall up to \$350 Million (i.e. a maximum drop of 60% compared to the mean).

## 5.9. Conclusions

This work studies a multi-period long-term multi feedstock LBSC under multiple and jointly occurring uncertainties in biomass supply, bioethanol demand and price. A two-stage stochastic MILP model is proposed to determine the optimal values of the strategic logistic decisions for maximizing the multiple objectives of financial profit, net reduction in carbon emissions, and job creation. The first-stage decisions include both continuous and integer decision variables.

The main computational burden of the stochastic model is due to the first-stage integer variables. In order to solve the proposed stochastic MILP model with greater accuracy and within

reasonable time, this work utilizes a 2-step solution approach involving sequential application of a modified SAA method and Benders decomposition to make the optimization problem computationally tractable. Using the first-stage binary decisions obtained from the modified SAA method as a surrogate solution for the stochastic environment reduces the MILP optimization problem to a LP optimization one. The reduced stochastic model (with only continuous variables) is then efficiently solved by the application of Benders decomposition. Results show that the two-step solution approach gives a higher financial profit with greater accuracy.

A case study based on the Midwestern state of Wisconsin demonstrate the effectiveness of the proposed stochastic model by determining the long-term (i.e. 10 years) infrastructure requirements over all the planning periods and short-term (i.e. 2 years) operational requirements within each planning period for bioethanol production. Results show that in a stochastic environment it is cost effective and environmentally sustainable to meet up to 20% of Wisconsin's annual demand of gasoline energy equivalent requirement from locally produced bioethanol by using switchgrass as the primary source of biomass feedstock. Crop residue and woody biomass are used as secondary sources of lignocellulosic feedstock. Result also shows that there is no single solution which simultaneously maximizes all 3 performance criteria. Maximization of job creation results in the smallest reduction in carbon emissions and vice versa. Similarly, profit is maximized when both the environmental and social performance are not at their highest levels. A goal programming framework is introduced to ensure that a set of feasible solutions is obtained that achieves specified levels of individual performances.

The research effort also assesses two different renewable energy policies by comparing the resulting economic performance of the LBSC. Policy evaluation shows that the variable subsidy policy does not result in a drop in expected profit nor increases the total amount of subsidies. Varying the subsidy greatly reduces the investment risk and encourages investment in bioethanol production.

Future work can propose more complex and efficient decomposition algorithms for solving larger scale LBSC optimization problems at the national level or continental level.

## 5.10. Nomenclature

### 5.10.1. Indices

- $e$  Bioethanol demand zones ( $e = 1, \dots, E$ )
- $i$  Lignocellulosic biomass supply zones ( $i = 1, \dots, I$ )
- $j$  Bioethanol conversion technologies ( $j = 1, \dots, J$ )
- $m$  Lignocellulosic biomass feedstocks ( $m = 1, \dots, M$ )
- $r$  Biorefinery locations ( $r = 1, \dots, R$ )
- $t$  Modeling horizon of 1 year with planning periods ( $t = 1, \dots, T$ )
- $\omega$  Stochastic scenarios ( $\omega = 1, \dots, N$ )

### 5.10.2. First stage decision variables

- $MG_{it}$  Marginal land used for switchgrass cultivation at supply zone  $i$  during planning period  $t$  (acres)
- $K_{rjt}$  Biomass processing capacity of biorefinery at location  $r$  with technology  $j$  during planning period  $t$  (tons/year)
- $Y_{rjt}$  {1, if biorefinery with conversion technology  $j$  setup in location  $r$  during period  $t$ ; Else 0}

### 5.10.3. Second stage decision variables

- $F_{mirjt}(\omega)$  Amount of biomass  $m$  sent from zone  $i$  to biorefinery  $r$  (with technology  $j$ ) in period  $t$  during scenario  $\omega$  (tons)
- $HV_{it}(\omega)$  Marginal land in supply zone  $i$  harvested for switchgrass in planning period  $t$  (acres)
- $L_{rjt}(\omega)$  Volume of unsubsidized ethanol sold from refinery  $r$  (with technology  $j$ ) in period  $t$  during scenario  $\omega$  (gallons)
- $O_{et}(\omega)$  Volume of unmet ethanol requirement in demand zone  $e$  in period  $t$  during scenario  $\omega$  (gallons)

$P_{rjet}(\omega)$  Volume of subsidized ethanol from refinery  $r$  (with technology  $j$ ) to zone  $e$  in period  $t$  during scenario  $\omega$  (gallons)

$S_{rjt}(\omega)$  Volume of mixed alcohol produced by biorefinery  $r$  (with technology  $j$ ) in period  $t$  during scenario  $\omega$  (gallons)

$X_{rjt}(\omega)$  Electricity generated by refinery  $r$  (with tech  $j$ ) in planning period  $t$  during scenario  $\omega$  (MWh)

$Z_{rjt}(\omega)$  Volume of ethanol produced by refinery  $r$  (with tech  $j$ ) in period  $t$  during scenario  $\omega$  (gallons)

#### 5.10.4. Deterministic parameters

$\Xi_i$  Switchgrass production cost parameter in supply zone  $i$  (\$/acre)

$\Theta_r$  Renewable electricity generation tax credit in location  $r$  (\$/MWh)

$B_i$  Marginal land area available for switchgrass cultivation in biomass supply zone  $i$  (acres)

$v_i$  Average switchgrass yield in biomass supply zone  $i$  (tons/acre)

$Cap_{rt}$  Carbon emission reduction target in location  $r$  during planning period  $t$  (tons CO<sub>2</sub> equiv.)

$C_{mj}$  Electricity generation parameter for biomass type  $m$  from conversion technology  $j$  (MWh/ton)

$D_{ir}$  Distance between biomass supply zone  $i$  and biorefinery  $r$  (mile)

$D_{re}$  Distance between biorefinery  $r$  and bioethanol demand zone  $e$  (mile)

$fb_{rj}$  Job creation parameter of refinery  $r$  with technology  $j$  (jobs created/ton of processing capacity)

$fm_i$  Job creation parameter of harvesting in supply zone  $i$  (jobs created/acre of harvested land)

$G_{rj}$  Annualized fixed cost of biorefinery at location  $r$  with conversion technology  $j$  (\$)

$H_{rj}$  Variable cost parameter of biorefinery at location  $r$  with conversion technology  $j$  (\$/ton)

$lc_i$  Switchgrass harvest cost parameter in supply zone  $i$  (\$/acre)

$Q_{Elt}$  Reduction in carbon emissions from renewable electricity (tons CO<sub>2</sub>-equiv./MWh)

$Q_{MA}$  Reduction in carbon emissions from mixed alcohols (tons CO<sub>2</sub>-equiv./ gallon)

$Q_{Eth}$  Reduction in carbon emissions from bioethanol (tons CO<sub>2</sub>-equiv./ gallon)

$pp_i$  Switchgrass densification cost parameter in supply zone  $i$  (\$/ton)



$U_{rj}$	Ethanol production cost parameter of refinery at location $r$ with technology $j$ (\$/gallon)
$\alpha_{mj}$	Carbon emission of processing biomass type $m$ with technology $j$ (tons CO <sub>2</sub> -equiv./ton)
$\beta_m$	Carbon emission of transporting biomass type $m$ (tons CO <sub>2</sub> -equiv./ton x mile)
$\gamma$	Carbon emission of transporting bioethanol (tons CO <sub>2</sub> -equiv./gallon x mile)
$\delta_{rt}$	Average sale price of renewable electricity generated at location $r$ in planning period $t$ (\$/MWh)
$\Lambda_m$	Carbon emission of harvesting biomass type $m$ (tons CO <sub>2</sub> -equiv./ton)
$\zeta_{mi}$	Amount of biomass type $m \neq 1$ available in supply zone $i$ (tons)
$\eta_{mir}$	Transport cost parameter of biomass $m$ from supply zone $i$ to biorefinery $r$ (\$/ton x mile)
$\iota_{rt}$	Average sale price of unsubsidized bioethanol at location $r$ in planning period $t$ (\$/gallon)
$\kappa_{mj}$	Bioethanol yield parameter for biomass type $m$ from conversion technology $j$ (gallons/ton)
$\lambda_{mit}$	Purchase price of biomass type $m \neq 1$ at supply zone $i$ in planning period $t$ (\$/ton)
$\mu_{mj}$	Mixed alcohol yield parameter for biomass type $m$ from conversion technology $j$ (gallons/ton)
$\nu_{et}$	Avg. bioethanol demand in zone $e$ during period $t$ (gallons)
$\rho_j^{max}$	Maximum amount of biomass that can be processed by refinery $r$ with technology $j$ (tons/year)
$\rho_j^{min}$	Minimum amount of biomass that must be processed by refinery $r$ with technology $j$ (tons/year)
$\tau_{re}$	Tax credit for bioethanol production in location $r$ for consumption in demand zone $e$ (\$/gallon)
$\varphi_e$	Penalty cost parameter for unmet bioethanol requirement at biofuel demand zone $e$ (\$/gallon)
$\chi_{rt}$	Average sale price of mixed alcohol at location $r$ in planning period $t$ (\$/gallon)
$\psi_{re}$	Transport cost parameter of ethanol from refinery $r$ to biofuel demand zone $e$ (\$/gallon x mile)
$\Gamma$	Ratio of annual gasoline demand to be satisfied from subsidized bioethanol

### 5.10.5. Stochastic parameters

$o_t(\omega)$	Supply level of switchgrass during scenario $\omega$
$\pi_t(\omega)$	Demand level of bioethanol during scenario $\omega$
$\sigma_t(\omega)$	Sale price level of energy during scenario $\omega$

## 5.11. References

- [1] Schnepf R, Yacobucci B. Renewable Fuel Standard (RFS): Overview and Issues. United States Congressional Research Service; 2013.
- [2] Carriquiry M, Du X, Timilsina G. Second generation biofuels: Economics & policies. *Energy Policy* 2011;39:4222–34.
- [3] Zhang J, Osmani A, Awudu I, Gonela V. An integrated optimization model for switchgrass-based bioethanol supply chain. *Applied Energy* 2013;102:1205–17.
- [4] Sokhansanj S, Mani S, Turhollow, Kumar A, Bransby D, Lynd L, Laser M. Large-scale production, harvest and logistics of switchgrass – current technology and envisioning a mature technology. *Biofuels, Bioprod. Bioref.* 2009;3:124–41.
- [5] Wu J, Sperow M, Wang J. Economic Feasibility of a Woody Biomass-Based Ethanol Plant in Central Appalachia. *Journal of Agricultural and Resource Economics* 2010;35:522–44.
- [6] Cherubini F, Ulgiati S. Crop residues as raw materials for biorefinery systems – A LCA case study. *Applied Energy* 2010;87:47–57.
- [7] U.S. Energy Independence and Security Act of 2007.
- [8] Mabee W, McFarlane P, Saddler J. Biomass availability for lignocellulosic ethanol production. *Biomass Bioenergy* 2011;35:4519–29.
- [9] Chen W, Wiecek M, Zhang J. Quality utility – A compromise programming approach to robust design. *Journal of Mechanical Design* 1999;121:179–87.
- [10] Awudu I, Zhang J. Stochastic production planning for a biofuel supply chain under demand and price uncertainties. *Applied Energy* 2013;103:189–96.
- [11] Gebreslassie B, Yao Y, You F. Design under uncertainty of hydrocarbon biorefinery supply chains: Multiobjective stochastic programming models, decomposition algorithm, and a comparison between CVaR and downside risk. *AIChE Journal* 2012;58:2155–79.

- [12] Osmani A, Zhang J. Stochastic optimization of a multi feedstock lignocellulosic-based bioethanol supply chain under multiple uncertainties. *Energy* 2013;59:157–72.
- [13] Escudero L, Garin M, Merino M, Perez G. An exact algorithm for solving large-scale two-stage stochastic mixed-integer problems: Some theoretical and experimental aspects. *European Journal of Operational Research* 2010;204:105–16.
- [14] Lam H, Klemes J, Kravanja Z. Model-size reduction techniques for large-scale-biomass production and supply networks. *Energy* 2011;36:4599–4608.
- [15] Papapostolou C, Kondili E, Kaldellis J. Development and implementation of an optimisation model for biofuels supply chain. *Energy* 2011;36:6019–26.
- [16] Van Dyken S, Bakken B, Skjelbred H. Linear mixed-integer models for biomass supply chains with transport, storage and processing. *Energy* 2010;35:1338–50.
- [17] Eksioglu S, Acharya A, Leightley L, Arora S. Analyzing the design and management of biomass-to-biorefinery supply chain. *Comput Ind Eng* 2009;57:1342–52.
- [18] Leduc S, Starfelt F, Dotzauer E, Kindermann G, McCallum I, Obersteiner M, Lundgren J. Optimal location of lignocellulosic ethanol refineries with polygeneration in Sweden. *Energy* 2010;35:2709–16.
- [19] Cucek L, Varbanov P, Klemes J, Kravanja Z. Total footprints-based multi-criteria optimisation of regional biomass energy supply chains. *Energy* 2012;44:135–45.
- [20] Giarola S, Zamboni A, Bezzo F. Spatially explicit multi-objective optimisation for design and planning of hybrid first and second generation biorefineries. *Computers and Chemical Engineering* 2011;35:1782–97.
- [21] Zamboni A, Shah N, Bezzo F. Spatially explicit static model for the strategic design of future bioethanol production systems. 2. Multi-objective environmental optimization. *Energy Fuels* 2009;23:5134–43.

- [22] Frombo F, Minciardi R, Robba M, Rosso F, Sacile R. Planning woody biomass logistics for energy production: A strategic decision model. *Biomass Bioenergy* 2009;33:372–83.
- [23] Kocoloski M, Griffin W, Matthews H. Estimating national costs, benefits, and potential for cellulosic ethanol production from forest thinnings. *Biomass Bioenergy* 2011;35:2133–42.
- [24] Kostin A, Guillen-Gosalbez G, Mele F, Bagajewicz M, Jimenez L. Design and planning of infrastructures for bioethanol and sugar production under demand uncertainty. *Chemical Engineering Research and Design* 2012;90:359–76.
- [25] Dal-Mas M, Giarola S, Zamboni A, Bezzo F. Strategic design and investment capacity planning of the ethanol supply chain under price uncertainty. *Biomass and Bioenergy* 2011;35: 2059–71.
- [26] Kim J, Realff M, Lee J. Optimal design and global sensitivity analysis of biomass supply chain networks for biofuels under uncertainty. *Computers and Chemical Engineering* 2011;35:1738– 51.
- [27] Chen C, Fan Y. Bioethanol supply chain system planning under supply and demand uncertainties. *Transportation Research Part E* 2010;48:150–64.
- [28] An H, Wilhelm W, Searcy S. A mathematical model to design a lignocellulosic biofuel supply chain system with a case study based in Central Texas. *Bioresour Technol* 2011;102:7860–70.
- [29] Osmani A, Zhang J. Economic and environmental optimization of a large scale sustainable dual feedstock lignocellulosic-based bioethanol supply chain in a stochastic environment. *Applied Energy* 2014;114:572–587.
- [30] Abdallah A, Farhat A, Diabat A, Kennedy S. Green supply chains with carbon trading and environmental sourcing: Formulation and life cycle assessment. *Applied Mathematical Modelling* 2011;36:4271–85.
- [31] Cruz J. Modeling the relationship of globalized supply chains and corporate social responsibility. *Journal of Cleaner Production* 2013;56:73–85.

- [32] You F, Tao L, Graziano D, Snyder S. Optimal design of sustainable cellulosic biofuel supply chains: Multiobjective optimization coupled with life cycle assessment and input–output analysis. *AIChE Journal* 2012;58:1157–80.
- [33] Huang Y, Chen C, Fan Y. Multistage optimization of the supply chains of biofuels. *Transportation Research Part E* 2010;46:820–30.
- [34] Cherubini F, Jungmeier G. LCA of a biorefinery concept producing bioethanol, bioenergy, and chemicals from switchgrass. *Int J Life Cycle Assess* 2010;15:53–66.
- [35] Lee D, Boe A. Biomass production of switchgrass in central South Dakota. *Crop Sci* 2005;45:2583–90.
- [36] Zhu X, Yao Q. Logistics system design for biomass-to-bioenergy industry with multiple types of feedstocks. *Bioresource Technology* 2011;102:10936–45.
- [37] Spatari S, MacLean H. Characterizing Model Uncertainties in the Life Cycle of Lignocellulose-Based Ethanol Fuels. *Environ Sci Technol* 2010;44:8773–80.
- [38] Badri H, Bashiri M, Hejazi T. Integrated strategic and tactical planning in a supply chain network design with a heuristic solution method. *Computers & Operations Research* 2013;40:1143–54.
- [39] Uster H, Easwaran G, Akcali E, Cetinkaya S. Benders Decomposition with Alternative Multiple Cuts for a Multi-Product Closed-Loop Supply Chain Network Design Mode. *Naval Research Logistics* 2007;54:890–907.
- [40] Kleywegt A, Shapiro A, Homem-De-Mello T. The sample average approximation method for Stochastic discrete optimization. *SIAM J. Optim.* 2001;12:479–502.
- [41] Linderoth J, Shapiro A, Wright S. The empirical behavior of sampling methods for stochastic programming. *Ann Oper Res* 2006;142: 215–41.
- [42] Shapiro A, Homem de Mello T. On the Rate of Convergence of Optimal Solutions of Monte Carlo Approximations of Stochastic Programs. *SIAM Journal on Optimization* 2000;11:70–86.

## CHAPTER 6. OPTIMAL GRID DESIGN AND LOGISTIC PLANNING FOR BIOMASS AND WIND BASED RENEWABLE ELECTRICITY SUPPLY CHAINS UNDER UNCERTAINTIES

### 6.1. Abstract

In this work, the grid design and optimal allocation of wind and biomass resources for renewable electricity supply chains under uncertainties is studied. Due to wind intermittency, generation of wind electricity is not uniform and cannot be counted on to be readily available to meet the demand. Biomass represents a type of stored energy and is the only renewable resource that can be used for producing biofuels and generating electricity whenever required. However, amount of biomass resources are finite and might not be sufficient to meet demand for electricity and biofuels. Potential of wind and biomass resources is therefore jointly analyzed for renewable electricity generation. Policies are proposed and evaluated for optimal allocation of finite biomass resources for electricity generation. A stochastic programming model is proposed that optimally balances the electricity demand across the available supply from wind and biomass resources under uncertainties in wind speed and electricity sale price. A case study set in the American Midwest is presented to demonstrate effectiveness of the proposed stochastic model by determining the optimal decisions for generation and transmission of renewable electricity. Sensitivity analysis shows that level of subsidy for renewable electricity production has a major impact on the decisions.

### 6.2. Introduction

The U.S. is the world's leading energy consumer with fossil fuels accounting for 83% of the energy supplied to the economy in 2012 [1]. Electricity generation consumes the largest share (i.e. 40%) of the U.S. energy resources [1]. There is growing public awareness that consumption of fossil fuels in large amounts is contributing to global warming by releasing increasing quantities of greenhouse gas (GHG) emissions. In addition, extraction of large quantities of coal, natural gas, and crude oil are leading to faster depletion of the finite reserves of fossil fuels. The depletion of fossil fuels

is likely to result in price fluctuations, uncertainties in the energy supply chain, and social upheaval due to job losses [1]. In June 2013 President Obama addressed the students of Georgetown University on the issue of climate change. In his speech the President expressed his administration's commitment to a green energy future for the U.S. by directing the Environmental Protection Agency (EPA) to "put an end to the limitless dumping of carbon pollution from our power plants, and complete new pollution standards for both new and existing power plants" [2]. Renewable energy sources have the potential to cost-effectively satisfy a large portion of U.S. electricity needs, while at the same time safeguarding the environment, and reducing dependence on fossil fuels [3, 4]. Research indicates that if optimally utilized, renewables can contribute up to 20% of total U.S. electricity generation by 2030 [4–7].

In 2012, 11% of the electricity generated in the U.S. was produced from renewables [1]. Hydropower generated the maximum share of 7% while the contribution of wind and biomass was 2% and 1.4% respectively [1]. The share of hydropower is not expected to increase as the hydroelectric resource has plateaued out with most of the promising large-scale hydropower sites in the U.S. already being tapped for electricity generation [1].

Wind energy is one of the highest potential renewable resources currently available for electricity generation in the U.S. [1, 4]. The estimated onshore wind energy has the annual potential to generate 5 million GWh of electricity [4]. In the U.S. wind power was used to generate 90000 GWh of electricity in 2012 [1], representing 23% of generation from renewables [4]. Even though wind generated electricity currently makes up only 2% of total U.S. electricity generation, wind power has grown at a 25% annual rate (from 2001 to 2010) and represents 35% of all new generating capacity [1]. Onshore wind technology is generally considered to be commercially available in the U.S. [4].

Currently there are some challenges that prevent a wide spread deployment of renewable electricity generated from intermittent resources like wind energy. Electricity generation from wind takes place where and when the wind blows. This intermittency is perceived as an obstacle to the

integration of wind generated electricity into the existing power grid [1, 8]. The biggest challenge is how to efficiently and economically supply electricity from diverse and dispersed wind farm sites to faraway electricity demand markets [8]. In the United States, most of the highest wind energy potential is located in the sparsely populated Midwestern states. However, highest demand for electricity is located in the densely populated urban areas of the Northeast, Southern California, and few major cities in the Midwest and Rocky Mountains [1].

Research on optimizing of a wind based renewable electricity supply chain (WESC) is extensive [9]. Research by [10–13] proposes stochastic optimization models that consider uncertainties in wind speeds, electricity demand and/or electricity sale price. A growing body of literature [14–18] also addresses the intermittency of wind in conjunction with energy storage mediums i.e. pumped water [19, 20], compressed air [21], deep-cycle batteries [22], etc. or traditional readily dispatchable electricity generators i.e. hydropower or natural gas fired. Work by [10, 23–25] studies a WESC where wind intermittency is balanced by use of pumped hydropower storage. While research by [26] studies a WESC where wind intermittency is balanced by use of compressed air energy storage. However, none of the currently available electricity/energy storage technologies are economically and efficiently capable of providing long-term power storage without significant conversion losses [1, 27].

Recently research is emerging on study of WESC optimization where the wind intermittency is balanced by another renewable resource. Work by [28–30] studies a WESC where wind intermittency is balanced by use of solar power. An optimization model is proposed that considers uncertainty in wind speeds and solar radiation. However, the use of multiple non-dispatchable renewable resources (i.e. solar and wind) is unlikely to eliminate the need of a readily dispatchable resource of electricity (e.g. natural gas fired generators) as a back-up [31].

Biomass resources represent a type of “stored” energy that can be used as feedstock to generate electricity whenever required and can act as a dispatchable resource for electricity generation without



the use of a fossil-fuel resource as a back-up. Recent studies [5] have highlighted the potential availability of a billion tons per year of biomass for energy production including electricity and liquid transportation fuels. In 2012 an estimated 63000 GWh was generated in the U.S. using biomass as feedstock [1], which represents 16% of generation from renewables [4]. Combustion technologies used to convert biomass to electricity are generally considered commercial [6]. Biomass procurement and feedstock quality are the key cost drivers that impact the cost of bioelectricity [7]. Currently, biomass is the only renewable source that can be used to generate both electricity and produce liquid transportation fuels [6, 7]. The amount of biomass resources are finite and might not be sufficient to meet demand for both electricity and biofuels in the U.S. due to the production mandates of the federal Renewable Fuel Standard. [1]. Accurate estimates for bioelectricity generation potential are difficult to obtain but are estimated to be around 1.4 million GWh annually if 40% of the available biomass is used for electricity generation [1].

This research aims to leverage the use of available wind and biomass resources for sustainable renewable electricity generation and transmission. Renewable energy policies are proposed for the optimal allocation of finite biomass resources for electricity generation. Each policy is evaluated across the economic objective (i.e. profit maximization) to select the optimal allocation ratio(s). The work also studies the design of an optimal grid infrastructure (from power production to transmission) that can integrate renewable electricity generated from wind and biomass resources into the power grid under uncertainties in wind speeds [32, 33]. To increase the supply and reliability of electricity generated from renewables it is necessary to upgrade the transmission lines (if they exist) between supply and demand zones so as to be able to cope with the additional electric load to be carried by the grid [4, 34]. Upgrading the transmission capacity will result in significant cost [35]. If no transmission lines are available between the electricity supply and demand zones, costly new transmission lines should be established [34, 35].

The unique contribution of this study is incorporating economic viability while optimizing a wind and biomass based renewable electricity supply chain (WBBRESC) by considering constraints on biomass availability, uncertainties in wind speed and electricity sale price. In this work wind energy is considered as the primary renewable resource for electricity production and wind farms are referred to as the “base-load” generators used for meeting a ratio of the off-peak electricity demand. Biomass is considered as the secondary renewable resource for electricity production and a biomass power plant (BMPP) is referred to as the “on-demand” generator used to compensate for shortage in electricity supply from wind farms due to wind intermittency. To the best of our knowledge this is the first research effort to study the optimal design of a WBBRESC that also considers the grid network and transmission capacities.

A two-stage stochastic mixed integer linear programming (SMILP) model is proposed that ensures the financial viability by balancing the electricity demand across the available supply from wind and biomass resources under uncertainties in wind speed and electricity sale price. The potential of wind energy, intermittency of wind electricity generation systems, biomass resource availability, electricity demand, and electricity sale price are used as constraints in the proposed model. The model integrates all the supply chain logistics for generation and transmission of renewable electricity to arrive at optimal decisions that include: 1) site selection for installation of wind farms, BMPPs, and grid stations; 2) generation capacity of wind farms and BMPPs; 3) grid connectivity; 4) transmission capacity of power lines; and 5) amount of renewable electricity to be supplied to demand zones.

A case study is used to demonstrate the effectiveness of the proposed SMILP model by optimally allocating the available wind and biomass resources for generating and transmitting up to 20% of the off-peak electricity demand of a U.S. Midwestern region by 2030. Sensitivity analysis is conducted to measure impact of renewable energy policy (i.e. subsidy level for renewable electricity generation) on the profit and the supply chain logistic decisions.

### 6.3. Problem statement

This research studies an integrated WBBRESC. A list of indices, parameters, and decision variables are given in the Nomenclature section. The conversion factors from the U.S. customary units to the metric units (SI) are given in Appendix C. This paper assumes that: 1) only road haulage is considered for the transportation of biomass; and 2) the off-peak electricity requirement is known and proportional to the population in each demand zone.

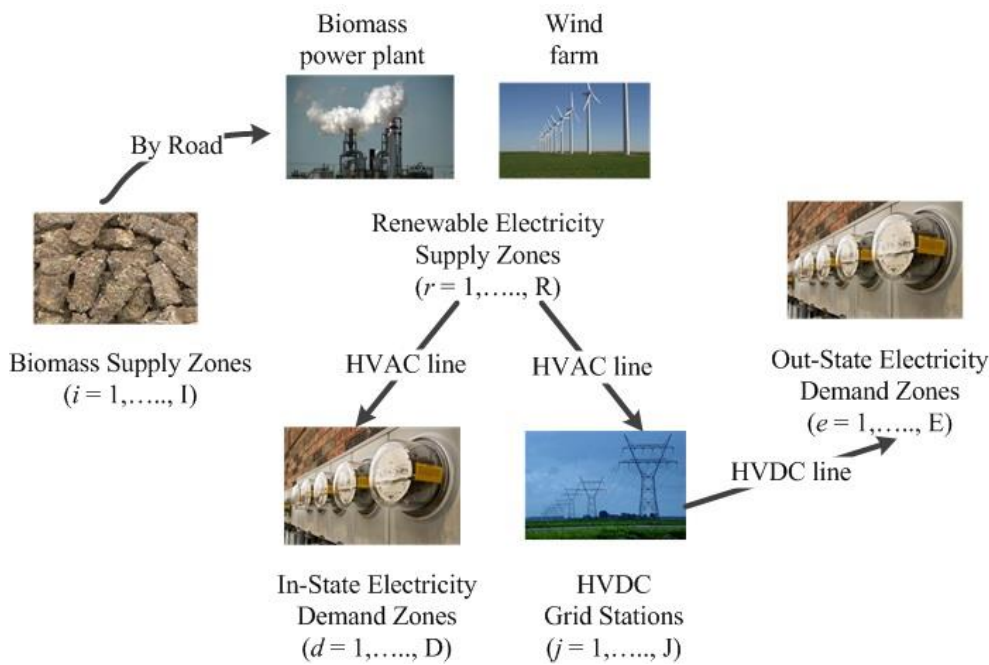


**Fig. 57. Major logistics activities in a WBBRESC**

The major logistics activities in a WBBRESC are shown in Fig. 57. Wind farms can be established in renewable electricity supply zone  $r$ . The generation capacity of wind farms is driven by the off-peak demand for renewable electricity, while the amount of electricity produced is limited by the availability of wind (of sufficient speed) and the maximum generation capacity of wind farms. BMPPs can also be installed in renewable electricity supply zone  $r$ . Biomass feedstock (in the form of densified crop residue pellets) can be procured from supply zone  $i$  and transported to BMPP located in renewable electricity supply zone  $r$ . The supplied biomass feedstock is combusted to generate electricity. The amount of bioelectricity produced is driven by the off-peak demand for renewable

electricity and limited by the availability of biomass and the maximum generation capacity of BMPPs. The amount of generated renewable electricity (from wind and/or biomass) is transmitted via high voltage alternating current (HVAC) power line from supply zone  $r$  to in-state demand zone  $d$  and/or high voltage direct current (HVDC) grid station  $j$ . Transmitting electricity using HVAC power lines over distances greater than 300 miles results in substantial line losses [4]. In case the amount of generated wind electricity is greater than the transmission capacity of the power line, the excess wind electricity amount is “purged” on-site and earns no revenue. The electricity received by HVDC grid station  $j$  is transmitted via HVDC power line to out-state demand zone  $e$ . HVDC power lines can be used for transmitting electricity over distances up to 1000 miles without incurring significant line losses [34]. In addition, the transmission capacity of HVDC power lines is more than double that of traditional HVAC power lines [4]. However, the investment needed to setup a HVDC line is many times more than that of traditional HVAC power lines [4]. If the amount of transmitted electricity is not sufficient to meet the required ratio of the off-peak demand, shortfall in electricity requirement incurs a high penalty cost [32, 34].

### **6.3.1. Logistics and supply chain decisions**

The strategic and tactical decisions are integrated and solved within a combined decision framework. In order to maximize the expected WBBRESC profit, the following logistics and supply chain decisions need to be optimized.

Strategic decisions must be made before the realization of the uncertain parameters. These include the following:

- Determining location of wind farm sites from  $r$  potential locations: In supply chain logistics, the technique of variability pooling is used to reduce the overall system variability [36, 37]. Along similar lines, the variation associated with wind intermittency can be reduced by establishing

wind farms in dispersed locations with uncorrelated wind speeds [34]. This substantially reduces the probability that all wind farms experience low wind speeds at the same time.

- Determining the location of BMPP sites from  $r$  potential locations. Co-locating a BMPP in close proximity to a wind farm allows a readily dispatchable generating resource like biomass to rapidly meet the electricity generation shortfalls as a result of wind intermittency. In addition, the transmission line costs can be allocated across both wind and bioelectricity generation sources in any given area [35]. However, it must also be noted that co-located wind farms and BMPPs are unlikely to be situated near their resource base i.e. areas with both high wind energy and biomass resource potential. Trade-off analysis is carried out to weigh the perceived benefit of co-location against the increased biomass feedstock transportation cost to the renewable electricity generation sites.
- Determining the generation capacity of wind farms and BMPPs: Adequate generation capacity needs to be allocated in order to meet the required electricity demand for in-state and out-state demand zones. Over allocation of generation capacity will result in increased costs while under allocation of generation capacity will result in high penalty cost due to unmet demand.
- Determining the transmission capacities of HVAC and HVDC power lines: Mainly as a result of the renewable portfolio standard (RPS) mandates [1], grid operators have to decide the optimal transmission capacity needed to economically and effectively distribute electricity generated from renewables [38]. If transmission line capacity is based on the maximum power generation potential of the renewable resource i.e. electricity output at peak wind speeds, then due to the intermittent nature of wind the transmission line will not be fully loaded apart from short durations of peak generation [36]. Conversely, if the transmission line is sized to align with average generating potential, then the wind farm will not be able to take advantage of peak favorable wind conditions to generate at full potential [34]. Nevertheless, no transmission line

dedicated solely to an intermittent renewable resource like wind can be expected to continuously operate with high utilization [29, 34].

Tactical decisions are taken for each scenario once the uncertainty is unveiled. These include the following:

- Determining the material flow of procured feedstock from biomass supply zone  $i$  to BMPP in location  $r$ .
- Determining amount of electricity generated by BMPP in location  $r$ .
- Determining amount of electricity generated by wind that is “purged” on-site  $r$  due to lack of transmission capacity.
- Determining the material flow of renewable electricity from supply zone  $r$  to in-state demand zone  $d$  and/or HVDC grid station  $j$ . Determining the material flow of renewable electricity from HVDC grid station  $j$  to out-state demand zone  $e$ .
- Determining amount of unmet off-peak electricity requirement for all demand zones.

### **6.3.2. Stochastic nature of the WBBRESC**

Literature review [1] has highlighted some of the key uncertainties inherent in the life cycle of a WBBRESC. As such the logistics and supply chain decisions taken need to be optimized over the entire range of the stochastic scenarios [1]. Uncertainty in energy prices and their level of supply/demand is commonly modeled using known probability distributions which are based on statistical analysis of historical data [39]. The following sections present the multiple uncertainties that are jointly considered in the proposed model.

Over the last 10 years the off-peak electricity demand in the U.S. has been very stable [40] and can be assumed to be deterministic. However, the off-peak electricity sale price is not deterministic and fluctuates mainly due to variation in fuel prices [40]. A probability function is used to model the

uncertainty in electricity sale price by analyzing historical electricity sale price data.  $A(\omega)$ , the electricity price level is modeled using Eq. 6.1.

$$A(\omega) = [\text{Electricity sale price}(\omega)/\text{Average electricity sale price}] \quad (6.1)$$

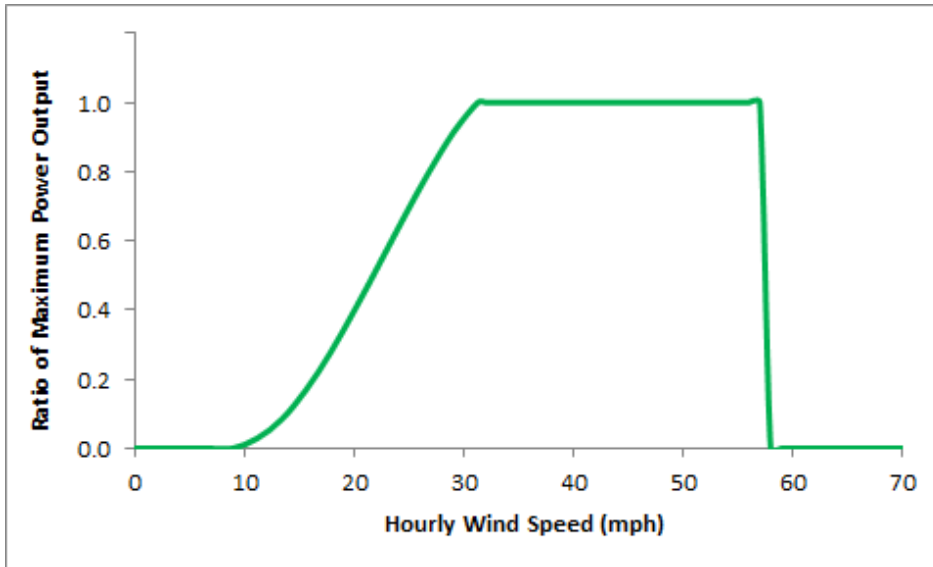


**Fig. 58. Power curve for a wind farm**

Fig. 58 shows that the power output of wind farms is highly correlated to the wind speed [4]. The statistical distribution of wind speeds varies depending upon local climate conditions, the landscape, and its surface [41, 42]. To assess the frequency of wind speeds at a particular location, a probability distribution function is often fit to the observed data [41]. The Weibull distribution closely mirrors the actual distribution of hourly wind speeds [41, 43]. The Weibull distribution curve is based on two parameters; the scale and the shape parameters. A value of 2 for the shape parameter is generally used to model the hourly wind speeds [43]. If the value of the shape parameter is between 3 and 4 the Weibull distribution approximates the Normal distribution [41].

The wind speeds can be converted into a ratio of maximum possible power output by applying the constraints of a power curve for a typical wind farm to the data [43]. The power curve depicted in Fig. 58 shows that when the wind speed is below 10 mph and above 57 mph no power is produced and the amount of power increases almost linearly between 10 mph and 30 mph, after which the power

output remains at its maximum up to the 57 mph cut off. The power production cuts off at an upper limit of 57 mph in order to prevent damage to the wind turbines in gale force conditions [43].

The approximately linear section of the power curve (wind speeds between 10 and 30 mph) is modeled as a first-order function in Eq. 6.2 where  $\Delta_r(\omega)$  is hourly wind speed in mph and  $C_r(\omega)$  is the power output level (as ratio of maximum output) of wind farm in location  $r$  during scenario  $\omega$ .

$$C_r(\omega) = 0.5 - 0.05\Delta_r(\omega) \quad \forall r \quad 10 \leq \Delta_r(\omega) \leq 30 \quad (6.2)$$

## 6.4. Model formulation

The goal of the study is to determine the optimal strategic configuration of the WBBRESC (i.e. first-stage decisions) along with the associated operational decisions (i.e. second-stage decisions) that maximizes its economic performance under uncertainties. A SMILP model is proposed to maximize the expected WBBRESC profit by determining the optimal values of the first-stage and the expected values of second-stage decision variables. The formulation (including the objective function and constraints) of the model is explained in the following sections. All continuous decision variables are non-negative, while all integer variables have 0–1 (i.e. binary) restriction.

### 6.4.1. Objective function of the WBBRESC

The objective function of the proposed stochastic model is to maximize the expected annualized WBBRESC profit (revenue – cost). There are 8760 hours (= 24 \* 365) in a year. Eq. 6.3 refers to the expected profit ( $\theta$ ) which needs to be maximized.

$$\begin{aligned} \theta = & - \sum_{r=1}^R (\alpha_r Z_r + \beta_r V_r) - \sum_{r=1}^R (\delta_r Y_r + \varepsilon_r U_r) - \sum_{j=1}^J \sum_{e=1}^E (\lambda W_{je} + \mu DST_{je} S_{je}) \\ & - \sum_{j=1}^J \Gamma_j X_j - \left( \sum_{r=1}^R \sum_{j=1}^J t_{rj} DST_{rj} T_{rj} + \sum_{r=1}^R \sum_{d=1}^D t_{rd} DST_{rd} T_{rd} \right) \\ & + E_\omega \left[ \begin{aligned} & 8760A(\omega) \left\{ \sum_{d=1}^D v_d N_d + \sum_{e=1}^E v_e N_e \right\} + 8760 \sum_{r=1}^R \varphi_r \{P_r(\omega) + M_r(\omega)\} \\ & - \sum_{i=1}^I \sum_{r=1}^R \rho_i Q_{ir}(\omega) - \tau \sum_{i=1}^I \sum_{r=1}^R DST_{ir} Q_{ir}(\omega) - 8760\psi \left\{ \sum_{d=1}^D G_d(\omega) + \sum_{e=1}^E G_e(\omega) \right\} \end{aligned} \right] \end{aligned} \quad (6.3)$$



In Eq. 6.3 the different components of  $\theta$  respectively represent the: 1) fixed and variable cost of BMPPs; 2) fixed and variable cost of wind farms; 3) fixed and variable cost of HVDC lines; 4) fixed cost of HVDC grid stations; 5) variable cost of HVAC lines; 6) revenue from sale of renewable electricity; 7) tax credits accrued from renewable electricity generation; 8) biomass purchase cost; 9) biomass transportation cost; and 10) penalty cost of unmet electricity demand.

#### 6.4.2 Constraints

$$\sum_{r=1}^R Q_{ir}(\omega) \leq \sigma RTO_i \zeta_i \quad \forall i, \omega \quad (6.4)$$

$$\gamma_{\min} Z_r \leq V_r \leq \gamma_{\max} Z_r \quad \forall r \quad (6.5)$$

$$P_r(\omega) \leq V_r \quad \forall r, \omega \quad (6.6)$$

$$U_r \leq \eta_r \quad \forall r \quad (6.7)$$

$$U_r \geq \zeta_{\min} Y_r \quad \forall r \quad (6.8)$$

$$O_r(\omega) \leq U_r \quad \forall r, \omega \quad (6.9)$$

$$T_{rj} \leq \kappa_{rj} \quad \forall r, j \quad (6.10)$$

$$T_{rd} \leq \kappa_{rd} \quad \forall r, d \quad (6.11)$$

$$K_{rj}(\omega) \leq T_{rj} \quad \forall r, j, \omega \quad (6.12)$$

$$K_{rd}(\omega) \leq T_{rd} \quad \forall r, d, \omega \quad (6.13)$$

$$\nu_{\min} W_{je} \leq S_{je} \leq \nu_{\max} Z_{je} \quad \forall j, e \quad (6.14)$$

$$H_{je}(\omega) \leq S_{je} \quad \forall j, e, \omega \quad (6.15)$$

Eq. 6.4 ensures that in each supply zone  $i$ , the amount of biomass sent to all BMPPs during each scenario  $\omega$  is not more than the amount of available biomass that can be procured. Eq. 6.5 represents the design limits on the generation capacity of a BMPP. Eq. 6.6 ensures that the amount of electricity produced by a BMPP does not exceed the generation capacity. Eq. 6.7 ensures that the installed generation capacity of a wind farm is not greater than the maximum potential for generating wind electricity at location  $r$ . Eq. 6.8 represents the minimum limits on the generation capacity of a wind farm. Eq. 6.9 ensures that during scenario  $\omega$  the amount of electricity produced by a wind farm does not exceed the generation capacity. Eq. 6.10 and Eq. 6.11 represent the maximum limits on the transmission capacity of HVAC power lines. Eq. 6.12 and Eq. 6.13 ensure that during scenario  $\omega$  the

electricity transmitted by a HVAC line does not exceed capacity. Eq. 6.14 represents the maximum and minimum limits on the transmission capacity of a HVDC power line. Eq. 6.15 ensures that during scenario  $\omega$  the electricity transmitted by a HVDC line does not exceed capacity.

$$\pi \sum_{i=1}^I Q_{ir}(\omega) = 8760P_r(\omega) \quad \forall r, \omega \quad (6.16)$$

$$C_r(\omega)U_r = O_r(\omega) \quad \forall r, \omega \quad (6.17)$$

$$M_r(\omega) + L_r(\omega) = O_r(\omega) \quad \forall r, \omega \quad (6.18)$$

$$M_r(\omega) + P_r(\omega) = \sum_{j=1}^J K_{rj}(\omega) + \sum_{d=1}^D K_{rd}(\omega) \quad \forall r, \omega \quad (6.19)$$

$$\sum_{r=1}^R K_{rj}(\omega) = \sum_{e=1}^E H_{je}(\omega) \quad \forall j, \omega \quad (6.20)$$

$$G_d(\omega) + \sum_{r=1}^R K_{rd}(\omega) = N_d \quad \forall d, \omega \quad (6.21)$$

$$G_e(\omega) + \sum_{j=1}^J H_{je}(\omega) = N_e \quad \forall e, \omega \quad (6.22)$$

$$\chi_{\min} O_d \leq N_d \leq \chi_{\max} O_d \quad \forall d \quad (6.23)$$

$$\chi_{\min} O_e \leq N_e \leq \chi_{\max} O_e \quad \forall e \quad (6.24)$$

Eq. 6.16 ensures that the entire amount of biomass procured by BMPP  $r$  is combusted to generate bioelectricity. Eq. 6.17 ensures that the entire amount of usable wind energy available to wind farm  $r$  is converted into electricity. Eq. 6.18 ensures that the amount of electricity generated by a wind farm is either transmitted or “purged” on site. Eq. 6.19 ensures that the amount of generated renewable electricity that is not purged is transmitted to HVDC grid stations and/or in-state demand zones. Eq. 6.20 ensures that the amount of electricity received by HVDC grid stations is transmitted to out-state demand zones. Eq. 6.21 ensures that the amount of unmet electricity requirement plus the amount of electricity transmitted (from all supply zones), is equal to the renewable electricity amount to be supplied to in-state demand zone  $d$ . Eq. 6.22 ensures that the amount of unmet electricity requirement plus the amount of electricity transmitted (from all HVDC grid stations), is equal to the renewable electricity amount to be supplied to out-state demand zone  $e$ . Eq. 6.23 and Eq. 6.24 ensure that the

amount of renewable electricity to be supplied must be between the allowable maximum and minimum limits for all the in-state and out-state demand zones.

$$U_r = (B_r + F_r) \quad \forall r \quad (6.25)$$

$$W_{je} \leq X_j \quad \forall j \quad (6.26)$$

Eq. 6.25 ensures that the existing generation capacity of wind farm in location  $r$  can be increased but not decreased. Eq. 6.26 ensures that renewable electricity can only be transmitted via HVDC line to out-state demand zone  $e$  if a HVDC grid station is established at location  $j$ .

## 6.5. Case study set-up and results

Parameters used in this case study are displayed in Tables A12–A14 (see Appendix A). In the United States, most of the highest wind energy and biomass resource potential is located in the Midwest. The case study is set in the typical Midwestern state of North Dakota (ND) and aims to show if 20% of the annual off-peak demand for electricity (by 2030) can be met by the generation of renewable electricity from wind energy and/or biomass resources. The National Renewable Energy Laboratory [4] has divided the state of North Dakota into 7 wind zones. Within a wind zone the average wind speeds are similar and correlated. However the wind speeds across different wind zones are not correlated. The case study also examines if there is enough surplus of renewable electricity to satisfy up to 20% of the annual off-peak demand for Chicago and Denver.

### 6.5.1. Model assumptions

The various indices used in the case study displayed in Table 15.

**Table 15. Indices used in the case study**

$d$	In-state electricity demand zones $d = 1$ (Entire state of ND)
$e$	Out-state electricity demand zones $e = 1$ (Chicago); $e = 2$ (Denver)
$i$	Biomass supply zones ( $i = 1, 2, \dots, 7$ )
$j$	HVDC grid station locations ( $j = 1, 2, \dots, 7$ )
$r$	Renewable electricity supply zones ( $r = 1, 2, \dots, 7$ )
$\omega$	Stochastic scenarios ( $\omega = 1, 2, \dots, \Omega$ )

The various assumptions used in this work are explained below.

- All 7 ND wind zones ( $r = 1, 2, \dots, 7$ ) are potential biomass supply zones, BMPP, wind farm, and HVDC grid station locations. Biomass and wind energy availability originate from the geographic center of each wind zone.

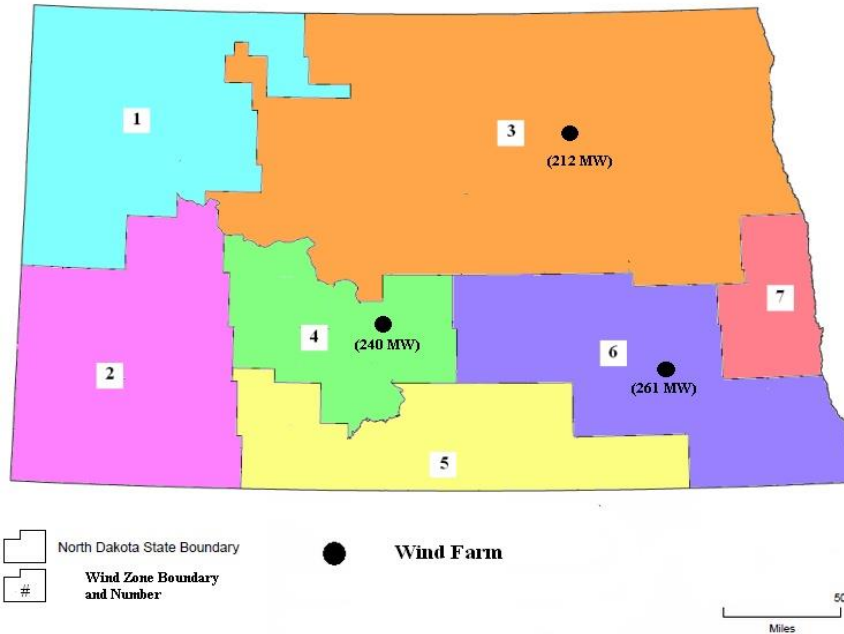


**Fig. 59. Capacities and locations of existing wind farms in ND**

- Existing wind farms (see Fig. 59) will not be shut down but incorporated into the proposed WBBRESC. Currently, in-service wind farms have a generating capacity of 700 MW [40].
- Only the currently available biomass (i.e. crop residues) can be procured as feedstock for a BMPP. Not all the crop residue is available for procurement, since significant portion of the residue should be kept on the field to prevent soil erosion. In this work only 30% of the total amount of crop residue ( $\zeta_i$ ) in biomass supply zone  $i$  can be sustainably removed [39].
- Supply chain revenues and operational costs are considered on an annual basis while capital costs are annualized using a discount rate of 5% [39]. The lifetime of BMPPs, wind turbines and HVAC transmission lines are assumed to be 20 years [4, 34, 39] while those for HVDC grid station and HVDC transmission lines is 40 years [34].

- Capital investment in wind farms, BMPPs, and transmission lines has economies of scale over the relevant capacity ranges. In this work a scaling factor of 0.9 is used [34]. Capital cost per unit of capacity decreases as capacity increases. When capacity is doubled the capital cost does not double and increase by a factor of  $2^{0.9}$ .
- This work assumes that the total electricity requirement for the state of ND is assigned to a “virtual” in-state demand zone composed of all the 53 counties in ND. The power requirement from each county is aggregated and assigned to the geographic center of the “virtual” demand zone. Findings by the North Dakota Transmission Authority [44] show that sufficient HVAC transmission capacity currently exists at the county level to allow transmission of an extra 20% of electric power within ND. No “line losses” are incurred as the maximum transmission distance within ND is less than 300 miles. Therefore there is no need to add HVAC transmission capacity from: a) renewable electricity supply zones to the “virtual” in-state demand zone; and b) the “virtual” in-state demand zone to each of the 53 counties in ND.
- Wind farms and/or BMPPs are assumed to be established in remote locations without adequate HVAC transmission capacity to HVDC grid stations [4]. This requires establishing of new HVAC transmission lines to transfer and manage renewable electricity generated from wind farms and/or BMPPs to HVDC grid stations.
- Fixed cost of wind farms include the cost of physical grid connection to the nearest existing HVAC grid station. The length of the HVAC connection link is assumed to be around 50 miles.
- HVDC grid stations are assumed to be established in remote locations without grid connectivity to faraway out-state electricity demand zones [4]. This requires establishing of new HVDC transmission lines and grid stations to transfer and manage renewable electricity generated from wind farms and/or BMPPs.
- Less than 1% of the available land to be used for establishing wind farms [4].

- The stochastic model has “full recourse”. Any shortfall in meeting the electricity demand is fully offset by incurring penalty cost ( $\varphi$ ) for each MWh of unmet electricity demand [32, 34].

### 6.5.2. Modeling the uncertainties in a WBBRESC

In this work, all stochastic scenarios are governed by 8 independent random variables (IRVs) which are not correlated. The first 7 IRVs,  $\Delta_r(\omega)$  are assumed to follow Weibull probability distribution (with a shape factor of 2) and are used to model the hourly wind speed in location  $r$ . The last IRV,  $A(\omega)$  is used to model price level of electricity and assumed to follow Normal probability distribution.

A set of possible scenarios with a given probability of occurrence are used to describe the random events. The use of continuous probability distributions to model the uncertainty will result in an infinite number of scenarios [39, 45]. The large number of stochastic scenarios need to be reduced (while maintaining the overall accuracy of the results) in order to ensure solution within reasonable computation time. To reduce the model size and the number of scenarios, a Monte Carlo sampling approach is used to generate a sample of  $\Omega$  scenarios [46, 47] with each scenario  $\omega$  (where  $\omega = 1, 2, \dots, \Omega$ ) equally likely to happen. A statistical method is used to determine the number of scenarios [48] needed to obtain solutions (for the proposed model) which fall within specific confidence intervals for a desired level of accuracy, Eq. 6.27 depicts the method which is effective for scenario reduction, particularly for problems with infinite scenarios,  $Z$  represents the  $z$ -value (e.g. 2.58 for 99% confidence level) and  $c$  represents the confidence interval expressed as decimal (e.g.  $\pm 1\% = 0.01$ ).

$$\Omega = (Z/2c)^2 \quad (6.27)$$

For a problem with almost infinite number of scenarios, a sample size of  $\Omega = 16000$  can find the true optimal solution with 99% probability with an accuracy of  $\pm 1\%$ . The reduced stochastic model is coded in GAMS and has 35 binary variables. The Sample Average Approximation method [45] is used to solve the reduced stochastic model, with 1% as the pre-set criteria for the optimality gap. For this

work an optimality gap of 0.97% is achieved from a sample of 40 sets, with each set populated with 400 scenarios randomly drawn without replacement from the 16000 scenarios.

### 6.5.3. Comparison of the deterministic model vs. proposed stochastic model

For the stochastic model, the optimal values of first-stage decisions and the expected profit (along with values of second-stage decisions) is obtained by solving its reduced counterpart over 16000 scenarios. For the deterministic model, the optimal values of first-stage decisions obtained by solving the problem for a single scenario using “mean” values of the input parameters are used in the stochastic model to calculate the expected profit (and values of second-stage decisions).

Value of stochastic solution (VSS) is used to compare the results of the proposed stochastic model with traditional deterministic model. VSS is defined as the difference between the expected profit of the stochastic model vs. the deterministic model under uncertainties [39, 45].

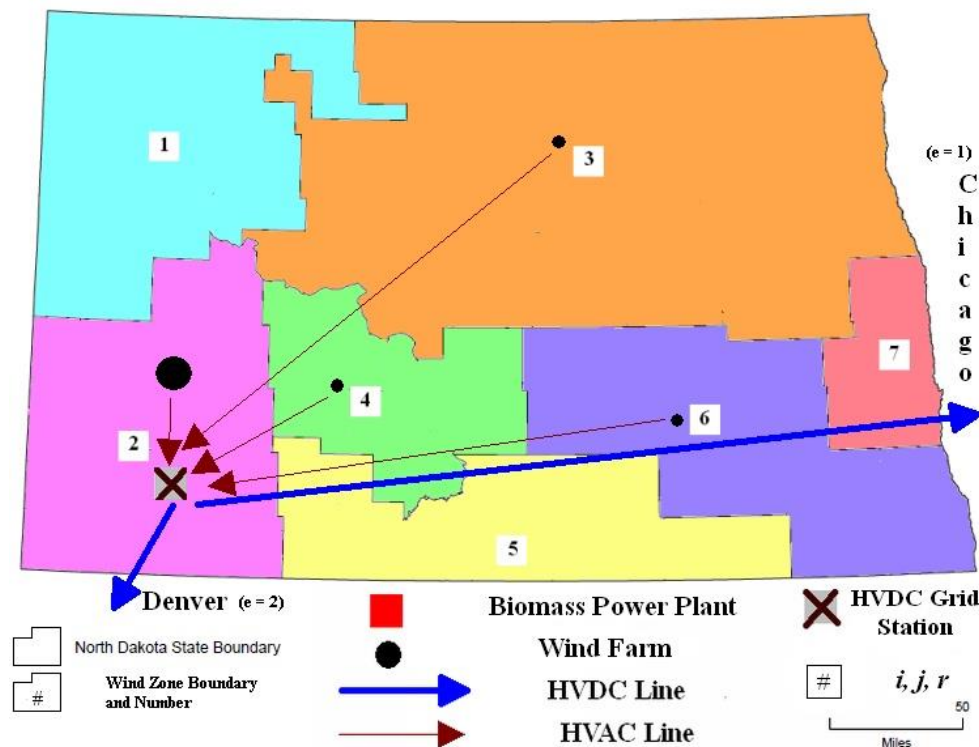


**Fig. 60. First-stage decisions (deterministic model)**

Results from the deterministic and stochastic models are displayed in Fig. 60 and Fig. 61.

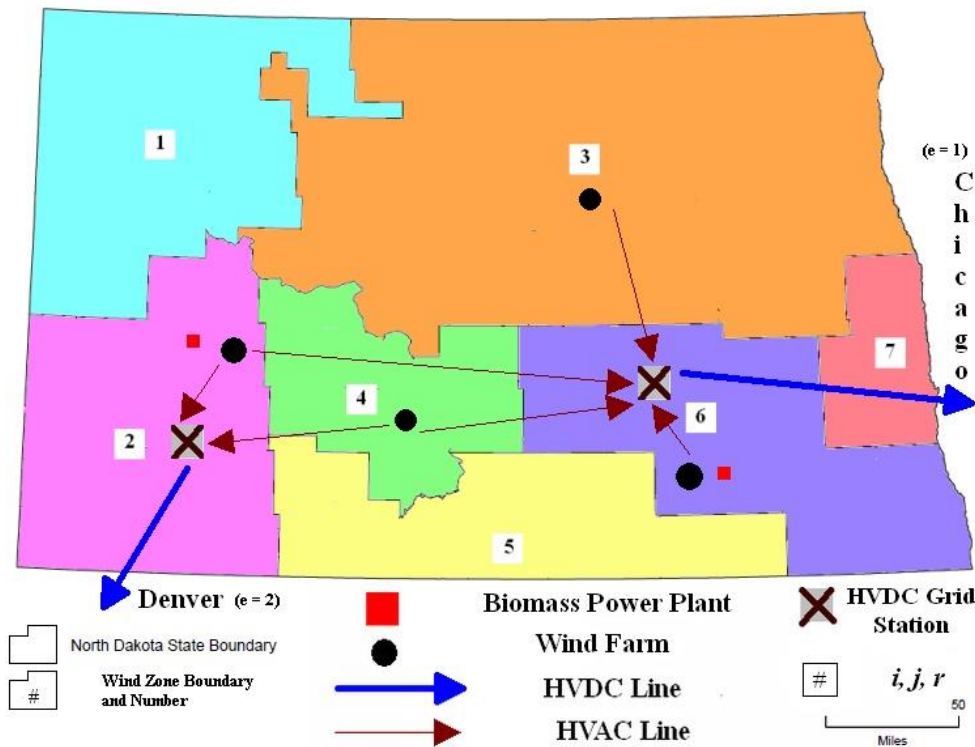


**Fig. 61. First-stage decisions (stochastic model)**

Table 16 summarizes the results. The proposed stochastic model gives robust decisions that lead to VSS of \$381 Million [= 283 – (–98)] for the WBBRESC. The deterministic model (under uncertainties) incurs higher penalty for unmet electricity demand due to establishing the bulk of the wind electricity generation capacity at a single wind farm without back-up generation from BMPPs. The stochastic model maximizes the profit by equitably distributing the wind electricity generation capacity across the 4 dispersed wind farm locations. 2 BMPPs are also established as back-up generators to mitigate wind intermittency and minimize the penalty cost of unmet electricity demand.

As the off-peak electricity demand is known with certainty, both the deterministic and stochastic models give the same results regarding the total transmission capacities of HVDC power lines and the amount of electricity to be supplied to demand zones. However the amount of electricity generated by each wind farm is stochastic. Therefore, both the deterministic and stochastic models give different results regarding the transmission line connectivity between renewable electricity supply zones, grid stations, and out-state electricity demand zones.



**Table 16. Comparison of the deterministic model vs. proposed stochastic model**

Expected annualized values	Model results	
	Deterministic	Stochastic
WBBRESC profit (\$ M) = i) – ii)	-98	283
i) WBBRESC revenues (\$ M) = a) + b)	2432	2486
a) Revenue from sale of renewable electricity (\$ M)	2150	2150
b) Tax credits from renewable electricity production (\$ M)	282	336
ii) WBBRESC costs (\$ M) = c) + d) + e) + f) + g) + h)	2530	2203
c) Cost of biomass power plants (\$ M)	0	114
d) Cost of wind farms (\$ M)	1276	1220
e) Cost of HVDC transmission lines (\$ M)	400	503
f) Cost of HVAC transmission lines (\$ M)	33	89
g) Cost of biomass procurement and transport (\$ M)	0	230
h) Penalty cost due to unmet electricity demand (\$ M)	821	47
<b>Key first-stage decision variables</b>		
<i>Total generation capacity of wind farms (MW)</i>	8139	7481
Total generation capacity of wind farm (MW) in supply zone $r = 1$	0	0
Total generation capacity of wind farm (MW) in supply zone $r = 2$	7426	1804
Total generation capacity of wind farm (MW) in supply zone $r = 3$	212	1882
Total generation capacity of wind farm (MW) in supply zone $r = 4$	240	1847
Total generation capacity of wind farm (MW) in supply zone $r = 5$	0	0
Total generation capacity of wind farm (MW) in supply zone $r = 6$	261	1948
Total generation capacity of wind farm (MW) in supply zone $r = 7$	0	0
<i>Total generation capacity of biomass power plants (MW)</i>	0	1173
Generation capacity of biomass power plant (MW) in supply zone $r = 1$	0	0
Generation capacity of biomass power plant (MW) in supply zone $r = 2$	0	557
Generation capacity of biomass power plant (MW) in supply zone $r = 3$	0	0
Generation capacity of biomass power plant (MW) in supply zone $r = 4$	0	0
Generation capacity of biomass power plant (MW) in supply zone $r = 5$	0	0
Generation capacity of biomass power plant (MW) in supply zone $r = 6$	0	616
Generation capacity of biomass power plant (MW) in supply zone $r = 7$	0	0
<i>Total transmission capacity of HVDC power lines (MW)</i>	3196	3196
Transmission capacity (MW) from Grid Stn $j = 2$ to demand zone $e = 1$	2511	0
Transmission capacity (MW) from Grid Stn $j = 6$ to demand zone $e = 1$	0	2511
Transmission capacity (MW) from Grid Stn $j = 2$ to demand zone $e = 2$	685	685
<i>Total amount of electricity supplied to demand zones (MWh)</i>	30800000	30800000
Amount of electricity (MWh) supplied to in-state demand zone $d = 1$	2800000	2800000
Amount of electricity (MWh) supplied to out-state demand zone $e = 1$	22000000	22000000
Amount of electricity (MWh) supplied to out-state demand zone $e = 2$	6000000	6000000

#### 6.5.4. Evaluating the decisions of the stochastic model

The results for transmission capacity of HVAC power lines from supply zone  $r$  to grid station  $j$  are summarized in Table 17. The parameter “ $Load\_AC$ ” (given by Eq. 6.28) is used to indicate HVAC transmission capacity utilization.

$$Load\_AC = [\text{Average utilization of HVAC capacity}/\text{Allocated HVAC capacity}] \quad (6.28)$$

**Table 17. Transmission capacity of HVAC power lines from  $r$  to  $j$**

$T_{rj}$	$K_{rj}(\omega)$	$Load\_AC^a$
$T_{22} = 790$ MW	$E_{\omega}(K_{22}) = 546$ MW	0.69
$T_{42} = 391$ MW	$E_{\omega}(K_{42}) = 231$ MW	0.59
$T_{26} = 223$ MW	$E_{\omega}(K_{26}) = 127$ MW	0.57
$T_{36} = 1114$ MW	$E_{\omega}(K_{36}) = 774$ MW	0.69
$T_{46} = 783$ MW	$E_{\omega}(K_{46}) = 522$ MW	0.67
$T_{66} = 1787$ MW	$E_{\omega}(K_{66}) = 1068$ MW	0.60

$$^a = [E_{\omega}(K_{rj})]/T_{rj}$$

The cost of a HVAC line are lower compared to a HVDC line over distances less than 300 miles, therefore the HVAC lines are not heavily loaded (i.e.  $Load\_AC < 0.7$ ). Each HVDC grid station is supplied electricity from multiple renewable electricity supply zones (see Fig. 61 for details) to ensure sufficient amount of electricity can always be transmitted from renewable electricity supply zones to the HVDC grid stations.

The results for transmission capacity of HVDC power lines are summarized in Table 18. The parameter “ $Load\_DC$ ” (given by Eq. 6.29) is used to indicate HVDC transmission capacity utilization.

$$Load\_DC = [\text{Average utilization of HVDC capacity}/\text{Allocated HVDC capacity}] \quad (6.29)$$

**Table 18. Transmission capacity of HVDC power lines**

$S_{je}$	$H_{je}(\omega)$	$Load\_DC^b$
$S_{61} = 2511$ MW	$E_{\omega}(H_{61}) = 2489$ MW	0.99
$S_{22} = 685$ MW	$E_{\omega}(H_{22}) = 677$ MW	0.99

$$^b = [E_{\omega}(H_{je})]/S_{je}$$

The fixed costs of HVDC lines are higher compared to HVAC lines. Therefore the allocated transmission capacity is optimized to ensure that the HVDC lines are heavily loaded (i.e.  $Load\_DC >$

0.95) to ensure adequate return on investment and avoid incurring loss from allocating excess capacity. To avoid the high fixed cost, each out-state electricity demand zone is only supplied renewable electricity from a single HVDC grid station via HVDC power transmission line (see Fig. 61).

The results for generation capacity of wind farms are summarized in Table 19. The parameters “ $Utlz\_W$ ” and “ $Trnsm\_W$ ” (given by Eq. 6.30 and Eq. 6.31) are respectively used to indicate wind generation capacity utilization and the ratio of generated wind electricity that is transmitted.

$$Utlz\_W = [\text{Avg utilization of wind generation capacity}/\text{Allocated wind generation capacity}] \quad (6.30)$$

$$Trnsm\_W = [\text{Avg transmission of wind electricity}/\text{Avg utilization of wind generation capacity}] \quad (6.31)$$

**Table 19. Generation capacity of wind farms**

$U_r$	$O_r(\omega)$	$M_r(\omega)$	$Utlz\_W^c$	$Trnsm\_W^d$
$U_2 = 1804 \text{ MW}$	$E_\omega(O_2) = 779 \text{ MW}$	$E_\omega(M_2) = 745 \text{ MW}$	0.43	0.96
$U_3 = 1882 \text{ MW}$	$E_\omega(O_3) = 782 \text{ MW}$	$E_\omega(M_3) = 742 \text{ MW}$	0.41	0.95
$U_4 = 1847 \text{ MW}$	$E_\omega(O_4) = 782 \text{ MW}$	$E_\omega(M_4) = 752 \text{ MW}$	0.42	0.96
$U_6 = 1948 \text{ MW}$	$E_\omega(O_6) = 783 \text{ MW}$	$E_\omega(M_6) = 782 \text{ MW}$	0.40	0.99

$$^c = [E_\omega(O_r)]/U_r \quad ^d = [E_\omega(M_r)]/[E_\omega(O_r)]$$

The stochastic model selects 4 dispersed locations all in different wind zones (see Fig. 61) for establishing wind farms. This ensures that the probability that wind farms in all the wind zones are simultaneously experiencing low wind speeds is very small. The results show that  $Utlz\_W > 0.4$  while a value of 0.36 is generally considered high due to wind intermittency [34].  $Trnsm\_W$  is very high (i.e. > 0.95) with almost all the generated electricity being transmitted with only a minimal ratio (i.e. < 0.05) being “purged” onsite due to lack of transmission capacity.

The results for generation capacity of BMPPs are summarized in Table 20. The parameter “ $Utlz\_B$ ” (given by Eq. 6.32) is used to indicate bioelectricity generation capacity utilization.

$$Utlz\_B = [\text{Avg utilization of biopower capacity}/\text{Allocated biopower capacity}] \quad (6.32)$$

The stochastic model selects 2 locations for installing BMPPs (see Fig. 61). The locations are invariably located in areas with high availability of biomass feedstock. Biomass feedstock has low density and is expensive to transport. Once the biomass is combusted to generate power, the resulting

electricity can be cheaply transmitted to the in-state demand zone and/or HVDC grid stations. As a result each of the 4 wind farm sites do not need an individual BMPP to be co-located to mitigate the effect of wind intermittency. The results show that the value of  $Utlz\_W$  is between 0.34 and 0.46.

BMPPs are only used to provide backup power when wind farms experience low wind speeds. As such BMPPs are not expected to operate at full capacity (i.e.  $Utlz\_W = 1$ ) all the time.

**Table 20. Generation capacity of BMPPs**

$V_r$	$P_r(\omega)$	$Utlz\_B^e$
$V_2 = 557 \text{ MW}$	$E_\omega(P_2) = 187 \text{ MW}$	0.34
$V_6 = 616 \text{ MW}$	$E_\omega(P_6) = 286 \text{ MW}$	0.46

$$^e = [E_\omega(P_r)]/V_r$$

The results for electricity supplied to out-state demand zones are summarized in Table 21. The stochastic model ensures that the value of  $UNMR$  is very low for all demand zones. The parameter “ $UNMR$ ” (given by Eq. 6.33) is used to indicate unmet electricity requirement for demand zones.

$$UNMR = [\text{Average unmet electricity requirement}/\text{Total electricity requirement}] \quad (6.33)$$

**Table 21. Amount of electricity supplied to out-state demand zones**

$N_e$	$G_e(\omega)$	$UNMR^g$
$N_1 = 22000 \text{ GWh}$	$E_\omega(G_1) = 194 \text{ GWh}$	0.01
$N_2 = 6000 \text{ GWh}$	$E_\omega(G_2) = 67 \text{ GWh}$	0.01

$$^g = [E_\omega(G_e)]/N_e$$

### 6.5.5. Sensitivity analysis

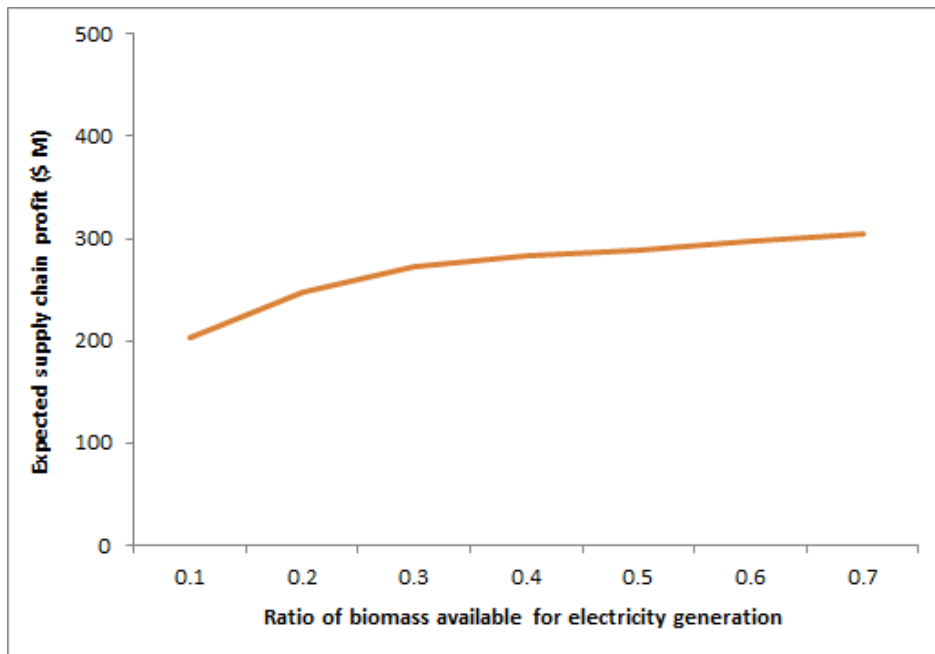
The impact of the uncertain parameters has already been incorporated into the stochastic model and sensitivity analysis is conducted to measure the impact of the following key deterministic parameters: a) ratio of available biomass that can be procured for electricity generation; b) biomass purchase price; and c) renewable electricity tax credit.

The ratio of available biomass that can be procured for electricity generation ( $\sigma$ ) is varied from 0.1 to 0.7 while the deterministic input parameter value used in this case study is 0.4 [1, 5]. Research shows that at least 30% of the available biomass in ND is needed for biofuel production. Therefore  $\sigma$

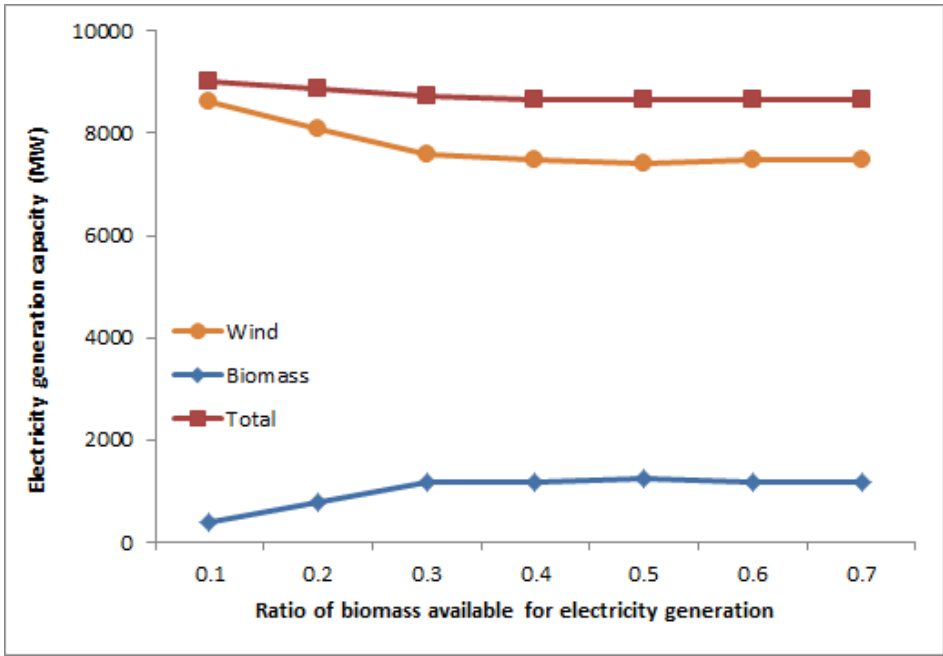
cannot exceed 0.7 [5]. Results show that location of HVDC grid stations and HVDC connectivity links are insensitive to the value of  $\sigma$ . Results also show that for all levels of  $\sigma$ , the maximum allowable amount of renewable electricity (i.e. 20% of total demand) is supplied to all demand zones.

Fig. 62 indicates that the value of  $\sigma$  positively impacts on the expected profit in a piece-wise linear manner. Once the value of  $\sigma$  exceeds 0.3 the slope of the profit line decreases. Fig. 63 indicates that as the value of  $\sigma$  increases from 0.1 to 0.3, generation capacity of wind farms decreases and that of BMPPs increases. As  $\sigma$  exceeds 0.3, generation capacity of wind farms and BMPPs remains constant.

Biomass purchase price ( $\rho$ ) is varied from \$20/ton to \$60/ton while the deterministic input parameter value used in this case study is \$40/ton [5]. Results show that location of HVDC grid stations and HVDC connectivity links are insensitive to the value of  $\rho$ . Results also show that for all levels of  $\rho$ , the maximum allowable amount of renewable electricity (i.e. 20% of total demand) is supplied to all in-state and out-state demand zones.



**Fig. 62. Impact on expected WBBRESC profit**



**Fig. 63. Impact on generation capacity**

Fig. 64 indicates that the value of  $\rho$  negatively impacts on the expected profit in almost a linear manner. Fig. 65 indicates that as the value of  $\rho$  increases, generation capacity of wind farms increases and that of BMPPs decreases. The rate of increase in wind generation capacity is greater than the rate of decrease in biomass generation capacity.

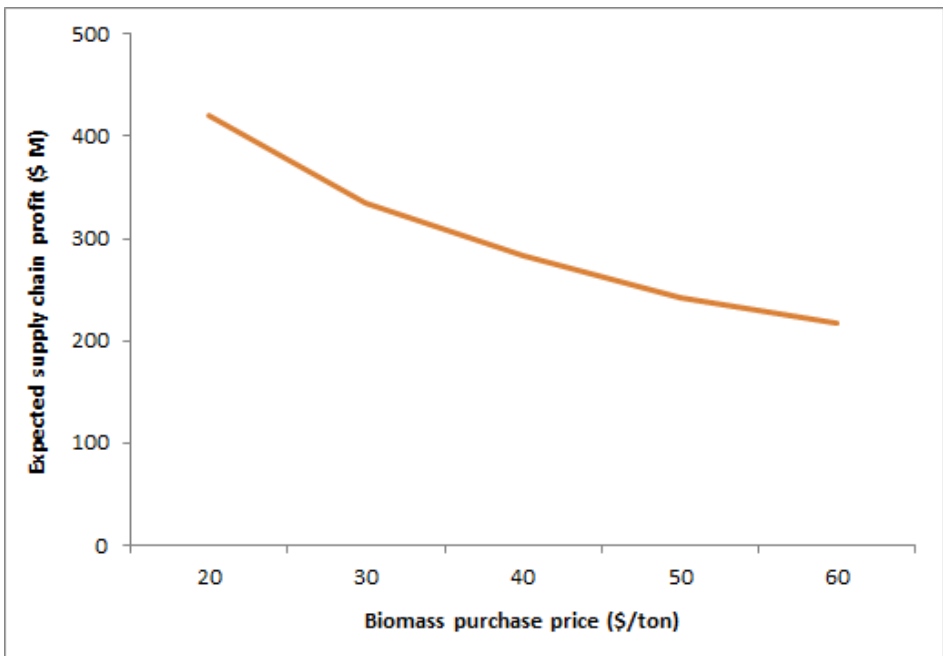


**Fig. 64. Impact on expected WBBRESC profit**

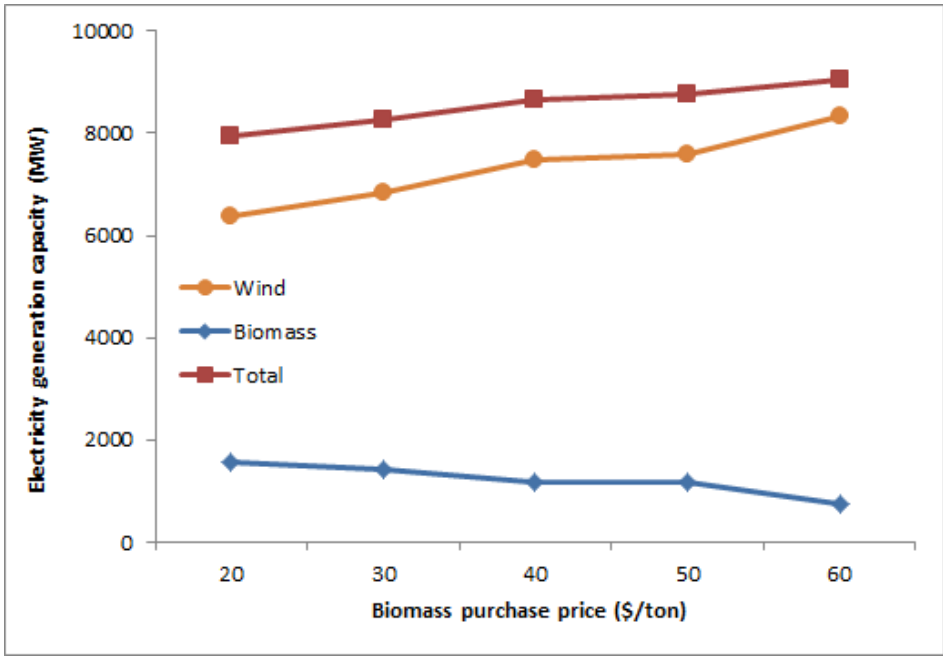


**Fig. 65. Impact on electricity generation capacity**

Renewable electricity tax credit ( $\phi$ ) is varied from \$0/MWh to \$11/MWh. The current federal tax credit of \$11/MWh [3, 4] expired in December 2012 and was renewed till December 2013 by the U.S. congress. As of now it is uncertain if the tax credit will be extended and/or reduced [40].

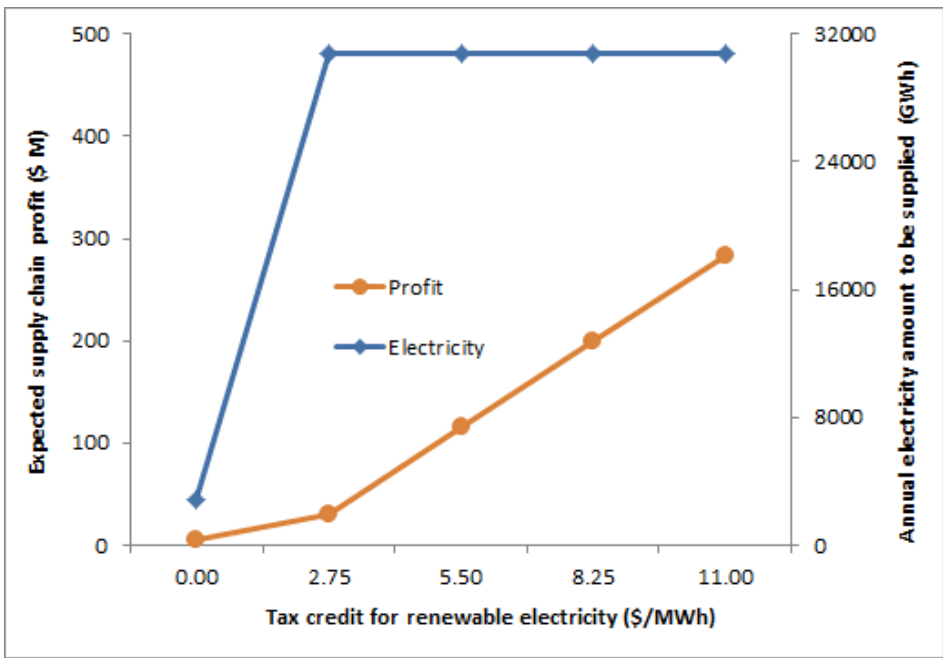


**Fig. 66. Impact on expected WBBRESC profit**

Fig. 66 indicates that when  $\varphi$  is less than \$2.75/MWh, renewable electricity is not supplied to the out-state demand zones as the subsidy is not sufficient to induce WBBRESC investors to incur the huge fixed costs in laying HVDC transmission lines from ND to Chicago and Denver. The value of  $\varphi$  positively impacts on the expected profit in a step-wise linear manner. Once the value of  $\varphi$  exceeds \$2.75/MWh the slope of the profit line decreases and the amount of electricity to be supplied to all demand zones reaches its maximum allowable limit (i.e. 20% of total off-peak demand) and plateaus.

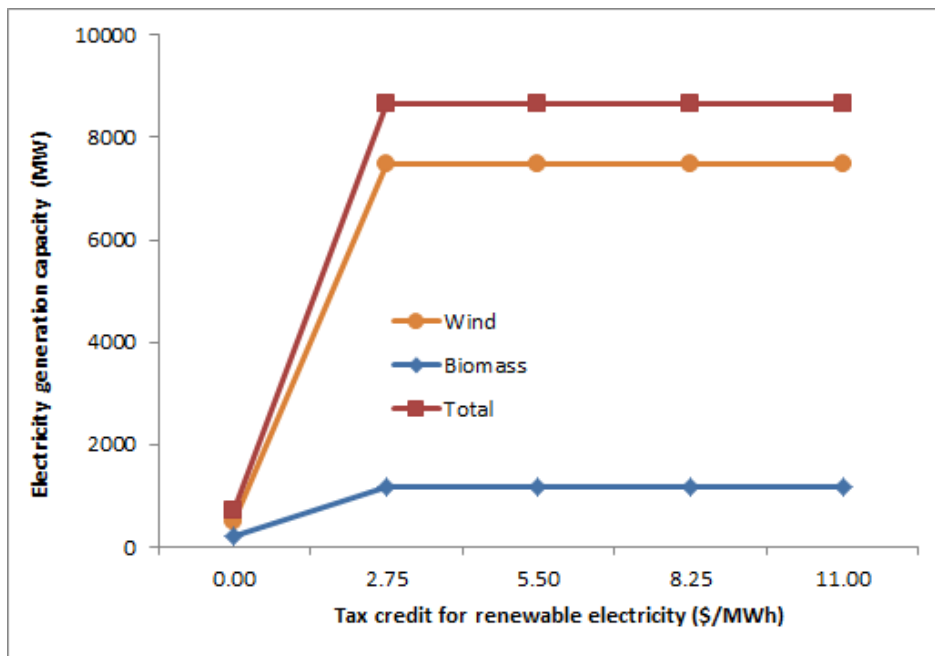


**Fig. 67. Impact on electricity generation capacity**

Fig. 67 indicates that as the value of  $\varphi$  increases from \$0/MWh to \$2.75/MWh, both wind and biomass generation capacity increases. As  $\varphi$  exceeds \$2.75/MWh, generation capacity of wind farms and BMPPs remains constant.

## 6.6. Conclusions

This paper studies the grid design and optimal allocation of wind and biomass resources for a WBBRESC. A two-stage SMILP model is proposed that ensures the financial viability by balancing the electricity demand across the available supply from wind and biomass resources under uncertainties in wind speed and electricity sale price. The model integrates all the supply chain logistics for



generation and transmission of renewable electricity to arrive at optimal first-stage decisions that include: 1) site selection for installation of wind farms, BMPPs, and grid stations; 2) generation capacity of wind farms and BMPPs; 3) grid connectivity and transmission capacity of power lines; and 4) amount of renewable electricity to be supplied to demand zones.

A case study set in the Midwestern state of North Dakota is presented to demonstrate the effectiveness of the proposed stochastic model. Results show that in a stochastic environment it is financially sustainable to meet 20% of annual off-peak electricity demand for the state of ND and the nearest major metropolitan centers of Chicago and Denver. The results demonstrate that the proposed stochastic model outperforms the counterpart deterministic model under uncertainties. The deterministic model underestimates the generation capacity of BMPPs and overestimates the generation capacity of wind farms. In addition the deterministic model incurs higher penalty for unmet electricity demand due to establishing the bulk of the wind electricity generation capacity at a single wind farm without back-up generation from BMPPs. The proposed stochastic model maximizes the expected profit by equitably distributing the wind electricity generation capacity across dispersed wind farm locations to mitigate wind intermittency and minimize the penalty cost. The deterministic and stochastic models give different results regarding the transmission line connectivity. However, the total transmission capacities of power lines and the amount of electricity to be supplied to demand zones are shown to be insensitive to the stochastic environment.

Sensitivity analysis is conducted to provide insights for efficiently managing the WBBRESC by evaluating the impact of key parameters. Results show that: 1) location of grid stations and connectivity links are insensitive to biomass availability, biomass purchase price, and renewable electricity tax credit; 2) allocating at least 30% of the available biomass represents the optimal biomass allocation policy for electricity generation; and 3) when renewable electricity tax credit is less than \$3/MWh, renewable electricity is not supplied to out-state demand zones as the subsidy is not sufficient to induce

WBBRESC investors to incur the huge fixed costs in laying HVDC transmission lines from ND to Chicago and Denver. The fixed investment costs for HVDC power lines will need to significantly decrease before the transmission of renewable electricity over large distances (i.e. > 600 miles) becomes commercially viable in the U.S. without needing subsidies.

This work optimizes WBBRESC by considering single objective of economic performance. Future work can optimize WBBRESC by considering multiple criteria such as economic, environmental [2] and social performances. Future work can also incorporate the uncertainties associated with “peak” electricity demand and additional renewable resources like solar power can also be considered for electricity generation.

## 6.7. Nomenclature

### 6.7.1. Indices

- $d$  In-state electricity demand zones ( $d = 1, \dots, D$ )
- $e$  Out-state electricity demand zones ( $e = 1, \dots, E$ )
- $i$  Biomass supply zones ( $i = 1, \dots, I$ )
- $j$  HVDC grid station locations ( $j = 1, \dots, J$ )
- $r$  Renewable electricity supply zones ( $r = 1, \dots, R$ )
- $\omega$  Stochastic scenarios ( $\omega = 1, \dots, \Omega$ )

### 6.7.2. First stage binary decision variables

- $Z_r$  {1, if biomass power plant established in location  $r$ ; Else 0}
- $Y_r$  {1, if wind farm established in location  $r$ ; Else 0}
- $X_j$  {1, if HVDC grid station established in location  $j$ ; Else 0}
- $W_{je}$  {1, if HVDC transmission line laid from grid station  $j$  to out-state demand zone  $e$ ; Else 0}

### 6.7.3. First stage continuous decision variables

- $V_r$  Generating capacity of biomass power plant at location  $r$  (MW)
- $U_r$  Total generating capacity of wind farm at location  $r$  (MW)
- $F_r$  New generating capacity of wind farm at location  $r$  (MW)
- $T_{rj}$  Transmission capacity of HVAC power line from electricity supply zone  $r$  to HVDC grid station  $j$  (MW)
- $T_{rd}$  Transmission capacity of HVAC power line from electricity supply zone  $r$  to in-state demand zone  $d$  (MW)
- $S_{je}$  Transmission capacity of HVDC power line from HVDC grid station  $j$  to out-state electricity demand zone  $e$  (MW)
- $N_d$  Annual amount of electricity to be supplied to in-state demand zone  $d$  (MWh)
- $N_e$  Annual amount of electricity to be supplied to out-state demand zone  $e$  (MWh)

### 6.7.4. Second stage decision variables

- $Q_{ir}(\omega)$  Annual amount of biomass sent from supply zone  $i$  to biomass plant  $r$  during scenario  $\omega$  (tons)
- $P_r(\omega)$  Hourly amount of renewable electricity generated by biomass plant  $r$  during scenario  $\omega$  (MWh)
- $O_r(\omega)$  Hourly amount of renewable electricity generated by wind farm  $r$  during scenario  $\omega$  (MWh)
- $M_r(\omega)$  Hourly amount of electricity that is transmitted from wind farm  $r$  during scenario  $\omega$  (MWh)
- $L_r(\omega)$  Hourly amount of electricity that is not transmitted from wind farm  $r$  during scenario  $\omega$  (MWh)
- $K_{rj}(\omega)$  Hourly amount of electricity transmitted from supply zone  $r$  to HVDC grid station  $j$  during scenario  $\omega$  (MWh)
- $K_{rd}(\omega)$  Hourly amount of electricity transmitted from supply zone  $r$  to in-state demand zone  $d$  (MWh)
- $H_{je}(\omega)$  Hourly amount of electricity transmitted from grid station  $j$  to out-state demand zone  $e$  (MWh)
- $G_d(\omega)$  Hourly amount of unmet electricity demand at in-state zone  $d$  during scenario  $\omega$  (MWh)
- $G_e(\omega)$  Hourly amount of unmet electricity demand at out-state zone  $e$  during scenario  $\omega$  (MWh)

#### 6.7.4. Deterministic parameters

$\alpha_r$	Annualized fixed cost of biomass power plant at location $r$ (\$)
$\beta_r$	Variable cost of biomass power plant at location $r$ (\$/MW)
$\gamma_{max}$	Maximum generation capacity of a biomass power plant (MW)
$\gamma_{min}$	Minimum generation capacity of a biomass power plant (MW)
$\delta_r$	Annualized fixed cost of wind farm at location $r$ (\$)
$\varepsilon_r$	Variable cost of wind farm at location $r$ (\$/MW)
$\zeta_{min}$	Minimum generation capacity of a wind farm (MW)
$\eta_r$	Maximum potential for generating wind electricity at location $r$ (MW)
$l_{rj}$	Variable cost of a HVAC transmission line from supply zone $r$ to grid station $j$ (\$/MW x mile)
$l_{rd}$	Variable cost of a HVAC line from supply zone $r$ to in-state demand zone $d$ (\$/MW x mile)
$\kappa_{rj}$	Maximum transmission capacity of a HVAC line from supply zone $r$ to grid station $j$ (MW)
$\kappa_{rd}$	Maximum transmission capacity of a HVAC line from supply zone $r$ to in-state zone $d$ (MW)
$\lambda$	Annualized fixed cost of a HVDC transmission line (\$)
$\mu$	Variable cost of a HVDC transmission line (\$/MW x mile)
$v_{max}$	Maximum transmission capacity of a HVDC power line (MW)
$v_{min}$	Minimum transmission capacity of a HVDC power line (MW)
$\varphi_r$	Renewable electricity generation tax credit in location $r$ (\$/MWh)
$\pi$	Electricity generation parameter from biomass (MWh/ton)
$\rho_i$	Purchase price of biomass at supply zone $i$ (\$/ton)
$\varsigma_i$	Amount of available biomass in supply zone $i$ (tons)
$\sigma$	Ratio of available biomass that can be procured for electricity generation
$\tau$	Transport cost parameter of biomass (\$/ton x mile)
$B_r$	Existing generating capacity of wind farm at location $r$ (MW)

- $DST_{ir}$  Distance between biomass supply zone  $i$  and biomass power plant  $r$  (miles)
- $DST_{rj}$  Distance between renewable electricity supply zone  $r$  and HVDC grid station  $j$  (miles)
- $DST_{rd}$  Distance between renewable electricity supply zone  $r$  and in-state demand zone  $d$  (miles)
- $DST_{je}$  Distance between HVDC grid station  $j$  and out-state demand zone  $e$  (miles)
- $v_d$  Sale price of electricity at in-state demand zone  $d$  (\$/MWh)
- $v_e$  Sale price of electricity at out-state demand zone  $e$  (\$/MWh)
- $o_d$  100% of annual electricity requirement at in-state demand zone  $d$  (MWh)
- $o_e$  100% of annual electricity requirement at out-state demand zone  $e$  (MWh)
- $\chi_{max}$  Maximum ratio of annual electricity demand to be satisfied from renewables
- $\chi_{min}$  Minimum ratio of annual electricity demand to be satisfied from renewables
- $RTO_i$  Ratio of available biomass that can be removed from supply zone  $i$
- $\psi$  Penalty cost parameter for unmet renewable electricity requirement (\$/MWh)
- $\Gamma_j$  Annualized fixed cost of HVDC grid station at location  $j$  (\$)

### 6.7.5. Stochastic parameters

- $A(\omega)$  Price level of electricity during scenario  $\omega$
- $\Delta_r(\omega)$  Hourly wind speed in location  $r$  during scenario  $\omega$  (mph)
- $C_r(\omega)$  Power output level (as ratio of maximum output) of wind farm in location  $r$  during scenario  $\omega$

### 6.8. References

- [1] Osmani A, Zhang J, Gonela V, Awudu I. Electricity generation from renewables in the United States: Resource potential, current usage, technical status, challenges, strategies, policies, and future directions. *Renewable and Sustainable Energy Reviews* 2013;24:454–472.
- [2] [www.whitehouse.gov/the-press-office/2013/06/25/remarks-president-climate-change](http://www.whitehouse.gov/the-press-office/2013/06/25/remarks-president-climate-change)
- [3] U.S. Energy Independence and Security Act of 2007 (EISA).

- [4] Department of Energy (DoE), 20% wind energy by 2030: Increasing wind energy's contribution to US electricity supply. Washington, DC (2008).
- [5] U.S. Department of Agriculture (USDA)/Department of Energy (DOE). Biomass as Feedstock for a Bioenergy and Bioproducts Industry: The Technical Feasibility of a Billion-Ton Annual Supply. Washington, DC (2005).
- [6] Bain R. Electricity from biomass in the United States: Status and future direction. *Bioresource Tech.* 1993;46:86-93.
- [7] Sims R. Electricity-generation from woody biomass fuels compared with other renewable energy options. *Renewable Energy* 1994;5:852–6.
- [8] Willis H, Scott W. *Distributed power generation: Planning and evaluation*. NY: Dekker; 2000.
- [9] Bazmi A, Zahedi G. Sustainable energy systems: Role of optimization modeling techniques in power generation and supply – A review. *Renewable and Sustainable Energy Reviews* 2011;15:3480–3500.
- [10] Garcia-Gonzalez J, de la Muela R, Santos L, Gonzalez M. Stochastic joint optimization of wind generation and pumped-storage units in an electricity market. *IEEE Transactions on Power Systems* 2008;23:460–468.
- [11] Rahimiyan M, Morales J, Conejo A. Evaluating alternative offering strategies for wind producers in a pool. *Applied Energy* 2011;88:4918–4926.
- [12] Pousinho H, Mendes V, Catalao J. A risk-averse optimization model for trading wind energy in a market environment under uncertainty. *Energy* 2011;36:4935–4942.
- [13] Meibom P, Barth R, Hasche B, Brand H, Weber C, O'Malley M. Stochastic Optimization Model to Study the Operational Impacts of High Wind Penetrations in Ireland. *IEEE Transactions on Power Systems* 2011; 26:1367–1379.

- [14] Brekken T, Yokochi A, Von Jouanne A, Yen Z, Hapke H. Optimal energy storage sizing and control for wind power applications. *IEEE Transactions on Sustainable Energy*, 2011;2: 69–77.
- [15] Jabr R, Pal B. Intermittent wind generation in optimal power flow dispatching. *IET Generation, Transmission & Distribution* 2009;3(1), 66-74.
- [16] Evans A, Strezov V, Evans T. Assessment of utility energy storage options for increased renewable energy penetration. *Renewable and Sustainable Energy Reviews* 2012;16:4141–4147.
- [17] Beaudin M, Zareipour H, Schellenberglabe A, Rosehart W. Energy storage for mitigating the variability of renewable electricity sources: An updated review. *Energy for Sustainable Development* 2010;14:302–314.
- [18] Connolly D, Lund H, Mathiesen B, Pican E, Leahy M. The technical and economic implications of integrating fluctuating renewable energy using energy storage. *Renewable Energy* 2012;43:47–60.
- [19] Varkani A, Daraeepour A, Monsef H. A new self-scheduling strategy for integrated operation of wind and pumped-storage power plants in power markets. *Applied Energy* 2011;88:5002–5012.
- [20] Tuohy A, O’Malley M. Pumped storage in systems with very high wind penetration. *Energy Policy* 2011;39:1965–74.
- [21] Sioshansi R. Increasing the Value of Wind with Energy Storage. *Energy Journal* 2011;32: 1–29.
- [22] Ekren B, Ekren O. Simulation based size optimization of a PV/wind hybrid energy conversion system with battery storage under various load and auxiliary energy conditions. *Applied Energy* 2009;86:1387–1394.
- [23] Castronuovo E, Usaola J, Bessa R, Matos M, Costa I, Bremermann L. et al. An Integrated Approach for Optimal Coordination of Wind Power and Hydro Pumping Storage. *Wind Energy* 2013. DOI: 10.1002/we.1600
- [24] Ding H, Hu Z, Song Y. Stochastic optimization of the daily operation of wind farm and pumped-hydro-storage plant. *Renewable Energy* 2012;48:571–578.

- [25] Duque A, Castronuovo E, Sanchez I, Usaola J. Optimal operation of a pumped-storage hydro plant that compensates the imbalances of a wind power producer. *Electric Power Systems Research* 2011;81(9):1767–1777.
- [26] Mauch B, Carvalho P, Apt J. Can a wind farm with CAES survive in the day-ahead market? *Energy Policy* 2012;48:584–593.
- [27] Rahman F, Rehman S, Abdul-Majeed M. Overview of energy storage systems for storing electricity from renewable energy sources in Saudi Arabia. *Renewable and Sustainable Energy Reviews* 2012;16:274–283.
- [28] Liang R, Liao J. A fuzzy-optimization approach for generation scheduling with wind and solar energy systems. *IEEE Transactions on Power Systems* 2007;22:1665–1674.
- [29] Currie R, Ault G, McDonald J. Methodology of economic connection capacity for renewable generator connections to distribution networks optimized by active power flow management. *IEEE Proceedings Generation Transmission & Distribution* 2006;153.
- [30] Al-Awami A, El-Sharkawi M. Coordinated Trading of Wind and Thermal Energy. *IEEE Transactions on Sustainable Energy* 2011;2:277–287.
- [31] De Jonghe C, Delarue E, Belmans R, D’haeseleer W. Determining optimal electricity technology mix with high level of wind power penetration. *Applied Energy* 2011;88:2231–2238.
- [32] Kim J, Powell W. Optimal Energy Commitments with Storage and Intermittent Supply. *Operations Research* 2011;59:1347–1360.
- [33] Capuder T, Pandzic H, Kuzle I, Skrlec D. Specifics of integration of wind power plants into the Croatian transmission network. *Applied Energy* 2013;101:142–150.
- [34] Pattanariyankool S, Lave L. Optimizing transmission from distant wind farms. *Energy Policy* 2010;38:2806–2815.
- [35] Marris E. Upgrading the grid. *Nature* 2008;454:570–3.



- [36] Bremen L. Large-scale variability of weather dependent renewable energy sources. In: Management of weather and climate risk in the energy industry. Springer; 2007:189–206.
- [37] Carpinelli G, Celli G, Mocci S, Pilo F, Proto D, Russo A. Multi-objective programming for the optimal sizing and siting of power-electronic interfaced dispersed generators. Proceedings of the 2007 IEEE power tech conference; 2007.
- [38] Zhu Y, Tomsovic K. Optimal distribution power flow for systems with distributed energy resources. *Int J Electr Power Energy Syst* 2007;29:260–7.
- [39] Osmani A, Zhang J. Stochastic optimization of a multi feedstock lignocellulosic-based bioethanol supply chain under multiple uncertainties. *Energy* 2013;59:157–172.
- [40] Energy Information Administration (EIA). [www.eia.gov/electricity](http://www.eia.gov/electricity)
- [41] Aksoy H, Toprak Z, Aytok A, Unal N. Stochastic generation of hourly mean wind speed data. *Renewable Energy* 2004;29:2111–2131.
- [42] Janke J. Multicriteria GIS modeling of wind and solar farms in Colorado. *Renewable Energy* 2010;35:2228–2234.
- [43] Sinden G. Characteristics of the UK wind resource: Long-term patterns and relationship to electricity demand. *Energy Policy* 2007;35:112–127.
- [44] North Dakota Transmission Authority, 2012 Annual Report. [www.nd.gov/ndic/ic-press/ta-annualreport-12.pdf](http://www.nd.gov/ndic/ic-press/ta-annualreport-12.pdf)
- [45] Osmani A, Zhang J. Economic and environmental optimization of a large scale sustainable dual feedstock lignocellulosic-based bioethanol supply chain in a stochastic environment. *Applied Energy* 2014;114:572–587.
- [46] Linderoth J, Shapiro A, Wright S. The empirical behavior of sampling methods for stochastic programming. *Annals of Operations Research* 2006;142:215–241.

- [47] Shapiro A, Homem-de-Mello T. On the rate of convergence of optimal solutions of Monte Carlo approximations of stochastic programs. *SIAM Journal on Optimization* 2000;11:70–86.
- [48] You F, Tao L, Graziano D, Snyder S. Optimal design of sustainable cellulosic biofuel supply chains: Multiobjective optimization coupled with life cycle assessment and input–output analysis. *AIChE Journal* 2012;58:1157–80.
- [49] EIA. Updated Capital Cost Estimates for Electricity Generation Plants. Washington, DC (2010).
- [50] Hoppock D, Patinoo-Echeverri D. Cost of Wind Energy: Comparing Distant Wind Resources to Local Resources in the Midwestern United States. *Environmental Science & Technology* 2010;44:8758–8765.

APPENDIX A. INPUT PARAMETERS

**Table A1. Values of input parameters ( $A_i, B_i, C_i, M_e^t$ )**

$e, i$	ND County	Population	$\delta_i$ (mm)	$B_i$ (hectare)	$C_i$ (\$/hectare)	$A_i$ (tonne/hectare)	$M_e^t$ (liter)
1	Slope	727	376	6,882	25.9	13.7	2,303,338
2	McIntosh	2,809	462	8,504	50.6	16.8	8,899,692
3	Golden Valley	1,680	389	5,081	23.0	14.1	5,322,706
4	Burleigh	81,308	429	13,536	37.0	15.6	257,606,315
5	Bottineau	6,429	470	21,623	32.1	17.1	20,368,857
6	Burke	1,968	427	15,505	20.7	15.5	6,235,170
7	Bowman	3,151	394	8,757	28.4	14.3	9,983,243
8	Towner	2,246	422	23,023	28.4	15.3	7,115,951
9	Foster	3,343	478	5,248	44.4	17.4	10,591,552
10	Grant	2,394	424	12,728	30.9	15.4	7,584,857
11	Pembina	7,413	465	19,249	29.6	16.9	23,486,442
12	Oliver	1,846	442	8,984	29.6	16.1	5,848,640
13	Griggs	2,420	523	12,155	32.1	19.0	7,667,232
14	Divide	2,071	378	12,531	22.2	13.8	6,561,503
15	Ramsey	11,451	480	23,556	29.6	17.5	36,279,947
16	Stark	24,199	417	10,171	38.3	15.1	76,669,150
17	Dickey	5,289	546	12,091	64.2	19.9	16,757,020
18	Cass	149,778	536	21,291	38.3	19.5	474,538,283
19	Wells	4,207	434	12,478	37.0	15.8	13,328,944
20	Steele	1,975	475	14,277	34.6	17.3	6,257,348
21	Sargent	3,829	523	11,433	72.8	19.0	12,131,335
22	Sioux	4,153	361	14,789	29.6	13.1	13,157,857
23	Walsh	11,119	467	33,116	29.6	17.0	35,228,079
24	Grand Forks	66,861	498	29,021	25.9	18.1	211,834,209
25	Adams	2,343	394	7,614	30.9	14.3	7,423,274
26	Traill	8,121	528	5,394	27.2	19.2	25,729,582
27	Stutsman	21,100	470	24,066	39.5	17.1	66,850,657
28	Nelson	3,126	457	20,096	29.6	16.6	9,904,036
29	LaMoure	4,139	470	15,604	53.1	17.1	13,113,501
30	Cavalier	3,993	460	24,725	27.2	16.7	12,650,932
31	Emmons	3,550	411	11,722	42.0	15.0	11,247,385
32	Ransom	5,457	513	9,076	58.0	18.7	17,289,291
33	Morton	27,471	434	11,513	38.3	15.8	87,035,754
34	Dunn	3,536	414	13,403	29.6	15.1	11,203,030
35	Sheridan	1,321	445	11,909	29.6	16.2	4,185,295
36	Billings	783	376	3,228	23.7	13.7	2,480,761
37	Benson	6,660	419	17,437	30.9	15.2	21,100,729
38	Ward	61,675	470	17,662	32.1	17.1	195,403,521
39	Renville	2,470	445	7,274	30.9	16.2	7,825,646
40	Hettinger	2,477	394	9,403	37.0	14.3	7,847,824
41	Logan	1,990	483	9,302	46.9	17.5	6,304,872
42	Eddy	2,385	457	9,304	35.8	16.6	7,556,342
43	Rolette	13,937	472	33,508	28.4	17.2	44,156,285
44	Pierce	4,357	465	12,710	33.3	16.9	13,804,186
45	Mountrail	7,673	500	16,918	22.5	18.2	24,310,194
46	Mercer	8,424	406	6,274	29.6	14.8	26,689,571
47	Kidder	2,435	475	20,471	38.3	17.3	7,714,756
48	McHenry	5,395	422	21,008	34.6	15.3	17,092,858
49	Barnes	11,066	480	15,982	44.4	17.5	35,060,160
50	Richland	16,321	556	29,425	53.1	20.2	51,709,459
51	McLean	8,962	452	24,821	28.4	16.4	28,394,104
52	McKenzie	6,360	366	13,275	20.2	13.3	20,150,246
53	Williams	22,398	361	15,904	24.4	13.1	70,963,082

**Table A2. Cumulative rate of switchgrass dry-matter weight loss for harvest methods**

	$t = 1$	$t = 2$	$t = 3$	$t = 4$	$t = 5$	$t = 6$	$t = 7$	$t = 8$	$t = 9$	$t = 10$	$t = 10$	$t = 12$
$L_{j=1}^t$	0.00	0.00	0.00	0.06	0.06	0.06	0.11	0.11	0.11	0.11	0.17	0.17
$L_{j=2}^t$	0.00	0.00	0.00	0.26	0.26	0.26	0.41	0.41	0.41	0.41	0.48	0.48

**Table A3. Values of other key input parameters**

Input Parameter	Value
Bioethanol yield (from switchgrass biomass) for biorefinery $r$ (liter/tonne)	$\beta_r = 313$ (for all $r$ )
Loose chop transportation cost from $i$ to $k$ (\$/tonne x km)	$\alpha_{ik} = 0.32$ (for all $i, k$ )
Traditional bales ( $j \neq 3$ ) transportation cost from $i$ to $r$ (\$/tonne x km)	$F_{1ir} = 0.22; F_{2ir} = 0.18$ (for all $i, r$ )
Densified bales transportation cost from $k$ to $r$ (\$/tonne x km)	$\gamma_{kr} = 0.11$ (for all $k, r$ )
Bioethanol transportation cost from $r$ to $e$ (\$/liter x km)	$\psi_{re} = 0.000028$ (for all $r, e$ )
Switchgrass harvest cost for method $j$ (\$/hectare)	$H_1 = 48.2; H_2 = 27.9; H_3 = 22.7$
Bioethanol processing cost for biorefinery $r$ (\$/liter)	$N_r = 0.20$ (for all $r$ )
Minimum capacity utilization rate of biorefinery $r$ with capacity $q$	$O_{rq} = 0.88$ (for all $r, q$ )
Switchgrass cultivation cost in supply zone $i$ (\$/hectare)	$P_i = 395$ (for all $i$ )
Switchgrass storage cost for harvest method $j \neq 3$ (\$/tonne)	$\xi_j = 21.7; \xi_3 = 21.7$
Minimum capacity utilization rate of preprocessing facility $k$	$\phi_k = 0.135$ (for all $k$ )
Maximum annual densification capacity of preprocessing facility $k$ (tonne)	$\lambda_k = 302,395$ (for all $k$ )
Maximum monthly production of 190 MLPY ( $q = 1$ ) biorefinery $r$ (liter)	$\rho_{r,1}^t = 15,833,333$ (for all $r, t$ )
Maximum monthly production of 380 MLPY ( $q = 2$ ) biorefinery $r$ (liter)	$\rho_{r,2}^t = 31,666,667$ (for all $r, t$ )
Preprocessing cost of loose chop biomass at facility $k$ (\$/tonne)	$U_k = 13.94$ (for all $k$ )
Annualized fixed cost of preprocessing facility $k$ (\$)	$W_k = 100,000$ (for all $k$ )
Annualized fixed cost of 190 MLPY ( $q = 1$ ) biorefinery $r$ (\$)	$G_{r,1} = 39,000,000$ (for all $r$ )
Annualized fixed cost of 380 MLPY ( $q = 2$ ) biorefinery $r$ (\$)	$G_{r,2} = 72,000,000$ (for all $r$ )

**Table A4. Values of key deterministic parameters**

Input parameter	Value
Bioethanol yield (from lignocellulosic biomass) for biorefinery $r$ (liter/tonne)	$\beta_r = 313$ (for all $r$ )
Crop residue transportation cost from $i$ to $r$ (\$/tonne x km)	$\eta_{ir} = 0.20$ (for all $i, r$ )
Densified switchgrass transportation cost from $i$ to $r$ (\$/tonne x km)	$\gamma_{ir} = 0.11$ (for all $i, r$ )
Bioethanol transportation cost from $r$ to $e$ (\$/liter x km)	$\psi_{re} = 0.000028$ (for all $r, e$ )
Switchgrass harvest cost as loose chop (\$/hectare)	$H_i = 22.73$ (for all $i$ )
Operational cost for biorefinery $r$ (\$/liter)	$N = 0.20$ (for all $r$ )
Switchgrass cultivation cost in supply zone $i$ (\$/hectare)	$\kappa_i = 395$ (for all $i$ )
Maximum ratio of available crop residue that can be removed from supply zone $i$	$\mu_i = 0.3$ (for all $i$ )
Maximum annual production capacity of biorefinery (MLPY)	$\rho_{max} = 380$
Minimum annual production capacity of biorefinery (MLPY)	$\rho_{min} = 190$
Pre-processing cost of loose chop switchgrass at supply zone $i$ (\$/tonne)	$U_i = 13.94$ (for all $i$ )
Sale price of densified switchgrass (\$/tonne)	$\chi = 49.59$
Tax credit for subsidized bioethanol production (\$/liter)	$\tau = 0.13$
Penalty cost for unmet bioethanol demand (\$/liter)	$\phi = 1.06$
Annualized fixed cost of biorefinery (\$)	$G = 8883500$
Annualized variable cost of biorefinery (\$/liter)	$T = 0.17$

**Table A5. Values of stochastic parameters**

Input parameter	Value
ND annual rainfall level (mm)	$\delta(\omega) \sim N(449, 5316)$ and truncated on the interval (218, 620)
* Crop residue purchase price (\$/tonne)	$\varepsilon(\omega) \sim N(83, 175)$ and truncated on the interval (51, 125)
Bioethanol sale price (\$/liter)	$l(\omega) \sim N(0.53, 0.006)$ and truncated on the interval (0.26, 0.79)
ND bioethanol demand (MLPY)	$M(\omega) \sim N(2133, 4138)$ and truncated on the interval (2006, 2280)

\* inversely correlated to annual rainfall level

**Table A6. “Mean” values of input parameters  $\delta_i, A_i, B_i, C_i, \zeta_i, M_e, a_i, b_i$**

$e, i$	ND County	$\delta_i$ (mm)	$B_i$ (hectare)	$C_i$ (\$/hectare)	$A_i$ (tonne/hectare)	$\zeta_i$ (tonne)	$M_e$ (MLPY)	$a_i$	$b_i$
1	Slope	376	6882	25.9	13.7	11706	2.30	0.80	28.24
2	McIntosh	462	8504	50.6	16.8	41031	8.90	1.00	9.96
3	Golden Valley	389	5081	23.0	14.1	4203	5.32	0.83	28.73
4	Burleigh	429	13536	37.0	15.6	36609	257.61	1.07	-42.84
5	Bottineau	470	21623	32.1	17.1	39652	20.37	1.14	-49.96
6	Burke	427	15505	20.7	15.5	8854	6.24	0.93	-17.55
7	Bowman	394	8757	28.4	14.3	15570	9.98	0.84	28.97
8	Towner	422	23023	28.4	15.3	42231	7.12	0.90	30.02
9	Foster	478	5248	44.4	17.4	40191	10.59	1.06	-0.34
10	Grant	424	12728	30.9	15.4	33270	7.58	1.05	-41.49
11	Pembina	465	19249	29.6	16.9	74175	23.49	0.99	33.44
12	Oliver	442	8984	29.6	16.1	8471	5.85	1.02	-7.89
13	Griggs	523	12155	32.1	19.0	35223	7.67	1.07	42.97
14	Divide	378	12531	22.2	13.8	0	6.56	0.83	-15.57
15	Ramsey	480	23556	29.6	17.5	66028	36.28	1.03	35.22
16	Stark	417	10171	38.3	15.1	39984	76.67	0.89	30.60
17	Dickey	546	12091	64.2	19.9	125108	16.76	1.18	11.30
18	Cass	536	21291	38.3	19.5	162951	474.54	1.09	44.58
19	Wells	434	12478	37.0	15.8	76603	13.33	0.97	-0.31
20	Steele	475	14277	34.6	17.3	68003	6.26	0.97	40.47
21	Sargent	523	11433	72.8	19.0	64162	12.13	1.13	11.08
22	Sioux	361	14789	29.6	13.1	11641	13.16	0.90	-33.83
23	Walsh	467	33116	29.6	17.0	85382	35.23	1.00	34.14
24	Grand Forks	498	29021	25.9	18.1	109418	211.83	1.07	36.43
25	Adams	394	7614	30.9	14.3	21146	7.42	0.84	28.58
26	Traill	528	5394	27.2	19.2	91057	25.73	1.08	45.21
27	Stutsman	470	24066	39.5	17.1	119103	66.85	1.04	-0.33
28	Nelson	457	20096	29.6	16.6	32018	9.90	0.98	33.15
29	LaMoure	470	15604	53.1	17.1	133191	13.11	1.01	10.13
30	Cavalier	460	24725	27.2	16.7	94095	12.65	0.98	33.88
31	Emmons	411	11722	42.0	15.0	102720	11.25	1.02	-37.69
32	Ransom	513	9076	58.0	18.7	64662	17.29	1.11	11.18
33	Morton	434	11513	38.3	15.8	40516	87.04	1.08	-39.57
34	Dunn	414	13403	29.6	15.1	24673	11.20	0.96	-7.39
35	Sheridan	445	11909	29.6	16.2	4985	4.19	0.99	-0.31
36	Billings	376	3228	23.7	13.7	4520	2.48	0.80	27.51
37	Benson	419	17437	30.9	15.2	67247	21.10	1.02	-45.03
38	Ward	470	17662	32.1	17.1	31113	195.40	1.03	-19.36
39	Renville	445	7274	30.9	16.2	0	7.83	0.97	-18.65
40	Hettinger	394	9403	37.0	14.3	52289	7.85	0.84	28.81
41	Logan	483	9302	46.9	17.5	36743	6.30	1.04	10.66
42	Eddy	457	9304	35.8	16.6	9279	7.56	1.02	-0.32
43	Rolette	472	33508	28.4	17.2	22838	44.16	1.15	-50.44
44	Pierce	465	12710	33.3	16.9	43215	13.80	1.13	-49.18
45	Mountrail	500	16918	22.5	18.2	17961	24.31	1.10	-21.04
46	Mercer	406	6274	29.6	14.8	5518	26.69	0.94	-7.26
47	Kidder	475	20471	38.3	17.3	28877	7.71	1.06	-0.34
48	McHenry	422	21008	34.6	15.3	30652	17.09	1.02	-44.44
49	Barnes	480	15982	44.4	17.5	100712	35.06	0.98	41.30
50	Richland	556	29425	53.1	20.2	189237	51.71	1.20	12.46
51	McLean	452	24821	28.4	16.4	71163	28.39	1.05	-8.07
52	McKenzie	366	13275	20.2	13.3	16165	20.15	0.85	-6.53
53	Williams	361	15904	24.4	13.1	5890	70.96	0.79	-15.12

The distances between county seats ( $D_{ir}, D_{re}$ ) are too numerous to display here.

**Table A7. Values of deterministic parameters**

Input parameter	Value
Price of carbon emissions in location $r$ (\$/ton CO <sub>2</sub> equiv.)	$\Xi_r = 40$ (for all $r$ )
Renewable electricity generation tax credit in location $r$ (\$/MWh)	$\Theta_r = 11$ (for all $r$ )
Electricity generation from biomass type $m$ for conversion technology $j$ (MWh/ton)	$C_{11} = 0.20$ ; $C_{12} = 0$ ; $C_{21} = 0.18$ ; $C_{22} = 0$
Annualized fixed cost of biorefinery at location $r$ with conversion technology $j$ (\$M)	$G_{r1} = 21.3$ ; $G_{r2} = 22.3$ (for all $r$ )
Variable cost of biorefinery at location $r$ with conversion technology $j$ (\$/ton)	$H_{r1} = 46$ ; $H_{r2} = 48$ (for all $r$ )
Reduction in carbon emissions from renewable electricity (tons CO <sub>2</sub> -equiv./MWh)	$N_{Elr} = 0.7$
Reduction in carbon emissions from mixed alcohols (tons CO <sub>2</sub> -equiv./gallon)	$N_{MA} = 0.0074675$
Reduction in carbon emissions from bioethanol (tons CO <sub>2</sub> -equiv./gallon)	$N_{Eth} = 0.005705$
Ethanol production cost of biorefinery at location $r$ with conversion technology $j$ (\$/gallon)	$U_{r1} = 0.907$ ; $U_{r2} = 0.859$ (for all $r$ )
Carbon emission of processing biomass type $m$ with technology $j$ (tons CO <sub>2</sub> -equiv./ton)	$\alpha_{11} = 0.08$ ; $\alpha_{12} = 0.09$ ; $\alpha_{21} = 0.08$ ; $\alpha_{22} = 0.09$
Carbon emission of transporting biomass type $m$ (tons CO <sub>2</sub> -equiv./ton x mile)	$\beta_m = 0.00011$ (for all $m$ )
Carbon emission of transporting bioethanol (tons CO <sub>2</sub> -equiv./gallon x mile)	$\gamma = 0.00000033$
Carbon emission of harvesting biomass type $m$ (tons CO <sub>2</sub> -equiv./ton)	$\Lambda_1 = 0.139$ ; $\Lambda_2 = 0.126$ ;
Transport cost of biomass $m$ from supply zone $i$ to biorefinery $r$ (\$/ton x mile)	$\eta_{mir} = 0.21$ (for all $m, i, r$ )
Sale price of unsubsidized bioethanol at location $r$ in time period $t$ (\$/gallon)	$i_{rt} = 2$ (for all $r, t$ )
Bioethanol yield for biomass type $m$ from conversion technology $j$ (gallons/ton)	$\kappa_{11} = 90$ ; $\kappa_{12} = 72$ ; $\kappa_{21} = 81$ ; $\kappa_{22} = 80$
Purchase price of biomass type $m$ at supply zone $i$ in time period $t$ (\$/ton)	$\lambda_{1it} = 75$ ; $\lambda_{2it} = 60$ (for all $i, t$ )
Mixed alcohol yield for biomass type $m$ from conversion technology $j$ (gallons/ton)	$\mu_{11} = 0$ ; $\mu_{12} = 13$ ; $\mu_{21} = 0$ ; $\mu_{22} = 14$
Bioethanol inventory cost in time period $t$ (\$/gallon)	$\Delta_t = 0.06$ (for all $t$ )
Maximum biomass amount that can be processed by refinery $r$ with technology $j$ (MTPY)	$\rho_j^{max} = 3$ (for all $j$ )
Minimum biomass amount that can be processed by refinery $r$ with technology $j$ (MTPY)	$\rho_j^{min} = 1$ (for all $j$ )
Inventory cost for biomass type $m$ in time period $t$ (\$/ton)	$\zeta_{1t} = 1.125$ ; $\zeta_{2t} = 0.900$ (for all $t$ )
Penalty cost for unmet bioethanol requirement at biofuel demand zone $e$ (\$/gallon)	$\phi_e = 1$ (for all $e$ )
Sale price of mixed alcohol at location $r$ in time period $t$ (\$/gallon)	$\chi_{rt} = 2.3$ (for all $r, t$ )
Transport cost of bioethanol from refinery $r$ to biofuel demand zone $e$ (\$/gallon x mile)	$\psi_{re} = 0.00017$ (for all $r, e$ )
Sale price of renewable electricity generated at location $r$ (\$/MWh)	$\delta_r = 77.5$ ( $r = 1, \dots, 102$ ); $70.4$ ( $r = 103, \dots, 201$ ); $77.4$ ( $r = 202, \dots, 288$ ); $93.5$ ( $r = 289, \dots, 360$ )
Tax credit for bioethanol production in location $r$ for satisfying demand in zone $e$ (\$/gallon)	$\tau_{re} = 0.50$ for ( $r, e = 1, \dots, 102$ ); ( $r, e = 103, \dots, 201$ ); ( $r, e = 202, \dots, 288$ ); ( $r, e = 289, \dots, 360$ ). Else = 0.25

**Table A8. Values of stochastic parameters**

Input parameter	Value
Biomass supply level	$o(\omega) \sim N(1, 0.0256)$ and truncated on the interval (0.52, 1.48)
Bioethanol demand level	$\pi(\omega) \sim N(1, 0.0121)$ and truncated on the interval (0.67, 1.33)
Biomass price level	$v(\omega) \sim N(1, 0.0144)$ and truncated on the interval (0.64, 1.36)
Energy price level	$\sigma(\omega) \sim N(1, 0.0225)$ and truncated on the interval (0.55, 1.45)

**Table A9. Discretized levels of independent random variables (IRVs)**

Supply level of biomass		Demand level of bioethanol		Price level of biomass		Price level of energy	
Level	Mean Value	Level	Mean Value	Level	Mean Value	Level	Mean Value
L_o01	0.72	L_π01	0.81	L_v01	0.80	L_σ01	0.74
L_o02	0.83	L_π02	0.88	L_v02	0.88	L_σ02	0.85
L_o03	0.89	L_π03	0.92	L_v03	0.91	L_σ03	0.90
L_o04	0.93	L_π04	0.96	L_v04	0.95	L_σ04	0.95
L_o05	0.98	L_π05	0.98	L_v05	0.98	L_σ05	0.98
L_o06	1.02	L_π06	1.01	L_v06	1.01	L_σ06	1.02
L_o07	1.07	L_π07	1.04	L_v07	1.04	L_σ07	1.05
L_o08	1.11	L_π08	1.07	L_v08	1.08	L_σ08	1.10
L_o09	1.17	L_π09	1.11	L_v09	1.12	L_σ09	1.15
L_o10	1.28	L_π10	1.19	L_v10	1.20	L_σ10	1.26

**Table A10. Values of stochastic parameters**

Input parameter	Value
Switchgrass supply level	$o(\omega) \sim N(1, 0.0342)$ and truncated on the interval (0.45, 1.55)
Bioethanol demand level	$\pi(\omega) \sim N(1, 0.0086)$ and truncated on the interval (0.72, 1.28)
Energy price level	$\sigma(\omega) \sim N(1, 0.0193)$ and truncated on the interval (0.58, 1.42)

**Table A11. Values of key deterministic parameters**

Input parameter	Value
Renewable electricity generation tax credit in location $r$ (\$/MWh)	$\Theta_r = 11$ (for all $r$ )
Electricity generation from biomass type $m$ for conversion technology $j$ (MWh/ton)	$C_{11} = 0.20; C_{21} = 0.20; C_{31} = 0.18; C_{m2} = 0$
Annualized fixed cost of biorefinery at location $r$ with conversion technology $j$ (\$ M)	$G_{r1} = 21.3; G_{r2} = 22.3$ (for all $r$ )
Variable cost of biorefinery at location $r$ with conversion technology $j$ (\$/ton)	$H_{r1} = 46; H_{r2} = 48$ (for all $r$ )
Reduction in carbon emissions from renewable electricity (tons CO <sub>2</sub> -equiv./MWh)	$Q_{Eth} = 0.7$
Reduction in carbon emissions from mixed alcohols (tons CO <sub>2</sub> -equiv./gallon)	$Q_{MA} = 0.0074675$
Reduction in carbon emissions from bioethanol (tons CO <sub>2</sub> -equiv./gallon)	$Q_{Eth} = 0.005705$
Ethanol production cost of biorefinery at location $r$ with conversion technology $j$ (\$/gallon)	$U_{r1} = 0.907; U_{r2} = 0.859$ (for all $r$ )
Carbon emission of processing biomass type $m$ with technology $j$ (tons CO <sub>2</sub> -equiv./ton)	$\alpha_{m1} = 0.08; \alpha_{m2} = 0.09$
Carbon emission of transporting biomass type $m$ (tons CO <sub>2</sub> -equiv./ton x mile)	$\beta_m = 0.00011$ (for all $m$ )
Carbon emission of transporting bioethanol (tons CO <sub>2</sub> -equiv./gallon x mile)	$\gamma = 0.00000033$
Carbon emission of harvesting biomass type $m$ (tons CO <sub>2</sub> -equiv./ton)	$\Lambda_1 = 0.175; \Lambda_2 = 0.139; \Lambda_3 = 0.126$
Transport cost of biomass $m$ from supply zone $i$ to biorefinery $r$ (\$/ton x mile)	$\eta_{mir} = 0.21$ (for all $m, i, r$ )
Sale price of unsubsidized bioethanol at location $r$ in planning period $t$ (\$/gallon)	$l_{rt} = 2$ (for all $r, t$ )
Bioethanol yield for biomass type $m$ from conversion technology $j$ (gallons/ton)	$\kappa_{11} = 90; \kappa_{21} = 90; \kappa_{31} = 81;$ $\kappa_{12} = 72; \kappa_{22} = 72; \kappa_{32} = 80$
Purchase price of biomass type $m \neq 1$ at supply zone $i$ in planning period $t$ (\$/ton)	$\lambda_{2it} = 70; \lambda_{3it} = 55$ (for all $i, t$ )
Mixed alcohol yield for biomass type $m$ from conversion technology $j$ (gallons/ton)	$\mu_{m1} = 0; \mu_{12} = 13; \mu_{22} = 13; \mu_{32} = 14$
Switchgrass harvest cost parameter in supply zone $i$ (\$/acre)	$lc_i = 9.2$ (for all $i$ )
Maximum biomass amount that can be processed by refinery $r$ with technology $j$ (MTPY)	$\rho_j^{max} = 3$ (for all $j$ )
Minimum biomass amount that can be processed by refinery $r$ with technology $j$ (MTPY)	$\rho_j^{min} = 1$ (for all $j$ )
Switchgrass densification cost parameter in supply zone $i$ (\$/ton)	$pp_i = 22$ (for all $i$ )
Penalty cost for unmet bioethanol requirement at biofuel demand zone $e$ (\$/gallon)	$\phi_e = 1$ (for all $e$ )
Sale price of mixed alcohol at location $r$ in planning period $t$ (\$/gallon)	$\chi_{rt} = 2.3$ (for all $r, t$ )
Transport cost of bioethanol from refinery $r$ to biofuel demand zone $e$ (\$/gallon x mile)	$\psi_{re} = 0.00017$ (for all $r, e$ )
Sale price of renewable electricity generated at location $r$ (\$/MWh)	$\delta_{rt} = 93.5$ (for all $r, t$ )
Ratio of gasoline equivalent annual demand to be satisfied from bioethanol	$\Gamma = 0.2$
Tax credit for bioethanol production in location $r$ for satisfying demand in zone $e$ (\$/gallon)	$\tau_{re} = 0.50$ (for all $r, e$ )

**Table A12. Values of key deterministic parameters**

Input parameter	Value
Annualized fixed cost of biomass power plant at location $r$ (\$ M)	$\alpha_r = 10$ (for all $r$ )
Variable cost of biomass power plant at location $r$ (\$/MW)	$\beta_r = 80,000$ (for all $r$ )
Maximum generation capacity of a biomass power plant (MW)	$\gamma_{max} = 1000$
Minimum generation capacity of a biomass power plant (MW)	$\gamma_{min} = 200$
Annualized fixed cost of wind farm at location $r$ (\$ M)	$\delta_r = 15$ (for all $r$ )
Variable cost of wind farm at location $r$ (\$/MW)	$\epsilon_r = 155,000$ (for all $r$ )
Minimum generation capacity of a wind farm (MW)	$\zeta_{min} = 200$
Variable cost of a HVAC transmission line from $r$ to $j$ (\$/MW x mile)	$\iota_{rj} = 230$ (for all $r, j$ )
Variable cost of a HVAC transmission line from $r$ to $d$ (\$/MW x mile)	$\iota_{rd} = 0$ (for all $r$ )
Maximum transmission capacity of a HVAC power line from $r$ to $j$ (MW)	$\kappa_{rj} = 2000$ (for all $r, j$ )
Maximum transmission capacity of a HVAC power line from $r$ to $d$ (MW)	$\kappa_{rd} = 100$ (for all $r$ )
Annualized fixed cost of a HVDC transmission line (\$ M)	$\lambda = 156$
Variable cost of a HVDC transmission line (\$/MW x mile)	$\mu = 100$
Maximum transmission capacity of a HVDC power line (MW)	$v_{max} = 4000$
Minimum transmission capacity of a HVDC power line (MW)	$v_{min} = 600$
Renewable electricity generation tax credit in location $r$ (\$/MWh)	$\phi_r = 11$ (for all $r$ )
Electricity generation parameter from biomass (MWh/ton)	$\pi = 1$
Purchase price of biomass at supply zone $i$ (\$/ton)	$\rho_i = 40$ (for all $i$ )
Ratio of available biomass that can be procured for electricity generation	$\sigma = 0.4$
Transport cost parameter of biomass (\$/ton x mile)	$\tau = 0.21$
Sale price of electricity at in-state demand zone $d$ (\$/MWh)	$v_1 = 67$
Sale price of electricity at out-state demand zone $e$ (\$/MWh)	$v_1 = 69; v_2 = 74$
100% of annual electricity requirement at in-state demand zone $d$ (GWh)	$o_1 = 14,000$
100% of annual electricity requirement at out-state demand zone $e$ (GWh)	$o_1 = 110,00; o_2 = 30,000$
Maximum ratio of annual electricity demand to be satisfied from renewables	$\chi_{max} = 0.2$
Minimum ratio of annual electricity demand to be satisfied from renewables	$\chi_{min} = 0.0$
Ratio of available biomass that can be removed from supply zone $i$	$RTO_i = 0.3$ (for all $i$ )
Penalty cost parameter for unmet renewable electricity requirement (\$/MWh)	$\psi = 160$
Annualized fixed cost of HVDC grid station at location $j$ (\$ M)	$\Gamma_j = 2.2$ (for all $j$ )

**Table A13. Values of stochastic parameters**

Input parameter	Value
Electricity price level	$A(\omega) \sim N(1, 0.0009)$
Hourly wind speed	$\Delta_r(\omega) =$ Weibull distribution with “shape parameter” of 2 (for all $r$ )*

\*The values of the “scale parameter” are given in Table A14.

**Table A14. Values of input parameters  $\zeta_i, B_r, \eta_r, \Delta_r$**

$i, r$	$\zeta_i$ (Million tons)	$B_r$ (MW)	$\eta_r$ (MW)	$\Delta_r$ [44] scale parameter
1	5.7	0	1783	14.1
2	4.4	0	9373	16.0
3	56.6	212	6998	13.1
4	2.7	240	4784	13.1
5	5.0	0	1874	13.4
6	25.7	261	6656	13.7
7	14.3	0	670	13.0

The distances ( $DST_{ir}, DST_{rj}, DST_{rd}, DST_{je}$ ) are too numerous to display here and are available upon request as a data file.



APPENDIX B. CONVERSION FACTORS FROM METRIC (SI) UNITS TO U.S. UNITS

1 mm = 0.039 inches

1 hectare = 2.471 acres

1 km = 0.621 miles

1 tonne = 1.102 tons

1 liter = 0.264 gallons

APPENDIX C. CONVERSION FACTORS FROM U.S. UNITS TO METRIC (SI) UNITS

1 inch = 25.4 mm

1 acre = 0.405 hectare

1 mile = 1.609 km

1 ton = 0.907 tonne

1 gallon = 3.785 liter